The Dissertation Committee for William Gibson Parker Jr. Certifies that this is the approved version of the following dissertation:

TAXONOMY AND PHYLOGENY OF THE AETOSAURIA (ARCHOSAURIA: PSEUDOSUCHIA) INCLUDING A NEW SPECIES FROM THE UPPER TRIASSIC OF ARIZONA

Committee:

Timothy Rowe, Supervisor

Christopher Bell

Julia Clarke

Sterling Nesbitt

Hans-Dieter Sues

TAXONOMY AND PHYLOGENY OF THE AETOSAURIA (ARCHOSAURIA: PSEUDOSUCHIA) INCLUDING A NEW SPECIES FROM THE UPPER TRIASSIC OF ARIZONA

by

William Gibson Parker Jr., B.S.; M.S.

Dissertation

Presented to the Faculty of the Graduate School of

The University of Texas at Austin

in Partial Fulfillment

of the Requirements

for the Degree of

Doctor of Philosophy

The University of Texas at Austin

May 2014

Dedication

To Linda, Zachary, and Elizabeth, who endured long periods of my time away from home as well as many late nights at the computer during its generation and completion. Despite these absences, physical and mental, they have been continuously supportive of my dream. I will always be deeply appreciative and I love you all.

Acknowledgements

I would like to thank Tim Rowe and Chris Bell for providing me the opportunity to initiate and complete my PhD at the University of Texas at Austin. Initially we were unsure if completing the degree while retaining my job in Arizona was feasible, but with their guidance it became a reality. I would also like to thank Julia Clarke and Hans-Dieter Sues for agreeing to serve on my committee and for all of their help and comments. Special thanks goes out to my committee member, friend, and colleague, Sterling Nesbitt, who continues to push me to be a better scientist and paleontologist. Thanks to Matthew Brown for giving me a place to stay during the 20 plus weeks that I was in Austin and for the many late night conversations about scientific ethics and standards. My fellow graduate students and colleagues Michelle Stocker, Adam Marsh, Kerin Claeson, Jen Olori, Heather Ahrens, and Katie Criswell offered much advice and guidance about my project as well as tips on managing graduate school.

I would also like the thank the management and staff of Petrified Forest National Park (PEFO), especially superintendents Cliff Spencer and Brad Traver, as well as my supervisor Pat Thompson who allowed me to pursue my degree while under their employment. This work never would have been completed without their support. For fieldwork assistance at the Petrified Forest I thank Daniel Woody, David Gillette, Sue Clements, Dan Slais, Randall Irmis, Sterling Nesbitt, Jeff Martz, Lori Browne, Michelle Stocker, Raul Ochoa, Chuck Beightol, Rachel Guest, Matt Smith, and Kenneth Bader. I also greatly appreciate the assistance provided by the Maintenance Division staff of PEFO in the final collection of many of these specimens. Preparation of PEFO specimens

was completed by Pete Reser, Matt Brown, Matt Smith, and Kenneth Bader. All specimens were collected under permit from the National Park Service.

Access to specimens under their care was provided by T. Scott Williams and Matt Smith (PEFO); Pat Holroyd, Mark Goodwin, and Kevin Padian (UCMP); David and Janet Gillette (MNA); Julia Desojo (MACN); Jaime Powell (PVL); Ricardo Martinez (PVSJ); Sandra Chapman, Lorna Steel, and David Gower (NHMUK); Lindsay Zanno and Vince Schneider (NCSM); Sankar Chatterjee and Bill Mueller (TTUP); Matthew Carrano (USNM); Tony Fiorillo and Ron Tykoski (DMNH); Alex Downs (GR); Charles Dailey and Dick Hilton (Sierra College); Tim Rowe, Lyndon Murray, Matt Brown, and Chris Sagebiel (VPL). Permission to discuss certain unpublished specimens was provided by Andrew Heckert, Rainer Schoch, Julia Desojo, and Tomajz Sulej. Photographs of specimens were provided by Sterling Nesbitt, Julia Desojo, Jeff Wilson, Jeff Martz, Randy Irmis, and Richard Butler. David Gower provided access to and permission to use Alick Walker's original notes and photographic slides of *Stagonolepis robertsoni*. Ben Creisler graciously developed the new taxonomic name for the Petrified Forest material.

Financial assistance for this project was provided by the Jackson School of Geosciences, the Lundelius Fund, the Francis L. Whitney Endowed Presidential Scholarship, the Ronald K. DeFord Scholarship Fund, the Petrified Forest Museum Association, Petrified Forest National Park, the Friends of the Petrified Forest, the Museum of Northern Arizona, the GSA Geocorp program, the Samuel and Doris Welles Fund, and the Systematics Association.

Finally I must acknowledge Philip Guerrero, the Graduate Program Coordinator from the Jackson School of Geosciences. Philip told me that his job was to "keep the students out of trouble" and at that he certainly excels. I would never have completed this degree without his patience and assistance.

TAXONOMY AND PHYLOGENY OF THE AETOSAURIA (ARCHOSAURIA: PSEUDOSUCHIA) INCLUDING A NEW SPECIES FROM THE UPPER TRIASSIC OF ARIZONA

William Gibson Parker, Jr. Ph.D

The University of Texas at Austin, 2014

Supervisor: Timothy Rowe

Abstract: Aetosaurians are a clade of pseudosuchian archosaurs that were globally dispersed during the Late Triassic Epoch. Aetosaurians are characterized by a suite of osteoderms that covered much of the body. These osteoderms are commonly recovered as fossils and possess characteristic surface ornamentation that can be diagnostic for taxa. The abundance of these osteoderms and the ease of identification have made aetosaurians ideal index taxa for Late Triassic biostratigraphy. Of special interest are specimens from South and North America and Europe that have been assigned to the genus *Stagonolepis*, which have been utilized for correlation of continental sedimentary units and to approximately date the timing of important biotic events. New finds have called the synonymy of these *Stagonolepis*-like specimens into question, jeopardizing their ability to serve as biochronological markers. Detailed examination of all of the specimens assigned to *Stagonolepis robertsoni* demonstrates that all of these specimens do not represent the same species. The South American material is assigned to the genera *Aetosauroides*, *Aetobarbakinoides*, and *Polesinesuchus*; the European material to

Stagonolepis; and the North American material to *Calyptosuchus, Adamanasuchus,* and a newly recognized taxon, *Scutarx deltatylus*. *Scutarx deltatylus* can be differentiated from other aetosaurians by the presence of a strongly raised, triangular boss, on the posteromedial corner of the paramedian osteoderms. *Scutarx deltatylus* also preserves the first good skull material from a *Stagonolepis*-like aetosaur from North America. A dorsoventrally thickened skull roof and an anteroposteriorly short parabasisphenoid further demonstrate the distinctness of this material from that of South America and Europe. A detailed phylogenetic analysis of all known aetosaurians further demonstrates the distinctness of these taxa. This new expanded analysis of 28 taxa and 83 characters recovers *Aetosauroides scagliai* as the sister taxon to all other aetosaurians. *Stagonolepis robertsoni* from Scotland does not clade with *Stagonolepis olenkae* from Poland. *Calyptosuchus wellesi* is the sister taxon to a clade consisting of *Scutarx deltatylus* and *Adamanasuchus eisenhardtae*. However, distribution of autapomorphies across these taxa precludes them from being synonymized. As a result the *Stagonolepis*-like aetosaurs cannot be used for global scale correlations of Upper Triassic strata, but do appear to be of utility for regional correlations, in particular those between the Chinle Formation and Dockum Group in the American Southwest.

Table of Contents

List of Tables

List of Figures

CHAPTER 1: INTRODUCTION

The Triassic Period is a key transitional point in Earth history, where remnants of the Paleozoic biotas are replaced by a more modern Mesozoic biota (e.g., Fraser, 2006). Prominent in this new radiation are the archosaurs, which includes the common ancestor of birds and crocodylians and all of its descendents (Gauthier, 1986). The early appearance and diversification of this important clade is of interest because beginning in the Triassic, the archosaurs almost completely dominated all continental ecosystems throughout the entire Mesozoic. Because the Triassic globe had a coalesced supercontinent, Pangaea, the Laurasian and Gondwanan continental faunas are often considered to be cosmopolitan in their distribution, presumably due to the lack of major oceanic barriers (Colbert, 1971). Thus many Triassic taxa were considered widespread and widely applicable for global biostratigraphy (e.g., Lucas, 1998a).

More recent work suggests that this is a gross oversimplification of the taxonomic diversity present at the time (e.g., Irmis et al., 2007a, Nesbitt et al., 2007; Nesbitt et al., 2009a, b) and new research on many Triassic groups is showing evidence for endemism of species-level taxa (e.g., Martz and Small, 2006; Parker, 2008a; Parker, et al. 2008; Stocker, 2010), with distinct patterns of radiation of more inclusive clades into new areas (e.g., Nesbitt et al., 2010). Key to this change in thinking are the utilization of testable techniques such as apomorphy-based identification of fossils (e.g., Irmis et al., 2007b; Nesbitt and Stocker, 2008) and improved phylogenetic approaches to archosaur relationships and paleobiogeography (e.g., Irmis, 2008; Nesbitt et al., 2010; Nesbitt,

2011). However, the majority of these new studies have focused mainly on the bird-line archosaurs and similar studies of the crocodile-line (Suchia) taxa are sorely needed.

Aetosaurians are quadrupedal, heavily armored, suchian archosaurs with a global distribution, restricted to non-marine strata of the Late Triassic (Figure 1.1; Desojo et al., 2013). Aetosaurians are characterized by their specialized skull with partially edentulous jaws, an upturned premaxillary tip, and laterally facing supratemporal fenestrae. Another key feature of aetosaurians is a heavy carapace consisting of four columns of rectangular dermal armor, two paramedian columns that straddle the midline, and two lateral columns (Figure 1.2; Walker, 1961). Ventral and appendicular osteoderms are also present in most taxa. Aetosaurian osteoderms possess detailed ornamentation on the dorsal surface, the patterning of which is diagnostic for taxa (Long and Ballew, 1985). Thus, the type specimens of several aetosaurian taxa consist solely of osteoderms (e.g., *Typothorax coccinarum* Cope, 1875; *Paratypothorax andressorum* Long and Ballew, 1985; *Lucasuchus hunti* Long and Murry 1995; *Rioarribasuchus chamaensis* Zeigler et al., 2003; *Apachesuchus heckerti* Spielmann and Lucas, 2012) or consist chiefly of osteoderms (e.g., *Calyptosuchus wellesi* Long and Ballew, 1985; *Typothorax antiquum* Lucas et al., 2003a; *Tecovasuchus chatterjeei* Martz and Small, 2006; *Adamanasuchus eisenhardtae* Lucas et al., 2007a; *Sierritasuchus macalpini* Parker et al., 2008). Aetosaurian osteoderms and osteoderm fragments are among the most commonly recovered fossils from Upper Triassic strata (Heckert and Lucas, 2000). Because of this abundance, in concert with the apparent ease of taxonomic identification, global distribution in non-marine strata, and limited stratigraphic range (e.g., Upper Triassic)

aetosaurians have been proposed as key index fossils for use in regional and global non-marine biostratigraphy (e.g., Long and Ballew, 1985; Lucas and Hunt, 1993; Lucas and Heckert, 1996a; Lucas et al., 1997; Lucas, 1998a; Heckert et al., 2007a, b; Lucas et al., 2007b; Parker and Martz, 2011). Four Land Vertebrate Faunachrons (LVF) were erected that use aetosaurians to divide the Late Triassic Epoch (Lucas and Hunt, 1993), from oldest to youngest these are the Otischalkian (middle Carnian); Adamanian (late Carnian); Revueltian (Norian), and the Apachean (Rhaetian). These were redefined as biozones by Parker and Martz (2011).

Proposed biostratigraphically significant aetosaurian taxa include *Longosuchus* for the Otischalkian, *Stagonolepis* (including *Calyptosuchus*) for the Adamanian, *Typothorax* and *Aetosaurus* for the Revueltian, and *Redondasuchus* for the Apachean (Long and Ballew, 1985; Lucas and Hunt, 1993; Lucas, 1998a). However, the global utility of aetosaurians for biochronology has been criticized (Schultz, 2005; Langer, 2005; Lehman and Chatterjee, 2005; Rayfield et al., 2005, 2009; Parker and Irmis, 2005; Parker, 2006; Parker, 2008a; Irmis et al., 2010; Desojo et al., 2013) and the regional utility (especially western North America) is still being tested (Parker and Martz, 2011). Response to these criticisms, as well as the more recent discovery of index taxa outside of their respective biozones, such as *Stagonolepis* in purported Otischalkian strata and *Typothorax* in presumed Adamanian strata, have led to several proposed revisions of those faunachrons (Hunt et al., 2005; Lucas et al., 2007c), all of which are still problematic (Irmis et al., 2010; Parker and Martz, 2011). Furthermore recent recalibration of the Late Triassic timescale has demonstrated that much of the Late Triassic strata in

North America are probably Norian to Rhaetian in age with Carnian strata restricted or absent (e.g., Furin et al. 2006; Irmis et al., 2011) and therefore the Adamanian is now considered to by early to middle Norian, and the Revueltian to be lmiddle Norian to early Rhaetian (Parker and Martz, 2011).The implications for aetosaurian distribution in light of this revised timescale is still being investigated (Desojo et al., 2013).

Much of the disagreement regarding the biochronological utility of aetosaurians stems from a lack of consensus among aetosaur workers regarding their taxonomy. One hypothesis (e.g., Lucas et al., 1997; Heckert and Lucas, 1999a, 2000, 2002a; Lucas, 2010) synonymizes several taxa (e.g., *Aetosauroides*, *Calyptosuchus*, *Stegomus*) into the genera *Aetosaurus* and *Stagonolepis* and then utilizes the resulting global distribution of those two taxa to correlate Upper Triassic strata worldwide. In turn, the co-occurrence of the earliest known dinosaurs with aetosaurs in some of these strata has led to the hypothesis that the earliest appearances of Dinosauria were globally synchronous (e.g., Heckert and Lucas, 1999b). A second hypothesis (e.g., Desojo, 2005; Langer, 2005; Martz and Small, 2006; Parker, 2007; Desojo and Ezcurra, 2011; Irmis et al., 2011; Desojo et al., 2012, 2013; Martz and Small, 2013; Roberto-da-Silva et al., 2014) maintains that the distribution of aetosaurian taxa was instead quite endemic and that the global distribution of the clade is much more taxonomically diverse limiting their applicability for long-range biostratigraphic correlations (Irmis et al., 2010). This second hypothesis has recently been supported by the recent redescription of many of the taxa considered to be junior synonyms of *Stagonolepis* (Heckert and Lucas, 2000, 2002a; Lucas and Heckert, 2001), which have instead been recovered as diagnosable taxa

distinct from *Stagonolepis*. Thus these *Stagonolepis*-like taxa would not useful for global-scale correlations (Desojo and Ezcurra, 2011; Desojo et al., 2012; Roberto-da-Silva et al., 2014), but this requires further testing. Likewise comparison of radioisotopic dates from the lower portion of the Chinle Formation of New Mexico and the lower part of the Ischigualasto Formation of Argentina has suggested that the appearance of the earliest dinosaurs was a globally diachronous event (Irmis et al., 2011). Therefore, many of the specimens assigned to *Stagonolepis* and *Aetosaurus* are in need of restudy to better ascertain their taxonomic and phylogenetic relationships (Parker, 2008a).

Phylogenetic relationships within Aetosauria are not entirely understood, largely because seemingly informative phylogenetic characters may be intermingled with character transformations owing to ontogeny and sexual dimorphism (Desojo et al., 2013). Furthermore, past phylogenetic analyses of the Aetosauria have been affected by coding errors, unclear character construction, and poorly supported topologies (Harris et al. 2003a; Desojo and Ezcurra, 2011).

The most recent phylogenetic analysis suggested that the Aetosauria (Archosauria: Pseudosuchia) can be divided into three distinct clades, Aetosaurinae, Typothoracinae, and Desmatosuchinae (Parker, 2007). Relationships within the last two clades are fairly well resolved (Parker et al. 2008; Desojo et al., 2012; Heckert et al., in press), but still require further testing in light of taxonomic revisions mentioned above as well as the recent discovery of many new aetosaurian fossils. However, the relationships of Aetosaurinae (aetosaurians more closely related to *Stagonolepis* and *Aetosaurus*, *sensu* Parker, 2007) are unresolved and the placement of the Typothoracinae in Aetosaurinae in

the study of Parker (2007) was weakly supported. Subsequent phylogenetic analyses that have rescored characters and added taxa to the matrix of Parker (2007) have not recovered a monophyletic Aetosaurinae (e.g., Desojo et al., 2012; Heckert et al., in press). Furthermore, although the original study recovered *Calyptosuchus*, *Aetosauroides*, and *Stagonolepis* in a single, but unresolved clade (Parker, 2007), subsequent studies have not recovered this clade.

AETOSAURIANS PREVIOUSLY ASSIGNED TO *STAGONOLEPIS*

Aetosaurians presently and historically assigned to the genus *Stagonolepis* consist of seven nominal taxa; *Stagonolepis robertsoni* Agassiz 1844 (Lossiemouth Sandstone Formation, Scotland), *Aetosauroides scagliai* Casimiquela 1961 (Ischigualasto Formation, Argentina; Sequence 2 of the Santa Maria Supersequence, Brazil), *Calyptosuchus wellesi* Long and Ballew 1985 (Chinle Formation, Dockum Group, southwestern USA), *Stagonolepis olenkae* Sulej, 2010 (Poland), *Adamanasuchus eisenhardtae* Lucas, Hunt and Spielmann, 2007a (Chinle Formation, southwestern USA), *Aetobarbakinoides brasiliensis* Desojo, Ezcurra, and Kischlat 2012 and *Polesinesuchus aurelioi* Roberto-da-Silva et al. (2014), both from the Santa Maria Supersequence (Sequence 2) of Brazil. An eighth taxon is named and described later in this dissertation. Historically all of these taxa, with the exception of *Adamanasuchus*, have been synonymized with *Stagonolepis*, mostly as *Stagonolepis robertsoni*, but also as *Stagonolepis wellesi*, based mainly on the presence of a radial ornamentation of grooves and ridges in concert with a posteriorly placed dorsal eminence on the trunk paramedian

osteoderms, as well as a general similarity of the lateral osteoderms.(e.g, Long and Murry, 1995; Lucas and Heckert, 1996a; Heckert and Lucas, 1999a, 2000, 2002a; Lucas and Heckert 2001; Parker and Irmis, 2005; Parker, 2006; Lucas et al. 2007d).

Detailed re-examination of the holotype of *Aetosauroides scagliai* identifies key differences of the skull from that of *Stagonolepis robertsoni*, most notably that the premaxillae and nasals meet behind the nares, restricting the maxilla from participating in the margin of the nares (see Chapter 3; Desojo and Ezcurra, 2011). The holotype specimens of *Aetobarbakinoides brasiliensis* and *Polesinesuchus aurelioi* from Brazil were thought to represent South American specimens of *Stagonolepis robertsoni* (Lucas and Heckert, 2001), but re-examination of the materials has recognized autapomorphies allowing them to be described as distinct taxa (Desojo et al., 2012; Roberto-da-Silva et al., 2014). The purpose of this study is to reexamine those taxa to reevaluate their potential taxonomic affinities utilizing an apomorphy-based approach and to review the phylogenetic relationships of these taxa. In sum, this study asks two main questions:

1) Does *Stagonolepis robertsoni* have a global distribution and what is its biostratigraphic significance? Material from Argentina, Brazil, Scotland, Poland, and North America has been assigned to *Stagonolepis robertsoni* (Lucas and Heckert, 2001; Heckert and Lucas, 2002a; Lucas et al., 2007d). This includes the holotype specimens of *Aetosauroides scagliai* and *Stagonolepis olenkae*. Furthermore, a second species of *Stagonolepis*, *Stagonolepis wellesi*, is recognized from North and South America (Long and Murry, 1995; Heckert and Lucas, 2002a). Both of these taxa are used to globally

correlate the Adamanian biozone, which is argued to be latest Carnian (Lucas, 2010) or early Norian (Irmis et al., 2011).

2) Do all of the *Stagonolepis*-like aetosaurs from the American Southwest belong to the same taxon? Originally all of the *Stagonolepis*-like aetosaurs were assigned to a single taxon, *Calyptosuchus* (=*Stagonolepis*) *wellesi* (Long and Murry, 1995). However, some specimens have been identified as possibly pertaining to *Stagonolepis robertsoni* (Lucas et al., 1997) and a partial skeleton from Petrified Forest National Park was noted as similar to *Calyptosuchus wellesi*, but possessing a few characteristics that could be used to refer it to a new species (Parker and Irmis, 2005). Lucas et al., (2007a) also named a new taxon, *Adamanasuchus eisenhardtae*, for material that also resembles that of *Calyptosuchus wellesi*.

Institutional abbreviations – **AMNH**, American Museum of Natural History, New York, USA; **ANSP**, Academy of Natural Sciences, Philadelphia, Pennsylvania, USA; **CPE2**, Coleção Municipal, São Pedro do Sul, Brazil; **DMNH**, Perot Museum of Natural History, Dallas, Texas, USA; **DMNH**, Denver Museum of Nature and Science, Denver, Colorado, USA; **FMNH**, Field Museum of Natural History, Chicago, IL, USA; **FR**, Frick Collection, American Museum of Natural History, New York, USA; **MCCDP**, Mesalands Community College Dinosaur Museum, Tucumcari, New Mexico, USA; **MCSNB,** Museo Civico di Scienze Naturali Bergamo, Bergamo, Italy; **MCP**, Museo de Ciencias e Tecnología, Porto Alegre, Brazil**;** **MCZ**, Museum of Comparative Zoology, Harvard University, Cambridge, Massachusetts, USA; **MCZD**, Marischal College

Zoology Department, University of Aberdeen, Aberdeen, Scotland, UK; **NCSM**, North Carolina State Museum, Raleigh, North Carolina, USA; **NHMUK**, The Natural History Museum, London, United Kingdom; **NMMNH**, New Mexico Museum of Natural History and Science, Albuquerque, New Mexico, USA; **MNA**, Museum of Northern Arizona, Flagstaff, Arizona, USA; **PEFO**, Petrified Forest National Park, Petrified Forest, Arizona, USA; **PFV**, Petrified Forest National Park Vertebrate Locality, Petrified Forest, Arizona, USA; **PVL**, Paleontología de Vertebrados, Instituto 'Miguel Lillo', San Miguel de Tucumán, Argentina; **PVSJ,** División de Paleontologia de Vertebrados del Museo de Ciencias Naturales y Universidad Nacional de San Juan, San Juan, Argentina, **SMNS**, Staatliches Museum für Naturkunde, Stuttgart, Germany; **TMM**, Vertebrate Paleontology Laboratory, University of Texas, Austin, Texas, USA; **TTUP**, Museum of Texas Tech, Lubbock, Texas, USA; **UCMP**, University of California, Berkeley, California, USA; **ULBRA PVT**, Universidade Luterana do Brasil, Coleção de Paleovertebrados, Canoas, Rio Grande do Sul, Brazil; **UMMP**, University of Michigan, Ann Arbor, Michigan, USA; **USNM**, National Museum of Natural History, Smithsonian Institution, Washington, D.C., USA; **VPL**, Vertebrate Paleontology Lab, University of Texas at Austin, Austin, Texas, USA; **YPM**, Yale Peabody Museum of Natural History, New Haven, Connecticut, USA; **VRPH**, Sierra College, Rocklin, California, USA; **ZPAL,** Institute of Paleobiology of the Polish Academy of Sciences in Warsaw, Warsaw; Poland.

MATERIALS AND METHODS

For this study the holotypes and main referred material of the major taxa that have been assigned to *Stagonolepis* were examined firsthand. These include *Aetosauroides scagliai* (PVL 2052; PVL 2073), *Calyptosuchus wellesi* (e.g., UMMP 13950, UMMP 7470, UCMP 27225) and *Stagonolepis robertsoni* (e.g., MCZD 2, NHMUK R4787a). Other *Stagonolepis*-like aetosaurs examined firsthand include *Adamanasuchus eisenhardtae* (PEFO 34638) and *Aetobarbakinoides brasiliensis* (CPE2 168). Detailed notes and photographs were taken of all specimens. I was unable to examine the *Stagonolepis olenkae* material firsthand, but excellent photographs of the material were provided to me by another researcher (see acknowledgements). Most of this material remains undescribed so I do not describe it for this project although it was scored in the phylogenetic analysis. Details on methods used for the phylogenetic analysis and individual descriptions of taxa are provided in the respective chapters.

Apomorphy-based identifications

Apomorphy-based identification is an explicit, conservative, and testable method that uses the presence of discrete synapomorphies to determine taxonomic placement of individual specimens (Bell et al., 2004; 2010; Bever, 2005; Nesbitt et al., 2007; Irmis et al., 2007b; Nesbitt and Stocker, 2008; Stocker, 2013b). This approach minimalizes the influence of geographical and/or stratigraphic factors in taxonomic assignment, allowing

for a broader comparative sample (Bever, 2005; Bell et al., 2010). This re-evaluation is needed for aetosaurians because the majority of specimens consist of isolated, fragmentary osteoderms and many prior referrals of this material to existing genera have been done on the basis of superficial resemblance and/or geographical or stratigraphic occurrence (e.g., Long and Ballew, 1985; Long and Murry, 1995; Heckert and Lucas, 2000; Parker and Irmis, 2005). These are significant biases that can cause significant misidentifications and taxonomical referrals, which can lead to misconceptions and circularity regarding ideas on biostratigraphy and faunal dynamics (Nesbitt and Stocker, 2008; Bell et al., 2010). Aetosaurs have been proposed as important index taxa for Late Triassic terrestrial biostratigraphy; however, in many instances stratigraphic position has been used to refine specimen identifications and then the same specimens used as evidence to develop biostratigraphic zonations based on these taxa (e.g., Lucas and Hunt, 1993; Lucas and Heckert, 1996a; Heckert et al., 2007a). This is clearly circular as biostratigraphically determined taxonomic assignments cannot be used as support for a biochronology (Parker and Martz, 2011).

There are several shortcomings to an apomorphy-based method of identification. For example, it is not always possible to identify specimens, especially fragmentary ones, down to the species or even genus level. This is primarily because discrete apomorphies may not be pre-determined for many skeletal elements (Bever, 2005; Bell et al., 2010). Furthermore, a lack of understanding of morphological differences resulting from individual variation, sexual dimorphism, and ontogeny can hinder identifications. Finally, in isolated specimens with limited preserved characters, it can be difficult to determine

whether the presence of certain character states is because of homoplasy or homology with the comparative sample (Bever, 2005). Aetosaurians are susceptible to several of these problems because; 1) historically aetosaurian taxonomy has been done utilizing only a limited character set, those of the osteoderms. Indeed many taxa are known solely from osteoderms; 2) individual, sexual, and ontogenetic variation are poorly understood; and 3) there is a fair degree of homoplasy in osteoderm characters making it difficult to recognize full suites of characters, which are necessary for accurate identifications of fragmentary specimens (Martz and Small, 2006; Parker, 2007, 2008a). As a result it is often not possible to resolve the taxonomy of many aetosaurian specimens down to the genus or species level. Fortunately for this study the key taxa to be examined (e.g., *Stagonolepis robertsoni*, *Stagonolepis olenkae*, *Calyptosuchus wellesi*, *Aetosauroides scagliai*, *Coahomasuchus kahleorum*) are known from well-preserved skeletally mature specimens, minimizing these effects. Furthermore, these taxa are also represented by endoskeletal material allowing the opportunity to discover apomorphies in a far wider variety of skeletal elements including those of the skull.

Naming Conventions for Aetosaurian Osteoderms

Traditionally, identification and naming of aetosaurian osteoderms, which cover the dorsal, ventral, and appendicular areas, utilizes terms first originated by Long and Ballew (1985). In this convention the dorsal armor consists of two midline 'paramedian' columns flanked laterally by two 'lateral' columns (Long and Ballew, 1985; Heckert and

Lucas, 2000). By convention, osteoderms of the dorsal region are named from the type of vertebrae they cover (e.g., cervical, dorsal, and caudal). However, the anteriormost paramedian osteoderms lack equivalent lateral osteoderms causing a potention numbering offset between the presacral paramedian and lateral rows (Heckert et al., 2010). Aetosaurians also possess ventral armor at the throat, as well as ventral armor that underlies the 'dorsal' (=trunk) and caudal vertebrae. The presence of ventral armor of the 'dorsal' series creates the awkward combination of 'ventral-dorsal' osteoderms. Therefore there is a need to standardize the positional nomenclature for aetosaurian osteoderms.

The term carapace properly refers only to the dorsally situated network of osteoderms, thus the term 'dorsal carapace' is incorrect and redundant. In this study the term carapace refers only to the dorsally situated osteoderms and the term ventral osteoderms is used for all ventrally situated osteoderms.

The carapace can be divided into four anteroposteriorly trending columns of osteoderms (Heckert et al., 2010). Those that straddle the mid-line are referred to as the paramedians and the flanking osteoderms are called the lateral armor (Long and Ballew, 1985). Each column is divided into rows and as noted above these have traditionally been given names based on the vertebral series they cover (in most taxa there is a 1:1 ratio between osteoderms and vertebrae).

The two anteriormost paramedian osteoderms fit into the back of the skull and are generally mediolaterally oval and lack corresponding lateral osteoderms. These osteoderms are termed the nuchal series (Figure 1.3; Sawin, 1947; Desojo et al., 2013). Posterior to these are roughly five, six, or nine rows of paramedian and lateral osteoderms

that cover the entire cervical vertebral series, termed cervical osteoderms (Figure 1.3; Long and Ballew, 1985). The patch of osteoderms beneath the cervical vertebrae in the throat area would be called the gular osteoderms, based on the name given to these osteoderms in phytosaurians (Long and Murry, 1995).

The next vertebral series initiates with the 10th presacral vertebra. On this vertebra the parapophysis has moved up to the top of the centrum, just below the level of the neurocentral suture. In the previous nine vertebrae (the cervical series), the parapophysis is situated at the base of the centrum, and in the eleventh vertebra the parapophysis is situated on the tranverse process. Thus the 10th presacral is transitional in form and has been considered to be the first of the 'dorsal' series (Walker, 1961; Parker, 2007), and that convention is followed here.

Historically in aetosaurians these vertebrae have been referred to as the dorsal series and osteoderms covering these vertebrae are the 'dorsal osteoderms' (e.g., Long and Ballew, 1985; Long and Murry, 1995; Heckert and Lucas, 2000; Desojo et al., 2013); however, this term has become problematic because whereas all of the osteoderms below the vertebral column are termed the ventral osteoderms, only those of above the vertebral column in the trunk region are called the dorsals. Thus technically the osteoderms beneath the caudal vertebrae would be the caudal ventral osteoderms and those beneath the 'dorsal' vertebrae would be the dorsal ventral osteoderms. This is non-sensical so I suggest that a new term be used for what have been known as the dorsal vertebrae and osteoderms in aetosaurians. The terms thoracic and lumbar vertebrae reflect the chest and loin areas respectively and are assigned depending on the presence or absence of free ribs. This is not readily applicable to aetosaurians where there are ribs through the entire series. Instead I recommend the term trunk vertebrae, which is commonly used for amphibians and lepidosaurs, which also tend to have a ribs throughout the entire series

(e.g., Wake, 1992). The osteoderms above the trunk vertebrae are the dorsal runk paramedian and dorsal trunk lateral osteoderms. The osteoderms located beneath the trunk vertebrae are the ventral trunk osteoderms and consists of numerous columns of osteoderms (Figure 1.3; Heckert and Lucas, 1999). Heckert et al. (2010) utilized the term ventral thoracic osteoderms, which effectively solves the 'ventral dorsal' problem; however, I prefer to use the term ventral trunk osteoderms to maintain consistency with the term dorsal trunk osteoderms.

The osteoderms above the caudal vertebrae are termed the dorsal caudal osteoderms and consist of paramedian and lateral columns (Figure 1.3; Long and Ballew, 1985). The osteoderms beneath the caudal vertebrae are the ventral caudal osteoderms (Heckert et al., 2010) and also consist of paramedian and lateral columns behind the cloacal area (fourth row) to the tip of the tail (Jepson, 1948; Walker, 1961), the first two lateral rows bear spines in *Typothorax coccinarum* (Heckert et al., 2010). An assemblage of irregular shaped osteoderms are located anterior to the cloacal area is preserved in *Stagonolepis robertsoni*, *Aetosaurus ferratus*, and *Typothorax coccinarum* (Walker, 1961; Schoch, 2007; Heckert et al., 2010), which can be called the cloacal osteoderms.

Small masses of irregular shaped osteoderms cover the limb elements of aetosaurians (e.g., Heckert and Lucas, 1999; Schoch, 2007; Heckert et al., 2010). These have collectively been termed as simply appendicular osteoderms. However, when found in articulation they can be differentiated by the limb that is covered, including the humeral, radioulnar, femoral, and tibiofibular osteoderms (Hill, 2011).

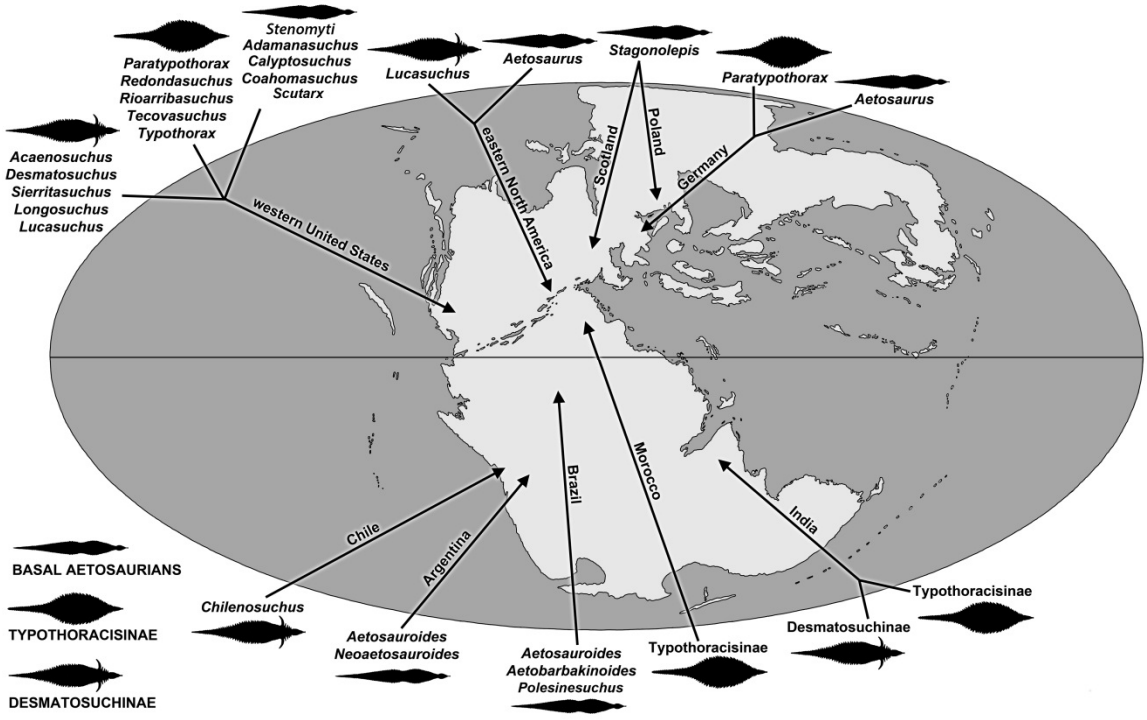

Figure 1.1. Global distribution of known aetosaurian taxa and specimens throughout Pangaea during the Late Triassic. Modified from Desojo et al., 2013.

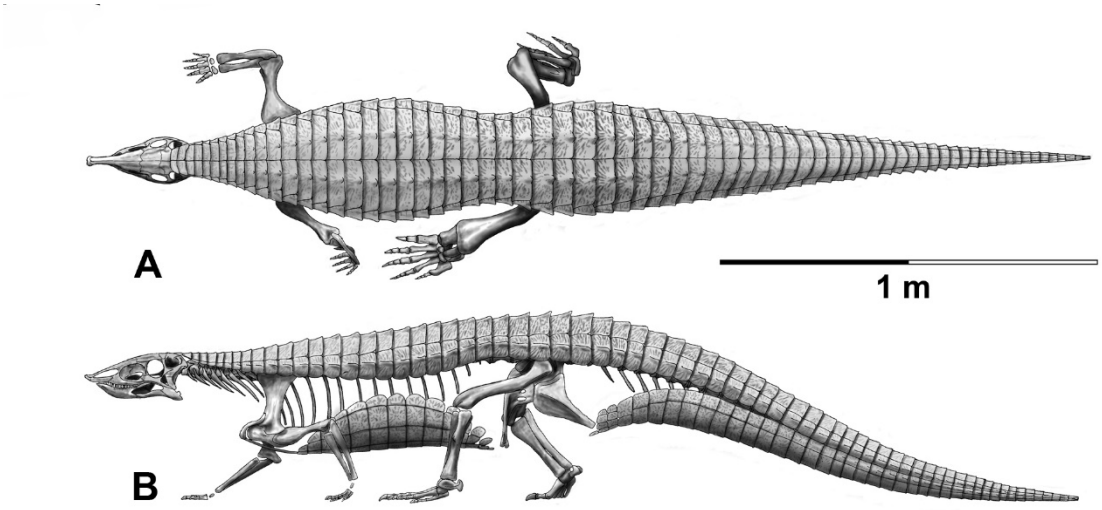

Figure 1.2. Skeletal reconstruction of *Stagonolepis robertsoni* in dorsal (A) and lateral (B) views. Courtesy of Jeffrey Martz.

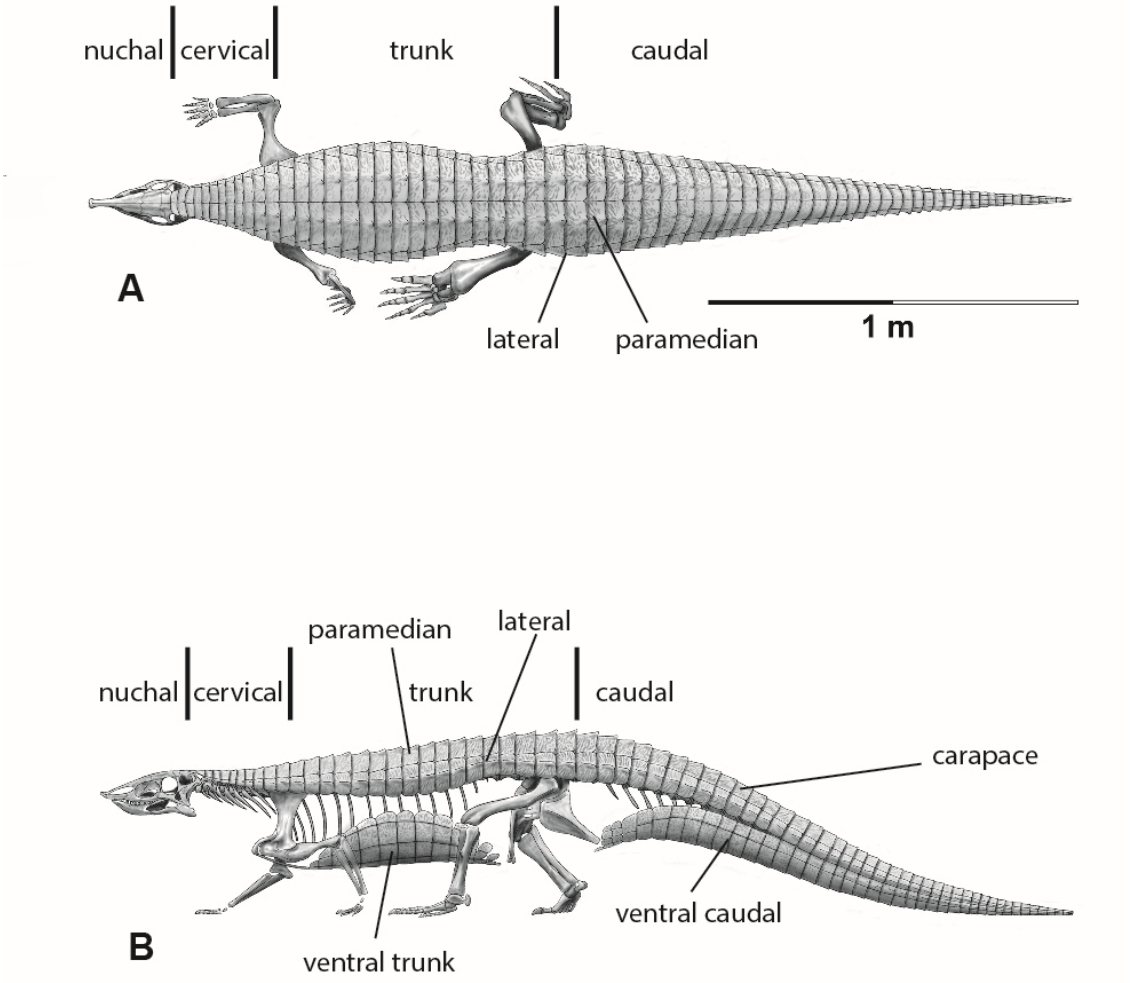

Figure 1.3. Differention and terminology for aetosaurian osteoderms. Reconstruction courtesy of Jeffrey Martz.

CHAPTER 2 – COMMENTS REGARDING SOME OF THE '*STAGONOLEPIS*-LIKE' AETOSAURIANS

INTRODUCTION

For this project I examined all of the aetosaurian taxa that have been synonymized in the past with *Stagonolepis robertsoni* (e.g., Heckert and Lucas, 1999a, 2000, 2002a; Lucas and Heckert, 2001) or assigned to the genus *Stagonolepis* (e.g., Long and Murry, 1995; Sulej, 2010); I collectively refer to them as '*Stagonolepis*-like' aetosaurians. These taxa, and several others including *Coahomasuchus kahleorum*, originally formed were included in the clade Aetosaurinae (Parker, 2007) and it was these taxa on which I focused for the purpose of determining their interrelationships within Aetosauria. Over the next few chapters I describe much of this material; however, in my opinion not all of my observations warranted full chapters and instead I have compiled them here. Taxa discussed in this chapter include *Stagonolepis robertsoni*, *Neoaetosauroides engaeus*, *Adamanasuchus eisenhardtae*, and *Coahomasuchus kahleorum*.

COMMENTS ON THE SKULL, VERTEBRAE, AND ARMOR OF *STAGONOLEPIS ROBERTSONI*

Although Alick Walker's (1961) description of *Stagonolepis robertsoni* is extremely detailed and still relevant, recent examination of the NHMUK material revealed some characteristics of the skull and vertebrae, which shed new light on this taxon, in particular the details of the vertebral laminae.

Skull

NHMUK R4787a is a cast of the lower portion of a skull in semi-articulation including much of the lower jaw, quadrate, portions of the palate and maxilla, and the premaxilla (Figure 2.1). These elements represent the left side of the skull, so the cast provides an internal (medial) view. The semi-articulated condition allows for the determination of the skull length which from the retroarticular process to the tip of the premaxilla is about 240 mm. The dentigerous elements show the presence of at least eight dentary teeth, four maxillary, and four premaxillary teeth. Alick Walker's PVC cast of this specimen shows even more details including the upper portions of the skull and the braincase. Thus block 4787 is the natural mold of a nearly complete skull of *Stagonolepis robertsoni* (Walker, 1961). An attempt was made to use the CT scanner at the NHMUK to scan the negative space in the block to get a three-dimension scan of the skull, but unfortunately the CT-scanner in the museum could not penetrate the hard sandstone matrix of the block. Details of this specimen include: 1) what looks to be a fifth tooth in the premaxilla, alternatively the tip could be the tip of the right premaxilla in articulation with the left; 2) a portion of the right squamosal and impressions of the skull roof, 3) the left quadrate in articulation with the left articular, and 4) impressions of the braincase, especially the basisphenoid including the left and right basal tubera and basipterygoid processes, showing that they were anteroposteriorly separated (distance equals 8 mm), and the cultriform process is also preserved.

A mold of the right maxilla from NHMUK R4787 (Figure 2.2) shows that overall this element is more slender than that of *Stagonolepis olenkae* (Sulej, 2010) with at least six alveoli, but the anterior portion is not preserved in the cast. A very distinct transverse ridge is present on the lateral surface of the maxilla along the anterior and ventral borders of the antorbital fossa that is not present in *Stagonolepis olenkae* (Sulej, 2010), making

the antorbital fossa extremely pronounced. The medial side of the maxillary body is marked by an elongate medial shelf that articulates with the palatal bones (Walker, 1961). The articulations with the lacrimal and jugal are each complex, with regions of overlap between the two bones. Finally, a pneumatic accessory cavity is present on the medial surface at the base of the ascending process as described for *Desmatosuchus smalli* (Small, 2002).

NHMUK R8586 is a cast of E.M. 38R (Figure 2.3), which was figured by Huxley (1877) and features the left side of the internal portion of the snout, including the premaxilla, maxilla, and nasals. The premaxilla measures 63 mm in length, bears four teeth and has an edentulous anterior portion typical for aetosaurians. The maxilla bears six teeth as preserved but is missing the posterior portion. The external naris is 22 mm at its deepest point and 72 mm in length, but missing the posteriormost section. The nasal has a pronounced ridge on the medial edge, which at a position just dorsal to the third premaxillary tooth migrates ventrally to the ventral margin of the nasal where it contacts the premaxilla. The anterior tip of the premaxilla bears a prominent ridge that divides the element into a flat surface that slopes into the external naris, and a second triangular area that slopes anteroventrally (Figure 2.3). The premaxilla bears a small dorsal protuberance that extends dorsally into the external naris, which also occurs in *Stagonolepis olenkae* (Sulej, 2010) and *Desmatosuchus smalli* (Small, 2002).

The best preserved skull material for *Stagonolepis robertsoni* is MCZD 2, which consists of seven small blocks that fit together to present much of the skull and the anterior section of the neck. The material consists of well-preserved bone and is not a natural mold as is most of the other material referred to *Stagonolepis robertsoni*. Walker (1961) and Gower and Walker (2002) described this specimen in great detail so this will

not be duplicated here although it was utilized to score characters for *Stagonolepis robertsoni* in the phylogenetic analysis (Chapter 6).

Cervical vertebrae and ribs

On NHMUK R4784a, which is a cast created from a natural mold and represents the postcranial skeleton associated with the skull R4787 (Walker, 1961), the occipital condyle and left paroccipital process of the skull are present. If the cervical vertebral count is nine (as in *Desmatosuchus spurensis*), the four anterior cervical vertebrae are missing (including the axis and atlas); however, cervical ribs are present for three of these positions. Striking are two greatly elongated, posteriorly projecting cervical ribs underlying the ventral surfaces of the two more posteriorly positioned ribs. The elongate ribs originate where the axis/atlas would be located and are very similar to the greatly elongate anterior cervical ribs found in *Alligator* (Reese, 1915). As exposed these ribs measure 85mm in length (the ends are covered), more than three times the lengths of the other exposed cervical ribs. The elongate ribs were not noted by Walker (1961) and have not previously been described for any aetosaur. The axis/atlas and third cervical are present in MCZD 2, but unfortunately are very poorly preserved; however, this block also preserves a very elongate first cervical rib.

The first well-preserved cervical vertebra in NHMUK R4784a is the eighth (Walker, 1961), which is visible in right lateral view and preserves details of the centrum and much of the neural arch and transverse process. A disarticulated cervical rib is present across the centrum and probably does not belong to this vertebra. The centrum measures 25 mm in length and the ventral surface is strongly keeled. The parapophysis is

low on the anterior rim of the centrum, but not completely at the base. The transverse process projects laterally and slightly ventrally, is 25 mm long, and bears a flaring sub-rectangular head in lateral view. A distinct posterior centrodiapophyseal lamina (*sensu* Wilson, 1999) stretches from the base of the transverse process to the posterior portion of the neurocentral suture. This is the "T-beam" structure described by Case (1922) for *Desmatosuchus spurensis* and reported as present in *Stagonolepis robertsoni* by Walker (1961). The right prezygapophysis is preserved but not enough is present to tell if a hyposphene was present. The neural spine is present, but lacks its apex.

The next three vertebrae are preserved in articulation. The parapophysis on the ninth cervical is still situated on the centrum, but slightly higher than its position in the preceding vertebra. The centrum is more elongate as well measuring 31 mm. Pre- and postzygadiapophyseal laminae (Wilson, 1999) are visible on the ninth and tenth presacrals. The tenth presacral is transitional between the cervical and dorsal trunk series as previously described for *Desmatosuchus spurensis* (Case, 1922; Parker, 2008b). The centrum is more elongate than the previous vertebra with a length of 36mm, and a slight ventral keel is present. The parapophysis has migrated upwards onto the base of the neural arch. The neurocentral suture appears to be open.

The 11th presacral is the first true dorsal trunk vertebra because the parapophysis is now situated on the posteroventral surface of the transverse process; unfortunately this cannot be seen clearly as it is broken away (Walker, 1961:fig. 7i). The centrum has a length of 39 mm and has a smooth ventral surface. The 12th presacral is present, but covered by broken ribs.

Caudal Vertebrae

NHMUK R4799b is a PVC cast of an isolated anterior caudal vertebra providing more details of the neural arch and spine (Walker, 1961: figs. 10c-e). The broad transverse processes (the left of which is 79 long) do not extend ventral to the base of the centrum; the postzygapophyses are oriented at 45 degrees above horizontal. The centrum is blocky, with equant width and height of about 40 mm, but the entire vertebral height is 112 mm, with the neural spine contributing 40 mm to this measurement. Spinopostzygapophyseal laminae (*sensu* Wilson, 1999) are present, as is an expanded neural spine table.

Osteoderms

Numerous osteoderms of *Stagonolepis robertsoni* are preserved as natural molds; however, often they only produce partial casts. Walker (1961) discussed the osteoderms in what we now consider superficial terms, therefore I redescribe one each of the best preserved dorsal trunk paramedian and lateral osteoderms. The dorsal trunk paramedian osteoderm (NHMUK 4790a) is from the left side and has a surface patterning that I call anastomosing, an interlacing network of high ridges surrounding circular and elongate pits closer to the posterior plate margin, and elongate, but irregular grooves on the anterior portion of the osteoderm (Figure 2.5a). This anastomosing ornamentation radiates from an elongate, but narrow, raised dorsal eminence that contacts the posterior osteoderm margin. This eminence is offset slightly medial to the center of the osteoderm. The anterior portion of the osteoderm bears a raised, transverse, smooth strip of bone called the anterior bar (Long and Ballew, 1985). The bar bears two distinct processes, an

anterolateral projection and an anteromedial projection. The anterior bar maintains an even width across the lateral portion of the osteoderm, but thins significantly medially before expanding again at the anteromedial projection. I term this distinct thinning, 'scalloping'. This feature occurs in several other aetosaurians including *Calyptosuchus wellesi* and *Paratypothorax andressorum*. The medial edge is straight and the lateral edge slightly sinuous in dorsal view. In posterior view the osteoderm is moderately arched.

The dorsal trunk lateral osteoderm (NHMUK 4789a; Figure 4.5b) is from the right side based on the presence of a distinct beveling of the anteromedial corner of the anterior bar, which represents an articular surface for the anterolateral process of the adjacent paramedian osteoderm. The bar is thin but extends across the entire anterior margin of the osteoderm. The osteoderm is trapezoidal in dorsolateral view and a ridge-like dorsal eminence that contacts the posterior margin divides the osteoderm into distinct dorsal and lateral flanges. The dorsal flange is roughly triangular in dorsal view, whereas the lateral flange is rectangular in dorsolateral view. The lateral flange is slightly larger than the dorsal flange. The surface ornamentation is anastomosing and very faint on the posterior portion of the osteoderm. The osteoderm is slightly flexed ventrally and the angle between the two flanges is obtuse. In dorsolateral view the lateral margin is gently rounded. The medial margin is angled posteromedially, corresponding with the shape of the adjacent paramedian osteoderm.

Status of the holotype of *Stagonolepis robertsoni* Agassiz, 1844

The holotype of *Stagonolepis robertsoni* is the impression of a fragment of the ventral trunk carapace of a single specimen (EM 27R) that shows several partial rows and columns of imbricated square to rectangular osteoderms (Figure 2.6). These osteoderms

have an anterior bar and a surface pattern of numerous drop shaped pits radiating from the osteoderm center; hence the name *Stagonolepis*, which means "drop scale". The specimen was described from a sketch by Agassiz (1944) who mistook it for the scales of a ganoid fish. At the time the deposit that had yielded the specimen was assigned to the Devonian Old Red Sandstone, and only the subsequent discovery of further remains of the a clearly reptilian vertebrate allowed for the realization that *Stagonolepis* was a reptile and that the strata were actually Triassic in age (Huxley, 1859, 1875, 1877). Much of the material was described and figured by Huxley (1877) who argued for a crocodilian affinity. Later authors (e.g, Camp, 1930) thought it to be phytosaurian. Huene (1936) assigned it to his 'Stagonolepinae', which he placed under the 'Pelycosimoidia' and considered to be distinct from the Aetosauridae, characterized by *Aetosaurus ferratus*. It was not until Walker's (1961) monograph that *Stagonolepis robertsoni* was fully recognized as an aetosaurian (i.e. closely related to *Aetosaurus ferratus*).

Subsequent authors assigned other specimens to *Stagonolepis robertsoni* based on similarities of the dorsal trunk paramedian osteoderms (e.g., Murry and Long, 1989; Long and Murry, 1995; Lucas and Heckert, 2001; Heckert and Lucas, 2002a; Lucas et al., 2007d). However, none of these authors have addressed the diagnostic status of the type specimen. Similar ventral trunk osteoderms are known from several taxa including *Coahomasuchus kahleorum*, *Calyptosuchus wellesi*, *Scutarx deltatylus*, *Aetosaurus ferratus*, and even the non-aetosaurian *Revueltosaurus callenderi*. Therefore, the holotype is not adequate to diagnose *Stagonolepis robertsoni* exclusive of other aetosaurians. Accordingly *Stagonolepis robertsoni* can be considered a *nomen dubium* and the name

should be restricted to the type specimen as presently it is impossible to refer any other specimens to *Stagonolepis robertsoni* based on the type specimen. However, the name *Stagonolepis* is firmly entrenched in the literature and it would be extremely confusing for systematics to rename this animal. Therefore the International Committee of Zoological Nomenclature should be petitioned to set aside the original holotype in favor of a neotype. For this purpose I would recommend either NHMUK R4799, the most complete dorsal paramedian osteoderm, or maybe MZCD 2, which represents a nearly complete skull and some associated osteoderms from a single specimen. It will be tricky to find a single specimen that exemplifies the taxon best, but this needs to be done to preserve taxonomic stability and validity to *Stagonolepis robertsoni*.

COMMENTS ON THE SKULL AND POSTCRANIA OF THE HOLOTYPE OF *NEOAETOSAUROIDES ENGAEUS*.

Desojo and Báez (2005, 2007) have described the skull and postcranial skeleton in great detail; however, there are a few additional noteworthy details. Bonaparte (1972) described the holotype (PVL 3525) as possessing a complete right and partial left mandibular ramus, and subsequent descriptions and phylogenetic scorings have utilized character states present in the right mandibular ramus. However, examination of the right mandibular ramus shows that it has been significantly altered during preparation (Figure 2.7). The bones surface was ground smooth, presumably during preparation and because of mineral encrustation. It has already been noted that the external mandibular fenestra is quite large and has been artificially expanded (Desojo and Báez, 2007). Just as

significant, however is that much of the anterior portion of the dentary is missing and has been completely recreated in plaster. This includes the area of the Meckelian foramen as well as the anterior tip. Thus the holotype cannot be used itself to determine if the mandibular ramus was indeed 'slipper-shaped' (*sensu* Walker, 1961). Fortunately another specimen (PULR 108) preserves the anterior tip of a dentary sowing that is was narrow and tapering (Desojo and Báez, 2007). The bone on the occlusal surface of the right dentary of PVL 3525 is ground smooth. Six alveoli are barely visible, but the area just beyond the sixth tooth position is reconstructed in plaster. A low dentary tooth count is considered an autapomorphy of *Neoaetosauroides* (Parrish, 1994; Heckert and Lucas, 2000). Desojo and Báez (2007) list the dentary tooth count for PVL 3525 as seven, but it cannot be dismissed that the number is actually higher. The posterior portion of the left mandibular ramus is also present in PVL 3525 and beautifully preserves the sutures between the various bones forming the element.

There has also been confusion regarding the surface ornamentation of the dorsal carapace in PVL 3525, which has been stated to be unornamented and an autapomorphy of *Neoaetosauroides* (Heckert and Lucas, 2000; Heckert et al., 2001). Examination of the holotype (PVL 3525) demonstrates that this lack of surface ornamentation is the result of overpreparation of the material. Furthermore, the osteoderms have been set in plaster and in the mounted specimen of *Neoaetosauroides* almost all of the anterior osteoderm rows (i.e. about the first 14 rows of cervical and anterior dorsal trunk osteoderms) are reconstructed in plaster. Thus the carapace was probably not as long as reconstructed in

the mount (see Desojo and Báez, 2005 for an alternate reconstruction) and the caudal osteoderms rows are not nearly as wide as depicted. Instead, these mid to distal caudal osteoderms rows were actually situated over the pelvis.

Those anterior caudal paramedian osteoderms show a clear radial ornamentation with elongate grooves and ridges radiating from a posteriorly placed, medially situated, pyramidal dorsal eminence. The anterior bar is raised and an anterolateral projection is present and is elongate (Figure 2.8). The lateral edge of the paramedian is angles posteromedially but lacks the extreme cut-off corner seen in typothoracines. Width/length ratios of the paramedian plates are close to 3.0.

The associated lateral plates are trapezoidal with triangular dorsal flanges. The eminence is an anteroposteriorly oriented keel. The lateral flange is very broad rectangular with a gently rounded lateral edge. Surface ornamentation consists of a radial pattern of pits and grooves (Figure 2.8). Osteoderms are flexed ventrally and the angle between the dorsal and lateral flanges is obtuse.

Overall the dorsal carapace is very similar to that of *Aetosauroides scagliai* and *Calyptosuchus wellesi* with the radial pattern, raised anterior bar and medially situated dorsal eminence. *Neoaetosauroides* shares with *Calyptosuchus* the strong anterolateral projection of the anterior bar and the strongly slanting lateral edge.

COMMENTS ON THE POSTCRANIA OF THE HOLOTYPE OF *ADAMANASUCHUS EISENHARTAE*.

The holotype of *Adamanasuchus eisenhardtae* as originally described consisted of 11 paramedian osteoderms, one lateral osteoderm, three vertebrae, and a nearly complete right femur (Lucas et al., 2007a). The associated specimen was collected from the upper part of the Blue Mesa Member in Petrified Forest National Park. Since the original description four more osteoderms have been recovered from the type locality and are part of the associated holotype. The new material consists of three left dorsal trunk paramedian osteoderms and a left dorsal trunk lateral osteoderm (Figures 2.9a-f). *Adamanasuchus* is very similar to *Calyptosuchus wellesi* and a new aetosaurian described below, *Scutarx deltatylus*, in possessing moderately wide paramedian osteoderms with a surface pattern of pits, grooves, and ridges that radiates from a medially offset pyramidal dorsal eminence that contacts the posterior osteoderm margin. The anterior bar is strongly raised and bears and anteromedial process as well as an elongate anterolateral process (Figures 2.9a-b, d). Like *Calyptosuchus wellesi*, it possesses a weak ventral strut (Figure 2.9c), unlike the strongly produced strut in *Typothorax coccinarum*. The lateral osteoderms are also very similar to those of aetosaurians such as *Calyptosuchus wellesi*, *Scutarx deltatylus*, and *Stagonolepis robertsoni* in possessing an anterior bar that has a beveled anteromedial corner for the overlap of the anterolateral process (Figure 2.9e). Like *Calyptosuchus* the lateral osteoderms bear large pyramidal dorsal eminences that divide the osteoderm into dorsal and lateral flanges (Figures 2.9e- h). The lateral flange is larger and the osteoderm is ventrally flexed with an angle of approximately 45 degrees (Figures 2.9f, h).

Differences from *Calyptosuchus wellesi* include the presence of a smooth triangular area on the posteromedial corner of the paramedian osteoderms (Figures 2.9a-b, d). This is similar to what is found in *Scutarx deltatylus*, except that in the latter this triangular patch is very strongly raised dorsally. *Adamanasuchus* differs from both *Calyptosuchus* and *Scutarx* in that the paramedian osteoderm ornamentation of radiating grooves and ridges is overprinted by a deep, coarse pitting that is unique among known Aetosauria (Figures 2.9a-b, d). Furthermore, many of the paramedian osteoderms in the holotype specimen have a very strongly sigmoidal lateral edge in dorsal view, where the posterolateral margin is sharply directed posteromedially giving the appearance that the corner was 'cut-off' (Figure 2.9d). *Calyptosuchus* and *Scutarx* also have paramedian osteoderms with strong sigmoidal lateral osteoderms, but lack the very strongly cut-off corner. Instead this is a character that is often found in typothoracine aetosaurians (e.g., *Paratypothorax*, *Typothorax*).

The rest of the material (figured in Lucas et al., 2007a) is relatively unremarkable. The femur is robust, and the large and medium sized vertebral centra unusual inbearing strong rib attachments on the anterolateral corners, forming much of the neurocentral suture and represent sacral vertebrae The distinct difference in size between the two centra suggests that they belong to different animals, with the largest assignable to *Adamanasuchus.* Despite the close similarities to *Calyptosuchus* and *Scutarx*, and although it overlaps in biostratigraphic range with *Calyptosuchus*, I consider *Adamanasuchus* valid based on the distinct pitting that overprints the base radial

ornamentation, the unraised and unornamented triangular patch on the dorsal trunk paramedian osteoderms, and also because of the strongly cut-off corners of the dorsal trunk paramedian osteoderms.

COMMENTS ON THE SKULL AND LATERAL OSTEODERMS OF THE HOLOTYPE SPECIMEN OF *COAHOMASUCHUS KAHLEORUM*

The holotype (NMMNH P-18496) of *Coahomasuchus kahleorum* consists of much of a carapace of an individual (Heckert and Lucas, 1999a). Unfortunately the specimen is crushed flat and poorly preserved and has been very roughly prepared making description of the various elements problematic. A proposed autapomorphy of *Coahomasuchus* is the presence of broad, flat lateral osteoderms with a surface ornamentation that radiates from the medial edge and lacking a dorsal eminence (Heckert and Lucas, 1999a, 2000). Indeed, the lack of a dorsal eminence of the lateral osteoderms would be unique in an aetosaurian. However, examination of the dorsal carapace of NMMNH P-18496 demonstrates that a dorsal eminence is present in *Coahomasuchus* and is in the form of a medially situated anteroposteriorly directed sharp keel. These are especially visible in the mid and posterior dorsal trunk laterals of the right side (Figure 2.10; Heckert and Lucas 1999a: fig. 3). On the dorsal mid-trunk laterals the dorsal flange is extremely reduced compared to the very broad lateral flange and in articulation the keel is situated very close to lateral edge of the corresponding paramedian osteoderm. Flattening of the carapace pushed the angled dorsal flange further ventrally, partly masking its presence. The eminence and flexion in the posterior caudal dorsal laterals is more apparent as the lateral flange is reduced compared to the dorsal flange and the angle of flexion is closer to 90 degrees as in the posterior dorsal laterals of *Calyptosuchus*

wellesi and *Scutarx deltatylus*. This increased flexion and reduction of the lateral flange helps form the 'waist' found in the dorsal carapace (Heckert and Lucas, 1999a: fig.3). Thus the lateral osteoderms are not autapomorphic and are actually very similar to other non-desmatosuchine aetosaurians.

Interpretation of the preserved right mandibular ramus of the holotype of *Coahomasuchus kahleorum* has also been problematic. Heckert and Lucas (1999a) listed the right quadrate, jugal, quadratojugal, and squamosal as being present in partial articulation with the right lower jaw in a single preserved block, although only the quadrate and purported quadratojugal are labelled in the figure (Heckert and Lucas, 1999a: fig. 5). The mandible was described in greater detail by Desojo and Heckert (2004) who also reinterpreted the bones in the upper portion of the block as only consisting of a portion of the quadrate. What had been initially interpreted as the posterior corner of the upper part of the skull was considered instead to represent a very large surangular (Desojo and Heckert, 2004: fig. 3b).

Although those authors improved the overall description of the mandible, their new interpretation is incorrect in identifying the uppermost bones in the block. The posteriormost bone of this set is the base of the right quadrate and then from back to front, the quadratojugal, the jugal, and possibly a small portion of the posterior ramus of the maxilla are present (Figure 2.11a). Those upper cranial bones have been forced ventrally, overlapping the dorsal and anterior portions of the surangular. The lower set of bones), comprises the articular, the posterior portion of the surangular, the angular, and the posteromedial process of the dentary (Desojo and Heckert, 2004). The splenial appears to be exposed beneath the anterior portion of the angular (Desojo and Heckert, 2004). The surangular foramen is readily visible on the posterolateral surface of the mandibular ramus (Figure 2.11a), but is a small opening posteroventral to the larger

crescentic opening indicated by Desojo and Heckert (2004), which actually is a gap between the quadratojugal and the surangular. In dorsal view, there is a hooked bone that forms a dorsomedially open concave surface that was labelled as the quadratojugal by Heckert and Lucas (1999a) (Figure 2.11b). I reinterpret this bone as the ectopterygoid, which articulates laterally with the posteromedial face of the jugal. Thus all of these bones are in their original articular contacts although the upper jaw has been forced ventrolaterally over the lateral side of the mandibular ramus.

DISCUSSION

Re-investigation of the holotypes of *Stagonolepis robertsoni*, *Neoaetosauroides engaeus*, *Adamanasuchus eisenhardtae*, and *Coahomasuchus kahleorum* clarifies our understanding of the anatomy of these specimens mostly in light of new discoveries made since these specimens were first described (Desojo et al., 2013). These include the recognition of an extensive series of vertebral lamina present within aetosaurians (e.g., Parker, 2008; Desojo and Ezcurra, 2011) as well as a new understanding of the anatomy of lateral osteoderms and their significance to aetosaurian phylogeny (Parker, 2007). These redescriptions allow for more clarity in scoring these taxa in a phylogenetic analysis and descriptions of the skull of *Aetosauroides scagliai*, referred material of *Calyptosuchus wellesi*, and the description of a new taxon based on material previously assigned to *Calyptosuchus wellesi* are found in the next three chapters.

Figure 2.1. NHMUK R4787a, cast of bones of *Stagonolepis robertsoni*, which represent much of the lower portion of a skull. Scale bar equals 1 cm. Abbreviations: an, angular; art, articular; d, dentary; fr, frontals; l, left; mx, maxilla; pmx, premaxilla; pra, prearticular; pt, pterygoid; qu, quadrate; r, right; sa, surangular.

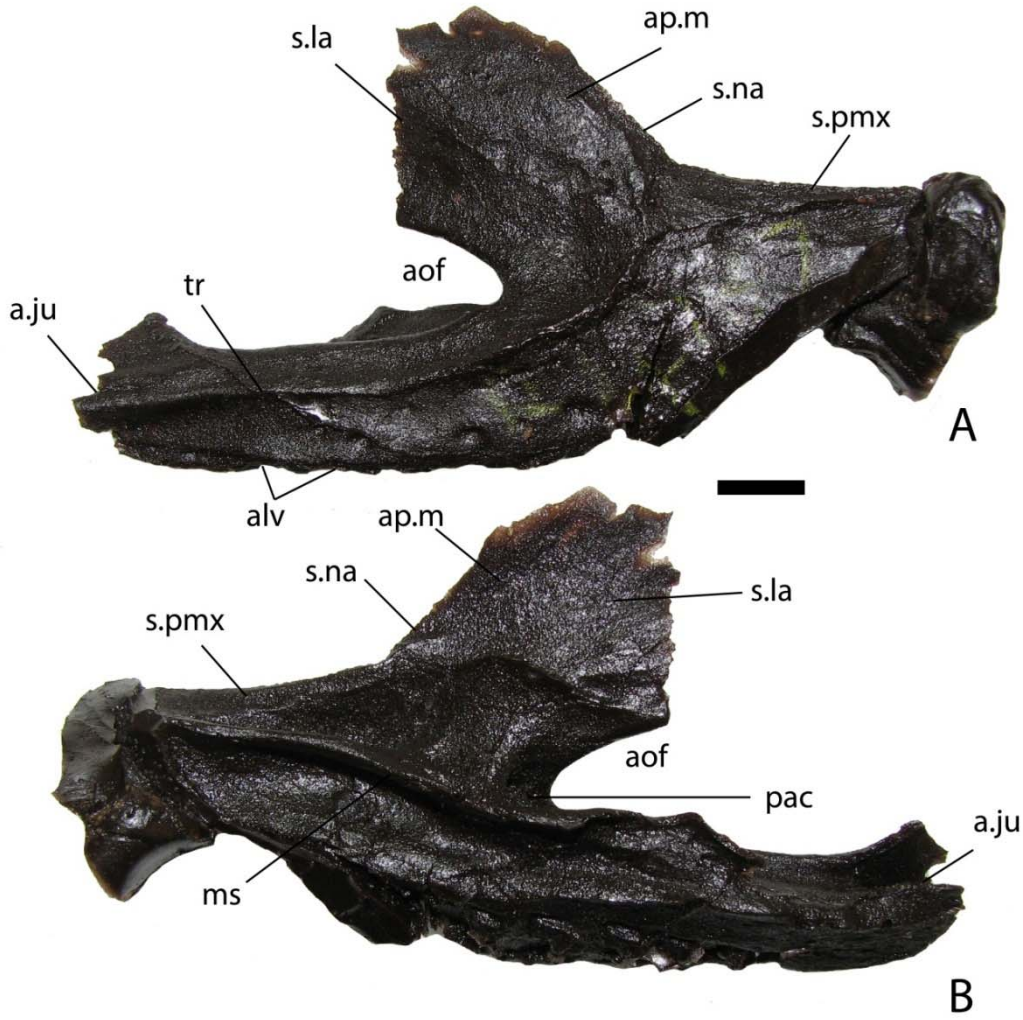

Figure 2.2. NHMUK R4787, cast of a right maxilla of *Stagonolepis robertsoni* in lateral (A) and medial (B) views. Scale bar equals 1 cm. Abbreviations: **a.**, articulation with listed element; **alv**, alveoli; **aof**, antorbital fenestra; **ap.m**, ascending process of the maxilla; **ju**, jugal; **la**, lacrimal; **ms**, medial shelf; **na**, nasal; **pac**, pneumatic accessory cavity; **pmx**, premaxilla; **tr**, transverse ridge.

Figure 2.3. Cast of the anterior part of the right side of the skull of *Stagonolepis robertsoni* in lateral view. Scale bar equals 1 cm. Abbreviations: **en**, external naris; **mx**, maxilla; **na**, nasal; **nr**, nasal ridge; **pmr**, premaxillary ridge; **pmx**, premaxilla.

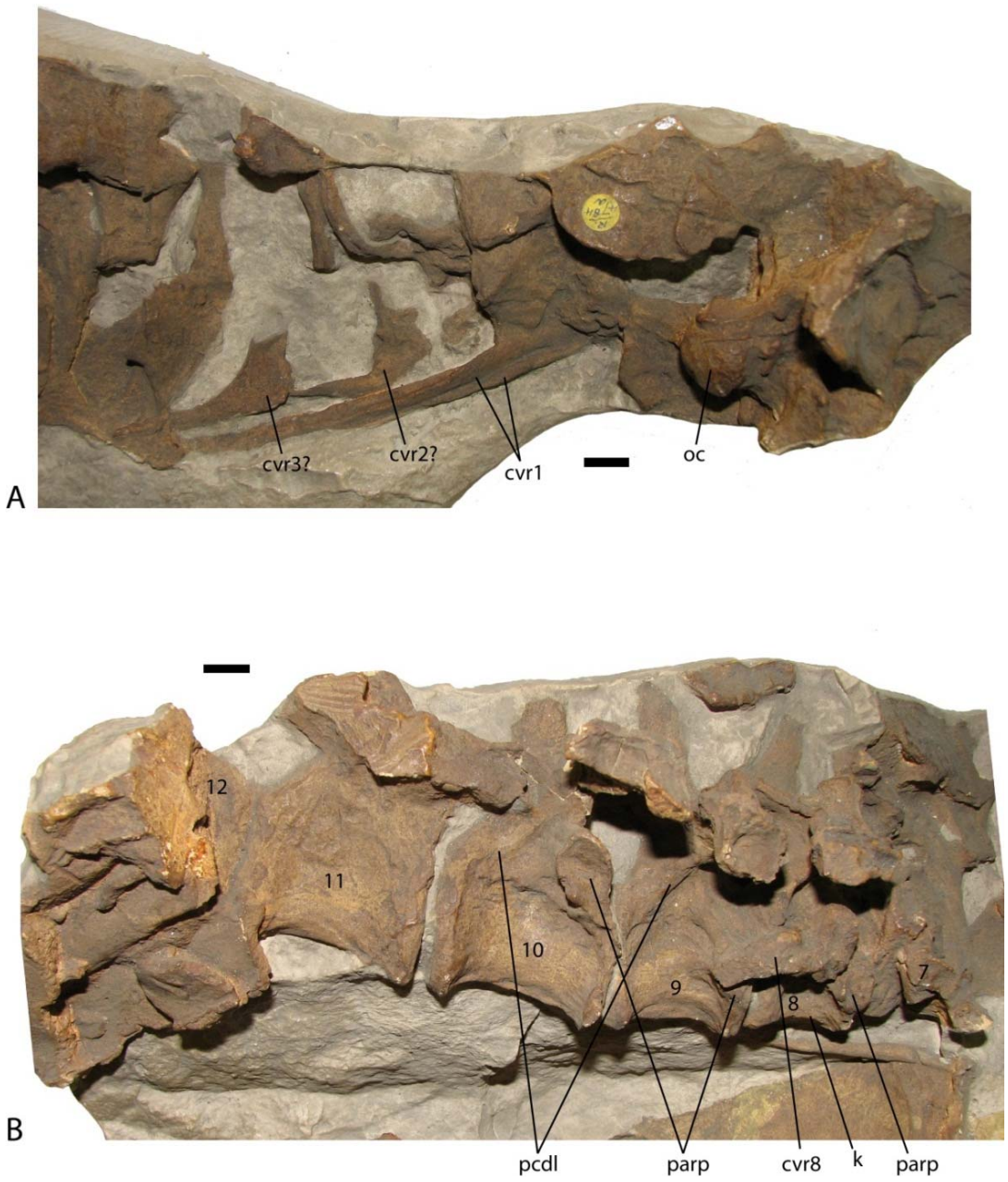

Figure 2.4. NHMUK 4784a, casts of articulated sections of the presacral vertebral column in lateral view including the rear of the skull through the fourth cervical position (A), and the seventh through the twelfth presacral vertebrae (B). Scale bars equal 1 cm. Abbreviations: **cvr**, cervical rib; **k**, ventral keel; **oc**, occipital condyle of the basicranium; **parp**, parapophysis; **pcdl**, posterior centrodiapophyseal lamina.

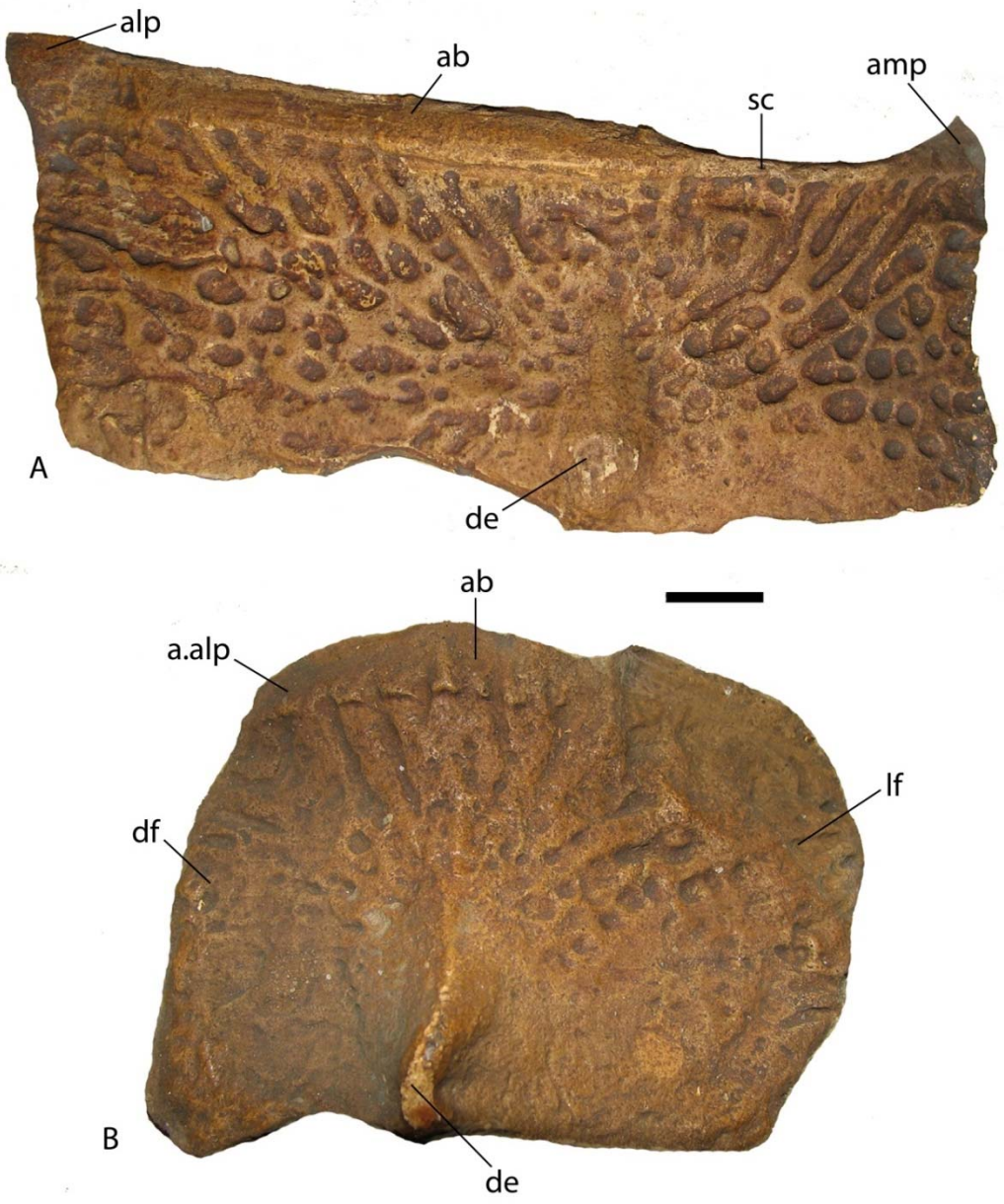

Figure 2.5. Casts of osteoderms of *Stagonolepis robertsoni*. A, left dorsal trunk paramedian (NHMUK 4790a) in dorsal view; B, right dorsal trunk lateral (NHMUK 4789a) in dorsolateral view. Scale bar equals 1 cm. Abbreviations: **a.**, articulation with listed element; **ab**, anterior bar; **alp**, anterolateral projection; **amp**, anteromedial projection; **de**, dorsal eminence; **df**, dorsal flange; **lf**, lateral flange; **sc**, scalloping of anterior bar margin.

Figure 2.6. Cast of EM 27R, the holotype specimen of *Stagonolepis robertsoni* Agassiz 1844. A series of imbricated osteoderms from the ventral trunk region.

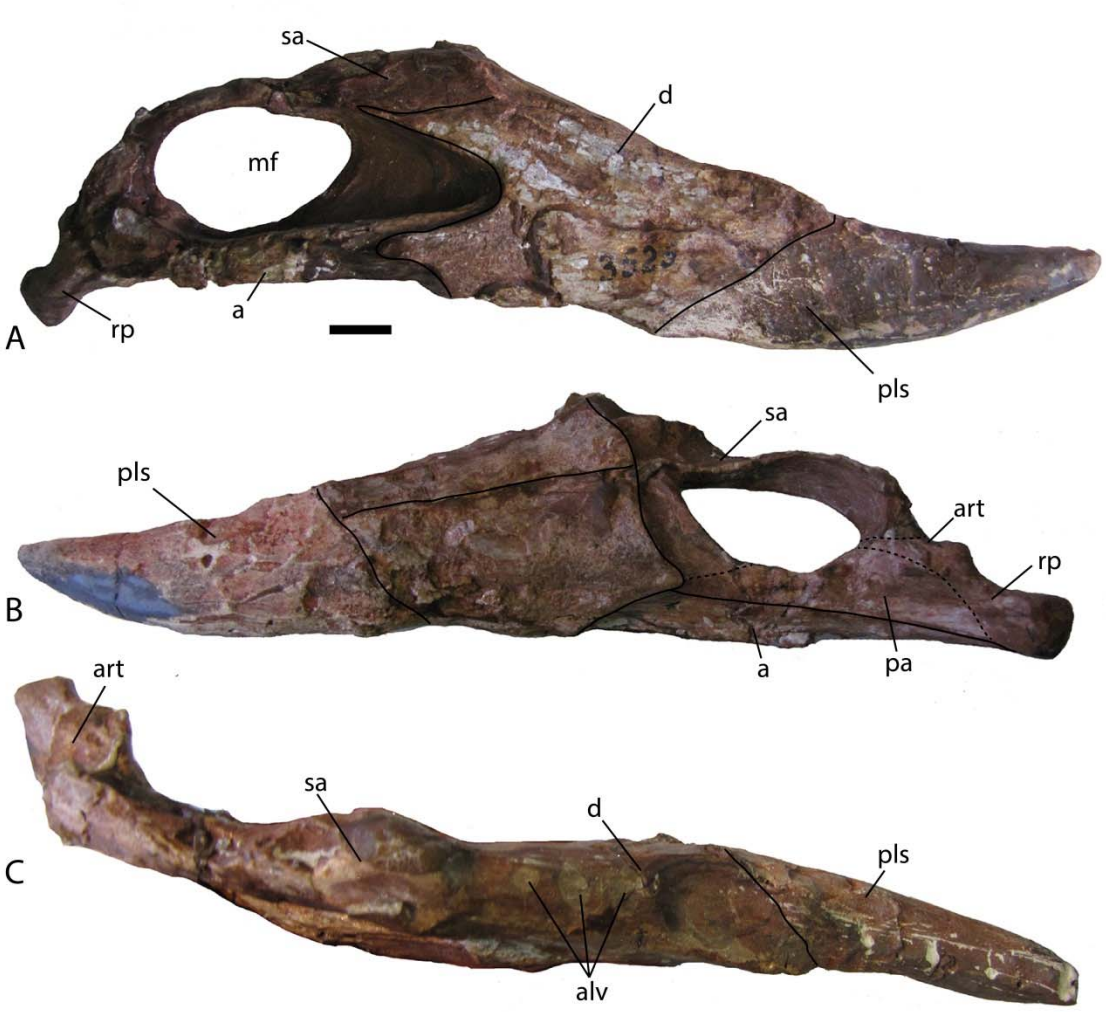

Figure 2.7. Left mandible of the holotype of *Neoaetosauroides engaeus* (PVL 3525) in lateral (A), medial (B), and occlusal (C) views. Scale bar equals 1 cm. Abbreviations: **a**, angular; **alv**, alveoli; **art**, articular; **d**, dentary; **mf**, mandibular fenestra; **pa**, prearticular; **pls**, plaster reconstruction; **rp**, retroarticular process of the articular; **sa**, surangular.

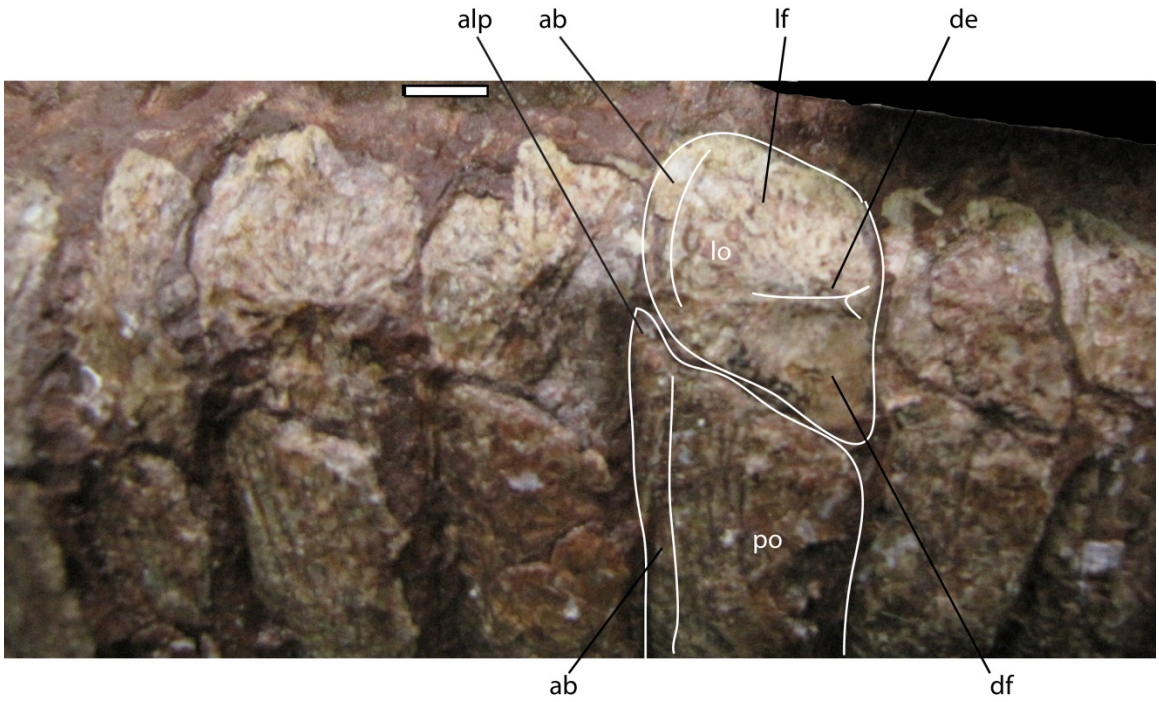

Figure 2.8. A portion of articulated right paramedian and lateral osteoderms from the trunk region of the holotype specimen of *Neoaetosauroides engaeus* (PVL 3525) in dorsolateral view. Note strong radial ornamentation of osteoderms. Scale bar equals 1cm. Abbreviations: **ab**, anterior bar; **alp**, anterolateral process; **de**, dorsal eminence; **df** dorsal flange; **lf**, lateral flange; **lo**, lateral osteoderm; **po**, paramedian osteoderm.

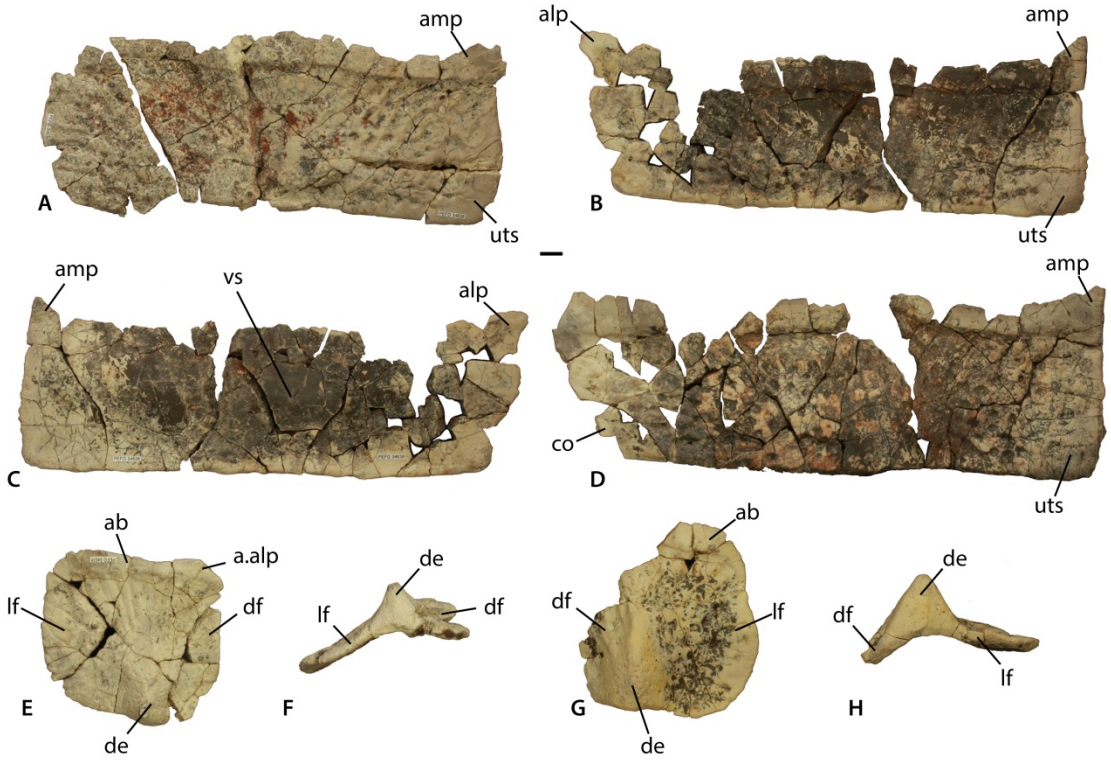

Figure 2.9. Additional osteoderms of the holotype of *Adamanasuchus eisenhardtae* (PEFO 34638). A, left dorsal trunk paramedian in dorsal view; B-C, left dorsal paramedian in dorsal (B) and ventral (C) views; D, left dorsal trunk paramedian in dorsal view; E-F, left dorsal trunk lateral in dorsolateral (E) and posterior (F) views. G-H, original right dorsal trunk lateral in dorsolateral (G) and posterior (H) views. Scale bar equals 1 cm. Abbreviations: **a.**, articulation with listed element; **ab**, anterior bar; **alp**, anterolateral projection; **amp**, anteromedial projection; **co**, cut-off corner; **de**, dorsal eminence; **df**, dorsal flange; **lf**, lateral flange; **uts**, unornamented triangular surface; **vs**, ventral strut.

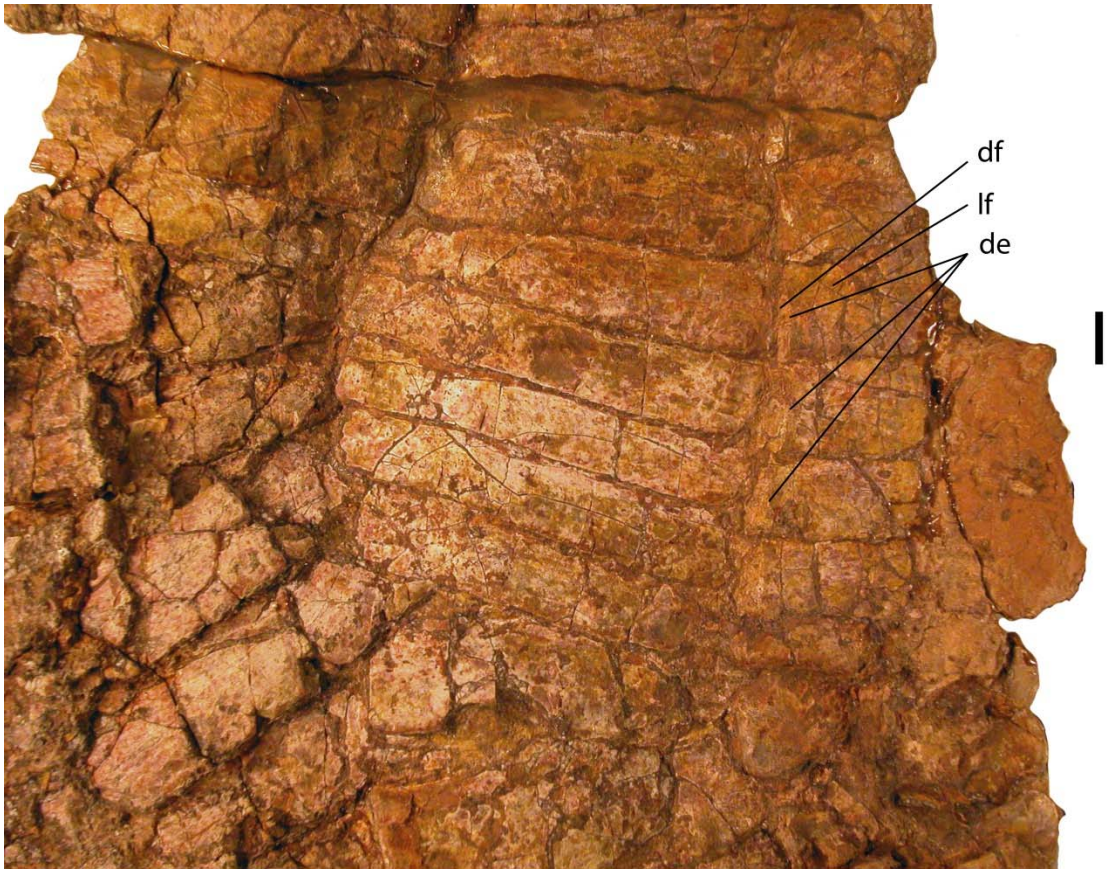

Figure 2.10. Portion of the mid-dorsal trunk paramedian and lateral carapace of the holotype of *Coahomasuchus kahleorum* (NMMNH P-18496) showing the presence of keeled dorsal eminences on the lateral osteoderms. Scale bar equals 1 cm. Abbreviations: **de**, dorsal eminence; **df**, dorsal flange; **lf**, lateral flange.

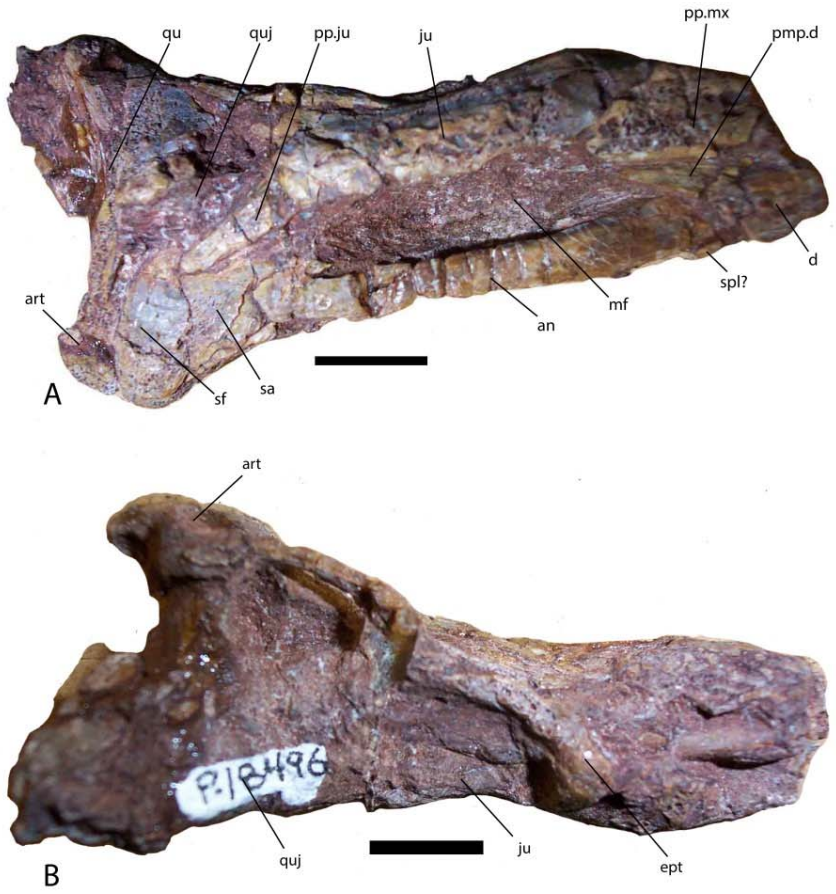

Figure 2.11. Mandible and posterior portion of the cranium of *Coahomasuchus kahleorum* (NMMNH P-18496) in ventrolateral (A), and dorsolateral (B) views. Scale bars equal 1 cm. Abbreviations: **an**, angular; **art**, articular; **d**, dentary; **ept**, ectopterygoid; **ju**, jugal; **mf**, mandibular foramen; **pmp.d**, posteromedial process of the dentary; **pp.ju**, posterior process of the jugal; **pp.mx**, posterior process of the maxilla; **qu**, quadrate; **quj**, quadratojugal; **sa**, surangular; **sf**, surangular foramen; **spl**, splenial.

CHAPTER 3: THE SKULL OF *AETOSAUROIDES SCAGLIAI* FROM THE UPPER TRIASSIC OF ARGENTINA

INTRODUCTION

Aetosauroides scagliai Casimiquela 1961 is a small (>2 m length) aetosaurian known exclusively from South America (Argentina and Brazil). *Aetosauroides* was first described by Casimiquela (1960, 1961) on the basis of material from the Ischigualasto Formation of Argentina and is known from much of the skeleton including a beautifully preserved articulated specimen consisting of much of the carapace and the underlying vertebral column and pelvis (PVL 2073) as well as a partial skull (PVL 2059). The published study of *Stagonolepis robertsoni* by Walker (1961) heavily influenced Casimiquela's (1967) subsequent description of new material (PVL 2052), which he then considered very closely related to *Stagonolepis*. The material was redescribed by Heckert and Lucas (2002a) who found it to be nearly identical to that of *Stagonolepis robertsoni* from the Lossiemouth Sandstone Formation of Scotland. This was used to propose a strong biostratigraphic correlation between Europe and North and South America (Heckert and Lucas, 2002a).

A well-preserved portion of a carapace from the Sequence 2 of the Santa Maria Supersequence of Brazil was assigned to "*Aetosauroides subsulcatus*" (Zacarias, 1982) and subsequently referred to *Stagonolepis robertsoni* (Lucas and Heckert, 2001). This material was eventually redescribed and assigned to *Aetosauroides* (Desojo and Ezcurra,

2011). Another aetosaurian specimen from Brazil (CPE2 168) originally assigned to *Aetosauroides* was reassigned to *Stagonolepis robertsoni* (Lucas and Heckert, 2001) and was subsequently designated as the holotype of *Aetobarbakinoides brasilensis* (Desojo and Ezcurra, 2011). The latter authors also noted significant differences between the skulls of *Aetosauroides scagliai* and *Stagonolepis robertsoni* that preclude their synonymy.

A goal of this project was to restudy the type and referred materials of *Aetosauroides scagliai* and compare them to other "*Stagonolepis*-like" aetosaurians such a *Calyptosuchus wellesi*, *Scutarx deltatylus*, and *Stagonolepis robertsoni* to determine its taxonomic affinities.

MATERIALS AND METHODS

The holotype (PVL 2073) and referred materials (PVL 2052; PVL 2059) of *Aetosauroides scagliai* from Argentina were examined first hand. The material was photographed and measurements taken with digital calipers. The holotype of *Aetobarbakinoides brasiliensis* (CPE2 168) was also studied first hand. Although extensive notes were taken on all specimens only the cranial material is described below. The postcranial material was used to score the taxon in the phylogenetic analysis (Chapter 6) and may be described elsewhere.

A third skull (PVSJ 326) assigned to *Aetosauroides scagliai* (Desojo and Ezcurra, 2011) features a well-preserved braincase but is in need of further preparation. This

specimen was also used to score the phylogenetic analysis and may also be described elsewhere if the specimen is prepared further.

SYSTEMATIC PALEONTOLOGY

Archosauria Cope, 1869 *sensu* Gauthier and Padian, 1985

Pseudosuchia Zittel, 1887-90 *sensu* Gauthier and Padian, 1985

Aetosauria Marsh, 1884 *sensu* Parker, 2007

Aetosauroides Casamiquela, 1960

Aetosauroides scagliai Casamiquela, 1960

(Figs. 3.1 – 3.4)

1960 *Aetosauroides scagliai*: Casamiquela, p. 2, figs. 1-2.
1961 *Aetosauroides scagliai*: Casamiquela, p. 4, figs. 1-26, pl. 1.
1967 *Aetosauroides scagliai*: Casamiquela, p. 173, figs. 1-3, pls. I-XV.
1971 *Aetosauroides scagliai*: Bonaparte, p. 671, figs. 15, 16.
1982 *Aetosauroides*: Bonaparte, p. 108, fig. 4d.
1985 *Aetosauroides inhamandensis*: Barbarena et al., p. 14.
2000 *Stagonolepis robertsoni*: Heckert and Lucas, p. 1552, fig. 4d.
2002a *Stagonolepis robertsoni*: Heckert and Lucas, p. 852, figs. 2-4.
2011 *Aetosauroides scagliai*: Desojo and Ezcurra, p. 596, figs. 2-6, 7a, 8.

Holotype: PVL 2073, partial postcranial skeleton including the majority of the dorsal carapace, vertebral column, and sacrum in articulation (Casimiquela, 1961).

Referred Specimens: PVL 2052, partial skeleton including a natural mold of a portion of the skull; PVL 2059, partial skull and associated postcranial skeleton; PVSJ 326; partial skull and associated postcrania.

Age – Late Triassic, Carnian, *Hyperodapedon* Assemblage Zone (Rogers et al., 1993; Furin et al., 2006; Martinez et al., 2011).

Occurrence – Cancha de Bochas Member, Ischigualasto Formation, Argentina; Sequence 2, Santa Maria Supersequence, Rio Grande do Sul State, Brazil (Casimiquela, 1961; Desojo and Ezcurra, 2011).

DESCRIPTION

Skull

Cranial material is preserved in two specimens (PVL 2059; PVL 2052), which together preserve much of the upper part of the skull and the jaws. Missing are the rear portions of both mandibular rami, the jugals, quadratojugals, quadrates, and squamosals, as well as the braincase. The maxillae, premaxillae, nasals, and postorbitals are incomplete. Some of the elements in PFV 2059 are distorted by crushing and/or have been incompletely prepared. PVL 2052 contains the natural mold of the antorbital, external nares portion of the right side of a much larger skull as well as a portion of the mandible. These specimens were previously described by Casamiquela (1967) and discussed by Heckert and Lucas (2002a) and Desojo and Ezcurra (2011).

Overall the dorsal surface of the skull of PFV 2059 is well-preserved and free from distortion (Figure 2.1). The dorsal surface descends gradually from the parietals to the premaxillae as in *Aetosaurus* (Schoch 2008, fig. 8). Some dorsoventral crushing has occurred, but in general the skull appears to have been very long and shallow with an

estimated length of about 190mm compared to a depth of about 50mm. The skull is widest at the anteriormost point of the frontals, tapers significantly anteriorly, and is slightly reduced posterior to that point, thus the parietals are equal to or just slightly narrower than the frontals. The skull roof is smooth and devoid of ornament in PVL 2059; however, this is most likely an artifact of preparation as many of the bones in PVL 2059 and PVL 2072 have been ground smooth. PVL 2052 preserves the impression of the surface of the skull roof, which is rugose, as is typical for aetosaurians (Figure 2.2). A reconstruction of the skull is provided in Figure 2.3.

Premaxilla

The posterior portions of both premaxillae are preserved in PVL 2059 (Figure 2.1). They are slender and elongate. The posteriormost portion tapers rapidly overlying the anterior portion of the maxilla and contacting the descending ramus of the nasal and slightly underlying it; thus the maxilla is excluded from participation in the margin of the external naris (Figures 2.1, 2.3). The posterior portion of the premaxilla bears teeth although the exact number is difficult to determine, although Heckert and Lucas (2002a) noted that five premaxillary teeth were present. This is a plausible number as I can see the remnants of four teeth and there is a spot for a fifth alveolus although it is covered by matrix and glue. Further preparation would help elucidate this. The anterior portion of the premaxilla is edentulous as is typical for aetosaurs. As preserved the upper portion of the left premaxilla is 40 mm in length, the ventral portion is 25 mm long. At the thickest portion, where the toothed portion articulates with the maxilla, it is about 7 mm deep and the anteriormost portion is 4 mm deep. The right side has corresponding measurements of

45 mm, 17 mm, 6 mm, and 4 mm respectively. Ventrally the symphysis is 19 mm long and the joined premaxillae are 12 mm wide at the maxillary junction and 8 mm wide at the anteriormost preserved point which would be close to the anterior part of the external naris. As preserved the external nares are ovate but compressed dorsoventrally with rounded margins. The incomplete length is 45 mm and at its deepest point (above the premaxilla/maxilla ventral suture) the naris is 13 mm deep, thus it is elongate and shallow. The rapid anterior tapering of the nasal is important regarding the determination of the presence or absence of a lateral expansion of the distal end ('shovel') because this portion is missing (but see discussion below) as aetosaurs with tapering nasals tend to lack the anterior premaxillary expansion (e.g., *Aetosaurus ferratus*). The premaxilla lacks the small triangular projection into the ventral portion of the external naris that is present in *Desmatosuchus smalli* (Small, 2002) and *Stagonolepis olenkae* (Sulej, 2010).

Only the posteriormost tip of the premaxilla is unambiguously preserved in PFV 2052 (Figure 2.2); however, enough is present to show the articulation of the premaxilla and descending process of the nasal excluding the maxilla from participation in the margin of the external naris. The external nares are elongate and shallow in this specimen as well, about 60mm long and 15mm deep. PFV 2052 shows what could be bone at the distal end of the snout forming the anterodorsal margin of the external naris. A clear demarcation in the cast shows a separation of this possible element from the ventral border of the nasal, thus this could represent a laterally flared anterior end of the premaxilla as seen in other aetosaurs. Unfortunately it is impossible to tell from the cast or the mold if this is a bony feature.

Maxilla

Much of both maxillae are preserved in PVL 2059 and consist of three main parts, anterior, posterior and the ascending process (Figures 3.1, 3.3). The anterior portion tapers anteriorly and meets the premaxilla anteriorly and dorsally. The upper articulation is concave progressing posterodorsally to underlie the descending process of the nasal and forming the upper margin of the ascending process of the maxilla. The posterior portion is incomplete but appears to taper posteriorly. It forms the ventral margin of the anterior portion of the antorbital fenestra. Much of the dorsal portion is a smooth dorsally and posteriorly directed beveled area which represents a sizeable antorbital fossa and is separated from the main body of the maxilla by a sharp longitudinal ridge. Anteriorly this ridge curves dorsally onto the ascending process of the maxilla. The ventral border of the maxilla is straight and tooth bearing. The left ramus bears 10 alveoli, and the right has nine some still with fragmented teeth. Because the elements are incomplete the numbers were almost certainly higher. The alveolar surfaces are still covered in glue and matrix and many are filled with broken teeth. The presence or absence of unfused interdental plates cannot be confirmed. The left maxilla is 55 mm long as preserved and the right about 45 mm. Comparison with *Aetosaurus ferratus* suggests that as much as 35 mm may be missing from the right side if the element originally terminated below the anterior portion of the orbit. Thus the maxilla was very elongate and gracile.

The ascending process is preserved mainly on the left maxilla and extends dorsally and posteriorly meeting the nasal dorsally, the lacrimal posteriorly, and forming the dorsal margin of the anterior portion of the antorbital fenestra (Figure 3.3). The

antorbital fossa continues onto this portion and makes up almost the entire lateral surface. The large extent of the antorbital fossa differs from aetosaurs such as *Desmatosuchus smalli* (TTU P-9023) where the fossa is extremely reduced. The articulation of the maxilla with the lacrimal is steep and oblique, and directed posterodorsally. The length of the dorsal margin of the maxilla from where it meets the premaxilla at the tooth row to its posterior articulation with the lacrimal is 53 mm. The distance from the top of the ascending process ventrally to the tooth row is 22mm.

As preserved the length of the antorbital fenestra in PVL 2059 could not have been much more than 23 mm. The length of the antorbital fossa is much more sizeable at about 43 mm. The height of the fenestra is 10 mm and the fossa is 22 mm. In the larger specimen, PVL 2052, the antorbital length is 50 mm for the fenestra and 65 mm for the fossa, whereas the heights are 15 mm for the fenestra and 35 mm for the fossa. Thus the fossa makes up less of the surface in the larger individual and possibly represents an ontogenetic transformation. The margins of the maxilla are not complete enough in PVL 2052 for measurements to be taken, (but can be estimated to be at least 90 mm for the ventral margin and 73 mm for the dorsal) but the anatomy of the element including the orientation of the anterior lacrimal/maxilla contact are identical to that of PVL 2059. The distance from the top of the ascending process to the tooth row in PVL 2052 is 43 mm. This larger specimen has a small foramen in the lateral surface of the maxilla at the level of the tooth row.

Lacrimal

In PVL 2059 the lacrimal is best preserved on the left side where most of the element is present. The lacrimal is bounded dorsally by the nasal and the prefrontal which effectively separates it from contact with the frontal. It forms the dorsal and posterior margins of the posterior portion of the antorbital fenestra. The majority of the preserved portion consists of the lacrimal contribution to the antorbital fossa which is sizeable in aetosaurs. The posterior portion of the lacrimal is poorly preserved but present in a fragment that has broken away and shifted slightly posteroventrally. This fragment probably represents the area just dorsal to the maxilla-jugal contact. The upper suture with the nasal can also be clearly seen on the right side of the skull, although the right lacrimal is barely preserved. As preserved the left lacrimal is 27 mm long and the upper portion dorsal to the antorbital fossa is 11 mm high. The posterior ramus was at least 18 mm high.

Prefrontal

In PVL 2059 this element is best preserved on the left side, where it forms a distinct triangular tuber on the lateral side of the skull roof between the antorbital fossa and the orbit. In ventral view it is possible to make out the suture with the posterodorsal margin of the lacrimal; however, the ventral portion including the elongate descending process that backs the lacrimal is missing or buried in matrix. Dorsally the sutures with the nasal anteriorly and frontal posteriorly can be clearly seen. The outer surface is faintly marked with the rugose ornamentation typical of aetosaur skulls. Posteriorly the element

tapers along its contact with the frontal and where it forms the anterodorsal margin of the orbit. This element is 32 mm long. Only a sliver of the right prefrontal is preserved; however, in dorsal view it shows the articulations with the surrounding bones, including the lacrimal.

Nasal

In PVL 2059 the area where the frontal-nasal contact occurs is heavily damaged (Figure 3.1b); however, under magnification the suture can be seen in at least two places, just above the anterior process of the left prefrontal and along the skull midline, which corresponds with the position of the suture in *Aetosaurus* (Schoch, 2008). The nasals are elongate, narrow anteriorly, and broaden significantly posteriorly. At their anteriormost extent (as preserved) the conjoined nasals are 8mm wide whereas at the posterior margin just anterior to the prefrontals they are 30mm wide. The nasals form the dorsal and posterior margins of the external nares and posteriorly overlie the maxilla, lacrimal, and the anteriormost portion of the prefrontal. Notably there is a strong triangular depression in the posterior portion of each nasal that meets its antimere medially forming a larger very broad triangular depression (40mm long by 24mm wide) across the skull roof that opens posteriorly and is confluent with the dorsal surface of the nasals (Figures 3.1a, b). Thus the center of the skull roof above the antorbital fenestra is flanked on each side by a narrow raised, rounded ridge that originates dorsal to the descending process of the nasal and continues posteriorly to the posterior extent of the prefrontal, with the upper portion of the prefrontal representing a continuation of this ridge. The anterior portion of the

nasals are relatively smooth, whereas the posterior portions possess of dispersed punctuate ornamentation of elongated pits.

The descending process of the nasal is an anteriorly recurved, and thus hooked, extension of the ventral surface of the nasal that forms the posterior border of the external naris. In most aetosaurs this process terminates short of any contact with the posterior process of the premaxilla and the maxilla forms part of the narial margin. However, in *Aetosauroides* (PVL 2052, 2059) the descending process of the nasal and the posterior process of the premaxilla meet along an extremely short contact, excluding the maxilla from the margin of the external naris (Figures, 3.1, 3.2, 3.3). This is the plesiomorphic condition for Archosauriformes and an autapomorphy of *Aetosauroides*. This configuration was originally suggested by Casamiquela (1961), considered ambiguous by Heckert and Lucas (2002a), and later reaffirmed by Desojo and Ezcurra (2011). My observations conform those of Casamiquela (1961) and Desojo and Ezcurra (2011).

Frontals

Both frontals are well preserved in PVL 2059 although the anterior and posterior margins are difficult to discern (Figure 3.1b). The frontal/parietal suture is barely visible on the skull roof just dorsal to the remnant of the postfrontal. The estimated length of the frontals is therefore about 45mm. The dorsal surfaces of PVL 2059 are relatively smooth but marked with the sparse punctuate ornamentation found in the posterior portion of the nasals; however, this may be an artifact of preservation as the cast of PVL 2052 demonstrates that the skull roof was very rugose, typical for aetosaurs (Figure 3.2). The frontals form most of the dorsal margin of the orbits and are raised relative to the rest of

the skull roof forming a broad rounded dome at the skull apex. The orbit is at least 37 mm wide in PVL 2059 and proportionally large for this skull, suggesting that the specimen represents a young ontogenetic stage for this taxon.

Postfrontal

A very small portion of the left postfrontal is preserved in PVL 2059 along the posterodorsal margin of the orbit. It articulates with the frontal medially and anteriorly and with the pareietal medially and posteriorly. Posteriorly it meets the postorbital. Other than being present its poor preservation precludes any useful description.

Postorbital

In PVL 2059 a small portion of the dorsal process of the postorbital is present along the margin of the skull roof. It forms the anterior border of the anterodorsal margin of the supratemporal fenestra and borders the postfrontal anteriorly and the parietal medially.

Parietals

The parietals are present but poorly preserved in PVL 2059 (Figure 3.1a). Anterior osteoderms have shifted anteriorly covering much of the right parietal. The surface of the left parietal is better preserved but difficult to discern details of because of the rugosity of the surface. It is unclear whether *Aetosauroides* possessed the posteriorly protruding shelf for articulation with the anteriormost osteoderms; however, a small triangular projection on the left parietal just anterior to the osteoderms probably represents this shelf as in lateral view it is strongly offset from the descending parietal

flange. This flange is anteroposteriorly thin, posteriorly smooth, and forms the posterodorsal margin of the supratemporal fenestra. It should articulate ventrally with the posterior portion of the squamosal; however, the latter element is not preserved.

The supratemporal fenestra is exposed almost fully laterally as is typical for aetosaurs. The preserved upper margin shows that is was round or oval in outline and at least 24mm in diameter, much smaller than the orbit.

Laterosphenoid

An inset ridge of bone beneath the orbit in PVL 2059 probably represents the upper margin of the laterosphenoid. A mass of bone covered in matrix medial and posterior to this probably represents more of the otic capsule of the braincase, but detailed preparation is needed to confirm this.

Dentary

Almost a complete right and much of the left dentary is preserved in PVL 2059 (Figures 3.1a, c). The right dentary is noticeably slender with a gently upward curving ventral margin in contrast to the sharp deflected margin found in many aetosaurs. The dentary measures 93mm in length with the symphysis making up more than half of this length (51mm). Two posterior projections bound an external mandibular fenestra. The dentary is tallest in this area (17mm). The outer surface possesses small ornament pits as well as a few faint elongate grooves. The posterior and anterior portions of the dentary are edentulous with 10 alveoli present in the midsection of the element. The second and third positions from the posterior end are the largest in diameter and the alveoli decrease diameter anteriorly. There are teeth in the fifth, sixth, and eighth positions from the front;

however, only the sixth tooth is complete. The alveoli are shallow, the teeth have a thecodont implantation, and the interdental plates are not fused.

A short, shallow groove is present in front of the anteriormost tooth position. Anterior to this groove is a slightly raised flat edentulous surface that extends anteriorly for the rest of the element length. The anterior tip of the dentary is oddly expanded dorsally and laterally (Figures 3.1a, c). Close examination shows that this expansion is real bone but it is unique to this specimen and any function currently unknown. The medial surface is rugose along the symphyseal area (Figure 3.1c). The Meckelian groove is not visible, being covered by what appears to be the splenial. The partial left dentary shows that the Meckelian groove is present, long and dorsoventrally shallow. The right dentary conforms in all aspects to the left except that it possesses 11 alveoli. There are broken teeth in the fifth and eighth positions from proximal end.

An impression of the outer surface of the right dentary is preserved in PVL 2052 (Figure 3.2). It provides no new details but reaffirms that the dentary is gracile, with a gently curved ventral margin and not 'slipper-shaped' as in other aetosaurs such as *Stagonolepis robertsoni* (Walker, 1961).

Splenial

What may be part of the splenial is covering the Meckelian groove on the inner surface of the right dentary in PVL 2059 (Figure 3.1c). Other than its possible presence no other details can be discerned.

Teeth

Both maxillary and dentary teeth are preserved in PVL 2059. Casamiquela (1961) described them as elliptical is cross-section with sharp, somewhat recurved apices. The maxillary tooth is indeed oval in cross-section, but is missing the distal tip. The base is covered in preservative and matrix and is in need of repreparation. The dentary teeth would benefit from further treatment as well. The best preserved dentary tooth is also oval in cross-section (medio-laterally compressed) and recurved. There is no indication of a swelling at the base of the crown. The posterior edge of the tooth crown is worn but there are three serrations visible along this edge and at least two more visible closer to the base. The serrations are small and measure 5 or 6 per mm. There is no evidence for a carina along the anterior tooth margin. This tooth also possesses longitudinal grooves or striations from base to apex.

DISCUSSION

The cranial material of *Aetosauroides scagliai* is important because it exemplifies the plesiomorphic aetosaurian skull condition, optimizing characters such as the exclusion of the maxilla from the external naris, the frontals being wider than the parietals, the nasals tapering anteriorly, the presence of a large triangular depression is present anterior to the frontals, the lack of a 'slipper-shaped' mandible, the lack of basal swelling of the tooth crowns, and the mediolaterally compressed teeth with recurved tips. It demonstrates conclusively that the skull is significantly different from that of *Stagonolepis robertsoni*, *Stagonolepis olenkae*, *Neoaetosauroides engaeus*, and *Calyptosuchus wellesi* and that characters of the osteoderms used to unite these taxa are

homoplasious (Desojo and Ezcurra, 2011; Parker 2008b). Finally, *Aetosauroides scagliai* cannot be utilized to correlate the Ischigualasto Formation with Adamanian age strata in North America, a finding further supported by recent radioisotopic dates (Irmis et al., 2011). This calls into question the reliability of the aetosaurian record to provide long-range intercontinental correlations of strata and emphasizes the strong need to provide independent support for hypothesized correlations using non-biostratigraphic methods such as high precision radioisotopic dates (Irmis et al., 2010).

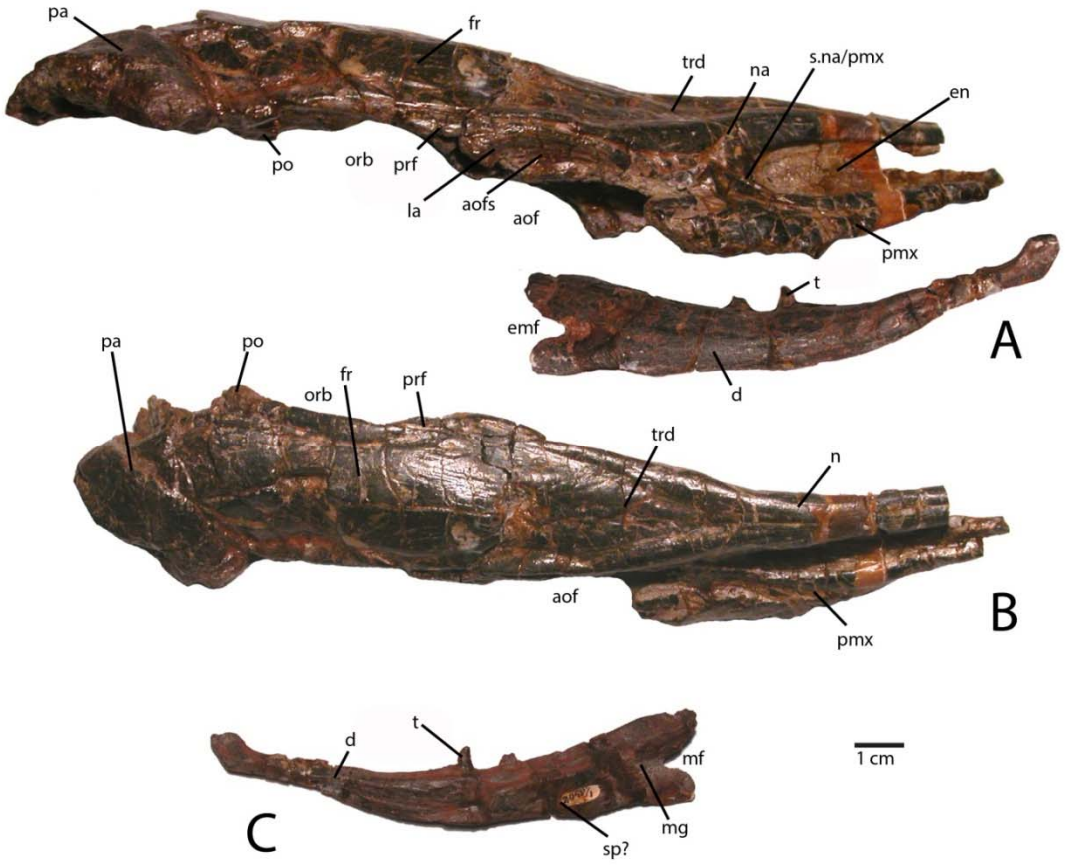

Figure 3.1. Partial skull of *Aetosauroides scagliai* (PVL 2059). A, cranium and associated dentary in right lateral view; B, cranium in dorsal view; C, right dentary in medial view. Scale bar equals 1 cm. Abbreviations: **aof**, antorbital fenestra; **aofs**, antorbital fossa; **d**, dentary, **en**, external naris; **fr**, frontal; **la**, lacrimal; **mf**, mandibular foramen; **mg**, Meckelian groove; **na**, nasal, **orb**, orbit, **pa**, parietal; **pmx**, premaxilla; **po**, postorbital; prf, prefrontal, **s.x/x**, suture between listed elements; **sp**, splenial; **t**, tooth; **trd**, triangular depression.

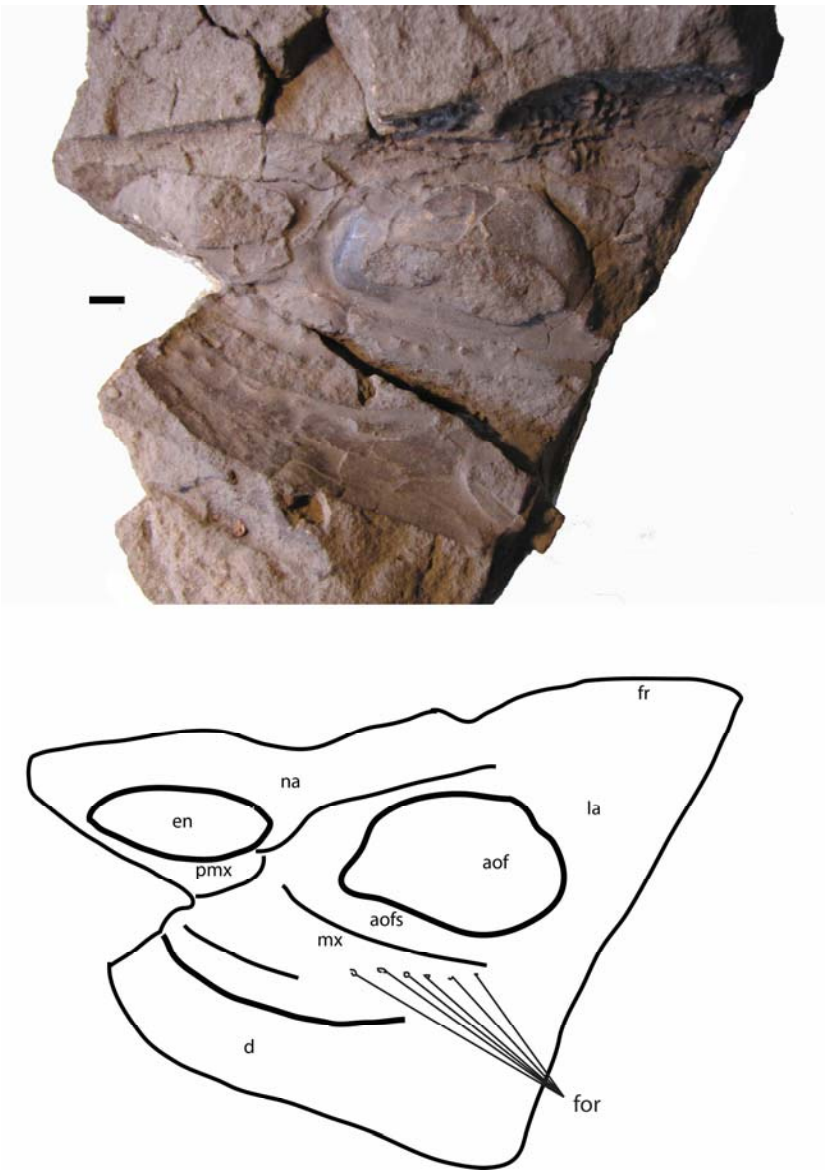

Figure 3.2. Photo of a sandstone block with a natural mold of much the right side of the skull of *Aetosauroides scagliai* (PVL 2052) with an interpretive drawing. Scale bar equals 1 cm. Abbreviations **aof**, antorbital fenestra; **aofs**, antorbital fossa; **d**, dentary; en , external nares; **for**, foramina; **fr**, frontal; **la**, lacrimal; **mx**, maxilla; **na**, nasal; **pmx**, premaxilla.

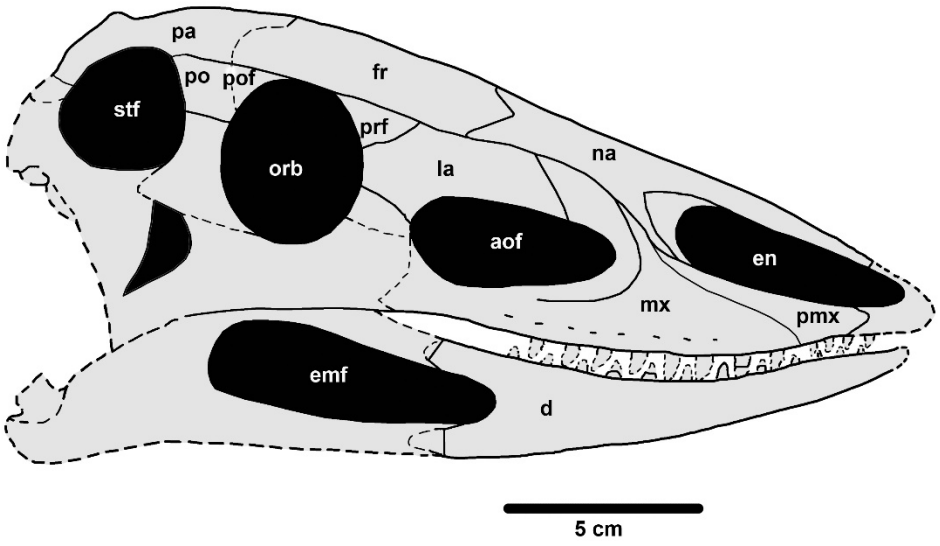

Figure 3.3. Skull reconstruction of *Aetosauroides scagliai*. Dashed lines indicate broken. Missing elements. Redrawn from Desojo and Ezcurra 2011.

CHAPTER 4: REDECRIPTION OF *CALYPTOSUCHUS WELLESI* FROM THE LATE TRIASSIC OF THE SOUTHWESTERN UNITED STATES

INTRODUCTION

In 1931 Ermine Cowles Case of the University of Michigan discovered a well-preserved articulated partial carapace with an associated vertebral column and pelvis of an aetosaurian in Upper Triassic strata of the Texas Panhandle. Although described in detail, the taxonomic affinities of the specimen were considered enigmatic and the material was assigned only to Phytosauria (Case, 1932).

The same year Charles Lewis Camp of the University of California at Berkeley began excavating a vast deposit of bones in the Upper Triassic Chinle Formation of Arizona at a site he christened the *Placerias* Quarry because of the large number of bones of the dicynodont *Placerias gigas* (=*Placerias hesternus*) he recovered there. In addition Camp recovered a large number of aetosaurian 'skin plates' as well as portions of the endocranial skeletons of dozens of individuals. In 1935 comparison of this material to that of *Stagonolepis robertsoni* from the Elgin Sandstone (now the Lossiemouth Sandstone Formation) of Scotland led Camp to believe that much of his Arizona material represented a very similar animal possibly of the same genus (C. L. Camp, unpublished notes, 1935). Unfortunately Camp never published descriptions or taxonomic notes regarding these specimens, only referring them in passing to "*Typothorax*" (as in *Longosuchus meadei*) and "*Episcoposaurus*" (as in *Desmatosuchus spurensis*) (Camp and Welles, 1956:259).

Both the Texas and Arizona material remained undescribed until the material was restudied as part of a field investigation of the Triassic of Arizona by crews from the UCMP (Long and Ballew, 1985). It was named *Calyptosuchus wellesi* in the mid-1980s

and Case's specimen was designated as the holotype of the new taxon (Long and Ballew, 1985). The genus name was only used for a very short time before it was noted again that the material appeared to be very similar to that of *Stagonolepis robertsoni*, and was reassigned to the genus *Stagonolepis*, as *Stagonolepis wellesi* (Long and Murry, 1989). *Stagonolepis wellesi* was differentiated from *Stagonolepis robertsoni* by the presence of short horns on the cervical lateral osteoderms (Long and Ballew, 1985; Long and Murry, 1995); however, these were later demonstrated to belong to a previously unrecognized paratypothoracin aetosaur that was present in the *Placerias* Quarry, probably *Tecovasuchus* (Parker, 2005a). Thus, specific characters to diagnose *Stagonolepis wellesi*, exclusive of other aetosaurians, are lacking. Initial comparisons of the dorsal osteoderms with those of *Stagonolepis robertsoni* for this study revealed strong differences (see discussion below) and the use of *Calyptosuchus wellesi* for the American material is recommended (e.g., Parker, 2008a; Parker and Martz, 2011; Desojo et al., 2013).

Scoring *Calyptosuchus wellesi* into a phylogenetic analysis is challenging because the holotype consists of the articulated carapace from just anterior to the pelvic region back through the middle of the tail and lacks both limb and cranial material. Furthermore, the specimen was set in plaster and mounted upright behind heavy glass in the UMMP. The associated vertebral column and pelvis were separated from the osteoderms and are presently in poor condition (W. Parker, pers. obs., 2000).

Besides Case's (1932) description of UMMP 13950 and his descriptions of an isolated pelvis and associated vertebrae (UMMP 7470; Case, 1922, 1929), *Calyptosuchus wellesi* has never been adequately described. The initial study in which the taxon was named only provides a general list of characters of the osteoderms (Long and Ballew, 1985). Superficial descriptions of various referred endoskeletal elements were provided

by Long and Murry (1995), who did not redescribe the type or referred osteoderms in more detail.

The largest collection of material referred to *Calyptosuchus wellesi* is from the *Placerias* Quarry and potentially contains bones from most portions of the skeleton including a few isolated skull bones and basicrania (see below). Long and Murry (1995) referred much of this material to *Calyptosuchus*; however, most of the elements have received unique catalogue numbers and any original association has been lost. Furthermore, Camp and Welles (1956) stated that little of the material was associated. Thus, it is not clear on what basis the endocranial material was assigned to *Calyptosuchus* by Long and Murry (1995). However, it is known that disarticulated specimens from the quarry fit together perfectly demonstrating that they belong to the same individual. The best example from the quarry is are five elements (UCMP 25962, right ilium, UCMP 25974, left ilium, UCMP 25999, pubis, UCMP 25993, ischium, UCMP 78719, sacral vertebrae), which can be combined to reconstitute a nearly complete pelvis of *Poposaurus gracilis* (Long and Murry, 1995:figs. 151, 153). The quarry also contains associated pelvic and limb material from a single individual of *Calyptosuchus wellesi* (Long and Murry, 1995:fig. 79), which is discussed in more detail below.

Fortunately, the collectors at the *Placerias* Quarry excavated utilizing a grid system (Camp and Welles, 1956) and physically marked the grid of collection in permanent ink on many of the bones. These numbers can be matched to the published quarry map (Camp and Welles, 1956:fig. 2), and although the exact placements of each bone have not been preserved, the numerous smaller grids measure about 2.25 square meters and the largest about 9 square meters (Camp and Welles, 1956), allowing for some degree of association to be estimated. With the exception of a few endocranial elements discussed in the text, only the osteoderm material can be assigned with any

certainty to the genera *Calyptosuchus* and *Desmatosuchus*. I created a spreadsheet listing all of the material (over 1000 specimens) assigned these taxa by Long and Murry (1995) along with the associated field/grid number when available. I then sorted these data by field/grid to look for potential associated specimens. The element types were then plotted onto the quarry map with the exception of the majority of the numerous caudal centra, which I find indeterminate to genus or species (Figure 4.1). No other aetosaurians were recognized in the plotted osteoderm sample even though rare paratypothoracin lateral osteoderms are recognized from collections from the area made at later dates (Parker, 2005a). Thus, I consider all of the material referable to *Calyptosuchus* or *Desmatosuchus* with the caveat that the slight possibility does exist that some of the endoskeletal bones could represent this extremely rare paratypothoracin.

Plotting the sorted data shows large accumulations of *Calyptosuchus wellesi* osteoderms in grids C71S and C72S, as well as in C64M and C65M. *Desmatosuchus spurensis* osteoderms are accumulated particularly in C75W, C64, and C62M. Thus there is some distinction between large accumulations of osteoderms of these taxa and it is possible that these associations could represent single individuals. This information was used to make suggestive referrals of material to *Calyptosuchus wellesi* and is discussed in more detail in the following description. Unfortunately there is no way to calculate a genuine minimum number of individuals for each taxon; however there are 14 aetosaurian basicrania in the overall sample (including three that lack field numbers). Numerous endoskeletal elements in CD1, CD2, CE1, CE2, CF1, CF2 are associated with very few osteoderms presenting a potentially interesting taphonomic question; however,

Camp and Welles (1956:259) note that in this portion of the excavation "most of the numerous isolated dermal scutes of *Typothorax*, as well as broken ribs and other fragmentary material, were not collected". Thus the majority of osteoderms in the sample was collected in 1931 from the west side of the quarry and in 1932, during excavation of the east side, the osteoderms were ignored. This is reflected in the plotted data (Figure 4.1). Note that by listing "*Typothorax*", Camp and Welles (1956) were actually referring to *Calyptosuchus*, although they are may also be using this name to encompass all of the paramedian osteoderms.

SYSTEMATIC PALEONTOLOGY

Archosauria Cope, 1869 *sensu* Gauthier and Padian, 1985

Pseudosuchia Zittel, 1887-90 *sensu* Gauthier and Padian, 1985

Aetosauria Marsh, 1884 *sensu* Parker, 2007

Stagonolepididae Lydekker, 1887 *sensu* Heckert and Lucas, 2000

Calyptosuchus Long and Ballew, 1985

Calyptosuchus wellesi Long and Ballew, 1985

(Figs. 4.2 - 4.18)

1922 Phytosaur: Case, p. 73, fig. 28b.
1929 Phytosaur: Case, p. 49, fig. 21.
1932 *Phytosaurus*?: Case, p. 57, figs. 1-6, pl. 1-3, pl. 4, fig. 1.
1953a *Typothorax*: Gregory, p. 13.
1953a *Desmatosuchus haplocerus*: Gregory, p. 15.
1961 Unnamed aetosaur: Walker, p. 157
1961 *Desmatosuchus haplocerus*: Walker, p. 181.
1961 *Typothorax*: Walker, p. 184.
1962 *Phytosaurus*: Gregory, p. 682.

1985 *Calyptosuchus wellesi*: Long and Ballew, p. 47, figs. 13b, 14b, 15-16, pl. 4-5. [non fig. 13a, 14a (= *Scutarx deltatylus*)].
1986 *Calyptosuchus*: Long and Padian, p. 165.
1986 *Calyptosuchus*: Parrish and Carpenter, p. 158.
1986 *Calyptosuchus wellesi*: Murry, p. 123.
1988 *Calyptosuchus wellesi*: Long and Houk, p. 50.
1989 *Stagonolepis wellesi*: Murry and Long, p. 32.
1995 *Stagonolepis wellesi*: Long and Murry, p. 1, figs. 68-70, 71a, c, d, 72a, c-d, f-g, 73-77, 79-81, 83-84. [non figs. 71b, 72b, e (=*Scutarx deltatylus*), 71e-f (=Paratypothoracini), 78, 82 (=Stagonolepididae)].
1996a *Stagonolepis wellesi*: Lucas and Heckert, p. 70.
1996b *Stagonolepis wellesi*: Lucas and Heckert, p. 60, fig. 4 (in part). [non fig. 4 (in part) (=*Scutarx deltatylus*)].
1997 *Stagonolepis*: Heckert and Lucas, p. 14.
1997 *Stagonolepis wellesi*: Lucas et al., p. 40.
1998b *Stagonolepis wellesi*: Lucas, p. 366, fig. 11b (in part). [non fig. 11b (in part) (=*Scutarx deltatylus*).
2000 *Stagonolepis wellesi*, Heckert and Lucas, p. 1543, figs. 4a-b
2002b *Stagonolepis wellesi*, Heckert and Lucas, p. 12.
2005a *Stagonolepis wellesi*: Heckert et al., p. 23.
2005a *Stagonolepis wellesi*: Parker, p. 38.
2005 *Stagonolepis wellesi*: Parker and Irmis, p. 50. [non fig. 4a (=*Scutarx deltatylus*)].
2005 *Stagonolepis wellesi*: Irmis, p. 77, fig. 6e.
2006 *Stagonolepis wellesi*: Parker, p. 47.
2007 *Stagonolepis wellesi*: Parker, p. 54.
2008 *Desmatosuchus haplocerus*: Lucas and Connealy, p. 26.
2010 *Stagonolepis*: Lucas, p. 464.
2011 *Calyptosuchus wellesi*, Parker and Martz, p. 240, fig. 3.
2013 *Calyptosuchus wellesi*: Desojo et al., p. 206.

Holotype – UMMP 13950, partial articulated skeleton consisting of the osteoderms of the posterior dorsal series through the mid-caudal region, the associated partial vertebral column and the sacrum (Case, 1932).

Referred Specimens – UMMP 7470, mostly complete pelvis with associated posterior trunk vertebrae and paramedian osteoderms; UCMP 27225, dentary fragment, dentigerous bone fragment, cervical centra, paramedian, lateral, and ventral osteoderms.

Much material from near St. Johns, Arizona is referable to *Calyptosuchus wellesi* (see description below).

Locality, Horizon, and Age – Blue Mesa Member, Chinle Formation, Arizona; Tecovas Formation, Dockum Group, Texas. Adamanian biozone, early Norian.

Revised Diagnosis – Characters shared with *Scutarx deltatylus*: medium (less than four meters length) sized aetosaur with large knob-like dorsal eminences that contact the posterior margin of the dorsal and caudal paramedian osteoderms; moderate width/length ratios of the dorsal trunk paramedian osteoderms; strongly radial pattern of ridges and furrows on paramedian osteoderms; anterolateral and anteromedial projections of the anterior bar of the paramedian osteoderms; triangular projection of the anterior bar anterior to the dorsal eminence on the dorsal trunk paramedian osteoderms; dorsal paramedian osteoderms with a 'scalloped' anterior margin of the anterior bar between the medial edge and the anterior triangular projection; dorsal trunk paramedian osteoderms with a weak ventral strut; cervical vertebrae are keeled ventrally; trunk vertebrae lack hyposphene -hypantrum articulations; base of the postzygapophyses of the trunk vertebrae bearing a posterior projection that rests upon the ventral bar of the prezygapophyses; neural spines taller than the centra in the mid-trunk vertebrae. Differs from *Scutarx deltatylus* in that the cervical and dorsal trunk paramedian osteoderms lacks a pronounced triangular protuberance in the posterolateral corner; dentary with nine tooth positions (*unknown in Scutarx deltatylus*).

DESCRIPTION

Cranial bones

The only skull bone unambiguously referable to *Calyptosuchus wellesi* is a partial right dentary from UCMP 27225, which was neither mentioned nor described by Long and Ballew (1985) or Long and Murry (1995). This partial dentary is missing all of the anterior portion as well as the posterior articulations with the angular and surangular (Figure 4.2a). The element is slightly crushed and still covered in part by a hematite crust, but many details can be discerned. Overall the element is dorsoventrally shallow and possesses the sharp inflexion on the ventral margin of the dentary described by Desojo and Ezcurra (2011) as present in *Desmatosuchus smalli*, *Stagonolepis robertsoni*, and *Neoaetosauroides engaeus*, and as lacking in *Aetosauroides scagliai*. The medial surface is inscribed by an elongate, tapering Meckelian groove, which extends anteriorly to the level of the third alveolus (Figure 4.2b). The anteroventral corner of the medial surface bears a rugose patch that represents the beginning of the dentary symphysis. The occlusal surface is slightly concave, edentulous anteriorly and preserving nine oval alveoli posteriorly. The alveoli are closely spaced and slightly imbricated (Figure 4.2c). No complete teeth are preserved although root fragments are present in some of the alveoli. A second dentigerous fragment in UCMP 27225 bears five alveoli and represents a portion of the maxilla.

There are numerous aetosaur frontals and parietals in the UCMP collection from the *Placerias* Quarry, but none can be referred with certainty to *Calyptosuchus*. There are

also approximately nine basicrania in the same collections. Two (UCMP 27414, UCMP 27419) possess anteroposteriorly elongate basisphenoids with divergent basipterygoid processes. These differ significantly from those of *Desmatosuchus* (TTU P-9023; UMMP 7476) and may belong to *Calyptosuchus*; however, this cannot be presently ascertained.

There are also two maxillary fragments that also differ in morphology from known specimens of *Desmatosuchus* (e.g., TTU P-9024; UMMP 7476) in possessing a distinct antorbital fossa delineated ventrally and anteriorly by a sharp rim (Figure 2-3). The first (UCMP 195193) is a fragment of a right maxilla which preserves the main body ventral to the anterior portion of the antorbital fossa including the base of the ascending process of the maxilla (Figure 2.3a-c). The lateral face is divided into two sections by a sharp horizontal ridge that forms the ventral border of the antorbital fossa. Anteriorly this ridge forms a broad dorsally sweeping curve that extends up onto the ascending process of the maxilla. A similar ridge is present in *Stagonolepis olenkae* (Sulej, 2010), *Aetosauroides scagliai* (PVL 2073), *Stagonolepis robertsoni* (Walker, 1961), and *Revueltosaurus callenderi* (PEFO 34561), but is absent or extremely weak in *Desmatosuchus* (e.g., TTU P-9024) and *Longosuchus meadei* (TMM 31100-98). In *Stagonolepis olenkae* the ventral portion is not as deep and as a result the ridge does not split the main body of the maxilla in two equal portions. This maxillary fragment is missing the anterior and posterior portions as well as the majority of the ascending process and as preserved has a length of 45.7 mm and a height of 36.8 mm. The height from the ventral margin to the antorbital fenestra is 18.2 mm. The margin of the antorbital fenestra is thin. The fenestra was longer than high, and ovate in outline. The

contact with the nasal is preserved as a shallow, concave groove with a sharp, medial ridge (s.na, Figures 2.3a-b). In lateral view this groove slopes anteroventrally.

In ventral view the anterior portion of the maxillary fragment is mediolaterally crushed. Four complete and part of a fifth alveoli are preserved. The third alveolus (from the front) preserves an unerupted tooth but no further details can be made out. Interdental plates are present, but unfused (Figure 2.3c). Medially there is a transverse ridge above the tooth row for articulation with the palate and forms a broad shelf bordering the antorbital fenestra (sh, Figure 2.3b). There is a marked foramen (corresponding to the pneumatic accessory cavity of Small, 2002) at the anteroventral corner of the antorbital fenestra, which is visible medially and dorsally. The anterior portion of the maxillary body is concave and a small ridge marks about where the upper border of the antorbital fenestra would be located. Dorsal to this is another smooth concave area.

The second specimen (UCMP 195194) is also from the right side and therefore from a different individual (Figure 2.3d-e). The anterolateral surface below the antorbital fossa is slightly rugose. The 'pneumatic accessory cavity' (Small, 2002) is visible in medial view and has possibly been enlarged by preparation. Anteriorly the nasal articulation is preserved and similar to the first specimen. Anterior to this is a thin rim of bone that represents the posteroventral margin of the external naris. Thus the maxilla enters the naris, differing from the condition in *Aetosauroides scagliai* (PVL 2073), where a thin contact of the premaxilla and the nasal exclude the maxilla from the margin of the external naris (Casimiquela, 1961; Desojo and Ezcurra, 2011). On the medial

surface, a sharp raised ridge is preserved anteriorly that represents the palatal process of the maxilla. Only three alveoli are preserved in this fragment.

Despite the strong possibility of these cranial elements belonging to *Calyptosuchus wellesi*, they should not be used to code phylogenetic characters until they can be assigned with absolute certainty.

Postcrania

Atlas/Axis

There are many axes in the collection from the *Placerias* Quarry. Case (1922) describes the ventral surface of the axis in *Desmatosuchus spurensis* as flat, and most of the specimens in the collection possess flat ventral surfaces. However, UCMP 139803 (from CF1) has a distinct ventral keel (Figure 4.4a) and therefore mostly likely is referable to *Calyptosuchus wellesi* which has keeled cervical vertebrae (e.g., UCMP 27225) rather than *Desmatosuchus spurensis* which has cervicals with a smooth ventral surface (e.g., UMMP 7476; MNA V9300). The upper portion of the neural arch, including the zygapophyses, is broken (Figures 4.4b-d). The altantal neural arches are also broken . The centrum of the axis has distinct concave sides that are overhung by a thickened ridge, which bears the diapophyses (Figure 4.4d). The parapophyses are situated anteroventrolaterally on the centrum and are connected ventrally by a thickened crescentic ridge that forms the anterior portion of the atlas intercentrum (Figure 4.4a). The suture between the atlas intercentrum and the axis centrum is visible in ventral view.

The parapophyseal facets are round and directed ventrolaterally and slightly posterior. The odontoid process is attached (Figure 4.4a-b, d-e); its sutures with the

centrum are still visible so the fusion is not complete. The dorsal surface of the odontoid process forms a slightly concave trough that opens posteriorly into the neural canal (Figure 4.4e). The canal is large, about one half the diameter of the posterior articular face of the centrum. In posterior view, the articular face of the centrum has a flat (horizontal) dorsal margin. The face is concave with well-developed rims. The length of the atlas/axis including the odontoid process is 48.7 mm. The axis centrum has a width of 30.6 mm and a height of 25.4 mm.

Postaxial cervical vertebrae

Numerous vertebrae were recovered in grid square CF1, where the atlas/axis (UCMP 139803) was recovered, including several cervical vertebrae. These centra possess cervical keels and therefore cannot be referred to *Desmatosuchus* (Long and Murry, 1995). Here they are assigned to *Calyptosuchus*. The presence of ventral keels on the cervical centra of *Calyptosuchus* is verified by specimen UCMP 27225. Long and Murry (1995:fig. 74) figured what presumably they thought to represent a cervical series of *Calyptosuchus*, but unfortunately did not provide explicit specimen numbers to identify the specimen further and it could not be located for the current study.

The cervical vertebrae of *Calyptosuchus* are amphicoelous, the anterior face being anteriorly concave and the posterior face nearly flat. Both faces are oval and taller than wide. On the anterior cervicals (e.g., UCMP 139793, 139794) the small, subrounded parapophysis is situated at the base of the centrum (Figures 4.4f-i). On more posterior centra (e.g., UCMP 139813) the parapophysis is located closer to the top of the centrum, below the neurocentral suture (Figures 4.4j-m). Anterior cervicals are also

anteroposteriorly shorter than the posterior cervicals (Figures 4.4h, k). The ventral keel is well developed and in some specimens (e.g., UCMP 78714) the keel is expanded posteriorly into a small tab (Figures 4.4n, o). UCMP 78714 also preserves a portion of the neural arch. Although crushed and distorted it shows that the zygapophyses were elongate (Figure 4.4p). Prezygadiapohyseal and postzygadiapophyseal laminae (*sensu* Wilson, 1999) are present.

Trunk vertebrae

The trunk vertebrae of *Calyptosuchus* are more difficult to identify than the cervical vertebrae from the mixed collection of material from the *Placerias* Quarry; however, there are vertebrae with more elongate neural spines that also lack typical accessory articulations (hyposphenes-hypantra) on the neural arch. This readily distinguishes them from the trunk vertebrae of *Desmatosuchus spurensis* which possess much shorter (dorsoventrally) neural spines as well as hyposphenes and hypantra (Parker, 2008b). The trunk centra of *Calyptosuchus* lack the lateral fossae present in *Aetosauroides scagliai* (Desojo and Ezcurra, 2011). There are also posterior trunk vertebrae preserved in the holotype (UMMP 13950; Case, 1932).

UCMP 139694 is most likely the 10th presacral (first trunk) vertebra as it is transitional in the position of the parapophysis between the cervical and trunk series (Figures 4.5a-b). The parapophysis is situated on the anterodorsal surface of the centrum and confluent with the transverse process, connected by a well-developed anterior centrodiapophyseal lamina (acdl; *sensu* Wilson, 1999). In *Desmatosuchus spurensis* this specific placement of the parapopohysis occurs in the 10th presacral position and in the

following vertebra (11th presacral) the parapophysis moves onto the transverse process (Case, 1922; Parker, 2008b). The neural arch of UCMP 139694 also bears a posterior centrodiapophyseal lamina (pcdl) but it is not as well developed as the anterior centrodiapophyseal lamina (acdl). The joining of these two laminae forms a ventrolaterally opening shallow triangular fossa situated ventral to the transverse process. A postzygadiapophyseal lamina (podl; Wilson, 1999) is developed as a well-developed thin ridge of bone connecting the transverse process and the postzygapophysis. The centrum is spool-shaped, amphicoelous, ventrally smooth, and measures 37.9 mm in length (Figure 4.5b). The centrum also has a height of 31.8 mm and a width of 31.6 mm.

UCMP 139796 from CF1 (Figures 4.5c-h) has the typical amphicoelous, spool-shape found in aetosaurs and represents a mid-trunk vertebra. The centrum measures 43.4 mm in length, with a height of 35.4 mm and a width of 32.4 mm; thus the lengths of the centra increase along the trunk portion of the vertebral column similar to *Desmatosuchus spurensis* (Parker, 2008b). The articular faces of the centrum are nearly flat, with expanded rims (Figures 4.5c-d). The neural arch is taller than the centrum articular faces and the oval neural canal is large (19.4 mm high) (Figure 4.5e). In right lateral view the transverse process is mostly broken away (Figure 4.5d), but a thick strut originates on the posterolateral corner of the neural arch and terminates on the ventral surface of what is left of the transverse process. This strut represents the posterior centrodiapophseal lamina (pcdl). A postzygadiapophyseal lamina (podl) forms a shelf from the posterior edge of the transverse process to the right postzygapophysis. A shallow postzygapophyseal centrodiapophyseal fossa (*sensu* Wilson et al., 2011) opens posterolaterally, formed by

the junction of these two laminae (Figure 4.5d). Although the posterior portion of the neural arch is broken it is clear that there is no deep hyposphene between the postzygapophyses as in *Desmatosuchus* (MNA V9300). The postzygapophyses are not steeply inclined, instead projecting at about 30 degrees above horizontal. The postzygapophyses project well posterior to the posterior face of the centrum (Figure 4.5f). Anteriorly on the neural arch there is a deep round fossa between the prezygapophyses and the neural spine, the spinoprezygapophyseal fossa (sprf, Wilson et al., 2011; Figure 4.5d). The neural spine is not anteroposteriorly elongate measuring only about 27mm at the base and the spinal laminae are present but weakly developed.

Another trunk vertebra from CF1 (UCMP 139702) preserves a few more details. In front of the anterior fossa (sprf) described for UCMP 139796, the prezygapophyses meet to form a broad shelf or ventral bar (Figure 4.5g) as in *Stagonolepis robertsoni* (Walker, 1961:fig. 7j). There is no hypantrum. The right transverse process is nearly complete. It is broad, about 26.7 mm in width, compared to the centrum, which has a width of 25.7 mm. The upper surface of the transverse process is flat and the ventral surface thickened with the strut described for UCMP 139796, which continues onto the base of the neural arch. The parapophysis is positioned 29.3 mm laterally from the origin of the transverse process. The distal end of the transverse process, the diapophysis, is not preserved but even incomplete the process has a length of 44.4 mm. The zygapophyses are inclined at close to 45 degrees to the horizontal. The centrum length is 39.9 mm long and 28.3 mm high.

A third trunk vertebra from CF1 (UCMP 139795) preserves the postzygapophyseal region extremely well. As with the other trunk vertebrae there are no accessory processes (hyposphene). Instead at the base of the medial union of the postzygapophyses there is a small posteriorly pointed projection that would rest on top of the ventral bar formed by the joined prezygapophyses of the subsequent vertebra. This pointed projection also occurs in *Scutarx deltatylus* (PEFO 34045). The ventral bar and posterior projection in the trunk vertebrae is also shared with some phytosaurians (e.g., *Smilosuchus*, TMM 43685-206).

Two other well preserved trunk vertebrae (Figure 2.6a-d) referable to *Calyptosuchus wellesi* are from UMMP 7470, which includes a partial sacrum and the two trunk vertebrae, as well as two paramedian osteoderms. The best preserved vertebra is a nearly complete anterior mid-trunk vertebra (Case, 1932: figs. 2-4). The centrum is laterally compressed and ventrally concave because of the flaring articular rims. It has a length of 48.7 mm, and width of 42.3 mm, and a height of 42.8 mm. The neural arch and spine are tall, twice the height of the centrum at 78.8 mm, with 55.2 mm for the neural spine height. The neural spine is mediolaterally thin, expanded anteroposteriorly (34.2 mm long) and terminates with a pronounced lateral expansion (spine table). The postzygapophyses extend posteriorly past the posterior articular face of the centrum and are oriented at 45 degrees above horizontal. The prezygapophyses form a flat plate almost indistinguishable from the transverse processes (Figures 4.6a, c). The transverse processes are broad with a flat dorsal surface, and nearly twice the width of the centrum (82.3 mm). The processes are of the typical aetosaurian arrangement with both rib

articulations situated on the transverse processes (Figures 4.6a, c). Transverse processes and postzygapophyses are connected by a thin sharp postzygapohyseal lamina (podl), which forms the deep spinopostzygapophyseal fossa (spof) just anterior to the postzygapophyses (Figures 4.6b, d).

Long and Murry (1995:fig. 75a) considered the transverse processes of the dorsal series extremely elongate throughout the entire column. However, they figured posterior trunk vertebrae of UMMP 13950 as an example, which have the ribs fused to the transverse processes, giving the appearance of greatly elongate processes (as noted by Case, 1932). This fusion of transverse process and rib is also found in *Scutarx deltatylus* (PEFO 34045) as well as *Desmatosuchus spurensis* (MNA V9300; Parker, 2008b). However, the processes in *Calyptosuchus wellesi* differ from those two taxa in that they are flat dorsoventrally and anteroposteriorly broad (Case, 1932: pl. 4, fig. 1). The centra of the posterior most trunk vertebrae are anteroposteriorly short in comparison with those of the mid-trunk vertebrae, with large flaring articular rims.

Sacral Vertebrae

The best preserved sacral vertebrae are in the holotype (UMMP 13950) as well as in the partial pelvis (UMMP 7470) and were well-described and figured by Case (1922, 1929, 1932). There are two vertebrae in the series, which differ from those of desmatosuchine aetosaurs in that they are not fused to each other (Parker, 2008b) although Case (1932) noted that the zygapophyses between the two sacral vertebrae were reduced in size. The articular faces of the centra are round. The neural arches are robust and bear the heavy,

expanded sacral ribs, and the neural spines are also robust and taller than the centra. The neural spines possess expanded apices or 'spine tables.'

An isolated specimen (UCMP 139785) from grid block C78W in the *Placerias* Quarry is most likely referable to *C. wellesi* as it does not show fusion to the other sacral as do others in the collection (e.g., UCMP 139787). The vertebra is very massive with the proximal portions of the sacral ribs firmly sutured to the neural arch (Figures 4.7a-d). The upper surface of the ribs is swept posteriorly (Figure 4.7b). The centrum faces are roughly 'heart-shaped' and the ventral surface lacks a keel (Figures 4.7c, d). The neural spine is broken off, but was obviously robust (thick and elongate) as in UMMP 7470. There is a distinct spinoprezygapophyseal fossa (Figure 4.7a) under the prezygapophyses.

Caudal Vertebrae

The *Placerias* Quarry collection contains dozens of aetosaur caudal centra with broken neural arches; however, at this time it is not possible the assign these elements to particular taxa. However, the first seventeen vertebrae of the caudal series of *Calyptosuchus wellesi* are well-preserved in articulation in the holotype (UCMP 13950) and were described by Case (1932). The most notable feature of the caudal series of UCMP 13950 is the height of the neural spines, which is greater than the height of the centrum. This differs from aetosaurs such as *Desmatosuchus spurensis* (MNA V9300) and *Paratypothorax* (PEFO 3004) where the height of the neural spine is equal to or less than the height of the centrum. It is similar to the condition in *Aetosauroides scagliai* (PVL 2073) and *Stagonolepis robertsoni* (Walker, 1961: fig. 10).

Long and Murry (1995:83) state that the ventral grooves of the caudal centra in *Calyptosuchus wellesi* are narrower than those of *Desmatosuchus spurensis* and "bear faint, longitudinal ridges". However, they provide no basis for their taxonomic referrals nor any specimen numbers, so this claim cannot be verified. The caudal ribs or transverse processes of paratypothoracins originate close to the base of the centrum (e.g., PEFO 3004). No centra with low caudal ribs are currently known from the *Placerias* Quarry, and thus all of the preserved centra presumably belong to *Calyptosuchus wellesi* or *Desmatosuchus spurensis* although they cannot be distinguished between those taxa.

Scapulocoracoid

No bones of the pectoral girdle are preserved in the holotype of *Calyptosuchus wellesi* (UMMP 13950). Long and Murry (1995) assign several scapulocoracoids (UCMP 78698, UCMP 32196, UCMP 27976) from the *Placerias* Quarry to *Calyptosuchus wellesi*; however these elements were recovered from areas CD and CE which provided many osteoderms of *Desmatosuchus spurensis* and none referable to *Calyptosuchus wellesi* (Figure 4.1). Furthermore, coracoids assigned to *Calyptosuchus wellesi* (UCMP 32196, UCMP 27976; Long and Murry, 1995) from C8 and C75W, also from areas that provided predominantly material of *Desmatosuchus* (Figure 4.1). Thus, none of the *Placerias* Quarry material can be unambiguously assigned to *Calyptosuchus wellesi*. Differences between the coracoids of *Desmatosuchus smalli* (TTU P-9023) and *Stagonolepis robertsoni* (Walker, 1961) pertain to the development of the subglenoid buttress. Unfortunately this area is not preserved in any of the *Placerias* Quarry specimens.

Forelimb

As with the shoulder girdle, no forelimb elements are present in the holotype of *Calyptosuchus wellesi* (UCMP 13950). Moreover, Long and Murry (1995) did not assign any forelimb material to *Calyptosuchus wellesi*. The UCMP *Placerias* Quarry collection contains numerous aetosaur humeri but none can be clearly referred to *Calyptosuchus wellesi*. All with preserved distal ends have an ectepicondylar foramen rather than a groove, which is a synapomorphy of *Desmatosuchus spurensis* and *Longosuchus meadei* (Small, 1985). Long and Murry (1995) reported a foramen as present in *Typothorax coccinarum* (UCMP 34240) and this was verified by Martz (2002). In *Aetosauroides scagliai* (PVL 2073) and *Stagonolepis robertsoni* (Walker, 1961) there is an ectepicondylar groove rather than a foramen on the lateral side of the radial condyle. Bonaparte (1971), Small (1985), and Martz (2002) stated that *Neoaetosauroides engaeus* possesses a foramen rather than a groove in the holotype (PVL 3525). Thus, the predicted condition in *Calyptosuchus* is equivocal and the distal ends of humeri from the *Placerias* quarry cannot be assigned with any certainty.

Pelvic Girdle

Several pelvic girdles have been referred to *Calyptosuchus wellesi* including the holotype (UCMP 13950; Figure 4.8), a specimen from the Dockum Group of Texas (UMMP 7470), and elements from the *Placerias* Quarry (Case 1929, 1932; Long and Murry, 1995). The *Placerias* Quarry elements include a left ilium (UCMP 32422) and a corresponding left ischium (UCMP 32148), both from grid CF1 (Figure 4.9a-b), and figured by Long and Murry (1995:figs. 79-80). The collection from CF1 also contains a

crushed, but complete right ilium (UCMP 25941) and a right ischium (UCMP 32153) (Figure 4.9c). These elements match the two figured by Long and Murry (1995) perfectly and all four elements probably belong to the same individual (Long and Murry, 1995). The difference in color between these elements in Figure 4.9 is a photographic lighting artifact. Grid CF1 contains a fair amount of material referable to *Calyptosuchus*, mainly cervical vertebrae, including some paramedian osteoderms, so referral of these pelvic elements to *Calyptosuchus wellesi* is supported.

The problem with assigning isolated ilia from the quarry to specific taxa is that the morphology of the ilium of *Desmatosuchus* is poorly understood. The holotype of *Desmatosuchus spurensis* (UMMP 7476) preserves only a fragmentary left ilium that is missing almost the entire posterior portion of the iliac blade. A referred specimen of *Desmatosuchus spurensis* (MNA V9300) as well a specimen of *Desmatosuchus smalli* (TTU P-9172) preserve nearly complete sacra; however, the anatomy of the ilia is difficult to interpret on these specimens because they are highly distorted, in part because of the complete fusion of the sacral ribs to the ilia (see Parker, 2008b). Long and Murry (1995:figs. 91-92) assigned an isolated right ilium from Crosby County Texas (UMMP 7322) to *Desmatosuchus spurensis*. This specimen possesses an acute angle between the anterior portion of the iliac blade and the anterior edge of the iliac body as well as a triangular (in lateral view) posterior iliac blade. The holotype ilium (UMMP 7476) as preserved is consistent with this although much of the anterior portion of the iliac blade is damaged. If UMMP 7322 is indeed referable to *Desmatosuchus spurensis* UCMP 32422 differs from it mainly in that the posterior iliac blade is squared off and not pointed as in

UMMP 7322. This is the character Long and Murry (1995) used to assign ilia to *Calyptosuchus wellesi* and this referral is followed here.

Ilium

The ilia in *Calyptosuchus wellesi* have ventrally directed acetabula; however, to make the following description easier to follow the element is described as if it is oriented vertically, thus the iliac blade is dorsal and the acetabulum ventral and lateral. The preacetabular process of the iliac blade in UCMP 25941 is short and does not extend far anterior of the pubic peduncle (Figures 4.9a-b). It is mediolaterally thick and triangular in lateral view with a ventrally curved tip and is 50 mm long. The postacetabular portion of the iliac blade extends well beyond the posterior edge of the pubic peduncle and is thickened very close to its proximal end. The entire iliac blade is 180 mm long, and 52 mm high above the acetabulum. The dorsal surface is highly rugose, marked with scars for the attachment of the *M. iliotibialis* 1-3 (Schachner et al., 2011). The acetabular area is roughly diamond-shaped in lateral view and delineated dorsally by a well-developed supraacetabular rim (Figure 4.9a). The main iliac body is slightly concave dorsal to the acetabulum, lacking the deep recess found between the supraacetabular rim and the posterior portion of the iliac blade in *Scutarx deltatylus*.

The pubic and iliac peduncles are thickened anteriorly and posteriorly respectively, and both are comma-shaped in ventral views. The two peduncles meet at a ventrally directed point ventral to the iliac portion of the acetabulum. Medially, there are scars for the two sacral ribs, which cover not only the iliac neck but also a large portion of the ilium ventral to the iliac blade and medial to the acetabulum (Figure 4.9b). This is

a result of the ventrally directed acetabula as in *Aetosauroides scagliai* (PVL 2073) and *Typothorax coccinarum* (PEFO 33967). The iliac blade thins dorsally from the sacral rib scars. Overall the ilium of *Calyptosuchus wellesi* is very similar to that of *Aetosaurides scagliai* (PVL 2073) and *Ebrachosaurus singularis* (Kuhn, 1936). It differs from *Neoaetosauroides engaeus* (PVL 3525) in having a much more robust anterior process of the iliac blade. It differs significantly from the ilium of *Typothorax coccinarum* (UCMP 122683) which has a taller, but anteroposteriorly shorter iliac blade, as well and a more gracile, and 'hooked' anterior process which does not extend anteriorly past the pubic peduncle (Long and Murry, 1995:figs. 106-107). The right ilium is well-preserved in the referred specimen UMMP 7470 (Case, 1922: fig. 28b). It is nearly identical to UCMP 25941 with the thickened, short, recurved anterior iliac blade. Both ilia are present in the holotype (UMMP 13950) but both are incomplete, crushed, and presently badly broken (Figure 4.8; Case, 1932, pl. II). Note that the photo of the pelvic girdle and vertebral column in Plate II in Case (1932) is reversed.

Ischium

The left ischium (UCMP 32148) associated with the UCMP ilium described above is nearly complete (Figure 4.9a). It is anteroposteriorly short, not much longer than tall, with a length of 110mm and a height of 97mm. This differs from the ischia of *Aetosauroides scagliai* (PVL 2073), *Stagonolepis robertsoni* (Walker, 1961); and *Aetosaurus ferratus* (Schoch, 2007), where the posterior process is more elongate. The pubic peduncle is comma-shaped in dorsal view and contacts the corresponding peduncle of the ilium. The oval acetabular surface is deeply concave and bordered posteriorly and

ventrally by a strongly raised, curved rim. The main body of the ischium is essentially a thickened 'rod' that curves posteriorly and dorsally. A mediolaterally thin flange of bone extends ventrally for the entire length of the 'rod' (Figure 4.9a). The ventral margin is straight. The lateral surface of the thin flange is rugose presumably for attachment of the third head of the *M. puboischiofemoralis externus* (Schachner et al., 2011). Medially there is an elongate suture for the opposing ischium. The anterior margin bears a distinct notch. This notch is also present on the right ischium of UMMP 7470. The posterior process of UMMP 7470 is more elongate than that of UCMP 32148, but still not as elongate as in Walker's (1961) reconstruction of *Stagonolepis robertsoni*. The ischia are also present in UMMP 13950 but are poorly preserved (Figure 4.8). Case (1932: pl. III) restores the ischium as dorsoventrally deep and anteroposteriorly short, consistent with UCMP 32148.

Pubis

The best preserved pubis from the *Placerias* Quarry material is a left element (UCMP 32150) from grid CF2 (Figures 4.9d-g). It shares the same preservation, color and size with the ilium and ischium described above, but does not quite articulate. The pubic rod is slender and its distal end is broken away (Figures 4.9d-e). The concave acetabular surface is reduced compared to the area on the ischium and there is a groove just ventral to this surface. The articular surface for the ilium is comma-shaped in dorsal view (Figure 4.9f). The obturator flange is broken away (Figure 4.9g) so the number of openings in this element cannot be determined. Walker (1961) restored the pubis of *Stagonolepis robertsoni* with two openings and a pubis of *Scutarx deltatylus* (PEFO

31217) also has two openings. Only a single opening is present in the pubis of *Desmatosuchus spurensis* (MNA V9300) and the number of openings is unknown in *Aetosaurus ferratus* (Schoch, 2007).

The proximal portion of the right pubis is present in UMMP 7470 (Case, 1922: fig. 28b). The posterior margin as preserved shows the anterior border of an obturator foramen but the element is not complete enough to determine if there was a second opening. The proximal head of UMMP 7470 bears a deep lateral groove that originates at the acetabular rim and extends parallel to the anterior margin of the pubis. The distal end of the element is broken away so that the extent of the groove cannot be determined. This groove is only weakly developed in UCMP 32150, which is also missing its distal end. UMMP 13950 preserves the distal end of the pubis, which expands into the broad pubic 'apron' typical for suchians (Case, 1932). Case (1932:pl. III) reconstructs the pubic as dorsoventrally shallow with the distal margin of the pubis at the same horizontal level as the ventral margin of the ischium. This differs greatly from the condition in *Desmatosuchus spurensis* (MNA V9300) where the pubis extends well below the level of the ischium, but is similar to the short pubes of *Typothorax coccinarum* (Long and Murry, 1995).

The distal end of the pubic rod extends slightly past the ventral margin of the pubic apron, as is typical for aetosaurs. This end is slightly swollen as in *Stagonolepis robertsoni* (Walker, 1961), but does not form the distinct knobby pubic boot found in *Desmatosuchus spurensis* (MNA V9300).

Femur

The best preserved femur that can be referred to *Calyptosuchus wellesi* is UCMP 25918, which is a left side element from CF1 (Figures 4.10a-d; Long and Murry, 1995:figs. 81, 83). It is of similar preservation and the right size to match the pelvic elements described above so it is very possible that all of these elements belong to a single individual. Long and Murry (1995) describe it as "more gracile" than femora from the quarry that they assign to *Desmatosuchus spurensis*. Overall it is less sigmoidal than the femur of phytosaurs, as is characteristic of aetosaurs (Figures 6.10a-c). It has a total length of 329 mm. The proximal head is badly eroded (Figures 4.10a-b). The fourth trochanter is a pronounced crescent-shaped ridge located about 120 mm ventral to the proximal end (Figure 4.10a). The distal femoral condyles are well preserved (Figure 6.10d). The medial condyle has a posteromedial corner with an angle of 90 degrees and a rounded anteromedial corner. The lateral condyle is larger than the lateral and anterolaterally bears a distinct crista tibiofibularis. The angle between the crista tibiofibularis and the lateral condyle is obtuse. The posterolateral corner of the lateral condyle is rounded and expanded posteriorly.

Tibia

UCMP 25887 from C64M occurs within a cluster of osteoderms of *Calyptosuchus wellesi*, but material referable to *Desmatosuchus spurensis* material occurs in that grid as well. Nonetheless, this left tibia is much more gracile than others found in the quarry (e.g., UCMP 25877), which probably belong to *Desmatosuchus* (Figure 4.11; Long and Murry, 1995). UCMP 25887 (Figure 4.12a-d) has a length of 186 mm, shorter than the

femur as is typical for aetosaurs. The proximal head is oval in proximal view with a width of 73 m, a length of 52 mm and is divided into two distinct sections by a nearly central ridge. The medial surface has slightly more area than the lateral surface and it concave, whereas the lateral surface is convex. A cnemial crest is absent (Nesbitt, 2011), and there is a distinct 'lip' posteriorly on the lateral portion of the head. The posterior portion of the distal end possesses a dorsoventrally oriented groove (Nesbitt, 2011: char. 337-1) for articulation with the astragalus. There is some damage to the medial condyle of the distal end in UCMP 25887. Overall there are few noticeable differences in the distal ends of UCMP 25887 and UCMP 25877 other than size. However, the proximal end in UCMP 25877 is much more expanded medially and has a distinct dorsal notch on the dorsolateral surface. There are two other gracile tibiae in the *Placerias* Quarry collection; UCMP 25896 (Figure 4.12e-g) is a left tibia from grid CH1, and UCMP 25894 is a left tibia from grid CH2 that was figured by Long and Murry (1995:fig. 84).

Fibula

UCMP 25802 from grid C67M is gracile compared to other fibulae in the *Placerias* Quarry collection and, as preserved, matches much of the material of *Calyptosuchus wellesi*. Long and Murry (1995) also assigned this element to *Calyptosuchus wellesi*. The specimen represents the proximal end of a left fibula. The iliofibularis trochanter is broken off. There is a small tubercle on the medial side of the shaft. Long and Murry (1995:84) state that "the diagonal ridge, so prominently exhibited along the medial fibular shaft of *Desmatosuchus* [*spurensis*], may not have been present

in [*Calyptosuchus*] *wellesi*." However, UCMP 25802 is not complete enough to evaluate this claim.

Astragalus

There are many astragali in the *Placerias* Quarry collection, but none fits the gracile tibiae in the collection that probably represent *Calyptosuchus wellesi*. Long and Murry (1995) figured and assigned a right astragalus from grid CF2 to *Calyptosuchus wellesi* (UCMP 34485); however, this specimen is currently on loan to another researcher and I was unable to examine it. Nonetheless, Long and Murry (1995) stated that they were unable to differentiate between the astragali of *Desmatosuchus* and *Calyptosuchus* and thus it is unclear how this assignment was originally made. Neither the type nor referred specimens of *Calyptosuchus wellesi* preserve the astragalus.

Calcaneum

As with the astragali there are lots of aetosaur calcanea in the collections as well, but as the calcaneum of *Desmatosuchus* is unknown, they cannot be differentiated. Long and Murry (1995:fig. 82) figured a left calcaneum (UCMP 34481) from CG1 as pertaining to *Calyptosuchus wellesi*. It is not clear what characters they used to make this assignment. UCMP 34481 is very similar to the calcaneum of *Aetosauroides scagliai* (PVL 2073) with a dorsoventrally flattened, mediolaterally expanded posterior tuber, and a deep concavity on the ventral surface of the anterior portion of the tuber. This deep concavity is sharply rimmed and also prominent in *Typothorax coccinarum* (AMNH FR 2713).

Osteoderms – The holotype of *Calyptosuchus wellesi* (UMMP 13950) preserves an articulated set of osteoderms starting with the posterior dorsal trunk series and extending back through much of the tail (Figure 4.13). These include trunk, lateral, and appendicular osteoderms and, importantly, they are associated with a vertebral column to aid with placement of specific rows. A significant landmark is the neural spine pushed up through the dorsal carapace, which is that of the first caudal vertebra (Case, 1929). Accordingly I have placed it between the first and second caudal paramedians where it pushed the first paramedian anteriorly and displaced the second paramedian posteriorly (Figures 4.13, 4.14). UMMP 13950 was thoroughly described by Case (1932) and is not in need of a full redescription.

Referred specimens from the St. Johns, Arizona area (Blue Hills, *Placerias* Quarry) provide more details regarding the mid-dorsal region as well as the ventral trunk osteoderms. Cervical osteoderms are currently unknown for *Calyptosuchus wellesi*. The cervical lateral plates assigned by Long and Ballew (1985) to *Calyptosuchus wellesi* that were reportedly characteristic of the genus (Long and Murry, 1995) actually belong to a paratypothoracin aetosaur, most likely *Tecovasuchus* (Parker, 2005a; Heckert et al., 2007b).

Paramedian Osteoderms

Trunk Series

The holotype of *Calyptosuchus wellesi* (UMMP 13950) preserves the last four presacral paramedians of the right side and the last two of the left side as well as the two sets that would have been situated over the sacrum (Figures 4.13, 4.14). The osteoderms

bear strongly raised anterior bars with anterolateral projections, sigmoidal lateral and straight medial margins. The dorsal eminence is a broad, low pyramidal structure that contacts and slightly overhangs the posterior plate margin. The boss is slightly situated medially on the osteoderm surface. A strongly developed pattern of pits and elongate grooves and ridges radiates from the position of the eminence. This ornamentation strongly differs from that of *Stagonolepis robertsoni* (NHMUK 4789a) and *Stagonolepis olenkae* (ZPAL AbIII 570/1) where the radiating grooves and ridges are more anastomosing. It also lacks the elongate parallel grooves and ridges found in *Aetosauroides scagliai* (PFV 2073). Furthermore, the posteromedial corners of the paramedians are flat and ornamented, lacking the distinct raised triangular boss of *Scutarx deltatylus* (PEFO 34616) or the triangular unornamented area of *Adamanasuchus eisenhardtae* (PEFO 34638). The lateral edge here is slightly indented for a short triangular process of the lateral osteoderm, but is not deeply "cut-off" as in typothoracines such as *Paratypothorax* sp. (PEFO 3004) or in *Adamanasuchus eisenhardtae* (PEFO 34638).

Isolated osteoderms from the *Placerias* Quarry (Figures 4.15a-k) demonstrate that at least some of the dorsal trunk paramedians had a weakly developed ventral strut (e.g., UCMP 136744; Figures 4.15b, d, e), an anterolateral projection (e.g., UCMP 126846; Figure 4.15f), "scalloping" of the medial portion of the anterior bar (e.g., UCMP 136744, UCMP 126844, UCMP 126801; Figures 4.15 g-h, j), and a distinct anteromedial projection (UCMP 136744, UCMP 126844, MNA V2930; UCMP 126801; Figures 4.15g-j). Some of the osteoderms (e.g., UCMP 136744; Figure 4.15c-e) are strongly

flexed ventrally. Osteoderms from smaller, presumably less mature, individuals have dorsal eminences in the form of elongate keels rather than blunt pyramidal bosses. This is similar to the condition in smaller sized taxa such as *Aetosaurus ferratus* (Schoch, 2007) and *Aetosauroides scagliai* (PVL 2073).

Closer to the end of the tail the paramedian osteoderms become longer than wide with strong pyramidal dorsal eminences (e.g, UCMP 126801; Figures 4.15j-k). Even more distally, the bosses become reduced and blunter, but the osteoderms thicken significantly and in some cases start to fuse to each other (e.g., UCMP 136744; Figures 4.16a-d). This is very similar to the condition in *Scutarx deltatylus* (PEFO 34045).

Lateral Osteoderms

The lateral osteoderms from the ninth dorsal trunk row (of 16 total) through the 16th caudal rows (of approximately 40 according to Schoch, 2007 for *Aetosaurus ferratus*) are present and well-preserved in the holotype (UMMP 13950). Thus, the positions of isolated lateral osteoderms with matching anatomy can be placed with confidence. Aetosaurian lateral osteoderms are roughly square to rectangular with a pronounced dorsal eminence. Typically the osteoderms are flexed to some degree, divided into two 'flanges' (dorsal and lateral or ventral) by the eminence. Importantly, all of the lateral osteoderms in UMMP 13950 have more rectangular dorsal flanges, however, lateral osteoderms with strongly triangular dorsal flanges are present in the referred material of *Calyptosuchus wellesi*. These osteoderms must be from positions anterior to the ninth dorsal row. All of the lateral osteoderms have prominent anterior

bars, pyramidal dorsal eminences, and a surface ornamentation of grooves and ridges radiating from the eminence.

The anteriormost lateral osteoderms of the trunk series are well represented in specimen UCMP 27225, a partial skeleton represented by osteoderms and vertebrae and collected by Charles Lewis Camp near St. Johns in 1926. They are quadrilateral in dorsal view with distinct dorsal and lateral flanges separately by an elongate keeled dorsal eminence with a pyramidal terminal end that projects just slightly beyond the posterior osteoderm margin (Figures 4.17a-d). The dorsal flange is distinctly triangular in dorsal view and is reduced in size compared to the lateral flange. The lateral flange appears to increase in width in more posteriorly situated osteoderms. The medial edge of the dorsal flange is strongly sigmoidal and the anterior bar is indented where the anterolateral projection of the adjacent paramedian osteoderm overlies it.

In the next positions, but still anterior to the ninth dorsal trunk row, the dorsal flanges retain their sigmoidal lateral edge, but become more quadrilateral in dorsal view (Figures 4.17e-f). The lateral flanges are very wide and rectangular. They are still significantly larger than the dorsal flange. The next form of lateral osteoderm occur in the 9^{th}-12^{th} dorsal trunk positions based on comparison with the holotype (UMMP 13950) and are best represented in the *Placerias* Quarry material by left and right osteoderms (UCMP 136744; Figures 4.17g-j).

The dorsal eminence is larger and very hook-like. The dorsal flange is quadrilateral in dorsal view and maintains the strongly sigmoidal medial margin. The lateral flanges are still much wider than the dorsal flanges but are no longer rectangular.

Instead they are strongly quadrilateral with a distinct mediolateral slant so that the anterior margin is much wider than the posterior margin. This forms a distinct anterolateral 'wing' that characterizes the osteoderms from this portion of the carapace. In posterior view the angle between the flanges is approaching 90 degrees, much more flexed than the preceding lateral osteoderms.

The sacral and anteriormost caudal lateral osteoderms are represented by a right (UCMP 78751) and two left (UCMP 136744, MNA V3744) osteoderms (Figures 4.17k-n). These osteoderms are reduced in overall width, the lateral flange remains larger than the dorsal flange, but only slightly and anterolateral 'wing' is no longer prominent. The dorsal eminence is still strong, but not as hook-like as the previous osteoderms.

At about the third caudal row the dorsal eminence of the lateral osteoderms becomes very rectangular, and the dorsal and lateral flanges are more equal in size. Overall the osteoderms are lengthening anteroposteriorly, corresponding with the increasing length of the caudal vertebrae. These positions are represented by two right osteoderms, UCMP 27048 from the Blue Hills area of St. Johns, and UCMP 136744 from the *Placerias* Quarry (Figures 4.17o-q). The dorsal eminence is taller but blunter, not hook-like. The angle of flexion between the dorsal and lateral flanges is a strong 90 degrees in these osteoderms.

Ventral Osteoderms

Ventral trunk osteoderms are best represented in UCMP 27225. They are square to broadly rectangular with a strong, but narrow anterior bar. The external surface

ornamentation consists of a fine pattern of grooves and ridges radiating from a central, unraised area on the osteoderm.

Appendicular Osteoderms

Numerous appendicular osteoderms are preserved close to life position in the holotype (UMMP 13950: Figure 4.13). They consist of small rounded to oval osteoderms with faint surface pitting. They would have been situated manly along the upper portion of the individual limbs.

DISCUSSION

Calyptosuchus wellesi has been considered one of the better known aetosaurian taxa from the American Southwest. However, it was never completely described and, whereas our knowledge of many of the other southwestern taxa (e.g., *Desmatosuchus spurensis*, *Typothorax coccinarum*) has increased because of the recovery of new specimens, hardly any new material of *Calyptosuchus* has been discovered. Several partial skeletons mentioned by Parker and Irmis (2005) and Parker and Martz (2011) including cranial material, are instead referable to a new taxon *Scutarx deltatylus*, which is described in the following chapter. Thus the best sources of character information on Calyptosuchus are the numerous osteoderms and endoskeletal elements from the *Placerias* Quarry. Unfortunately past assignments of this material to various taxa are problematic because no methodology for assigning material is discussed (e.g., Long and Murry, 1995). I have attempted here to use the only source of data remaining from the original excavations, the grid numbers, to look for clues regarding possible association of endoskeletal elements with the diagnostic osteoderms, however, in many cases the data are unequivocal because of the mixture of osteoderms of more than one aetosaurian taxon

and because the original workers did not collect the majority of the osteoderms from the east side of the quarry.

In recent years the east side of the quarry, as well as the nearby Downs quarry, (Jacobs and Murry, 1980) has been reopened by crews from the North Carolina State Museum and Appalachian State University. Results are still forthcoming, but hopefully these sites will prove rich in associated remains of *Calyptosuchus* and help further clarify the osteology of this taxon.

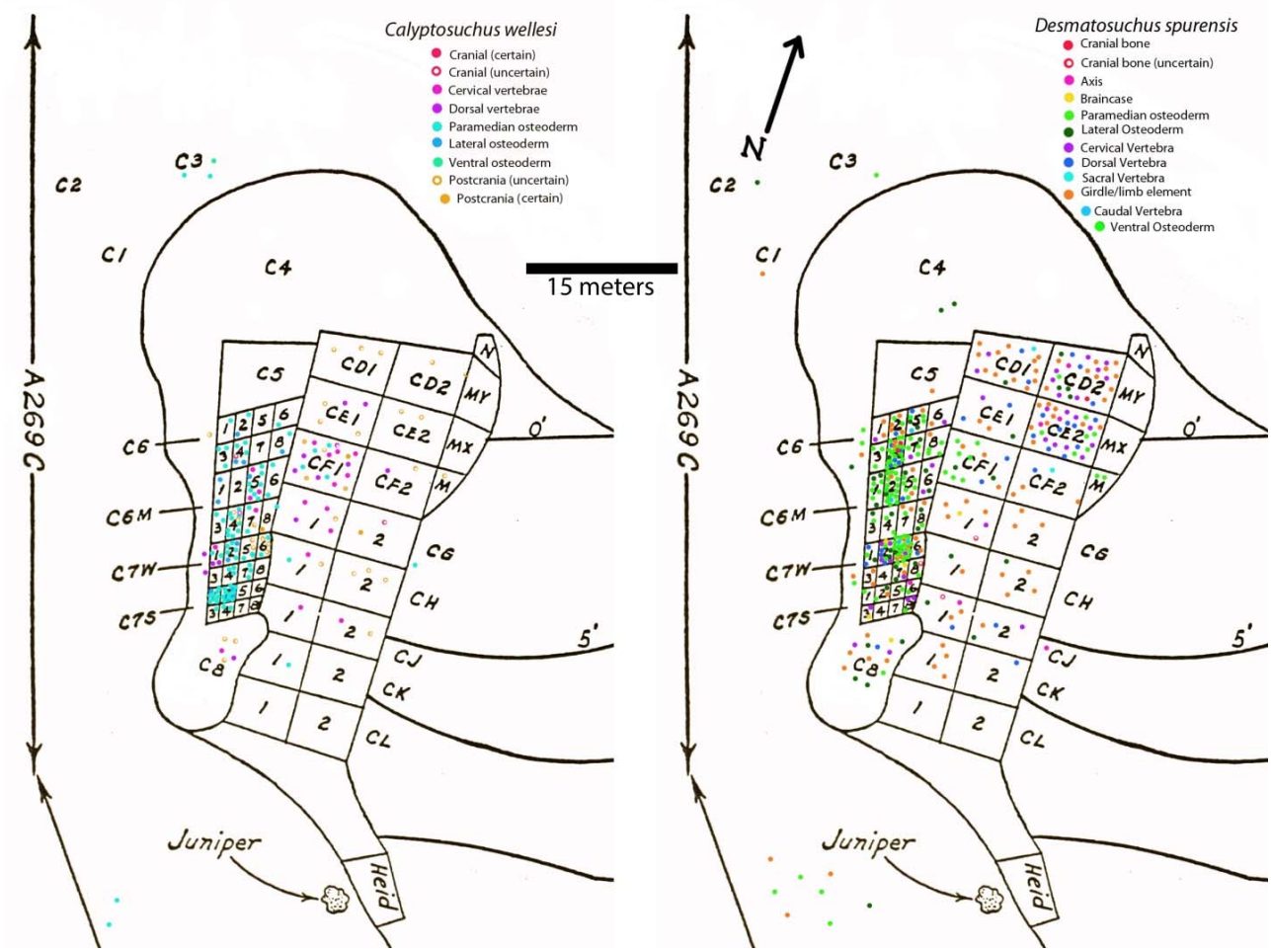

Figure 4.1. Recovered elements of *Calyptosuchus wellesi* and *Desmatosuchus spurensis* plotted on the map of the *Placerias* Quarry. Map modified from Camp and Welles (1956).

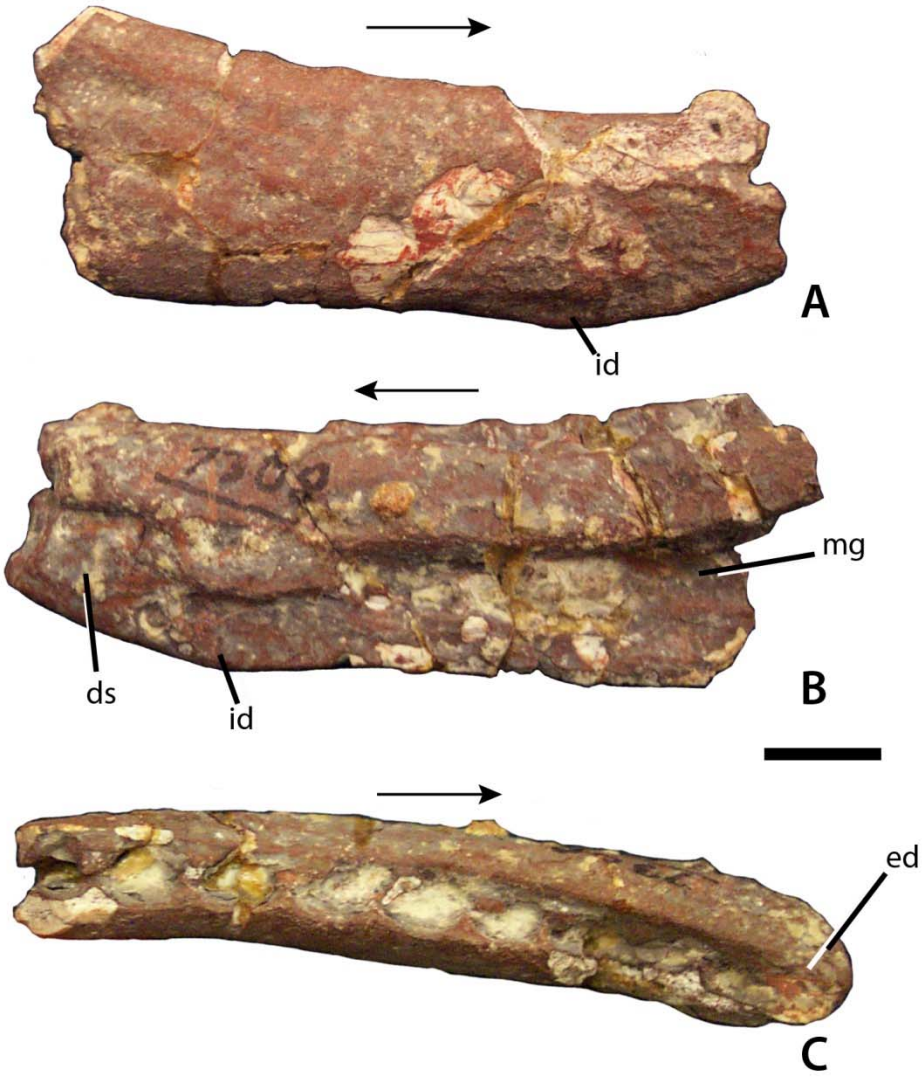

Figure 4.2. Partial right dentary of *Calyptosuchus wellesi* (UCMP 27225) in lateral (A), medial (B), and occlusal (C) views. Scale bar = 1cm. Arrows indicate anterior direction. Abbreviations: ds, dentary symphysis; ed, edentulous area; id, dentray infexion; mg, Meckelian groove.

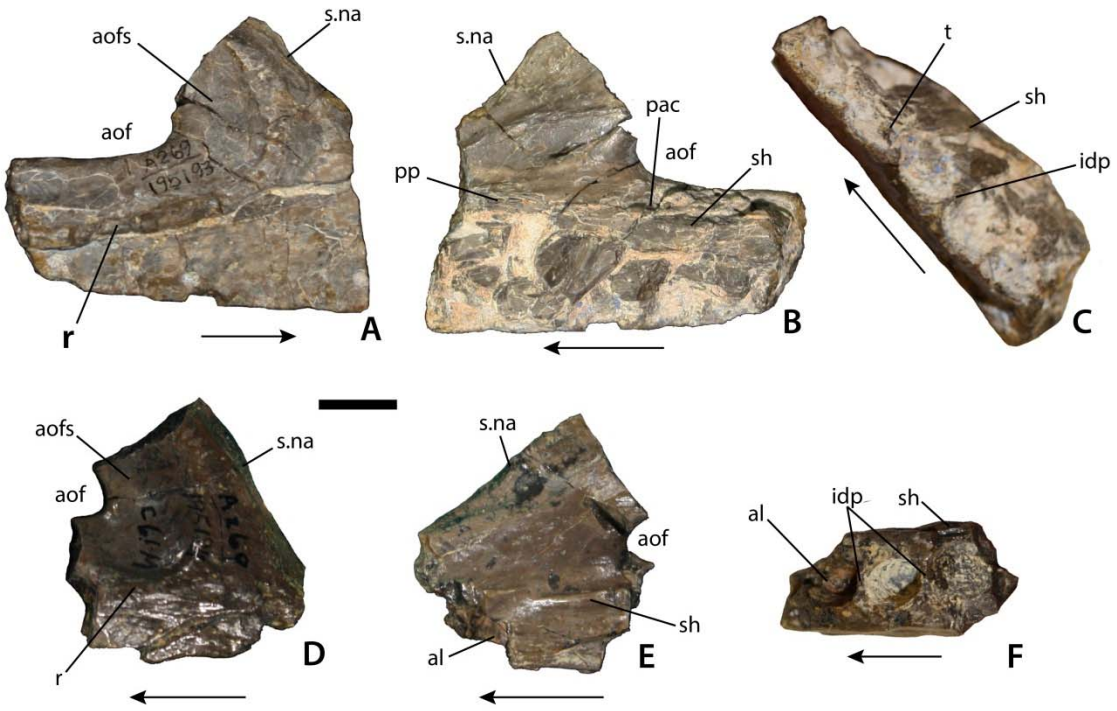

Figure 4.3. Maxillary fragments possibly referable to *Calyptosuchus wellesi*. A-C, right maxilla (UCMP 195193) in lateral (A), medial (B), and occlusal (C) views. D-F, right maxilla (UCMP 195194) in lateral (D), medial €, and occlusal (F) views. Scale bar equals 1 cm. Arrows indicate anterior direction. Abbreviations: al, alveolus; aof, antorbital fenestra; aofs, antorbital fossa; idp, interdental plate; na, nasal; pac, pneumatic accessory cavity; pp, palatal process of the maxilla; s.x, suture with indicated element; sh, maxillary shelf; t, tooth.

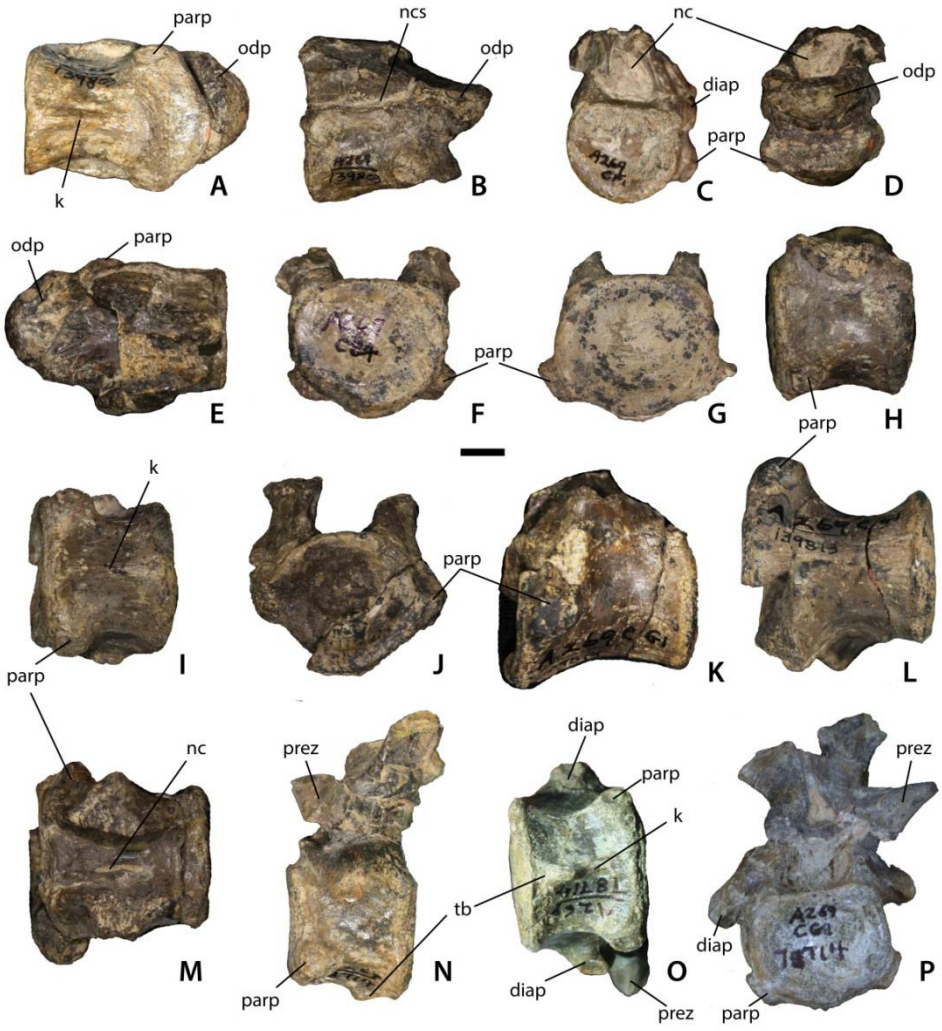

Figure 4.4. Axial and post-axial cervical vertebrae of *Calyptosuchus wellesi*. A-E, Axis (UCMP 139803) in ventral (A), lateral (B), posterior (C), anterior (D), and dorsal (E) views; F, anterior cervical (UCMP 139793) in anterior view; G, anterior cervical (UCMP 139794) in posterior view; H-I, anterior cervical (UCMP 139793) in lateral (H) and ventral (I) views; J-M, posterior cervical (UCMP 139813) in anterior (J), lateral (K), ventral (L), and dorsal (M) views; N-P, mid-cervical (UCMP 78714) in lateral (N), ventral (O), and anterior (P) views. Scale bar equals 1 cm. Abbreviations: diap, diapophysis; k, keel; nc, neural canal; ncs, neurocentral suture; odp, odontoid process; parp, parapophysis; prez, prezygapophyses; tb, ventral tab.

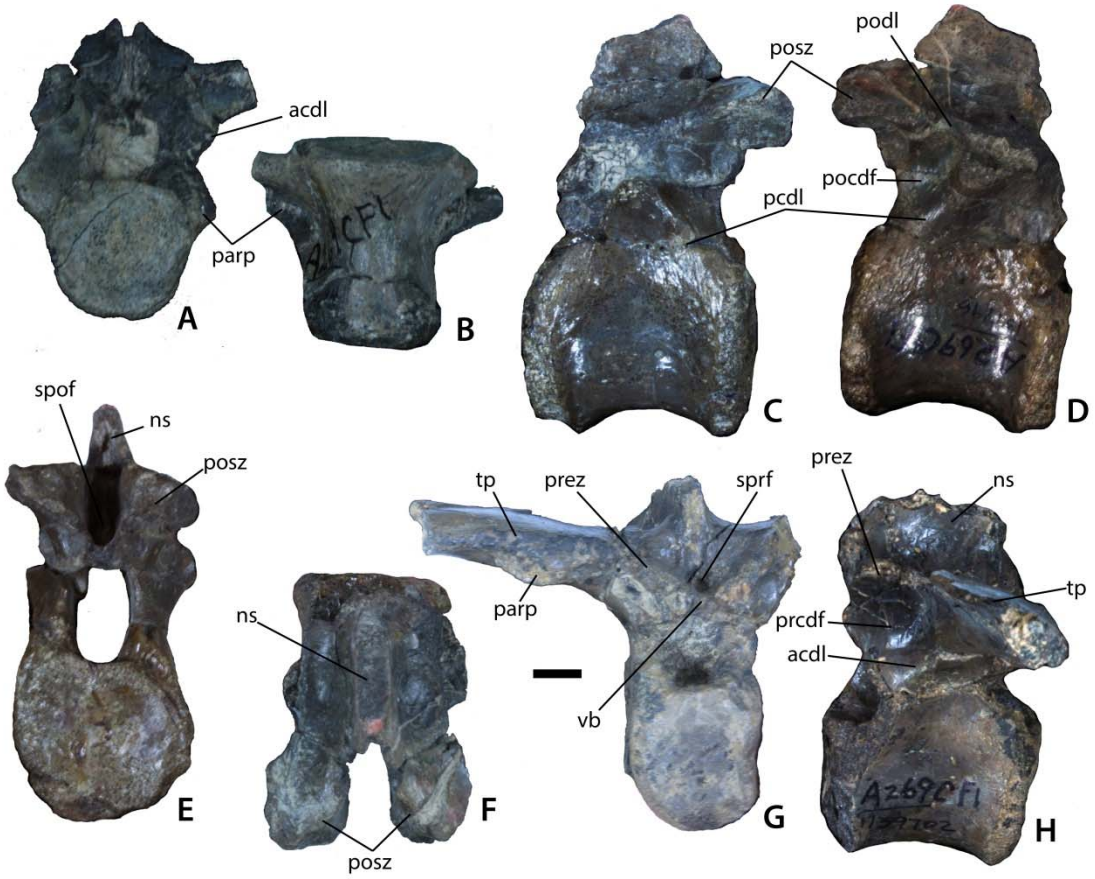

Figure 4.5. Trunk vertebrae of *Calyptosuchus wellesi*. A-B, UCMP 139694, 10th presacral vertebra in anterior (A) and ventral (B) views; C-F, UCMP 139796, mid-trunk vertebra in left lateral (C), right lateral (D), posterior (E), and dorsal (F) views; G-H, UCMP 139702, posterior trunk vertebra in anterior (G) and lateral (H) views. Scale bar equals 1 cm. Abbreviations: acdl, anterior centrodiapophyseal lamina; ns, neural spine; parp, parapophysis; pcdl, posterior centrodiapophyseal lamina; pocdf, postzygapophyseal centrodiapophyseal fossa; podl, postzygapophyseal lamina; posz, postzygapophysis; prcdf, prezygapophyseal centrodiapophyseal fossa; prez, prezygapophysis; spof, spinopostzygapophseal fossa; sprf, spinoprezygapophyseal fossa; tp, transverse process; vb, ventral bar.

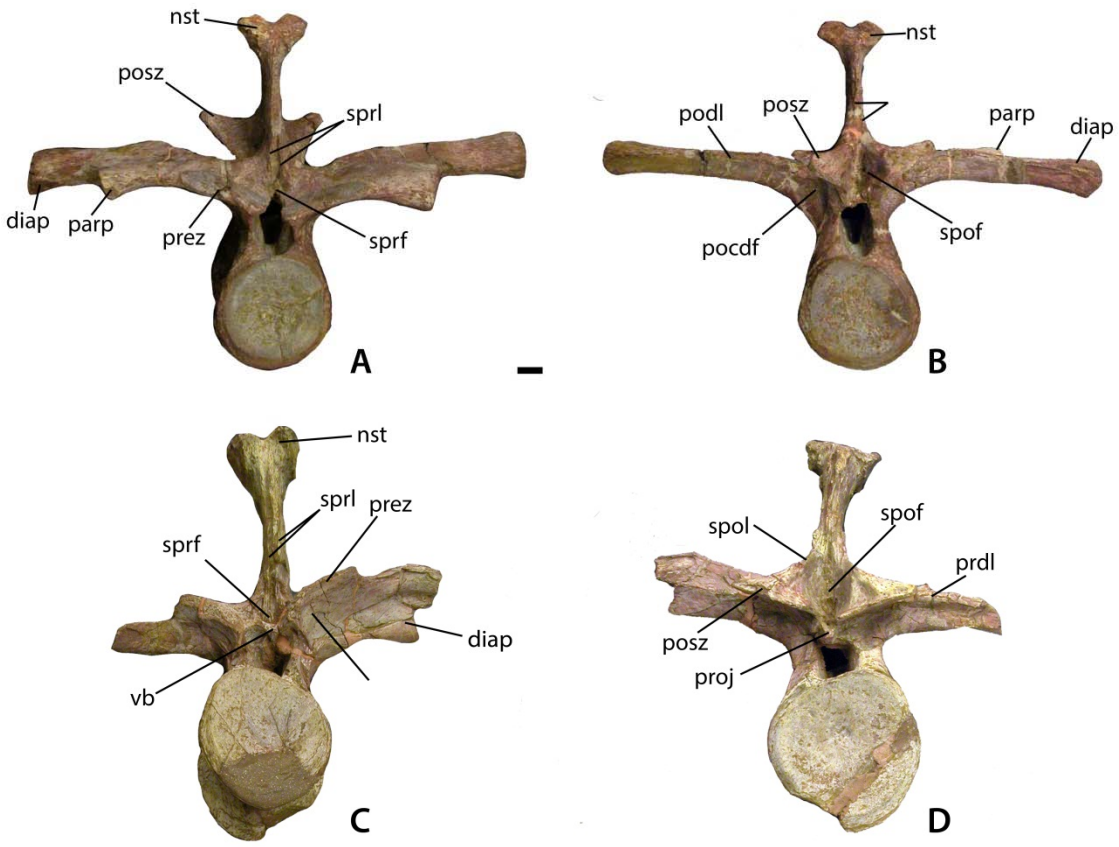

Figure 4.6. Mid-trunk vertebrae of *Calyptosuchus wellesi* (UMMP 7470). A-B, vertebra in anterior (A) and posterior (B) views. C-D, vertebra in anterior (C) and posterior (D) views. Scale bar equals 1 cm. Abbreviations: nst, neural spine table; parp, parapophysis; prdl, prezygapophyseal lamina; pocdf, postzygapophyseal centrodiapophyseal fossa; podl, postzygapophyseal lamina; posz, postzygapophysis; prcdf, prezygapophyseal centrodiapophyseal fossa; prez, prezygapophysis; proj, posterior projection; spof, spinopostzygapophseal fossa; spol, spinopostzygapophyseal lamina; sprf, spinoprezygapophyseal fossa; sprl, spinoprezygapophyseal lamina; vb, ventral bar.

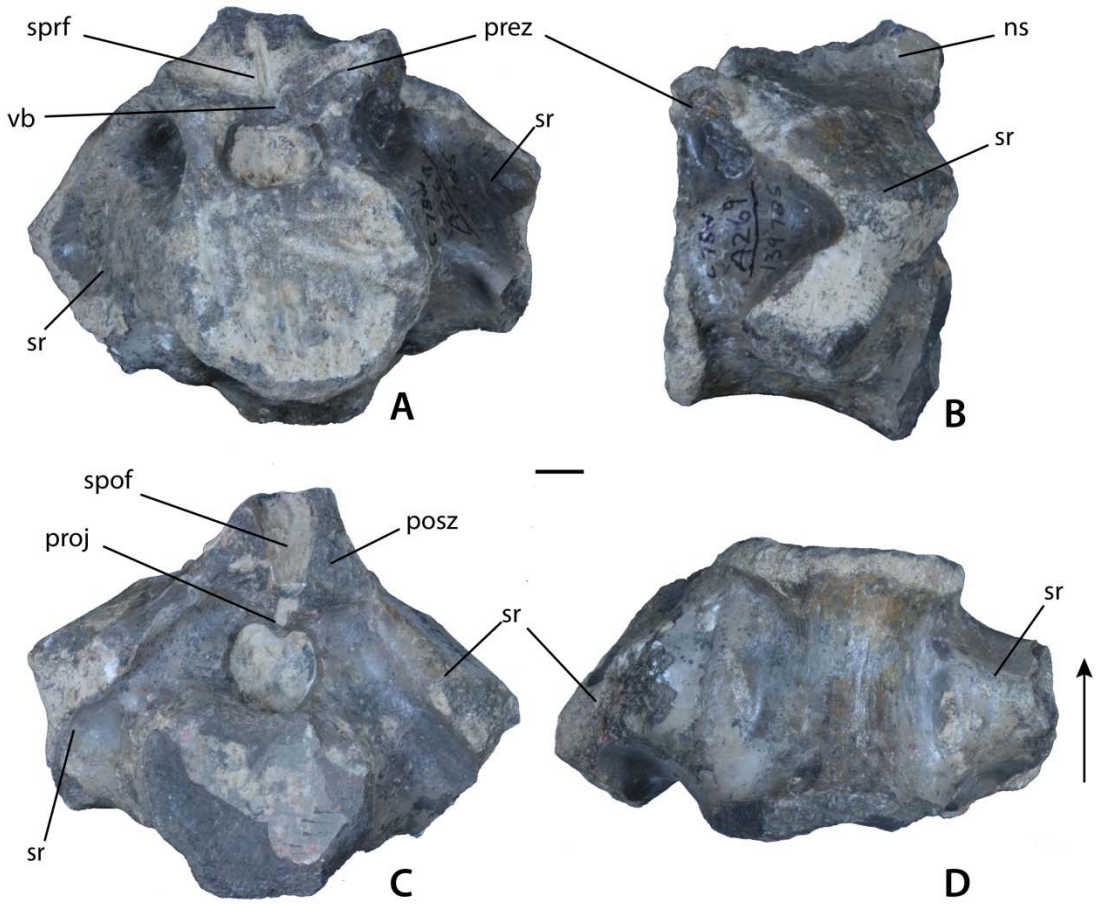

Figure 4.7. A-D, Sacral vertebra of *Calyptosuchus wellesi* (UCMP 139785) in anterior (A), lateral (B), posterior (C), and ventral (D) views. Scale bar equals 1 cm. Abbreviations: posz, postzygapophysis; prez, prezygapophysis; proj, posterior projection; spof, spinopostzygapophseal fossa; sprf, spinoprezygapophyseal fossa; sr, sacral rib; vb, ventral bar.

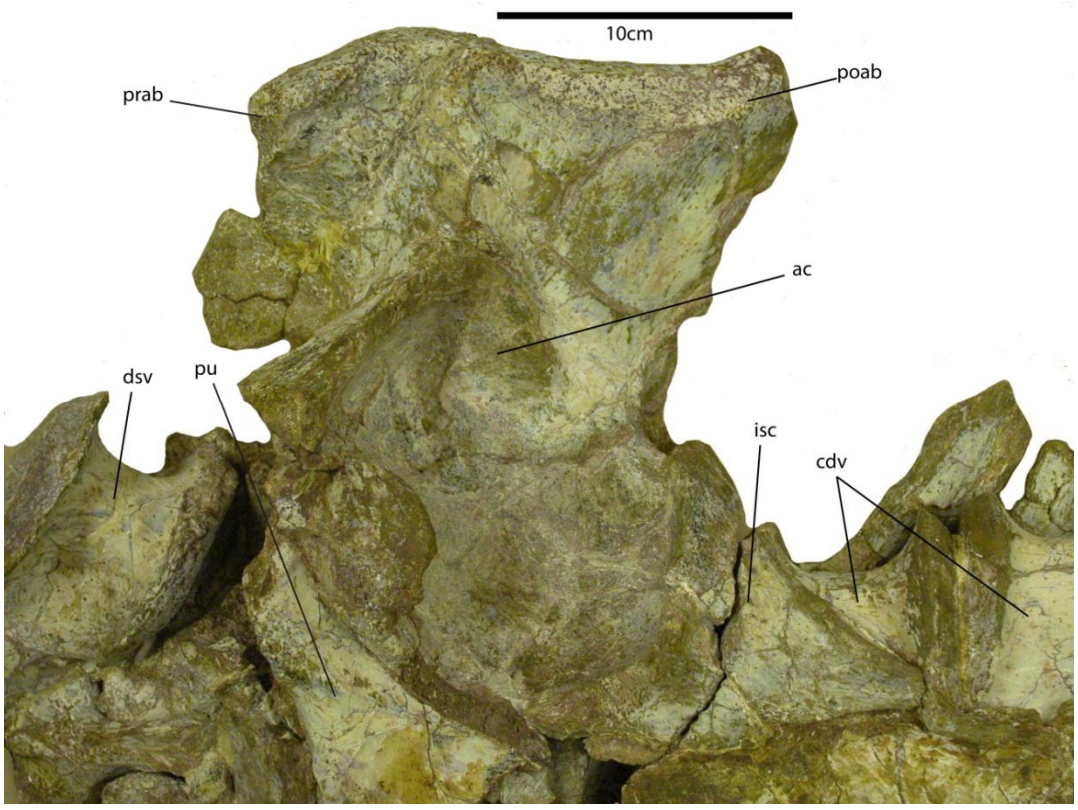

Figure 4.8. Portion of the sacrum and vertebral column of the holotype specimen of *Calyptosuchus wellesi* (UMMP 13950) in ventral view. Abbreviations: ac, acetabulum; cdv; anterior caudal vertebra; dsv, posterior trunk vertebra; isc, left ischium; poab, postacetabular blade of the left ilium; prab, preacetabular blade of the left ilium; pu, left pubis.

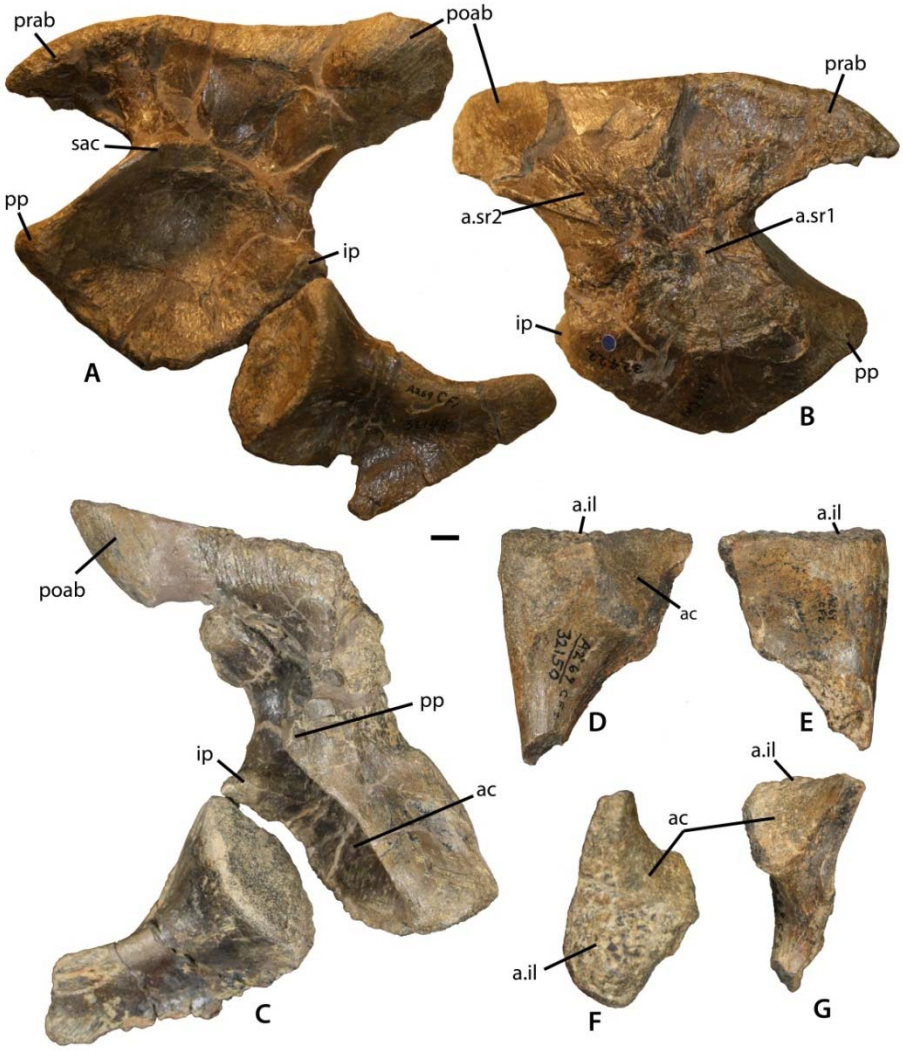

Figure 4.9. Pelvic elements of *Calyptosuchus wellesi*, possibly from a single individual. A, left ilium (UCMP 25941) and ischium (UCMP 32148) in lateral view (see text about anatomic directions for the pelvic elements); B, left ilium (UCMP 25941) in medial view; C, right ilium (UCMP 25941) and ischium (UCMP 32153) in lateral view; D-G, left pubis (UCMP 32150) in lateral (D), medial (E), dorsal (F), and posterior (G) views. Scale bar equals 1 cm. Abbreviations: a.x, articular surface with specified element; ac, acetabulum; il, ilium; ip, ischiadic peduncle; poab, postacetabular blade; pp, public peduncle; prab, preacetabular blade; sac, supraacetabular crest; sr, sacral rib.

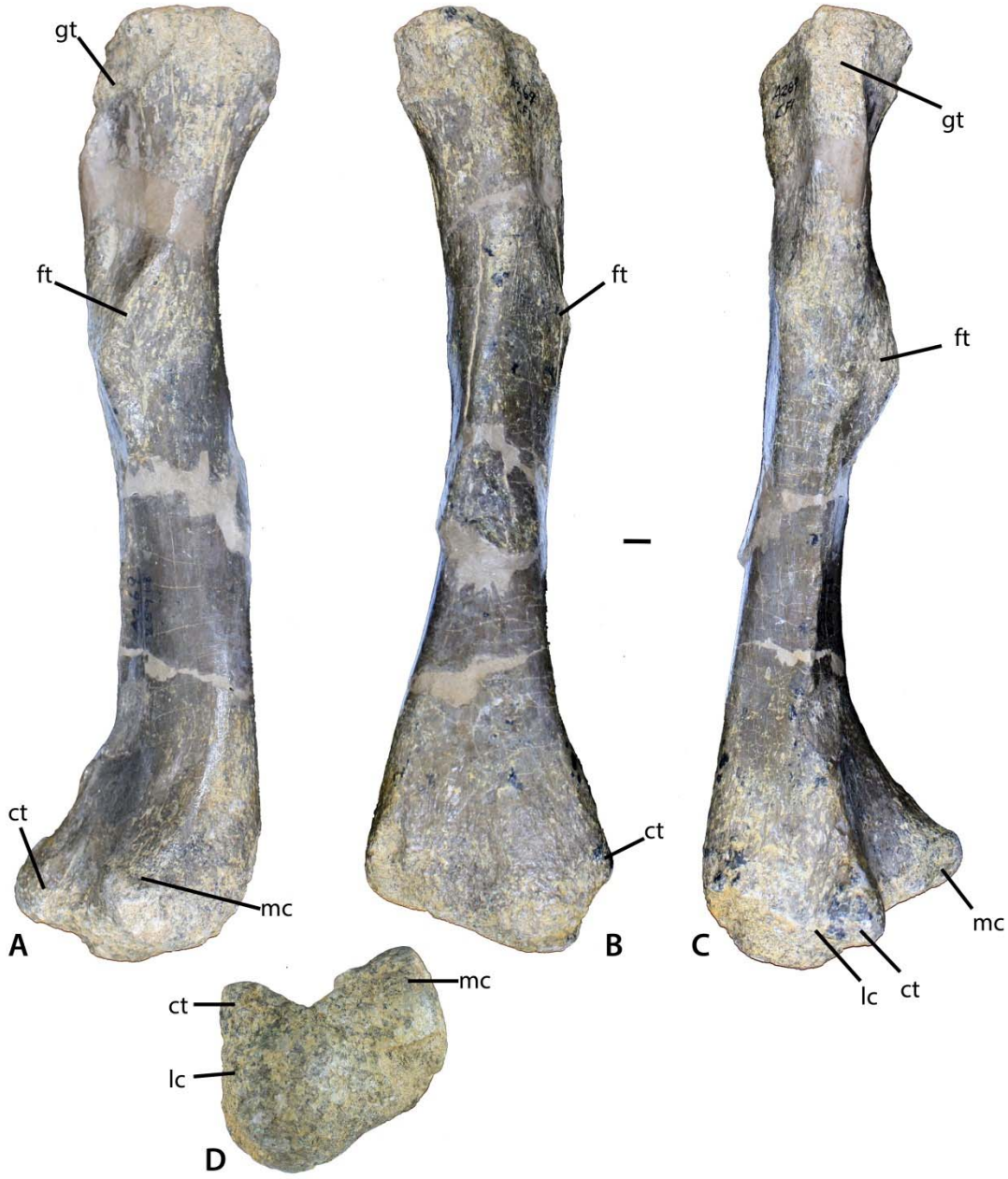

Figure 4.10. A-D, left femur of *Calyptosuchus wellesi* (UCMP 25918) in posteromedial (A); medial (B), lateral (C), and distal (D) views. Scale bar equals 1 cm. Abbreviations: ct, crista tibiofibularis; ft, fourth trochanter; gt, greater trochanter; lc, lateral condyle; mc, medial condyle.

Figure 4.11. Aetosaurian tibiae from the *Placerias* Quarry. A-C, *Desmatosuchus spurensis* left tibia (UCMP 25877) in proximal (A), posterior (B), and distal (C) views. D-F. *Calyptosuchus wellesi* left tibia (UCMP 25887) in proximal (D), posterior (E), and distal (F) views. Scale bar equals 1 cm.

Figure 4.12. Tibiae of *Calyptosuchus wellesi*. A-D, UCMP 25887, left tibia in posterior (A), medial (B), proximal (C), and distal (D). E-G, UCMP 25896, proximal end of left tibia in posterior (E), anterior (F), and proximal (G) views. Scale bar equals 1 cm. Arrows indicate anterior direction.

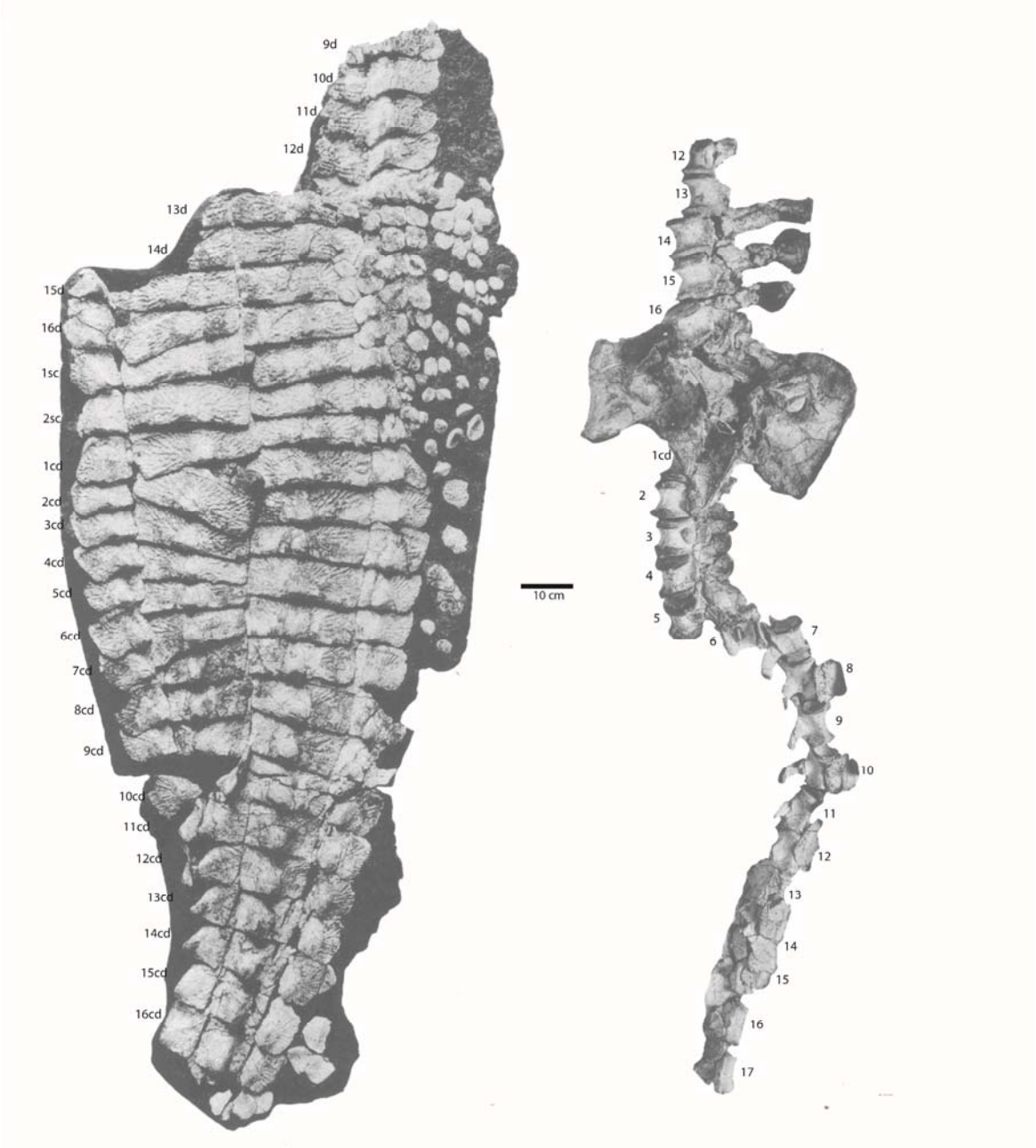

Figure 4.13. Holotype specimen of *Calyptosuchus wellesi* (UMMP 13950) showing assigned positions of osteoderms, pelvis, and vertebral column. Modified from Case, 1932. Abbreviations: d, trunk position; sc, sacral position; cd, caudal position.

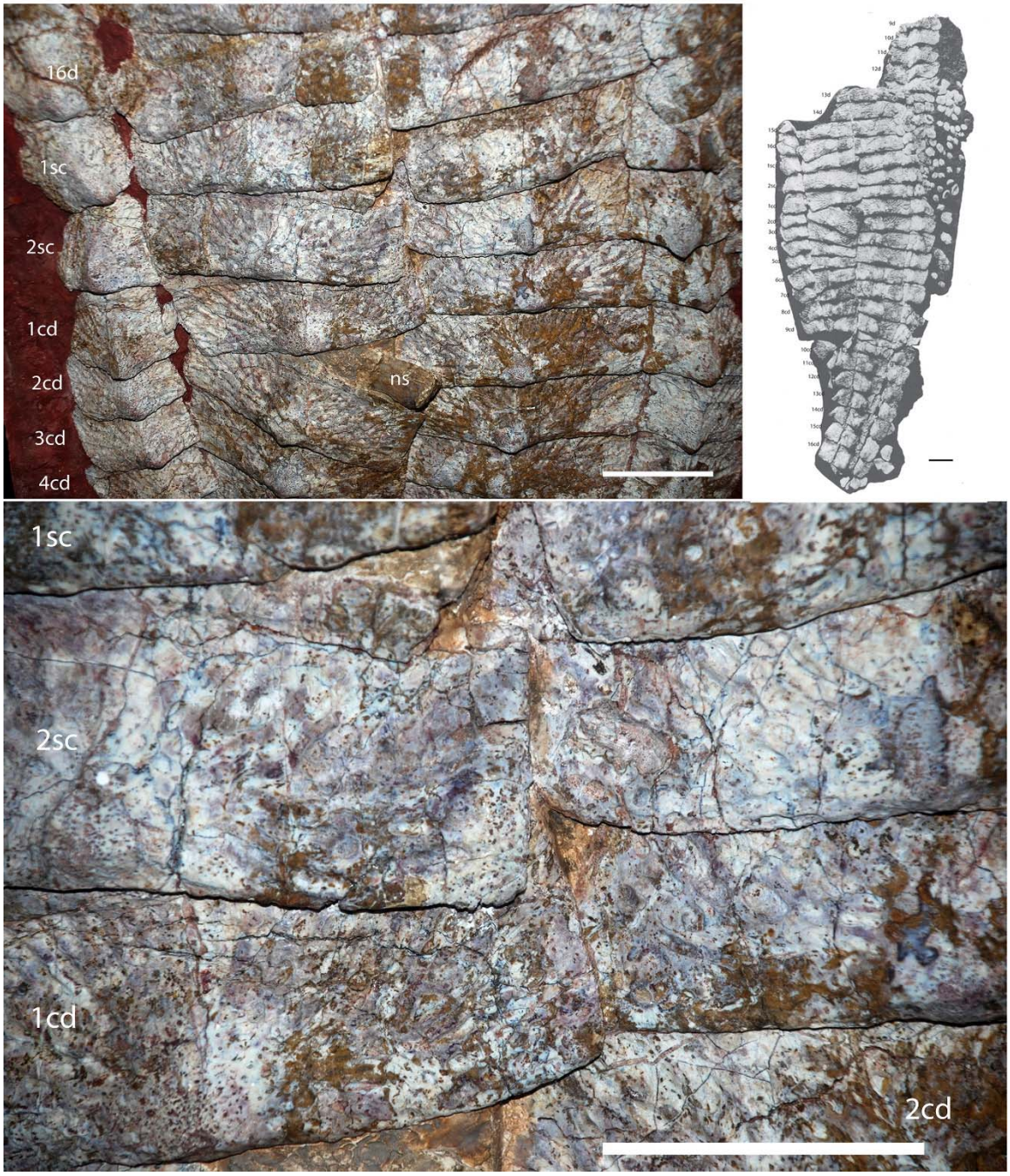

Figure 4.14. Close-ups of the carapace of the holotype of *Calytosuchus wellesi* (UMMP 13950) showing details of the paramedian osteoderms. Abbreviations: d, dorsal trunk row; sc, sacral row; cd, caudal row. Scale bars equal 10 cm.

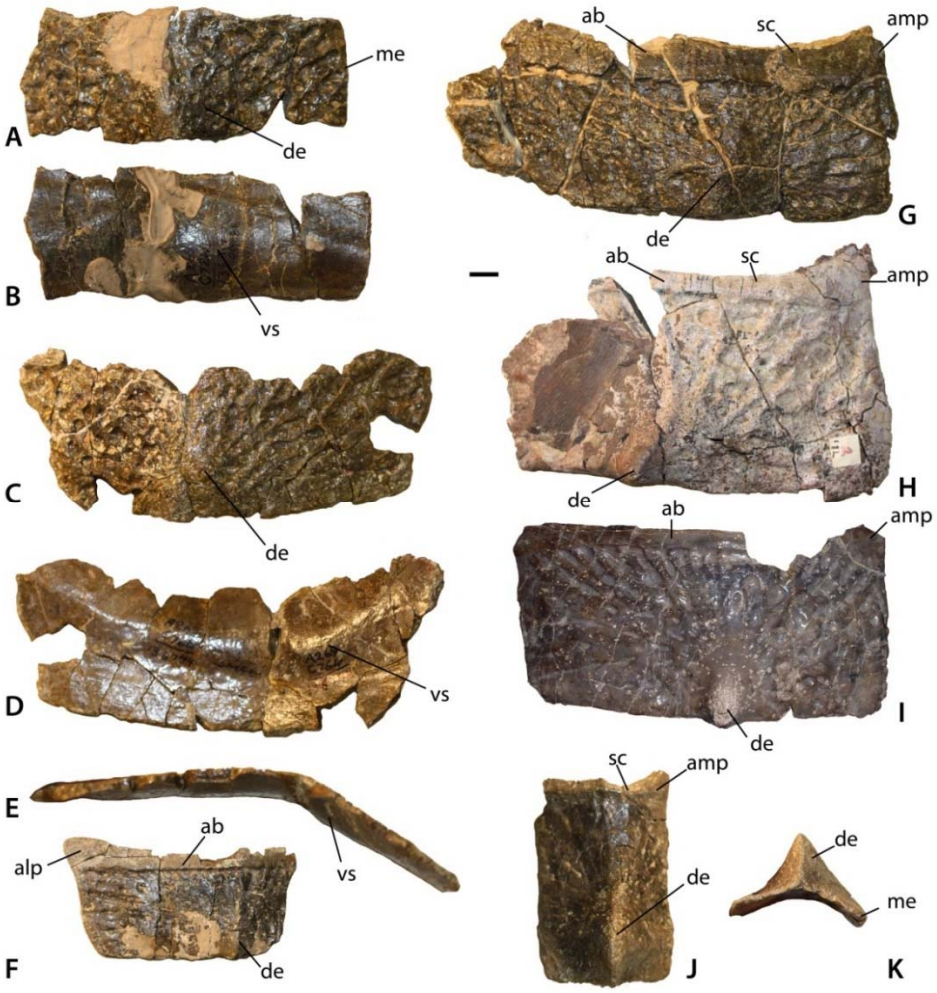

Figure 4.15. Paramedian osteoderms of *Calyptosuchus wellesi*. A-B, UCMP 136744, left anterior dorsal trunk osteoderm in dorsal (A) and ventral (B) views; C-E, UCMP 136744, right posterior dorsal trunk osteoderm in dorsal (C), ventral (D), and anterior (E) views; F, UCMP 126846, left dorsal trunk osteoderm in dorsal view; G, UCMP 136744, left dorsal mid-trunk osteoderm in dorsal view; H, UCMP 126844, left dorsal mid-trunk osteoderm in dorsal view; I, MNA V2930, left posterior dorsal trunk osteoderm in dorsal view; J-K, left posterior mid-caudal osteoderm in dorsal (J) and posterior (K) views. Scale bar equals 1 cm. Abbreviations: ab, anterior bar; alp, anterolateral process; amp, anteromedial process; de, dorsal eminence; me, medial edge; sc, scalloped area of anterior bar; vs, ventral strut.

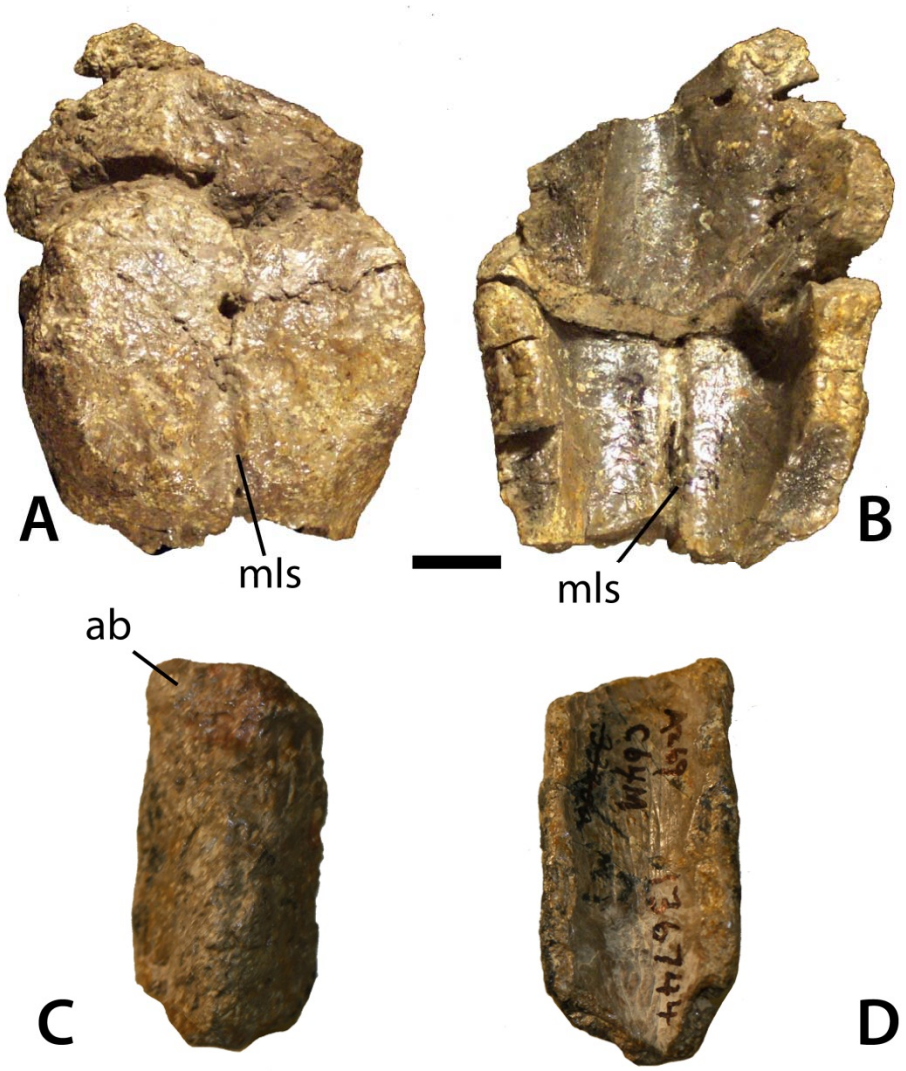

Figure 4.16. Distal caudal paramedian osteoderms of *Calyptosuchus wellesi* (UCMP 136744). A-B, Two semi-articulated sets of fused paired osteoderms in dorsal (A) and ventral (B) views; C-D, isolated osteoderm in dorsal (C) and ventral (D) views. Scale bar equals 1 cm. Abbreviations: ab, anterior bar; mls, mid-line suture.

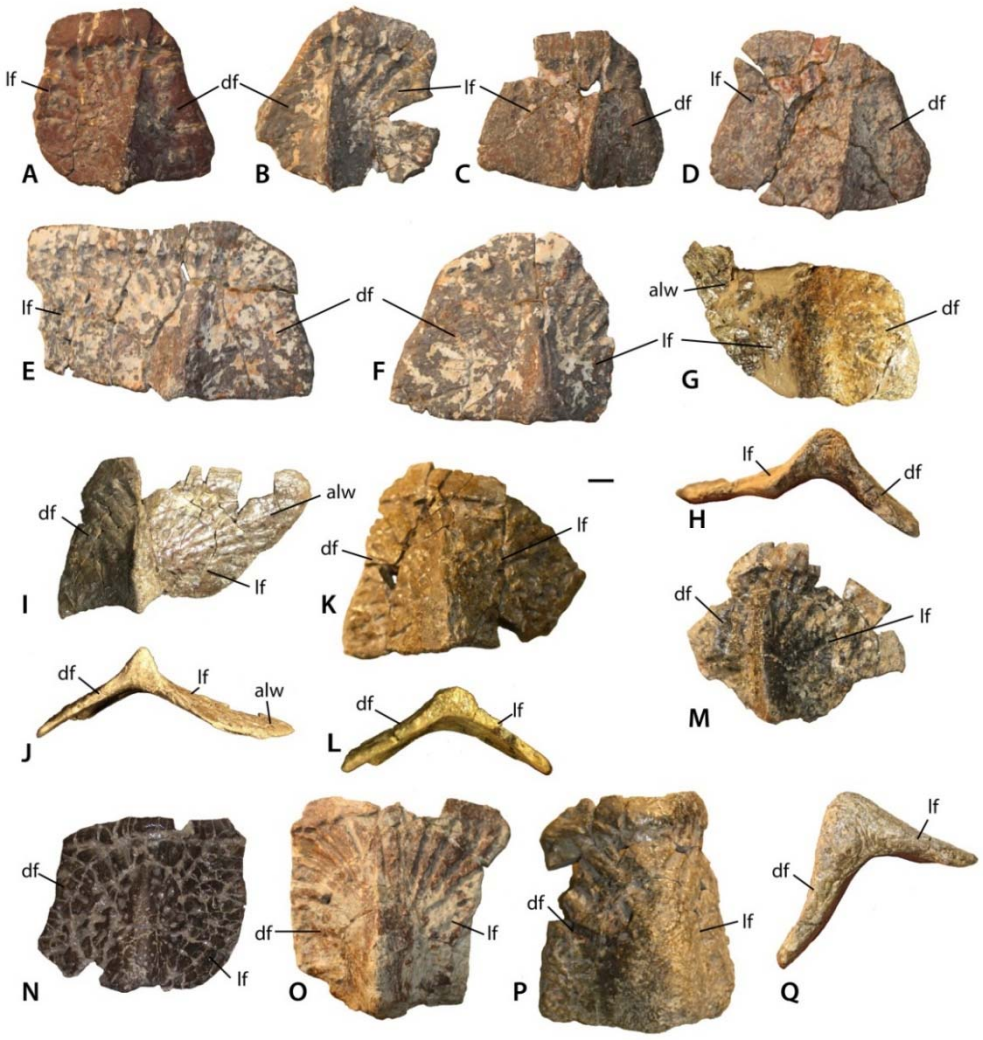

Figure 4.17. Lateral osteoderms of *Calyptosuchus wellesi*. A-D, anteriormost dorsal trunk lateral osteoderms (UCMP 27225) from the left (A, C-D) and right (B) sides in dorsal view; E-F, anterior dorsal trunk lateral osteoderms (UCMP 27225) from the left (E) and right (F) sides in dorsal view; G-J, posterior dorsal trunk lateral osteoderms (UCMP 136744) from the left (G-H) and right (I-J) sides in dorsal (G, I) and posterior (H, J) views; K-N, sacral and anteriormost caudal lateral osteoderms (UCMP 78751, K-L; UCMP 136744, M; MNA V3744, N) of the right side in dorsal (K, M-N) and posterior (L) views; O-Q, anterior-mid-caudal lateral osteoderms (UCMP 27048, O; UCMP 136744, P-Q) of the right side in dorsal (O-P) and posterior (Q) views. Scale bar equals 1 cm. Abbreviations: df, dorsal flange, lf, lateral flange.

Figure 4.18. Ventral and appendicular osteoderms of *Calyptosuchus wellesi*. A, UCMP 175148, ventral osteoderm in ventral view; B, UCMP 136744, ventral osteoderm in ventral view; C-N, UCMP 27225, ventral osteoderms in ventral view; O, UCMP 136744, external surface of an appendicular osteoderm. Scale bar equals 1 cm.

CHAPTER 5: *SCUTARX DELTATYLUS*, A NEW AETOSAURIAN FROM THE UPPER TRIASSIC CHINLE FORMATION OF ARIZONA

INTRODUCTION

Aetosaurians are one of the most commonly recovered vertebrate fossils in the Upper Triassic Chinle Formation at Petrified Forest National Park (PEFO), Arizona. Paleontological investigations in the park between 2001 and 2009 resulted in the discovery of four partial skeletons that are considered here to represent a single taxon. The first (PEFO 31217), discovered in 2001 and collected in 2002 from Petrified Forest Vertebrate Locality (PFV) 169 (Battleship Quarry; Figure 5.1), was initially assigned to *Calyptosuchus* (=*Stagonolepis*) *wellesi* based on characters of the armor and vertebrae (Parker and Irmis, 2005). The second partial skeleton was collected in 2004 from PFV 304 (Milkshake Quarry), at the south end of the park (Figure 5.1). That specimen (PEFO 34045) was also mentioned by Parker and Irmis (2005), who noted differences in the armor from *Calyptosuchus wellesi* and suggested that might represent a distinct species. The other two specimens were collected in 2007 and 2009. The first (PEFO 34616), from the Billings Gap area (PFV 355; Figure 5.1) is notable because it included the first aetosaurian skull to be recovered in the park. The second specimen (PEFO 34919) was recovered from the Saurian Valley area of the Devils Playground (PFV 224: Figure 5.1). All four of these specimens were assigned to *Calyptosuchus wellesi* by Parker and Martz (2011) and used to construct the stratigraphic range for that taxon. *Calyptosuchus* is

considered to be an index taxon of the Adamanian biozone (Lucas and Hunt, 1993;Parker and Martz, 2011).

Subsequent preparation and more detailed examination of these four specimens led to the discovery that they all shared a key autapomorphy, the presence of a prominent, raised triangular protuberance in the posteromedial corner of the paramedian osteoderms. The protuberance is not present on any of the osteoderms of the holotype of *Calyptosuchus wellesi* (UMMP 13950). It is also absent on the numerous paramedian osteoderms of *Calyptosuchus wellesi* recovered from the *Placerias* Quarry of Arizona in collections at the UCMP and the MNA. That autapomorphy and several features of the cranium and pelvis differentiate these specimens from all other known aetosaurians and form the basis for assigning these materials to a new taxon, *Scutarx deltatylus* gen. et sp. nov.

GEOLOGICAL SETTING

The four localities from which the new material of *Scutarx deltatylus* was collected all occur in the lower part of the Sonsela Member of the Chinle Formation (Martz and Parker, 2010; Figures 5.1, 5.2). In the PEFO region the Sonsela Member can be divided into five distinct beds, the Camp Butte, Lot's Wife, Jasper Forest, Jim Camp Wash, and Martha's Butte beds (Martz and Parker, 2010). The Lot's Wife, Jasper Forest, and Martha's Butte beds are sandstone dominated, cliff forming units with source areas to the south and west (Howell and Blakey, 2013), whereas the Lot's Wife and Martha's Butte beds are slope forming units with a higher proportion of mudrocks than sandstones

(Martz and Parker, 2010). All of these localities represent proximal floodplain facies associated with a braided river system (Woody, 2006; Martz and Parker, 2010, Howell and Blakey, 2013).

PFV 169 and PFV 224 occur in the upper part of the Lot's Wife beds, PFV 355 is situated in the base of the Jasper Forest bed, and PFV 304 marks the highest stratigraphic occurrence, located in the lower part of the Jim Camp Wash beds (Figure 5.2). All of these sites are below the 'persistent red silcrete,' a thick, chert, marker bed that approximates the stratigraphic boundary between the Adamanian and Revueltian biozones (Martz and Parker, 2010; Parker and Martz, 2011).

A high concentration of volcanic material in mudrocks of the Chinle Formation includes detrital zircons and allows for determination of high precision radioisotopic dates for studied beds (Figure 5.2; Ramezani et al., 2011). Zircons from the top of the Lot's Wife beds provided an age of 219.317 ± 0.080 Ma (sample SBJ; Ramezani et al., 2011). The base of the unit is constrained by an age of 223.036 ± 0.059 Ma for the top of the underlying Blue Mesa Member (sample TPs; Ramezani et al., 2011). Ages of 218.017 ± 0.088 Ma (sample GPL) and 213.870 ± 0.078 (sample KWI) are known from the Jasper Forest bed and the overlying Jim Camp Wash beds constraining the upper age for the fossil specimens (Ramezani et al., 2011).

MATERIALS AND METHODS

All specimens were excavated utilizing small hand tools, although a backhoe was used initially to remove overburden at PFV 304. B-15 Polyvinyl Acetate "Vinac" (Air Products & Chemicals, Inc.) and B-76 Butvar (Eastman Chemical Company) dissolved in

acetone were used as a consolidant in the field. PEFO 31217 was discovered partly in unconsolidated, heavily weathered sediment with numerous plant roots growing over and through the bones. Small handtools, including brushes, caused damage to the bone surface so plastic drinking straws were used to blow away sediment from the bone surface, which was then quickly hardened with a consolidant. In the lab the same specimen quickly deteriorated upon exposure, and liberal amounts of extremely thin Paleobond cyanoacrylate (Uncommon Conglomerates) was applied to stop disintegration. Because of the delicate nature of this specimen and the application of the cyanoacrylate, many of the bones cannot be prepared further or removed from the original field jackets. Furthermore, during collection the condition of the bones and surrounding matrix proved to be so poor that a portion of the jacket with the scapulocoracoid in it was lost during turning. This lost material consisted mostly of trunk vertebrae, ribs, and osteoderms.

The other three skeletons were consolidated in the lab using B-72 Butvar (Eastman Chemical Company), with Paleobond (Uncommon Conglomerates) cyanoacrylate used in many cases for permanent bonds. Paleobond (Uncommon Conglomerates) accelerator was originally used on some of the bones in PEFO 34045, but was halted because it was causing discoloration of the bone surface during the curing process. PEFO 34919 is coated with thin layers of hematite as is common for fossil specimens recovered from sandy facies in the Devils Playground region of PEFO. Mechanical preparation with pneumatic tools damaged the bone surface upon removing the coating and revealed that the hematite had permeated numerous microfractures in the bones, expanding them slightly, or in some bones significantly. As a result, the non-osteoderm bones from PFV 224 are highly deformed and often ‘mashed’ into the

associated osteoderms. Further preparation to remove the hematite coating was not attempted.

SYSTEMATIC PALEONTOLOGY

Archosauria Cope, 1869 *sensu* Gauthier and Padian, 1985.

Pseudosuchia Zittel 1887-90 *sensu* Gauthier and Padian, 1985.

Aetosauria Marsh, 1884 *sensu* Parker, 2007.

Stagonolepididae Lydekker, 1887 *sensu* Heckert and Lucas, 2000.

Scutarx deltatylus gen. et sp. nov.

(Figs. 5.3 – 5.24)

1985 *Calyptosuchus wellesi*: Long and Ballew, p. 54, fig. 13a.
1995 *Stagonolepis wellesi*: Long and Murry, p. 82, figs, 71b, 72b, e.
2005 *Stagonolepis wellesi*: Parker and Irmis, p. 49, fig. 4a.
2005a *Stagonolepis wellesi*: Parker, p. 44.
2005b *Stagonolepis wellesi*: Parker, p. 35.
2006 *Stagonolepis wellesi*: Parker, p. 53.
2011 *Calyptosuchus wellesi*: Parker and Martz, p. 242.
2013 *Calyptosuchus wellesi*: Martz et al., p. 342, figs. 7a-d.
2014 *Calyptosuchus wellesi*: Roberto-Da-Silva et al., p. 247.

Holotype **–** PEFO 34616, posterior portion of skull with braincase, cervical and dorsal trunk paramedian and dorsal trunk lateral osteoderms, ventral osteoderms, rib fragments, and paired gastral ribs.

Paratypes **--** PEFO 31217, much of a postcranial skeleton including vertebrae, ribs, pectoral and pelvic girdles, osteoderms; PEFO 34919, much of a postcranial

skeleton including vertebrae, ribs, osteoderms, girdle fragments, ilium; PEFO 34045, much of a postcranial skeleton including vertebrae, ribs, and osteoderms.

Referred Specimens -- UCMP 36656, UCMP 35738, dorsal trunk paramedian and dorsal trunk lateral osteoderms (lower part of the Chinle Formation, Nazlini, Arizona); TTU P-09240, left and right dorsal trunk paramedian osteoderms (Cooper Canyon Formation, Dockum Group, Post, Texas).

Etymology -- *Scutarx* 'shield fortress,' from Latin *scutum* 'shield' + Latin *arx* 'fortress, castle;' *deltatylus* 'triangular protuberance,' from Greek delta + Greek tylos 'knob, knot, swelling, callous, protuberance.'

Locality, Horizon, and Age -- PFV 255 (The Sandcastle), Petrified Forest National Park, Arizona; lower part of the Sonsela Member, Chinle Formation; Adamanian biozone, Norian, ~217 Ma (Ramezani et al., 2011).

Diagnosis -- Medium-sized aetosaurian diagnosed by the following autapomorphies; the cervical and dorsal trunk paramedian osteoderms bear a strongly raised, triangular tuberosity in the posteromedial corner of the dorsal surface of the osteoderm; the occipital condyle lacks a distinct neck because the condylar stalk is mediolaterally broad; the base of the cultriform process of the parabasisphenoid bears deep lateral fossae; the frontals and parietals are very thick dorsoventrally; and there is a distinct fossa or recess on the lateral surface of the ilium between the supraacetabular crest and the posterior portion of the iliac blade. *Scutarx deltatylus* can also be differentiated from other aetosaurs a unique combination of characters including moderately wide dorsal trunk paramedian osteoderms with a strongly raised anterior bar

that possesses anteromedial and anterolateral processes (shared with all aetosaurians except Desmatosuchini); osteoderm surface ornamentation of radiating ridges and pits that emanate from a posterior margin contacting a dorsal eminence (shared with *Calyptosuchus wellesi*, *Stagonolepis robertsoni*, *Adamanasuchus eisenhardtae*, *Neoaetosauroides engaeus*, and *Aetosauroides scagliai*); lateral trunk osteoderms with an obtuse angle between the dorsal and lateral flanges (shared with non-desmatosuchines); adorsoventrally short pubic apron with two proximally located 'obturator' fenestrae (shared with *Stagonolepis robertsoni*); and an extremely anteroposteriorly short parabasisphenoid, with basal tubera and basipterygoid processes almost in contact and a reduced cultriform process (shared with *Desmatosuchus*).

DESCRIPTION

Skull

Much of the posterodorsal portion of the skull is present in PEFO 34616 (Figures 5.3-5.9). Elements preserved include much of the left nasal, both frontals (the right is incomplete), both postfrontals, the left parietal (badly damaged), the left and right squamosals, the right postorbital, a portion of the left postorbital, and a nearly complete occipital region and braincase. The skull was already heavily eroded when discovered and although the skull roof/braincase portion was collected in situ, the remaining elements had to be carefully pieced back together from many fragments collected as float. Accordingly many of the skull roof elements are incomplete.

Much of the skull appears to have separated originally along some of the sutures, notably those between the prefrontal-frontal, squamosal-quadrate, and postorbital-

quadratojugal contacts. The left frontoparietal suture is also visible because of bone separation, and the sockets in the squamosals for reception of the proximal heads of the quadrates are well-preserved. Thus, the skull appears to have mostly fallen apart before burial and many of the anterior and ventral elements were presumably scattered and lost during disarticulation, with the exception of the left nasal, which is represented as an isolated piece. Similar preservation exists for the skull roof of the holotype of *Stagonolepis olenkae* (ZPAL AbIII/466/17) in which the frontal, parietals, occipital, and braincase are preserved as a single unit. This may suggest that the posterodorsal portion of the skull fuses earlier in ontogeny in these taxa. The skull of *Scutarx deltatylus* features a well-preserved braincase, which is described in detail below. Sutures are difficult to observe because of the state of preservation of the specimen, and the skull of *Longosuchus meadei* (TMM 31185-98) was used to infer the locations of various sutures, based on observable landmarks present in PEFO 34616.

Nasal

The proximal half of the left nasal is preserved, consisting of the main body and the posterior portion of the anterior projection through the mid-point of the external naris (Figure 5.3). The main body is dorsoventrally thick and the entire element is slightly twisted dorsomedially so that the dorsal surface is noticeably concave. Any surface ornamentation is obscured by a thin coating of hematite. The midline symphysis is straight and slightly rugose (Figure 5.3a). The lateral surface is damaged along the lacrimal suture; however, more anteriorly, the sutural surface for the ascending process of the maxilla is preserved and is strongly posteroventrally concave (Figure 5.3b).

Anteriorly the nasal narrows mediolaterally where it forms the dorsal margin of the external naris. The ventral process of the nasal that borders the posterior edge of the naris is missing its tip but it is clear from what is preserved that it was not elongate as in *Aetosauroides scagliai* but rather short as in *Stagonolepis olenkae* (ZPAL AbIII/346).

Frontal

Both frontals are present, with the left nearly complete and the right missing the posterior portion (Figure 5.4). The extreme dorsoventral thickness of the element is evident, as the dorsoventral thickness is 0.35 times the midline length of the element. The frontals appear to be hollow; however, this is most likely from damage during deposition and subsequent weathering before the skull roof was collected and pieced back together. In dorsal view the posterior margin of the frontal is slanted posterolaterally as in *Stagonolepis robertsoni* (Walker, 1961) so that the lateral margin of the frontal is longer than the medial margin, forming a distinct posterolateral process (Figure 5.4). The anterior portion of that process meets the postfrontal laterally and the parietal posteriorly as in *Stagonolepis olenkae* (Sulej, 2010). Just anterior to the posterolateral process the frontal forms the dorsal margin of the orbit. The position of the suture with the postfrontal is not clear, but it should have been present as in all other aetosaurians.

The dorsal surfaces of the frontals are rugose, ornamented with deep pits, some associated with more elongate grooves. Laterally above the round orbits and anteriorly there is are wider, anteroposteriorly oriented grooves as in *Stagonolepis olenkae* (Sulej, 2010). These grooves demarcate a raised central portion of the frontals as described for

Stagonolepis robertsoni by Walker (1961). The anterolateral margins of the frontals are dorsoventrally thick, rugose, anteromedially sloping areas that are bounded posteriorly by a thin curved ridge. These are the sutures for the prefrontals (Figs. 5.4, 5.5). There is no clear evidence for articulation of a palpebral bone at this position as in *Stenomyti huangae* (Small and Martz, 2013), but the posteriormost portion of the articular surface (Figure 5.5) is probably a suture for a palpebral as in *Longosuchus meadei* (TMM 31184-98). The anterior margins of the frontals are thick and rugose for articulation with the nasals (Figures, 5.4, 5.6). The frontal/nasal suture is nearly transverse. The frontal also lacks the distinct, raised midline ridge present in *Stenomyti huangae* (Small and Martz, 2013).

The ventral surfaces of the frontals are broadly ventrally concave and smooth (Figure 5.6). Medial to the orbital fossa is a distinct, slightly curved ridge that is the articulation point with the laterosphenoid.

Postfrontal

The postfrontals are roughly triangular bones that form the posterodorsal margin of the orbit. Both are certainly preserved in PEFO 34616, as in all aetosaurians, but the positions of their sutures are not clear.

Parietal

The dorsal portions of both parietals are mostly missing, although the posterolateral corner of the left one remains as well as a small fragment of the posterior portion of the right where it contacts the dorsal process of the squamosal (Figure 5.4). The frontal/parietal suture is visible along the posterior margin of the frontals, so it is

clear that these elements were not fused. The posterolateral portion forms the dorsal border of the supratemporal fenestra, but few other details are visible.

The posterior flanges of both parietals are preserved (Figure 5.7). Their posteroventrally sloping surfaces form the upper portion of the back of the skull. Ventrally, they contact the paroccipital processes of the opisthotics. There is no evidence of a posttemporal fenestrae, which may have been obliterated by slight ventral crushing of the skull roof. The parietal flanges contact the supraoccipital medially and the posterior process of the squamosal laterally. The upper margins are damaged so that the presence of a shelf for articulation of the nuchal paramedian osteoderms cannot be confirmed.

Squamosal

The majority of both squamosals is present. As is typical for aetosaurians the squamosals are elongate bones that are fully exposed in lateral view, forming the posterior corner of the skull, as well as the posteroventral margin of the oval supratemporal fenestra (Figure 5.5). The anterior and posterior portions are separated by a dorsoventrally thin neck. The anterior portion divides into two distinct rami, a large, but mediolaterally thin, ventral lobe that presumably contacted the upper margin of the quadratojugal, and a much smaller triangular dorsal ramus that forms much of the anteroventral margin of the supratemporal fenestra. These two rami are separated by a posterior process of the postorbital. On the right side of PEFO 34616, the dorsal ramus is broken, clearly showing the articulation with the postorbital and exposing the prootic in

this view (Figure 5.5). The ventral margin of the main body is concave and bears a flat surface that is the articulation surface with the quadrate (s.qu; Figure 5.6). Anterior to that articular surface the ventral margin of the anterior portion of the squamosal is confluent with the ventral margin of the postorbital. This arrangement suggests that the squamosal contributed little if anything to the margin of the lateral temporal fenestra. This is similar to the condition in *Stagonolepis robertsoni* (Walker, 1961) and differs from that in *Stenomyti huangae* (Small and Martz, 2013) in which the ventral margin of the squamosal is situated much lower that the ventral margin of the postorbital, and the squamosal contributes significantly to the margin of the infratemporal fenestra.

The posterior portion of the squamosal expands dorsally into dorsal and ventral posterior processes. The dorsal process forms the posterior border of the supratemporal fenestra and is mediolaterally thickened with a smooth anterior concave area that represents the supratemporal fossa. The apex of the upper process contacts the parietal. The ventral posterior process forms a small hooked knob that projects off of the back of the skull. Medial to this is a deep pocket in the medial surface of the squamosal that receives the dorsal head of the quadrate.. Dorsomedial to this pocket is the contact between the squamosal and the distal end of the paroccipital process of the opisthotic (Figure 5.6).

Postorbital

A portion of the left and almost the complete right postorbital are preserved in PEFO 34616 (Figures 5.5, 5.6). They are mediolaterally thin, triradiate bones that contact the postfrontal and parietal dorsally, the jugal anteriorly, and the squamosal posteriorly.

The upper bar forms the posterior margin of the orbit and the anterior margin of the supratemporal fenestra. The posterior process is triangular and inserts into a slot in the anterior portion of the squamosal. The ventral margin is flat, and forms the dorsal border of the infratemporal fenestra and more anteriorly that edge bears an articular surface with the jugal. The tip of the anterior process is broken, but it would have overlain the posterior process of the jugal and formed the posteroventral margin of the orbit.

Supraoccipital

The supraoccipital is present but poorly preserved (Figure 5.7). A median element, it forms much of the dorsal portion of the occiput and roofs the foramen magnum. Laterally it contacts the parietal flanges and ventrally the otooccipitals.

Exocipital/opisthotic

The exocciptals and opisthotics are indistinguishably fused into a single structure, the otooccipital. The exoccipital portions form the lateral margins of the foramen magnum (Figure 5.7). A protuberance is present on the left exoccipital at the dorsolateral corner of the foramen magnum (Figures 5.4, 5.7). The presence of similar structures in *Neoaetosauroides engaeus* (e.g., PVL 5698) was noted by Desojo and Báez (2007), and interpreted by them to be facets for reception of the proatlantes. Those authors considered the facets located on the supraoccipital; however, in *Longosuchus meadei* (TMM 31185-84) they are located on the exoccipital and the same appears to be true for PEFO 34616.

Anteriorly, a strong lateral ridge forms the posteroventral margin of the 'stapedial groove' as is typical for aetosaurs (Gower and Walker, 2002). In aetosaurians there are typically two openings for the hypoglossal nerve (XII) that straddle the lateral ridge

(Gower and Walker, 2002); however, they are not apparent in PEFO 34616, and where the posterior opening of the left side should be situated there is a fragment of bone missing.

Both paroccipital processes are present and well-preserved (Figures 5.4-5.7). They are mediolaterally short (14 mm) and stout, dorsoventrally taller than anteroposteriorly long (8 mm tall, 4 mm long), and contact the parietal flanges dorsally and the squamosal laterally. The distal end expands slightly dorsoventrally (Figure 5.7). The posterior surface is flat and distally the process forms the posterior border of the pocket for reception of the quadrate head, therefore there was a sizeable contact between the opisthotic and the quadrate.

The proximoventral portion of the paroccipital process opens into the 'stapedial groove'. That groove continues into the main body of the opisthotic, bounded by the lateral ridge of the exoccipital posteroventrally and the crista prootica anterodorsally Figure 5.8). Here there is a large opening for the fenestra ovalis and the metotic foramen; however, the two cannot be distinguished because the ventral ramus of the opisthotic that divides the two openings in aetosaurians (Gower and Walker, 2002) is not preserved (Figure 5.8). It is not clear if the ventral ramus was never originally preserved or if it was removed during preparation of the braincase. Thus the perilymphatic foramen is not preserved as well. The embryonic metotic fissure is undivided in aetosaurs and therefore the glossopharyngeal, vagal, and accessory (IX, X, XI) nerves and the jugular vein would have exited the braincase via a single opening, the metotic foramen (Rieppel, 1985; Walker, 1990; Gower and Walker, 2002). Just lateral to the metotic foramen on the

ventral surface of the crista prootica there should be a small opening for the facial nerve (VII); however, it is not visible through the hematite build-up on the lateral wall of the cranium.

A second distinct groove extends from the ventral border of the fenestra ovalis anteroventrally along the lateral face of the parabasisphenoid to the posterodorsal margin of the basipterygoid process, and is bordered anterodorsally by the anteroventral continuation of the crista prootica (Figure 5.8). The termination of that groove houses the entrance of the cerebral branch of the internal carotid artery (Gower and Walker, 2002; Sulej, 2010).

Prootic

The entire braincase is slightly crushed and rotated dorsolaterally so that the left side of the otic capsule is easier to view (Figure 5.8). Both prootics are preserved. Posteriorly, the prootic overlaps the opisthotic medially, and ventrolaterally forms a thin ridge (crista prootica), which is bounded ventrally by the upper part of the 'stapedial groove' and the groove in the parabasisphenoid leading to an opening for the internal carotid. Anteroventrally, the prootic meets the anterior portion of the parabasisphenoid, just posterior to the hypophyseal fossa. Anteriorly and anterodorsally, the prootic meets the laterosphenoid and dorsally it is bounded by the parietal. The uppermost margin is deformed by a thick anteroposteriorly oriented mass of bone, which could represent crushing of the parietal margin. Just posterior to the anterior suture with the laterosphenoid is the opening for the trigeminal nerve (V) which is deformed and closed

by crushing (Figure 5.8). In PEFO 34616 the opening for the trigeminal nerve is completely enclosed by the prootic.

Laterosphenoid

The laterosphenoids are ossified but poorly preserved. On the left side anterodorsal to the opening for the trigeminal nerve (V), there is the cotylar crest, which is crescentic and opens posteriorly (Figure 5.8). No other details of the laterosphenoid can be determined.

Basioccipital/Parabasisphenoid

The basioccipital and parabasisphenoid are complete and together comprise the best preserved and most distinctive portion of the braincase in *Scutarx deltatylus* (Figure 5.9). The occipital condyle is transversely ovate in posterior view rather than round like in other aetosaurs such as *Longosuchus meadei* (TMM 31185-98). The dorsal surface is broad with a wide shallow groove for the spinal cord.

The condylar stalk is also broad (25 mm wide), and wider than the condyle. Thus there is no distinct 'neck,' nor does a sharp ridge delineate the condyle from the stalk as in *Longosuchus meadei* (TMM 31185-98; Parrish, 1994) or *Desmatosuchus smalli* (TTU P-9024; Small, 2002). The ventral surface of the condylar stalk bears two low rounded 'keels' separated by a shallow, but distinct, oblong pit. The broad stalk, lack of a distinct neck, and ventral keels all appear to be autapomorphic for *Scutarx deltatylus*. Anterolaterally the condylar stalk expands laterally to form the ventral margin of the metotic fissure. The contacts with the exoccipitals are dorsal and posterior to that margin.

The right basal tuber of the basioccipital is present, but the left is missing. The basioccipital tuber is separated from the crescentic basal tuber of the parabasisphenoid by an unossified cleft, typical for aetosaurians and other suchians (Figure 5.9; Gower and Walker, 2002). The basal tubera of the basioccipital are divided medially by an anteroposteriorly oriented bony ridge that bifurcates anteriorly to form the crescentic basal tubera of the parabasisphenoid and enclose the posterior portion of the basisphenoid recess (*sensu* Witmer, 1997). Posteriorly that bony ridge is confluent with the posteriorly concave posterior margin of the basioccipital basal tubera (Figure 5.9). The short, anterolaterally directed basipterygoid processes are located anteriorly and in contact posteriorly with the anterior margin of the basal tubera of the parabasisphenoid.. The upper portion of the distal end of the left basipterygoid process is broken, but the right is complete and bears a slightly expanded and slightly concave distal facet that faces anterolaterally to contact the posterior process of the pterygoid.

The basipterygoid processes and the basal tubera are positioned in the same horizontal plane (Figure 5.8), which is typical for aetosaurians and differs significantly from the condition in *Revueltosaurus callenderi* (PEFO 34561) and *Postosuchus kirkpatricki* (TTU P-9000; Weinbaum, 2011) in which the basicranium is oriented more more vertically, with the basipterygoid processes situated much lower dorsoventrally than the basal tubera.

Scutarx deltatylus differs from aetosaurians such as *Stagonolepis robertsoni* (MCZD 2) and *Aetosauroides scagliai* (PVSJ 326) in that there is a broad contact between the basal tubera and the basipterygoid processes and that the basipterygoid

processes are not elongate (Figure 5.9). This is nearly identical to the condition in *Desmatosuchus smalli* (TTU P-9023) and *Desmatosuchus spurensis* (UMMP 7476; Case, 1922). There are two basicrania (UCMP 27414, UCMP 27419) from the *Placerias* Quarry with widely separated (anteroposteriorly) basal tubera and (elongate) basipterygoid processes that apparently do not pertain to either *Desmatosuchus* or *Scutarx deltatylus*, and may belong to *Calyptosuchus wellesi*. This would demonstrate a potential important braincase difference between *Calyptosuchus wellesi* and *Scutarx deltatylus*, despite the nearly identical structure of the osteoderms shared between these two taxa.

In the anteroposteriorly short area between the basal tubera and the basipterygoid processes, a deep, more or less rounded fossa (Figure 5.9) represents the basisphenoid recess (=median pharyngeal recess of Gower and Walker, 2002; =parabasisphenoid recess of Nesbitt, 2011), which is formed by the median pharyngeal system (Witmer, 1997). The presence of a 'deep hemispherical fontanelle' (= basisphenoid recess) between the basal tubera and the basipterigoid processes has been proposed as a synapomorphy of *Desmatosuchus* and *Longosuchus* (Parrish, 1994), but as discussed by Gower and Walker (2002), that condition is present in many archosauriforms. The number of aetosaurian taxa with this feature was expanded by Heckert and Lucas (1999a), who also reported that a 'hemispherical fontanelle' is absent in *Typothorax* and *Aetosaurus*. Unfortunately they did not list catalog numbers for examined specimens, and scoring of character occurrences cannot be replicated. The basisphenoid recess is actually

present in *Aetosaurus* (Schoch, 2007) and *Typothorax* (TTU P-9214; Martz, 2002). Thus, the presence of that recess is an aetosaurian synapomorphy.

Small (2002) found the shape and size of the basisphenoid recess to be variable in his hypodigm of *Desmatosuchus haplocerus*, and recommended that the character be dropped from phylogenetic analysis pending further review. However, rather than utilizing the presence or absence of the structure, it has been proposed that the shape and depth may be of phylogenetic significance (Gower and Walker, 2002). As noted above, it appears that there are two types of aetosaurian basicrania, those with anteroposteriorly short parabasisphenoids and those with long parabasisphenoids. These differences were used as rationale for splitting *Desmatosuchus haplocerus* into two species (Parker, 2005c). Among taxa with short parabasisphenoids, *Scutarx deltatylus* (PEFO 34616) and *Desmatosuchus spurensis* (UMMP 7476) have deep, more or less round basisphenoid recesses, and *Desmatosuchus smalli* has a shallow subtriangular recess. In *Longosuchus meadei* (TMM 31185-98) the recess is round and shallow. Among taxa with elongate basisphenoids, *Aetosauroides scagliai* (PVSJ 326) has a shallow, round recess and *Tecovasuchus chatterjeei* (TTU P-545) has a deep, round recess. However, in *Coahomasuchus kahleorum* (NMMNH P-18496; TMM 31100-437), which has an elongate basisphenoid, the recess has the form of a moderately deep, anteroposteriorly elongate oval (Desojo and Heckert, 2004; pers. obs. of TMM 31100-437). Thus, the shape of this structure is highly variable and most likely not phylogenetically informative, although the elongate form of the recess in *C. kahleorum* may prove autapomorphic.

Anterior to the basisphenoid recess and between the bases of the basipterygoid processes there is another shallow, anteroventrally opening recess (Figure 5.9). This recess is at the base of the parasphenoid process, in the same position as the subsellar recess in theropod dinosaurs (Witmer, 1997; Rauhut, 2004) and may be homologous to the latter. However, the function and origin of the recess are not understood (Witmer, 1997).

Dorsal to the basipterygoid processes, two crescentic and dorsally expanding clinoid processes flank the circular, concave hypophyseal fossa, which housed the pituitary gland (Figure 5.8). No openings are visible because of poor preservation, but the dorsum sellae should be pierced by two canals for the abducens (VI) nerves (Hopson, 1979; Gower and Walker, 2002). At the base of the hypophyseal fossa in *Stagonolepis robertsoni* (MCZD 2) and *Longosuchus meadei* (TMM 31185-98) there is a triangular flange of bone termed the parabasisphenoid prow (Gower and Walker, 2002). This structure is mostly eroded in PEFO 34616, although its base is preserved as a small dorsal protuberance.

Anterior to this, the cultriform process of the parasphenoid is completely preserved (Figures 5.8, 5.9). This structure is delicate and usually missing or obscured in the few known aetosaur skulls, making comparisons difficult. However, the process is notably short in PEFO 34616, barely extending past the anterior margins of the orbits (Figure 5.8). In PEFO 34616 the basisphenoid has a length of 34.2 mm, whereas the cultriform process measures 20.2 mm in length (cultriform process/basisphenoid ratio = 0.59). This is noticeably different from the parabasisphenoid in *Aetosauroides scagliai*

(PVSJ 326) which has a basisphenoid length of 51 mm and a cultriform process length of at least 63 mm, although the anterior end of the process is concealed (ratio = 1.23) beneath the left pterygoid. The cultriform process is also preserved in *Desmatosuchus spurensis* (UMMP 7476), which has a relatively short parabasisphenoid and a cultriform process/basisphenoid ratio of 0.96.

The cultriform process is elongate and tapers anteriorly. It is Y-shaped in cross-section with a ventral ridge, and dorsal trough for the ethmoid cartilage. Its posterolateral margins bear distinct oval recesses bound posterodorsally by strong ridges that are confluent with the posterodorsal edge of the process (Figures 5.8, 5.9). Thus the process is broader posteriorly, with these recesses contributing greatly to the thinning of the element anteriorly. The parasphenoid recesses appear to be unique to PEFO 34616, although the general lack of known aetosaurian cultriform processes makes it difficult to determine this with certainty.

Postcranial skeleton

Vertebrae

Cervical Series

Axis/Atlas

The axis and atlas are not preserved in any presently known specimens of *Scutarx deltatylus*.

Post-axial Cervicals

Two articulated cervical vertebrae are preserved in PEFO 31217 (Figure 5.10). Although both are crushed mediolaterally, they are nearly complete and preserve many details. The centra are taller than long (Figure 5.10a) suggesting they represent part of the anterior (post-axial) series (i.e., positions 3-6). Most notably, the difference in dimensions is not as pronounced as in *Typothorax coccinarum* and *Neoaetosauroides engaeus*, in which the centra are greatly reduced in length (Long and Murry, 1995; Desojo and Báez, 2005). The centrum faces are subcircular in anterior and posterior views and slightly concave, with slightly flared rims (Figures 5.10b-c). The ventral surface of each centrum consists of two concave, ventromedially inclined, rectangular surfaces divided by a sharp and deep mid-line keel (Figure 5.10d).

The short parapophyses are oval in cross-section and situated at the anteroventral corners of the centrum. The parapophyses are directed posteriorly, and each forms the beginning of a prominent ridge that continues posteriorly to the posterior margin of the centrum. The lateral faces of the centra are concave mediolaterally and dorsoventrally forming discrete, but shallow, lateral fossae that contact the neural arch dorsally (Figure 5.10a). However, PEFO 31217 lacks the deep lateral fossae, which are considered an autapomorphy of *Aetosauroides scagliai* (Desojo and Ezcurra, 2011). The neurocentral sutures are not apparent on this specimen, suggesting closure of the sutures and that this individual is osteologically 'mature' although this cannot be completely confirmed without histological sectioning of the sutural contact (Brochu 1996; Irmis, 2007).

The diapophyses are centrally located at the base of the neural arch (Figure 5.10b). The best preserved vertebra shows that they are slightly elongate, oval in cross-section, and curved ventrolaterally. Because none of the diapophyses appears to be complete their exact length cannot be determined. The neural canal is round in posterior view (Figure 5.10c) rather than rectangular as in *Desmatosuchus spurensis* (UMMP 7504). The entire neural arch is taller than the corresponding centrum face. The zygapophyses are well-formed, elongate, and oriented at approximately 45 degrees from the horizontal.

Aetosaurian vertebrae bear several vertebral laminae and associated fossae. The terminology for these structures follows Wilson (1999) and Wilson et al. (2011). There is a weakly developed posterior centrodiapophyseal lamina (pcdl) that originates at the posteroventral corner of the diapophysis and continues posteroventrally to the posterior edge of the neurocentral suture. The only other apparent vertebral laminae are paired intrapostzygapophyseal laminae (tpol) that originate on the posteroventral surface of the postzygapophyses and form two sharp ridges (laminae) that meet at the dorsomedial margin of the neural canal (Figure 5.10b). Those laminae delineate the medial margins of a pair of distinct subzygapophyseal fossae, called the postzygapophyseal centrodiapophyseal fossae (pocdf), as well as a sizeable intrazygapophyseal fossa, called the spinopostzygapophseal fossa (spof). This represents the first recognition of distinct intrapostzygapophyseal laminae in an aetosaurian. *Desmatosuchus spurensis* (MNA V9300) has struts of bone from the dorsomedial margins of the postzygapophyses that join medially and then extend ventrally as a single thickened unit to form a Y-shaped

hyposphene (Parker, 2008b: fig. 10a), similar to the pattern formed by the intrapostzygapophyseal laminae in *Scutarx deltatylus*. Thus, it is possible that the structure of the hyposphene in aetosaurians is homologous (i.e., the hyposphene is actually formed by paired vertebral laminae) with the presence of paired (but not joined) intrapostzygapophyseal laminae, but this interpretation requires further investigation.

The neural spines are not complete; however, the base of the one on the second preserved vertebra shows that the spine was anteroposteriorly elongate, with prominent spinopostzygapophyseal laminae (spol) that are confluent with the dorsal surfaces of the postzygapophyses (Figure 5.10b). Spinopostzygapophyseal laminae are also present on the cervical vertebrae of *Desmatosuchus spurensis* (Parker, 2008b).

Trunk Series

Mid-trunk vertebrae

Four mid-trunk vertebrae are preserved in PEFO 34045. In aetosaurs the cervical to trunk transition occurs when the parapophysis fully migrates from the base of the neural arch, laterally onto the ventral surface of the transverse process (Case, 1922; Parker, 2008b). PEFO 34045/FF-51 is well preserved, missing only the postzygapophyses (Figures 5.11a-c). The articular faces of the centra are round and slightly concave with broad flaring rims. The centrum is longer (45.78 mm) than tall (41.81 mm), its lateral faces are deeply concave, and its ventral surface is narrow and smooth. The neural canal is large and in anterior view, the margins of the neural arch lateral to the canal are mediolaterally thin with sharp anterior edges.

The prezygapophyses are inclined at about 45 degrees from the horizontal and are confluent laterally with a short horizontally oriented prezygadiapophyseal lamina (prdl) that terminates laterally at the parapophysis (Figure 5.11b). Between the prezygapophyses and ventral to the base of the neural spine there is a well-developed broad, sub-triangular spinoprezygapophyseal fossa (sprf). In combination with the flat prezygapophyses this creates a broad shelf for reception of the posterior portion of the neural arch of the preceding vertebra (Figure 5.11b). There is a horizontal, ventral bar that roofs the opening of the neural canal between the ventromedial edges of the prezygapophyses (Figure 5.11d); thus, there is no developed hypantrum as in *Desmatosuchus spurensis* or *Aetobarbakinoides brasiliensis* (Parker, 2008b; Desojo et al., 2012). The ventral bar also occurs in *Stagonolepis robertsoni* (Walker, 1961: fig. 7j). Ventrolateral to the prezygapophysis there is a deep fossa termed the centroprezygapophyseal fossa (cprf), which is bordered posteriorly by the main strut of the transverse process (Figure 5.11b). Although the positions of these fossae are homologous with those of saurischian dinosaurs because they share distinct topological landmarks, it is not clear if these features are similarly related to the respiratory system (Wilson et al., 2011; Butler et al., 2012).

In posterior view, the postzygapophyses (best preserved in PEFO 34045/14-R) are also oriented about 45 degrees above the horizontal. They are triangular in posterior view with a well-developed lateral postzygodiapophyseal lamina (podl). That lamina extends laterally to the diapophysis and forms a broad dorsal shelf of the transverse process in dorsal view (Figure 5.11a). The shelf is wider proximally and significantly narrows

distally along the transverse process. Along the dorsal surface of the shelf, between the postzygapophyses and the neural spine is a pair of shallow postzygapophyseal spinodiapophyseal fossae (posdf).

The neural spine is short (32.3 mm) relative to the centrum height as in *Desmatosuchus spurensis* (MNA V9300) and *Typothorax coccinarum* (TTU P-9214). The spine is anteroposteriorly elongate, equal in length to the proximal portion of the neural arch, and the distal end is mediolaterally expanded (spine table). The anterior and posterior margins of the neural spine possess paired vertical spinoprezygapophyseal (sprl) and spinopostzygapophyseal (spol) laminae as in *Desmatosuchus spurensis* (MNA V9300).

The postzygapophyses bound deep oval spinopostzygapophyseal fossa (spof). This fossa is much taller than wide and is bounded laterally by thin, nearly vertical intrapostzygapophyseal laminae (tpol). These laminae meet medially at a thickened triangular area dorsal to the neural canal. Here the vertebra bears a strong posteriorly pointed projection that inserts into the ventral portion of the spinoprezygapophyseal fossa just above the ventral bar. That projection is also present in *Calyptosuchus wellesi* (e.g., UCMP 139795). Ventrolateral to the postzygapophyses there are two deep centropostzygapophyseal fossae (cpof) in the proximal portions of the transverse processes.

The transverse processes extend laterally with a length of 81.6 mm in PEFO 34045/FF-51. However, in two of the other vertebrae (PEFO 34045/14-R; PEFO 34045/19-V) the transverse processes are directed more dorsolaterally (Figures 5.11d-e).

This difference also occurs in *Stagonolepis robertsoni* (Walker, 1961) and occurs in the more anteriorly positioned trunk vertebrae. Furthermore, the ventral surface of the centrum in these two vertebra (PEFO 34045/14-R; 19-V) is more constricted forming a blunt ventral 'keel'. The keel and the orientation of the transverse process are the only visible differences between and anterior and mid-trunk vertebrae in *Scutarx deltatylus*.

Posterior trunk vertebrae

The currently available material of *Scutarx deltatylus* includes seven posterior trunk vertebrae; three from PEFO 34045, three from PEFO 31217, and one from PEFO 34919. As in *Desmatosuchus spurensis* (MNA V9300; Parker, 2008b), the posterior trunk vertebrae are much more robust than the anterior and mid-dorsals (Figures 5.11g-h; 5.12a-c). Notable differences between the mid- and posterior trunk vertebrae in *Scutarx deltatylus* include an increase in the height of the neural spines and a lengthening of the transverse processes, which coincide with the loss of distinct parapophyses and diapophyses along the series. Furthermore, the centra become anteroposteriorly shorter than they are dorsoventrally tall (Figure 5.11h). The neural spine characteristics are identical to those of the mid-trunk vertebrae with regard to the presence of the various vertebral laminae and associated fossae. An isolated posterior trunk vertebra from PEFO 31217 (Figure 5.12c) shows that the prezygodiapophyseal laminae are even more strongly developed and extend farther laterally. In that vertebra, the length ratio between the transverse process length (86.84 mm) and centrum width (53.26 mm) equals 1.63, thus the process is more than 1.5 times the width of the centrum. This is comparable to a ratio of 1.58 for the mid-trunk vertebrae.

This same vertebra from PEFO 31217 also lacks distinct diapophyses and parapophyses and a single-headed rib is fused onto the distal end of the process (Figure 5.12c). This is also seen in *Desmatosuchus spurensis* (Parker, 2008b) and in *Stagonolepis robertsoni* (Walker, 1961) and *Calyptosuchus wellesi* (UMMP 13950). An isolated posterior trunk vertebra from PEFO 34045 (Figures 5.12a-b) preserves the entire transverse processes and the associated fused ribs. However, the specimen differs from the previously described vertebra from PEFO 31217 in that the parapophysis and diapophysis are distinct and the rib is double-headed (Figures 5.12a-b). Although the ribs and transverse processes are fused, the fusion is incomplete; gaps are present within the individual articulations and a gap is apparent between the anterior surface of the distal end of the transverse process and the medial surface of the capitulum of the rib (Figure 5.12b). This suggests that several vertebrae in the posterior trunk series fuse with the ribs, and loss of a distinct parapophysis and diapophysis of the transverse process and of the tuberculum and capitulum of the dorsal ribs only occurred in the last one or two presacrals. Examination of UMMP 13950 (Case, 1932; Long and Murry, 1995) suggests that this loss occurs in the last three presacrals. In *Stagonolepis robertsoni* that condition occurs in the final two presacral vertebrae (Walker, 1961). There is no evidence in *Scutarx deltatylus* that the last presacral was incorporated into the sacrum as in *Desmatosuchus spurensis* (Parker, 2008b). The last presacral in PEFO 31217 also shows a distinct vertical offset in the ventral margins of the articular faces of the centra with the anterior face situated more ventrally. This is also the case in *Stagonolepis robertsoni* (Walker, 1961) and *Desmatosuchus spurensis* (Parker, 2008b).

Another posterior trunk vertebra, PEFO 34045/22 (Figures 5.11g-h), lacks the transverse processes, but preserves other key characteristics of the posterior presacrals. Its neural spine is taller (81.94 mm) than the height of the centrum (61.24 mm), differing from the condition in the anterior and mid-trunk vertebrae where the neural spine is shorter than the centrum (Figure 5.11g). This transition occurs at the beginning of the posterior trunk vertebrae series, because the specimen from PEFO 34045 with the fused ribs, but distinct rib facets (Figures 5.12a-b), has a centrum and neural spine of equal height. PEFO 34045/22 also preserves the pointed posterior projection above the neural arch that is present throughout the trunk series (Figure 5.11h).

Sacral vertebrae

A sacral vertebra, probably the second, is visible in ventral view in PEFO 31217 in articulation with the rest of the pelvis (Figure 5.13). It is recognizable by the presence of a strong, broad sacral rib that laterally expands anterodorsally to contact the posterodorsal margin of the left ilium. Unfortunately no other details are available for that specimen.

Caudal series.

Vertebrae

Eight vertebrae occur in semi-articulation in PEFO 31217 posterior to the sacral vertebra described above (Figure 5.13). The first two are robust with thick flaring rims on the centra. The first vertebra has a length of 57.3 mm, and its anterior face is indistinguishable from the posterior face of the preceding sacral vertebra. Furthermore,

the centrum is constricted which is unusual for an aetosaur, because the sacrals and anterior caudals usually have wide ventral surfaces (e.g., *Desmatosuchus spurensis*, MNA V9300). The vertebra in PEFO 31217 lacks a ventral groove and chevron facets. It is possible that this is a sacral vertebra that has been forced backwards, but the poor preservation of the specimen does not allow a firm determination. The second caudal vertebra (assuming the first described is from the caudal series) has a centrum length of 52.2 mm and a width of 61.6 mm, thus it is wider than long as is typical for the anterior caudals of aetosaurians (Long and Murry, 1995). The centrum is ventrally broad and a chevron is articulated to the posterior margin. The base of the caudal rib originates from the base of the neural arch, but laterally the rib is incomplete.

Two anterior caudal vertebrae are also known from PEFO 34045, which roughly correspond in morphology to the second and third caudal centra of PEFO 31217 (Figures 5.14a-f). These two vertebrae have blocky centra that are wider (flared centrum faces) than long. The ventral surfaces are broad, with a deep median trough bordered by two lateral ridges. These ridges terminate posteriorly into two posteroventrally facing hemispherical chevron facets (Figures 5.14d-e). The articular faces of the centra are round in anterior and posterior views, and in lateral view these faces are offset from each other (Figure 5.14f). The ventral margin of the posterior face is situated much farther ventrally than that of the anterior face, as is typical for aetosaurs (e.g., *Desmatosuchus spurensis*, MNA V9300). Although the neural spines are missing, it is apparent that the neural arch complex was much taller than the height of the centrum (Figure 5.14c). The neural canal is oval with a taller dorsoventral axis.

The pre- and postzygapophyseal stalks are thickened and the facets are closely situated medially. They are oriented at about 30 degrees from the horizontal. The neural arch is directed posterodorsally and the postzygapophyses project posteriorly significantly beyond the posterior centrum face (Figure 5.14c). The caudal vertebrae lack diapophyseal and zygapophyseal laminae, but spinozygapophyseal fossae occur between the prezygapophyses (Figures 5.14a-b). The caudal ribs are fully fused to the centrum. They are anteroposteriorly broad and dorsoventrally thin with flat dorsal surfaces and buttressed ventral margins. The ribs are directed slightly posteriorly and laterally they arc ventrally (Figures 5.14a-c). Unfortunately their lateral extent is unknown.

The third and fourth caudal vertebrae in PEFO 31217 are longer than wide, with the centrum narrowing mediolaterally and with reduced flaring of the rims as in the previous vertebrae (Figure 5.13). The posteroventral margins possess chevron facets. The caudal ribs are broad, flat, and were elongate, as in *Desmatosuchus spurensis* (MNA V9300), even though the distal ends are not preserved. The third centrum has a length of 56.4 mm and the fourth has a length of 56.4 mm. Details of the neural arches and spines are buried in the block and irretrievable by mechanical preparation.

The fifth and sixth caudal vertebrae are mostly concealed beneath armor, bone fragments, and what are probably the eighth and ninth caudal vertebrae. Only the left caudal ribs are apparent, jutting out of the block. They are dorsoventrally flat and laterally elongate, typical for aetosaurs, but they are poorly preserved and no other details are apparent.

The anterior face of what is probably the seventh caudal vertebra is visible underneath matrix and an osteoderm about six centimeters behind where the sixth caudal vertebra is buried in the block, breaking the line of articulation. The neural canal is prominent on this vertebra and what is visible of the neural arch shows that it was tall. The centrum is amphicoelous and mediolaterally constricted. The ventral surface consists of a median ventral groove bounded laterally by two sharp ridges. The ridges would terminate posteriorly with the chevron facets, but the relevant area is obliterated. A vertebra from approximately the same position is preserved in PEFO 34919 (Figures 5.15a-c) and provides more details.

The centrum is much longer than wide (57 mm to ~30 mm), mediolaterally compressed, and grooved ventrally. Its rims flare minimally, but the articular faces are deeply concave (Figure 5.15b-c). The neural arch is dorsoventrally shorter than in the more anteriorly positioned caudal vertebrae, but the neural spine was certainly tall in this position as well (Figure 5.15b). The zygapophyses are reduced and each pair is closely situated medially. The postzygapophyses do not project far posteriorly. The caudal rib is situated anteroventrally on the neural arch. It is broad and flat, extends laterally (~50 mm), and is slightly arcuate in anterior view (Figure 5.15b).

What are probably the eighth and ninth caudal vertebrae are well-preserved at the edge of the block in PEFO 31217 (Figure 5.13). The centra are much longer than wide. The ninth centrum has a length of 66.3 mm and a width of 40.2 mm. The lateral faces of the centrum are concave and, as on the preceding centra, the ventral face is narrow with a deep median groove terminating at the chevron facets. The neural arches and spines are

complete and tall, with a height of 100.9 mm in the eighth vertebra and 98.4 mm in the ninth. The neural spines are tall and roughly triangular in lateral view, with an anteroposteriorly broad base and tapering distally. The zygapophyses are closely situated medially and extend anteriorly and posteriorly beyond the articular faces of the centra. The caudal ribs are greatly reduced in lateral length.

An isolated vertebra from PEFO 34045 represents the mid-caudal series (Figure 5.15d). The centrum is longer than tall (65 mm to 35 mm) and mediolaterally compressed. Its articular faces are deeply concave and oval with the longest axis situated dorsoventrally. The neural arch is dorsolaterally reduced and mediolaterally compressed. The caudal ribs are greatly reduced and eroded. The neural spine is elongate, but its full dorsal extent is unknown (Figure 5.15d).

Chevrons

Only half of a single chevron and part of the head of a second are preserved in PEFO 34045 (Figures 5.16a-b). A few are smashed beneath other elements in PEFO 34919 and a badly preserved chevron is present beneath the second caudal vertebra of PEFO 31217. Although the details are poor the latter suggests, in accordance with the lack of facets on the first caudal vertebra of PEFO 31217, that chevrons started on the second centrum. This is different from the condition in *Desmatosuchus spurensis*, in which they first appear on the third caudal centrum (Parker, 2008b), but similar to the condition in *Typothorax coccinarum* (Heckert et al., 2010). The two preserved chevrons in PEFO 34045 are of the 'slim' elongate type and, therefore, from the anterior portion of the tail (Parker, 2008b).

Ribs

Presacral

No cervical ribs are preserved in any of the specimens, but trunk ribs are common. The sacral and caudal ribs have been described above along with their associated vertebrae. The anterior and mid-trunk ribs are double-headed (Figure 5.16c-d). They extend laterally for the first quarter of their total length and then sharply turn ventrolaterally, are straight for another two quarters of the length, and then gently turn more ventrally. Proximally the rib body is oval in cross-section, becoming ovate and then flattened more distally; it is broadest at the point of the sharp ventrolateral turn.

The capitulum is oval in cross-section, with a sharp posterior projection. The capitulum and tuberculum are separated along the neck by 44 mm. The dorsal surface of the neck is marked by a transverse groove that terminates at a fossa on the proximal surface of the tuberculum (Figure 5.16e). That groove probably hosted the ventral portion of the vertebrarterial canal as in *Alligator* (Reese, 1915). A thin flange of bone originates on the dorsal surface of the tuberculum and extends laterally, becoming confluent with the rib body just lateral to the ventrolateral hook. That flange forms a deep, elongate groove along the posterodorsal surface of the rib. Dorsally the rib is flattened and forms a thin anterior blade.The posteriormost ribs are single headed and fused with the transverse processes of the dorsal vertebrae (Figure 5.12c).

Gastralia

It has been suggested that aetosaurians lack gastralia (Nesbitt, 2011), but they are present in *Typothorax coccinarum* (Heckert et al., 2010). In that taxon (e.g., NMMNH P-

56299), the gastralia are preserved in the posteroventral portion of the thoracic region, are medially fused and laterally elongate. A single gastralia set is preserved in PEFO 34616 demonstrating that they were present in *Scutarx deltatylus* as well (Figure 5.16f). This set consists of incomplete but medially fused ribs with a short anterior projection.

Appendicular Girdles

Scapulocoracoid

The left scapulocoracoid is preserved in PEFO 31217; unfortunately the coracoid is covered by osteoderms that cannot be removed without causing significant damage, so only the dorsal-most portion of the coracoid where it sutures to the scapula, is visible. In lateral view the general outline of the scapula of PEFO 31217 (Figure 5.17a) strongly resembles the scapulocoracoid of *Stagonolepis robertsoni* (Walker, 1961: fig. 12a). The proximal end is expanded anterolaterally with the posterior projection situated more dorsally than the anterior projection. The posterior projection has a rounded posterior margin, as in *Stagonolepis robertsoni* (Walker, 1961) differing from the pointed projection in *Stagonolepis olenkae* (ZPAL AbIII/694). The anterior projection is poorly preserved but appears to be pointed as in *Stagonolepis robertsoni* (Walker, 1961). The scapular blade is gently bowed medially and the posterior edge is straight except for a slight posterior projection (the triceps tubercle) about 62 mm above the glenoid lip (Figure 5.17a). The anterior edge of the blade is straight for most of its length until it strongly flares anteriorly, forming a prominent deltoid ridge (=acromion process; Brochu, 1992; Martz, 2002). Below this there is a prominent foramen, although its anterior edge is broken away. Likewise the ventral margin of the posterior edge of the scapular blade

strongly flares posteriorly forming the supraglenoid buttress. The glenoid facet opens posteriorly. Laterally there is a sharp ridge, which probably represents deformation and crushing along the scapulocoracoid suture.

Ilium

Ilia are preserved in PEFO 34919 (right ilium) and PEFO 31217 (both ilia). The ilia of *Scutarx deltatylus* were oriented in life so that the acetabula faced ventrally; however, to avoid confusion in this description, the anatomical directions will be provided as if the reader is viewing the ventral surface laterally (see Figure 5.17b-c). The right ilium of PEFO 34919 is nearly complete, missing only a portion of the anterior margin of the acetabulum (Figures 5.17b-c). As usual for the bones from this specimen, the ilium is covered with a thin layer of weathered hematite that cannot be removed without damaging the underlying bone. The iliac blade is complete with a length of 196 mm and a mid-height of 66.8 mm. The 'dorsal' margin of the iliac blade is mediolaterally narrow, expanding anteriorly so that the dorsal margin of the anterior process is thicker and more robust than the rest of the blade. The anterior portion of the iliac blade is triangular in lateral view, and does not extend anteriorly beyond the edge of the pubic peduncle. There is a prominent recess on the dorsal surface between the supraacetabular crest and the posterior iliac blade (Figure 5.17b) that appears to be unique to *Stagonolepis deltatylus*.

The posterior portion of the iliac blade quickly narrows in its dorsoventral height posteriorly, terminating in a point. From there the posteroventral margin slopes anteroventrally into a curving posterior margin that distally hooks posteriorly and

thickens to form the ischiadic peduncle. The posterior projection of the ischiadic peduncle is proportionally larger and more pointed than the same structure in *Aetosauroides scagliai* (PVL 2073) and *Stagonolepis robertsoni* (NHMUK R4789a), and more like that of TMM 31100-1, which represents a desmatosuchine aetosaurine. The ventral margins of the pubic and ischiadic peduncles meet at an angle of 90 degrees ventral to the acetabulum, with the ilium contributing to the majority of the acetabulum. In ventral view the margins of the peduncles are comma-shaped, thinning into the ventral margin of the broadly concave acetabulum. The medial side of the acetabulum is smooth and slightly convex.

Dorsal to the iliac neck, the medial side of the posterior portion of the iliac blade bears a prominent ventral ridge that forms a shelf for sacral rib articulation (Figure 5.17c). The rib scar is situated just above the ridge and forms a concave sulcus that extends anteriorly to just dorsal to the anterior margin of the neck.

Both ilia are present in PEFO 31217 as portions of a complete sacrum. Of the two the left is the better preserved. The acetabula are deeply concave and oriented ventrally (Figure 5.13). Originally this was thought to be the result of crushing of the pelvis; however, the acetabula are oriented ventrally in many other uncrushed aetosaurian specimens including *Aetosauroides scagliai* (PVL 2073) and the holotype of *Typothorax antiquum* (Lucas et al., 2003a). The supraacetabular ridge in these ilia is strongly produced, but not as strong as in rauisuchids. As in PEFO 34919 there is a deep fossa/recess on the dorsal surface between the supraacetabular ridge and the posterior portion of the iliac blade, a condition that appears to be autapomorphic for this taxon.

That fossa is bordered posteroventrally by the thickened margin of the neck, a feature which is ventrally confluent with the ischiadic peduncle. The left iliac blade measures 188.6 mm in length and 67.4 mm in height, producing a relatively tall iliac blade. The posterior portion of the iliac blade has a posterior margin that projects well beyond the iliac peduncle. The extent of the ventral portions of the ilia is hard to determine because they are indistinguishably fused to the ischia and pubes; however, the left acetabulum is more or less rounded, 116.5 mm tall and 111 mm wide.

Ischium

The left ischium and part of the right are present, but poorly preserved. The ischium consists of the main body with a sharp, rounded acetabular rim, and an elongate posterior process. The upper margin of the posterior process slopes gradually from the posterior margin of the ischiadic peduncle, and the entire ischium measures 183 mm in length. The anteroventral margin is flat where the two ischia are fused, forming a wide, slightly concave ventral shelf. Overall the ischium is similar to that of other aetosaurians such as *Stagonolepis robertsoni* (Walker, 1961), but lacks the prominent ventral kink found in *Desmatosuchus spurensis* (MNA V9300; Parker, 2008b).

Pubis

Both pubes are present and in articulation with the pelvis although they are moderately distorted by crushing and were damaged by weathering before collection. The body of the pubis consists of an elongate, narrow ’tube‘ that curves anteroventrally and expands medially into two broad sheets of bone that meet in a median symphysis. This pubic apron is convex anteriorly and concave posteriorly. It is dorsoventrally short,

barely extending past the ventral margin of the puboischiadic plate, more like the condition in *Typothorax coccinarum* (Long and Murry, 1995) rather than the extremely deep pubic apron found in *Desmatosuchus spurensis* (MNA V9300). Two distinct oval foramina pierce the pubic apron in the proximal part of the element. The bone is broken around the more anterior foramen of the right pubis, but it is clear that it was the larger of the two openings (Figure 5.13). Two pubic foramina are also described for *Stagonolepis robertsoni* (Walker, 1961), and the upper (anterior) opening considered homologous to the single foramen found in other aetosaurs (e.g., MNA V9300, *Desmatosuchus spurensis*). The distal ends of the pubes are shaped like elongate commata, narrow and curving into the symphysis (Figure 5.13), different from the strong, knob-like projections (pubic boots) found in *Desmatosuchus spurensis* (MNA V9300).

Osteoderms

Paramedian osteoderms

Cervical

Cervical osteoderms are present in PEFO 31217, PEFO 34045, and PEFO 34616. All of the osteoderms are wider than long (w/l ratio of 1.85). The cervical osteoderms are dorsoventrally thick with well-developed anterior bars (sensu Long and Ballew, 1985), which bear prominent anteromedial projections. The lateral edges are strongly sigmoidal, and lack anterolateral projections (Figures 5.18a, c; 5.19a).

The dorsal surface is relatively featureless, with the ornamentation poorly developed. The dorsal eminence is low, broad, and mounded, contacting the posterior plate margin (Figures 5.18a, c). The eminence is also offset medially, closer to the

midline margin. The characteristic triangular protuberance that diagnoses *Scutarx deltatylus* is present in the posteromedial corner of the osteoderm, but is greatly reduced in area (Figure 5.18c). In the cervical paramedian osteoderms the shape of that protuberance is more of a right triangle than the equilateral triangles found in the trunk series (see below).

In posterior view, the osteoderms are gently arched (Figures 5.18b, d). The median margins are sigmoidal in medial view and dorsoventrally thick as is typical for aetosaurians. *Scutarx deltatylus* lacks the 'tongue-and-groove' lateral articular surfaces present in *Desmatosuchus* (e.g., MNA V9300) and *Longosuchus meadei* (TMM 31185-84b).

The more posterior cervical paramedian osteoderms are similar, but increase in width (w/l ratio of 2.05) and lack the strongly sigmoidal lateral margin. The margin is still sigmoidal but bears a strong anterolateral projection (Figure 5.19a). Moreover, the anterior and posterior plate margins are gently curved anterolaterally. In posterior view, these osteoderms have a lesser degree of arching and are dorsoventrally thinner than the more anteriorly situated osteoderms. The dorsal eminence is strongly offset medially and slightly more developed, becoming raised and more pyramidal in shape, although this could be an individual variation (see description of caudal paramedian osteoderms).

Trunk

The osteoderm transition between the cervical and trunk series is difficult to identify, but anterior dorsal trunk osteoderms are considered here to have higher width/length ratios and be dorsoventrally thinner than the cervical paramedian osteoderms. Furthermore, the triangular protuberance is more equilateral. However, it is difficult to differentiate these osteoderms from those of the anterior caudal region.

Osteoderms with the maximum width/length ratio (2.72) are found in the mid-trunk region. They bear a strongly raised anterior bar with prominent anteromedial and anterolateral projections. The dorsal eminence is medially offset, and forms a broad, low mound. Anterior to this on the anterior bar is a prominent, pointed anterior projection. The area of the anterior bar medial to this process is 'scalloped out,'and is deeply concave. The length of the anterior bar decreases significantly within the arc of this concavity. The triangular protuberance is equilateral (Figures 5.18e-k).

The lateral margin is sigmoidal, and the anterior portion just posterior to the anterior bar is slightly embayed for slight overlap of the associated lateral osteoderm. In posterior view the osteoderm is only slightly arched Figure 5.18h). In what are presumed to be more posteriorly positioned osteoderms, the osteoderme is more strongly arched (Figures 5.18l, m). The ventral surface of the dorsal trunk paramedian osteoderms are smooth, with a slight embayment situated on the underside of the dorsal eminence.

The surface ornamentation of the dorsal trunk paramedian osteoderms is barely apparent in PEFO 34045, but much better developed in the other specimens. The ornament consists of pitting surrounding the dorsal eminence and radiating grooves and ridges over the rest of the surface.

There is no direct evidence for a constriction ('waist') in the carapace anterior to the pelvis as in *Aetosaurus ferratus* (Schoch, 2007), and *Calyptosuchus wellesi* (Case, 1932); however, because the lateral osteoderm shapes in *Scutarx deltatylus* are identical to those of *Calyptosuchus wellesi* (see description below), it is probable that *S. deltatylus* also possessed a 'waisted' carapace although this cannot be confirmed.

Caudal

Like the cervical-trunk transition, the trunk-caudal transition is also difficult to determine in unarticulated aetosaurian carapaces (Parker, 2008b). The latter transition is generally characterized by reduction of osteoderm width-length ratios and greater development of the dorsal eminences (Heckert and Lucas, 2003). The extreme is found in *Rioarribasuchus chamaensis*, in which the barely visible dorsal eminences in the mid-dorsal region transition posteriorly to elongate, anteromedially curved spines in the anterior caudal region (Parker, 2007).

The trunk-caudal transition for *Scutarx deltatylus* is best preserved in PEFO 34919 in which the dorsal eminences show a marked increase in height from 16.35 in the mid-trunkregion to 40.07 mm in the anterior dorsal caudal region. Width/length ratios across this same transition are 2.54 to 2.16, showing the corresponding decrease. The dorsal eminence is a tall pyramid, with a posterior vertical keel (Figure 5.20). In all other respects the anterior caudal osteoderms are similar to those of the trunk region.

Dorsal mid-caudal paramedians are relatively equal in width and length (w/l ratio = 1.08). Those osteoderms still possess the pronounced dorsal eminence (Figures 5.21a-j), as well as the anteromedial and anterolateral projections of the anterior bar. In PEFO 34045 these osteoderms are extremely thickened (Figures 5.21a-b, e-f).

The posterior dorsal caudal paramedians (Figures 5.21k-n) become longer than wide (w/l ratios of 0.73 and 0.66), and the dorsal eminence is reduced to a raised, anteroposteriorly elongate keel with a posterior projection that extends beyond the posterior margin of the osteoderm. Presumably these continue until they become elongate strips of bone as in *Aetosaurus ferratus* (Schoch, 2007).

Lateral osteoderms

The best guide for the distribution of the lateral osteoderms is UMMP 13950, the holotype of *Calyptosuchus wellesi*, which preserves the posterior dorsal armor and much of the caudal lateral armor in articulation (Case, 1932). *Scutarx deltatylus* possesses lateral plates that are identical in shape to those of *Calyptosuchus wellesi* allowing for determination of caudal and posterior dorsal osteoderms. Therefore, any lateral osteoderms falling outside of those morphotypes probably are from more anterior regions. Anterior dorsal lateral osteoderms are preserved in the articulated holotype of *Aetosauroides scagliai* (PFV 2073), which can be used to help assign isolated osteoderms.

Lateral osteoderms can be distinguished from paramedian osteoderms primarily by the lack of the prominent anterolateral projection. Furthermore, the anteromedial corner of the osteoderm is 'cut-off' and beveled for reception of the anterolateral projection of the associated adjacent paramedian osteoderm (poa; Figure 5.22).

Cervical

There are no lateral osteoderms in the material present that can unequivocally be assigned to the cervical region.

Trunk

Anterior lateral trunk osteoderms are not preserved in the holotype of *Calyptosuchus wellesi*, but they are preserved in *Aetosaurus ferratus* (Schoch, 2007). In *Aetosaurus* those osteoderms are strongly asymmetrical with the dorsal flanges roughly half the dimensions of the lateral flanges. Furthermore, the dorsal flanges are triangular

or trapezoidal in dorsal view rather than rectangular, with a slight, medially projecting posterior tongue.

Two osteoderms from the left side in PEFO 34616 and a third from the right side in PEFO 34045 match this anatomy and are probably from the anterior portion of the carapace (Figures 5.22a-d). In addition to the features just mentioned, those osteoderms possess a distinct anterior bar. The anteromedial corner of the anterior bar is beveled for articulation with the anterolateral process of the paramedian osteoderm. The dorsal eminence of the lateral osteoderm is a prominent pyramidal boss that contacts the posterior plate margin and extends anteriorly, covering two-thirds of the osteoderm length. Surface ornamentation consists of elongate grooves and ridges radiating from the dorsal eminence. In posterior view, the osteoderms are only slightly angulated, with the angle between flanges strongly obtuse (Figure 5.22b, d). Similarly shaped osteoderms are found in the anterior lateral trunk region of *Aetosauroides scagliai* (PVL 2073).

Posterior-mid trunk osteoderms (from roughly the ninth through 12th positions) are sub-rectangular with a distinct, posteromedially sloping lateral edge (Figures 5.22e-h; Case, 1932). The dorsal flange is sub-rectangular in dorsal view. The medial edge of the dorsal flange is beveled and slightly sigmoidal with a 'cut-off' anterior corner for the anterolateral projection of the paramedian plate. The osteoderm is moderately flexed with the lateral flange extending at about 45 degrees relative to to the dorsal flange (Figures 5.22f, h). Both flanges are roughly the same size although the sloping lateral edge produces a small anteromedial 'wing' that extends that edge a bit farther laterally and provides a trapezoidal shape for the lateral flange (alw; Figures 5.22e, g). The dorsal eminence is pyramidal, and the degree of its development differs between specimens, from a low mound in PEFO 34045 to a distinct tall, triangular boss in PEFO 34919. On the dorsal surface a distinct anterior bar is present and the surface ornamentation consists

of small pits and elongate grooves radiating from the dorsal eminence. Ventrally the osteoderms are smooth, except for longitudinal striations along the posterior margin where this margin would overlap the anterior bar of the preceding lateral osteoderm.

The posteriormost lateral trunk osteoderms (15th and 16th positions) are similar to the posterior mid-trunk osteoderms but lack the anterolateral 'wing' and are much more strongly flexed, enclosing an angle of approximately 90 degrees in posterior view (Figures 5.22i-j). They are similar to the posterior lateral trunk osteoderms in *Calyptosuchus wellesi* (Case, 1932).

Caudal

Caudal lateral osteoderms are more equal in dimension, and bear rectangular dorsal flanges (Figures 5.22k-p). The angle enclosed between the dorsal and lateral flanges is about 45-50 degrees (Figures 5.22l, n, p). Overall these osteoderms possess some of the same surficial features as the other osteoderms, such as an anterior bar, radial ornamention, and a posteriorly placed dorsal eminence. However, the anterior caudal osteoderms in some specimens (e.g., PEFO 34919) possess some of the tallest dorsal eminences in the carapace (Figures 5.20; 5.22n). The caudal lateral osteoderms also decrease in width posteriorly (Figure 5.22m, n). The height of the dorsal eminence is gradually reduced and becomes and elongate sharp ridge.

Ventral trunk osteoderms

Ventral trunk osteoderms are preserved in all of the PEFO specimens, including an articulated, but badly preserved, set in PEFO 31217. They consist mainly of square to rectangular osteoderms, with reduced anterior bars, no dorsal eminence and a surface

ornamentation of pits and elongated pits in a radial pattern (Figures 5.23a-f). Because no complete set is preserved the exact numbers of rows and column cannot be determined.

Appendicular osteoderms

A few irregular, small, rounded osteoderms most likely represent appendicular osteoderms that covered the limbs. There are two types: one featureless except for a distinct raised keel, and the other with a surface ornamentation of radial pits (Figures 5.23g, i). A triangular osteoderm (Figure 5.23h) from PEFO 34616 could represent a different type of appendicular osteoderm, or it could also be an irregularly shaped osteoderm from the ventral carapace.

Broken osteoderms?

An interesting aspect of PEFO 34045 is the presence of many irregularly shaped osteoderms recovered with the specimen (Figure 5.24). All of the edges on these osteoderms are compact bone and do not represent recent breaks. Close examination shows that these specimens are the lateral ends of dorsal paramedian osteoderms because they possess anterior bars with strong anterolateral projections and sigmoidal edges (Figures 5.24a-d). It is unclear why these osteoderms are incomplete but two possibilities exist. The first possibility is that these osteoderms were incompletely ossified. Alternatively, they were broken and then the edges rehealed during the life of the animal. However, there is no visible sign of pathology because the edges are smooth and the dorsoventral thickness of the osteoderms remains constant. The osteoderms are also from opposite sides of the body precluding a cause from a single injury if they are pathologic

in nature. Histological examination could help determine the ontogeny of these elements. If growth rings are uniform throughout the specimen, it would demonstrate that either damage occurred at a young age or that the remainder of the element did not ossify. If the osteoderms were broken at a later ontogenetic stage and healed, then that should be reflected in the bone histology showing a disruption in the growth rings, or establishment of new rings along the broken edge.

DISCUSSION

Scutarx deltatylus represents another good example of the importance of utilizing a detailed apomorphy-based approach to differentiate Late Triassic archosauromorph taxa (e.g., Nesbitt et al., 2007; Nesbitt and Stocker, 2008; Stocker, 2010). The material here referred to *Scutarx deltatylus* was originally assigned to *Calyptosuchus wellesi* (Long and Murry, 1995; Parker and Irmis, 2005; Parker and Martz, 2011, Martz et al., 2013), which was differentiated from *Stagonolepis robertsoni* by the presence of the triangular protuberance on the paramedian osteoderms (Martz et al., 2013). However, reexamination of the holotype of *Calyptosuchus wellesi* (UMMP 13950) as well as referred material from the *Placerias* Quarry of Arizona shows that material of *Calyptosuchus wellesi* actually lacks the triangular protuberance. Moreover, the skull of *Scutarx deltatylus* possesses characters of the braincase (e.g., foreshortened parabasisphenoid) that are more similar to *Desmatosuchus* than to other aetosaurians that are similar to *Stagonolepis*. Unfortunately, the skull of *Calyptosuchus wellesi* is still unknown. The *Placerias* Quarry contains a number of isolated aetosaurian skull bones, most notably basicrania, with differing anatomical characteristics, but none of these can be ascribed with certainty to *Calyptosuchus wellesi*. Nonetheless, prior to the discovery

of the skull of *Scutarx deltatylus*, *Calyptosuchus wellesi* was assumed to have a skull more like that of *Stagonolepis robertsoni* and *Aetosauroides scagliai* (i.e., with an elongate parabasisphenoid). That assumption can no longer be maintained. The presence of a aetosaurian with armor similar to *Stagonolepis*, but with a skull more like that of desmatosuchians provides further support that certain characteristic of the armor that were once used to unite taxa, such as paramedian osteoderm ornamentation (Long and Ballew, 1985; Long and Murry, 1995; Heckert and Lucas, 2000), may have wider distributions across Aetosauria than previously recognized (Parker, 2008a). I explore this in a separate analysis (Chapter 6).

Assigning Names to Genera

The genus-level name is possibly the most subjectively determined rank of the Linnaean taxonomic system (e.g., Clarke, 2004; Stuessy, 2009; Vences et al., 2010); however, the current enacted taxonomic codes (e.g., the International Code of Zoological Nomenclature [ICZN]) require establishment of the Linnaean binomial name including a distinct generic name. Yet, despite the voluminous amount of published literature dedicated to the 'species problem' (see Mayden, 1997; Wiens, 2004; de Queiroz, 2007 and references therein), comparatively little is written regarding concepts of how to delimit genera. To be descriptively useful a genus-group taxon should be 1) monophyletic, 2) reasonably compact (i.e., not containing too many species-group taxa), and 3) ecologically, morphologically, or biologically distinct (Gill et al., 2005). This fits well with the traditional view that a genus is an assemblage of species that have more significant features in common amongst themselves then with any other species (Stuessy,

2009). Review of recent volumes (2010) of the Journal of Vertebrate Paleontology demonstrates that many paleontologists accept that genera should be monophyletic, and that paraphyletic genera may require new taxonomic names at the genus-level (e.g., Lyson and Joyce, 2010; Maxwell, 2010; Cadena et al., 2010). However, this approach tends to result in the erection of monotypic genera (e.g., Lyson et al., 2010; Cadena et al., 2010), which has been considered problematic by some workers (e.g., Platnick, 1976, 1977a, b; de Queiroz and Gauthier, 1992; Loeuille et al., 2014).

It has been argued that monotypic genera are paraphyletic because if speciation originates from a cladogenesis event the monotypic genus "must exclude at least one other species that is a descendent of the most recent common ancestor" (Platnick, 1976:198). However, it can be assumed that at one point in their history (through the speciation of their common ancestor) all higher taxa must have been monotypic; therefore if they are currently monophyletic they must have always been so (Wiley, 1977). However, monophyletic higher taxa do not come into existence until a speciation event splits the ancestral taxon into two new entities (Platnick, 1977b). Nonetheless, it would seem that if a single species consists of a monophyletic grouping of organisms (specimens), then the inclusive monotypic genus-group taxon (technically defined the same as the species-group taxon) must also be monophyletic.

Monotypic genera have also been criticized as redundant because they offer no information regarding phylogenetic relationships at the genus level, in that they do not provide an operational name for a clade of terminal taxa (e.g., de Queiroz and Gauthier, 1992; Lee, 2003; Dayrat et al., 2008). In a phylogenetic study utilizing only terminal taxa

at the genus-group level, the structure of branching events in the phylogenetic analysis requires that in the outermost nodes of the recovered tree each terminal taxon should have a sister taxon at roughly the equivalent taxonomic level. Thus, it appears fair to assume that if genera are to be treated as clades, then all of the species within these clades should be provided the same genus-level name (e.g., Clarke, 2004; Lyson and Joyce, 2010; Stocker, 2013a). However, choosing the node at which to define these genera is subjective. This is of extreme importance because the genus-group level is often the taxonomic level utilized in higher level studies exploring biostratigraphy, biochronology, biogeography, and extinction. Thus it is important that genus-level taxa are not only monophyletic, but also that they only define stable clades (Lucas and Kondrashov, 2004; Vences et al., 2010). Within Aetosauria, *Scutarx deltatylus* appears to share the most anatomical features with *Calyptosuchus wellesi* (Parker and Irmis, 2005; Parker and Martz, 2011). The phylogenetic analysis from this study (Chapter 6) supports a close relationship between *Scutarx deltatylus* and *Adamanasuchus eisenhardtae*; however, it also demonstrates that as the sister taxon to *Scutarx* + *Adamanasuchus*, *Calyptosuchus welle*si is also very closely related. Therefore, it is plausible that these three species could all be assigned to the genus *Calyptosuchus*, as this is the oldest valid genus-level name available. However, overall clade support is weak and consideration of the results recovered from past studies that provide modifications to existing phylogenies of the Aetosauria (e.g, Desojo et al., 2012; Heckert et al., in press) strongly demonstrates that future modifications to character scoring or the addition of new taxa could significantly alter the constituency of this clade and the position of those individual taxa.

Monotypic genera tend to indicate unclear relationships between species through a lack of synapomorphies (i.e., the monotypic taxon is highly autapomorphic) or a lack of resolution between a group of taxa (i.e., polytomous phylogenetic relationships) (Loeuille et al., 2014). When first developed, the purpose of the genus-level rank was to serve as a means to group what were hypothesized to be closely related species. With the advent of phylogenetic systematics this role is no longer required as the individual trees determine relationships not the first name of the given binimen. Autapomorphic taxa that do not fit readily into existing monophyletic groups (i.e., genus-level terminals) should be coded separately in phylogenetic analyses, so that their relationships can be tested *a posteriori* (Schrire and Lewis, 1996). In cases where recovered genus-level clades are unstable and the exact internal relationships ambiguous, it is probably best to erect monospecific taxa to promote taxonomic stability and eliminate the ambiguity caused by frequent shifting of species within genera (Martz and Small, 2006; Vences et al., 2010). This in turn can provide clarity to and avoid compounded analytical mistakes in higher level studies that utilize supraspecific taxa (e.g, biostratigraphy and biogeography).

Implications for Late Triassic Vertebrate Biochronology

The holotype and all of the referred specimens of *Scutarx deltatylus* were originally assigned to *Calyptosuchus wellesi* (Long and Murry, 1995; Parker and Irmis, 2005; Parker and Martz, 2011; Martz et al., 2013), a proposed index taxon of the Adamanian biozone (Lucas and Hunt, 1993; Parker and Martz, 2011), which is earliest Norian in age (Irmis et al, 2011). However, all of the recognized specimens of *Scutarx*

deltatylus originate only from the Adamanian portion of the Sonsela Member of the Chinle Formation and the middle part of the Cooper Canyon Formation of Texas (Parker and Martz, 2011; Martz et al., 2013). The reassignment of this material restricts the stratigraphic range of *Calyptosuchus wellesi* to the Bluewater Creek and Blue Mesa members of the Chinle Formation as well as the Tecovas Formation of Texas (Long and Murry, 1995; Heckert, 1997), which are stratigraphically lower than the Sonsela Member and middle part of the Cooper Canyon (Martz et al., 2013).

It has been suggested that the Adamanian biozone (*sensu* Parker and Martz, 2011) can possibly be subdivided into sub-zones (Martz et al., 2013). Those authors provided a list of Adamanian taxa of the Chinle Formation, and noted which are known solely from the Blue Mesa Member and which are known only from the lower part of the Sonsela Member. The list of taxa shared by both units is small and consists of *Placerias hesternus* (a dicynodont synapsid), the archosauromorph *Trilophosaurus dornorum*, the poposaurid *Poposaurus gracilis*, a paratypothoracin aetosaur similar to *Tecovasuchus chatterjeei*, and *Calyptosuchus wellesi* (Martz et al., 2013). The reassignment of the Sonsela material previously placed in *Calyptosuchus wellesi* to a new taxon further reduces that list. *Scutarx deltatylus* also occurs in the upper Adamanian Post Quarry of Texas, which contains taxa elsewhere only found in the lower part of the Sonsela Member (e.g., *Desmatosuchus smalli*, *Trilophosaurus dornorum*, *Typothorax coccinarum*, *Paratypothorax* sp.; Martz et al., 2013). Thus, *Scutarx deltatylus* can presently be considered an index taxon of the upper Adamanian biozone.

CONCLUSIONS

Scutarx deltatylus is a new taxon of aetosaurian from the middle Norian (late Adamanian) of the American Southwest that was originally assigned to *Calyptosuchus wellesi*. This taxon is known from several carapaces as well as rare skull material rom western North America. *Scutarz delatatylus* differs from all other aetosaurians in the presence of a raised triangular boss in the posteromedial corner of the presacral paramedian osteoderms, a dorsoventrally thickened skull roof, and an anteroposteriorly shortened parabasisphenoid. A phylogenetic analysis (Chapter 6) places it as the sister taxon of *Adamanasuchus eisenhardtae* near the base of Desmatosuchinae. *Scutarx deltatylus* is further evidence of the distinctness of the western North American material from *Stagonolepis robertsoni*, and appears to have utility as an index taxon for the late Adamanian biozone.

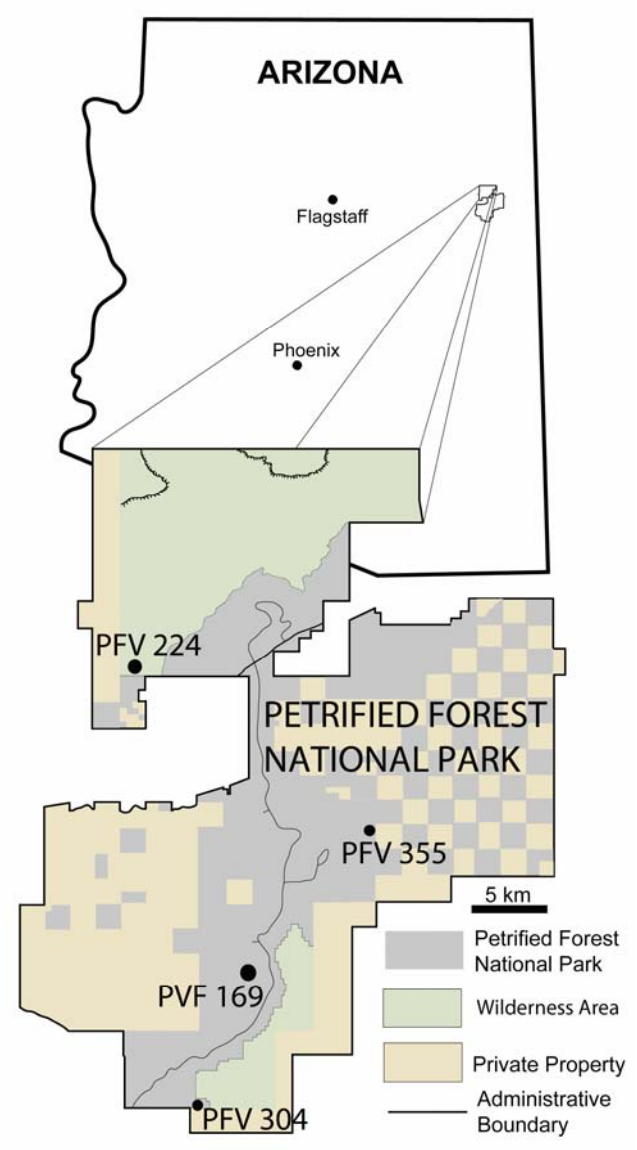

Figure 5.1. Map of Petrified Forest National Park showing relevant vertebrate fossil localities. Modified from Parker and Irmis (2005).

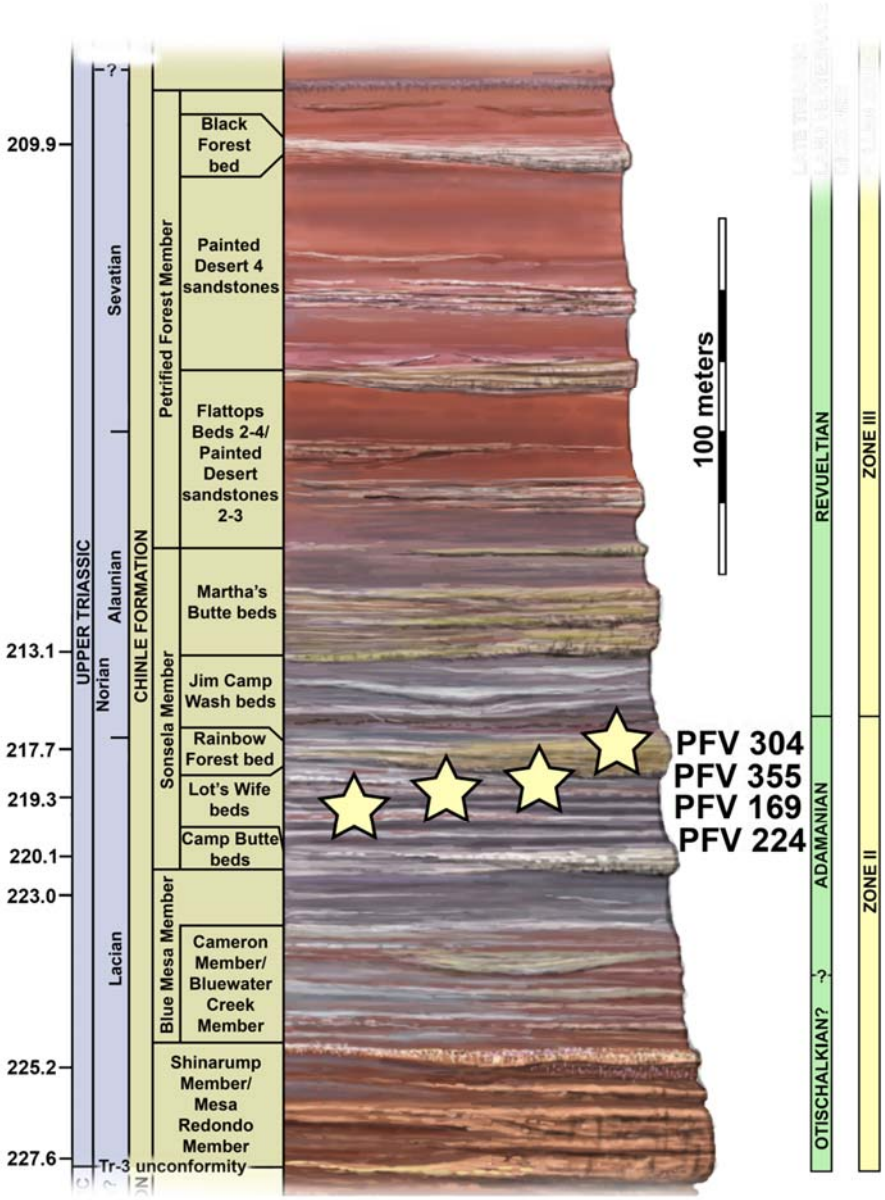

Figure 5.2. Regional stratigraphy of the Petrified Forest area showing the stratigraphic position of the localties discussed in the text. All occurrences are in the lower part of the Sonsela Member of the Chinle Formation and are within the Adamanian biozone. Stratigraphy from Martz and Parker, 2010. Biozones from Parker and Martz, 2011 and Reichgelt et al., 2013. Ages from Ramezani et al., 2011 and Atchley et al., 2013.

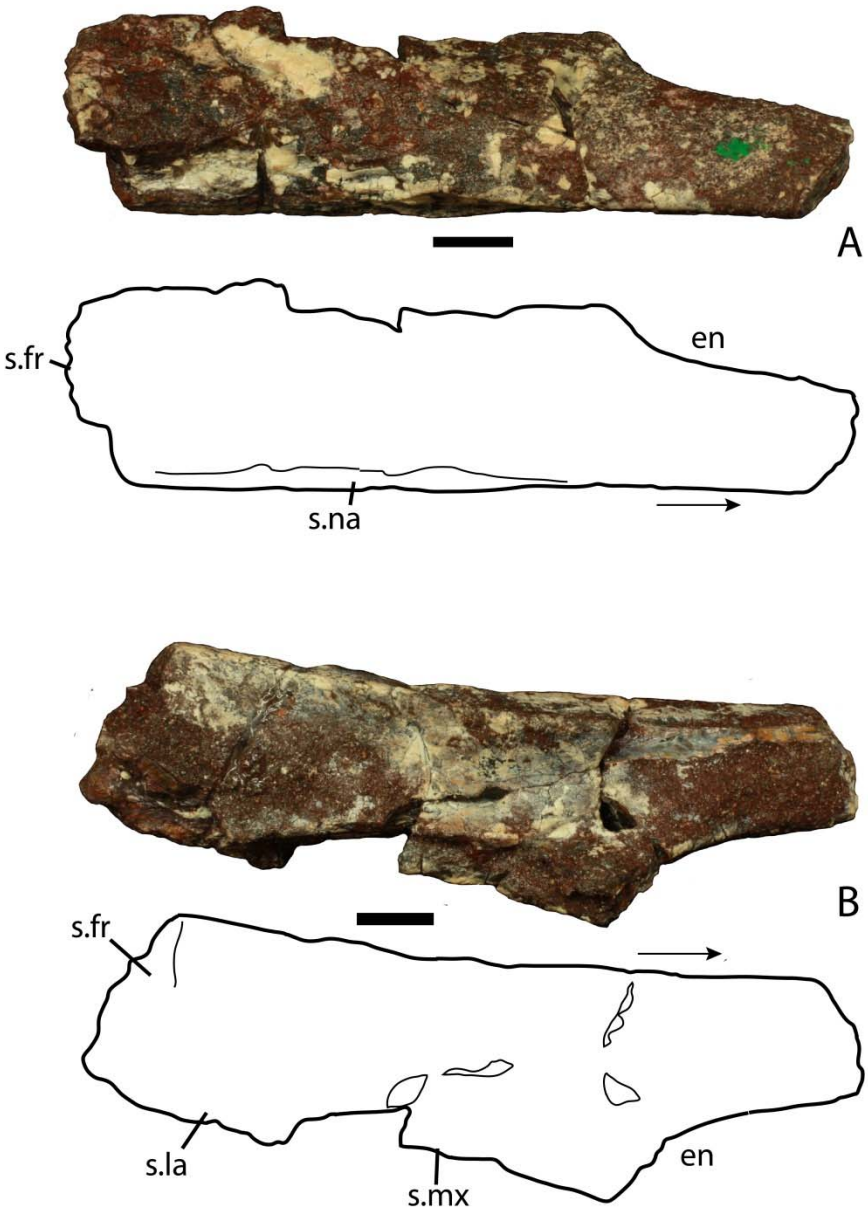

Figure 5.3. Photos and interpretive sketches of the left nasal (PEFO 34616) in dorsal (A) and ventral (B) views. Arrows point anteriorly and scale bars equal 1 cm. Abbreviations: en, external nares; fr, frontal; la, lacrimal; mx, maxilla; s., suture with listed element.

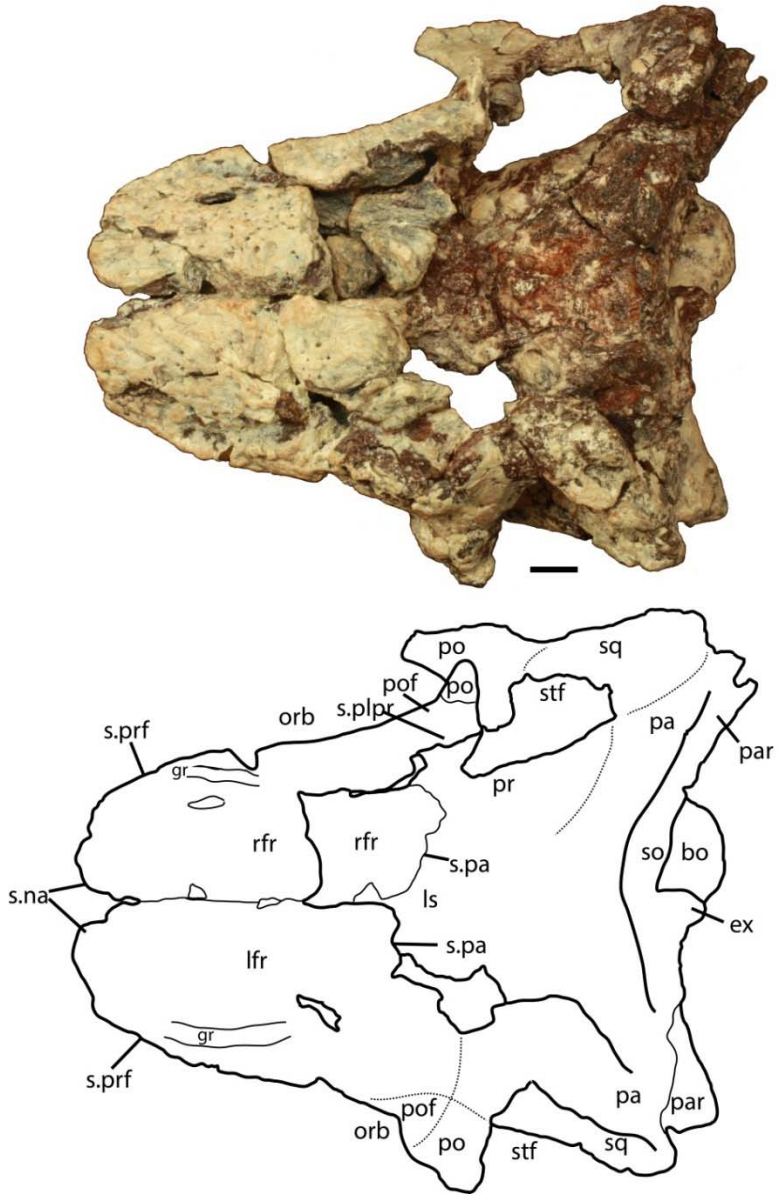

Figure 5.4. Photo and interpretive sketch of posterodorsal portion of the skull of *Scutarx deltatylus* in dorsal view. Scale bar equals 1 cm. Abbreviations: bo, basioccipital; gr, groove; ex, exoccipital; lfr, left frontal; ls, laterosphenoid; na, nasal; orb, orbit; pa, parietal; par, paroccipital process of the opisthotic; plpr, palpebral; po, postorbital; pof, postfrontal; pr, prootic; prf, prefrontal; rfr, right frontal; s., suture with listed element; so, supraoccipital; sq, squamosal; stf; supratemporal fenestra.

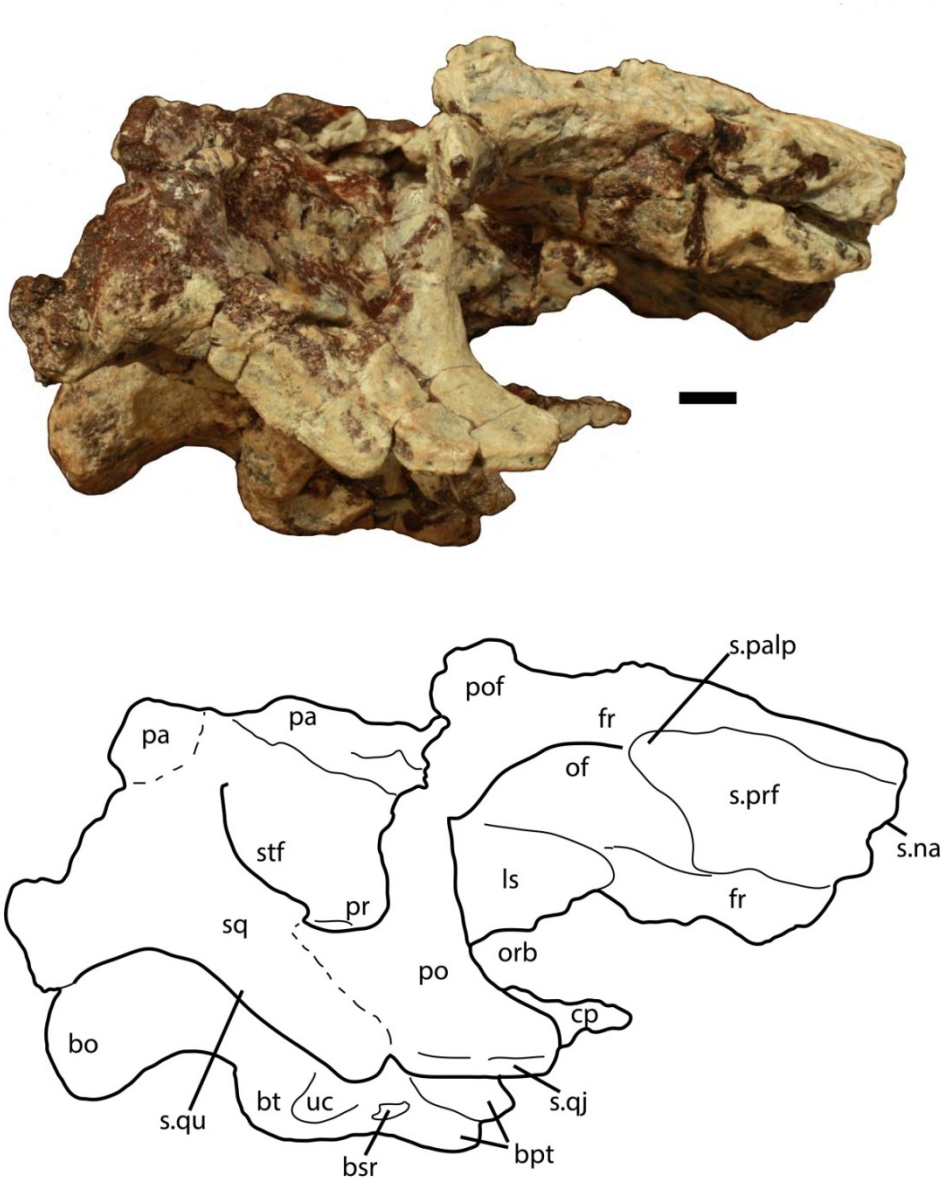

Figure 5.5. Partial skull of *Scutarx deltatylus* (PEFO 34616) in right lateral view. Scale bar equals 1 cm. Abbreviations: bo, basioccipital; bpt, basipterygoid processes; bsr, basisphenoid recess; bt, basal tubera; cp, cultriform process; fr, frontal; ls, laterosphenoid; na, nasal; of, orbital fossa; orb, orbit; pa, parital; palp, palpebral; po, postorbital; pof, postfrontal; pr, prootic; prf, prefrontal; qj, quadratojugal; qu, quadrate; sq, squamosal; stf, supratemporal fenestra; uc, unossified cleft of the basal tubera.

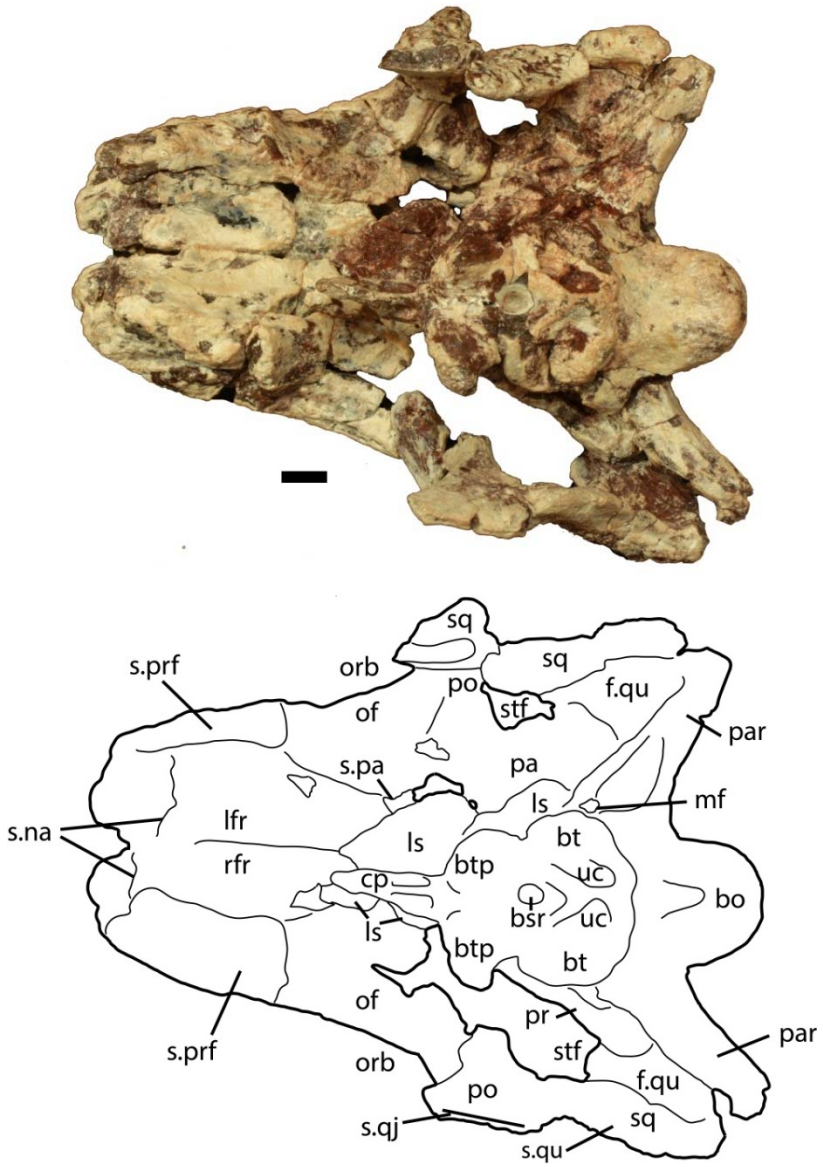

Figure 5.6. Partial skull of *Scutarx deltatylus* (PEFO 34616) in ventral view. Scale bar equals 1 cm. Abbreviations: bo, basioccipital; btp, basipterygoid processes; bsr, basisphenoid recess; bt, basal tubera; cp, cultriform process; f., fossa for specified element; lfr, left frontal; ls, laterosphenoid; mf, metotic fissure; na, nasal; of, orbital fossa; orb, orbit; pa, parietal; palp, palpebral; par, paroccipital process of the opisthotic; po, postorbital; pof, postfrontal; pr, prootic; prf, prefrontal; qj, quadratojugal; qu, quadrate; rfr, right frontal; sq, squamosal; stf, supratemporal fenestra; uc, unossified cleft of the basal tubera.

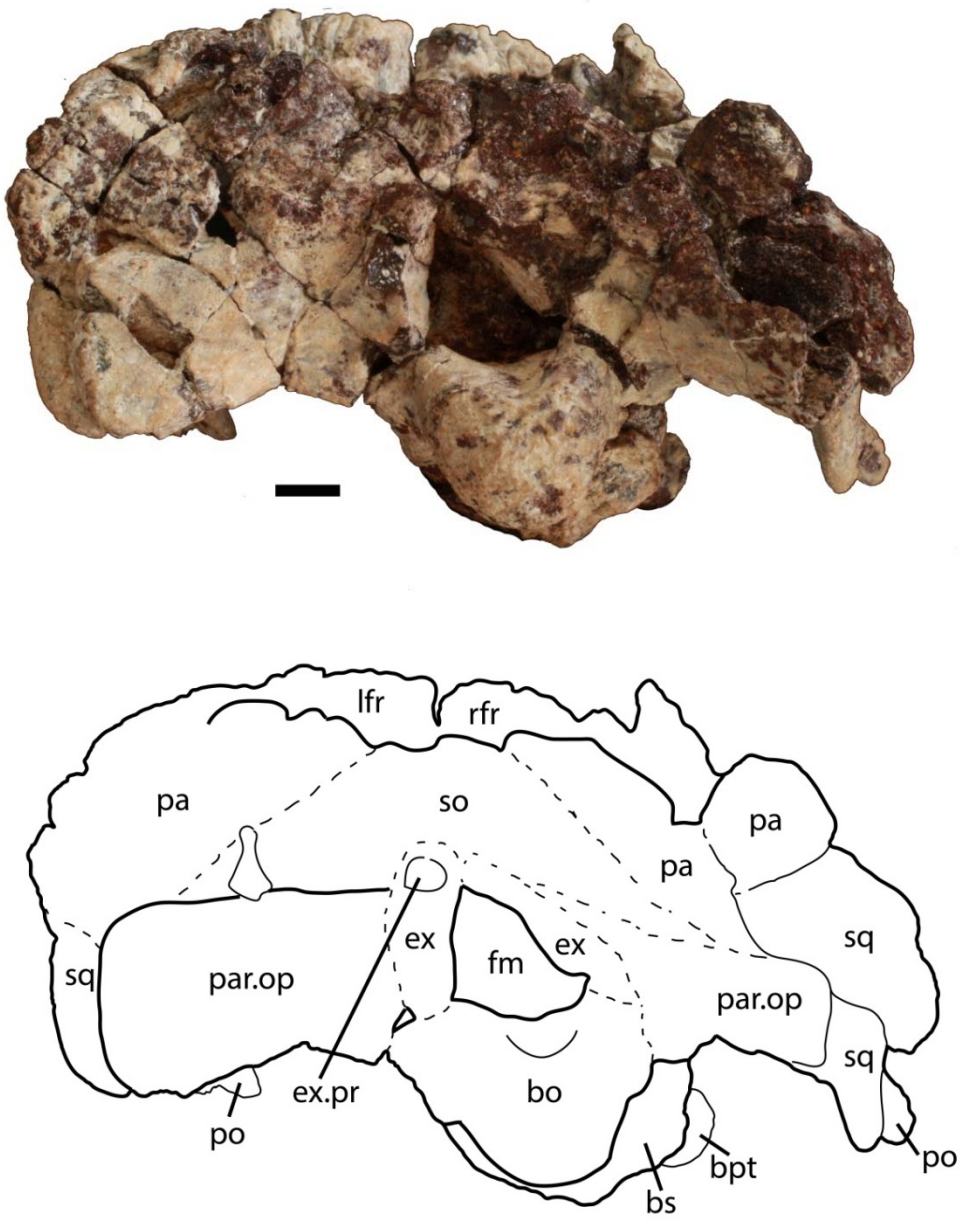

Figure 5.7. Partial skull of *Scutarx deltatylus* (PEFO 34616) in posterior view. Scale bar equals 1 cm. Abbreviations: bo, basioccipital; bpt, basipterygoid processes; bs, basisphenoid; ex, exoccipital; ex.pr; exocippital prong; fm, foramen magnum; lfr, left frontal; pa, parietal; par.op, paroccipital process of the opisthotic; po, postorbital; rfr, right frontal; sq, squamosal.

Figure 5.8. Braincase of *Scutarx deltatylus* (PEFO 34616) in ventrolateral view. Scale bar equals 1 cm. Abbreviations: bpt, basipterygoid processes; bsr, basisphenoid recess; bt, basal tubera; cc, cotylar crest; clp, clinoid process; cp, cultriform process; crp, crista prootica; fo, foramen ovale; hypf, hypophyseal fossa; ic, exit area of the internal carotid artery; lfr, left frontal; lr, lateral ridge; ls, laterosphenoid; mf, metotic foramen; na, nasal; oc, occipital condyle; orb, orbit; pa, parietal; par, paroccipital process of the opisthotic; po, postorbital; pr, prootic; prf, prefrontal; psr; parasphenoid recess; rfr, right frontal; s., suture with designated element; sq, squamosal; uc, unossified cleft of the basal tubera; V, passageway for the Trigeminal nerve.

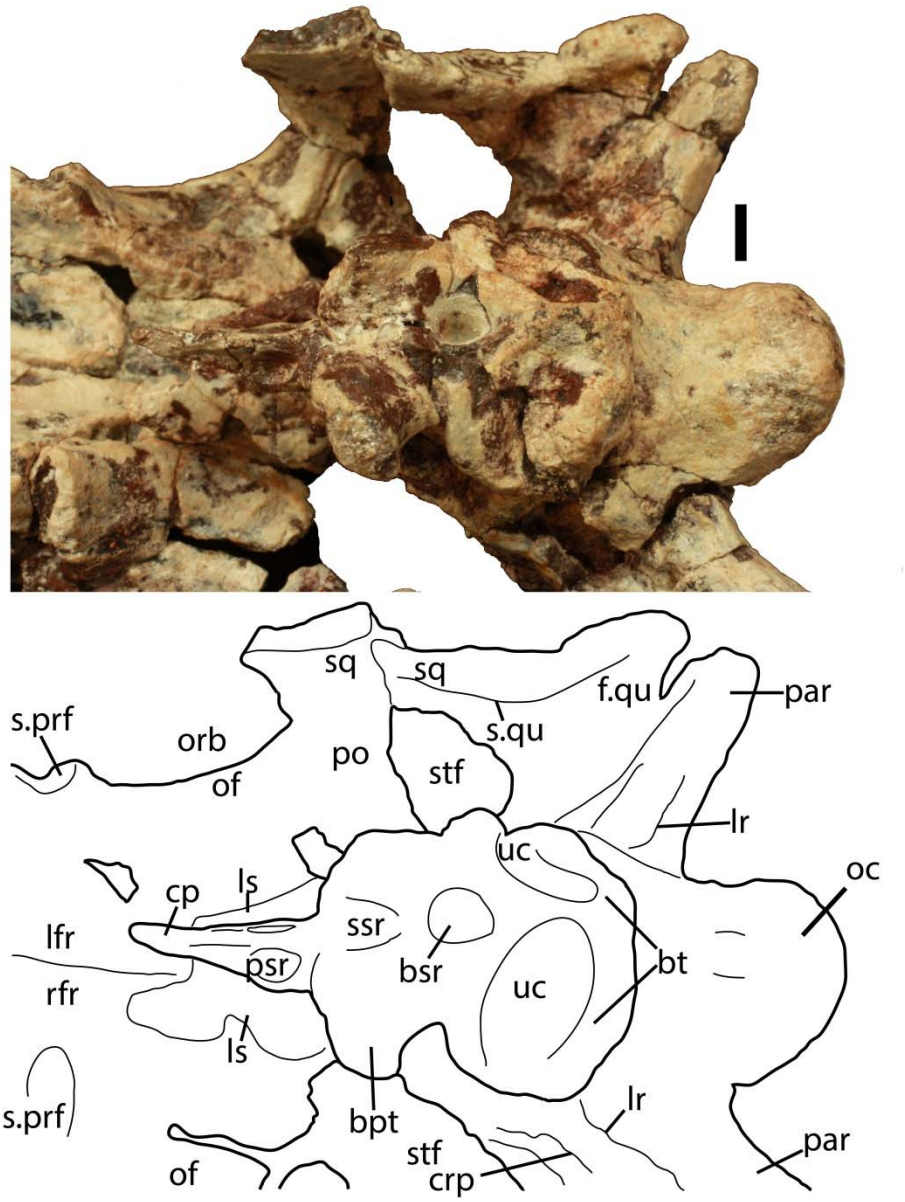

Figure 5.9. Parabasisphenoid of *Scutarx deltatylus* (PEFO 34616) in ventral view. Scale bar equals 1 cm. Abbreviations: **bpt**, basipterygoid processes; **bsr**, basisphenoid recess; **bt**, basal tubera; **cp**, cultriform process; **crp**, crista prootica; **f.**, fossa for specified element; **lfr**, left frontal; **lr**, lateral ridge; **ls**, laterosphenoid; **of**, orbital fossa; **orb**, orbit; **par**, paroccipital process of the opisthotic; **po**, postorbital; **prf**, prefrontal; **pr**, prootic; **prf**, prefrontal; **psr**, parasphenoid recess; quadrate; **rfr**, right frontal; **sq**, squamosal; **ssr**, subsellar recess; **stf**, supratemporal fenestra; **uc**, unossified cleft of the basal tubera.

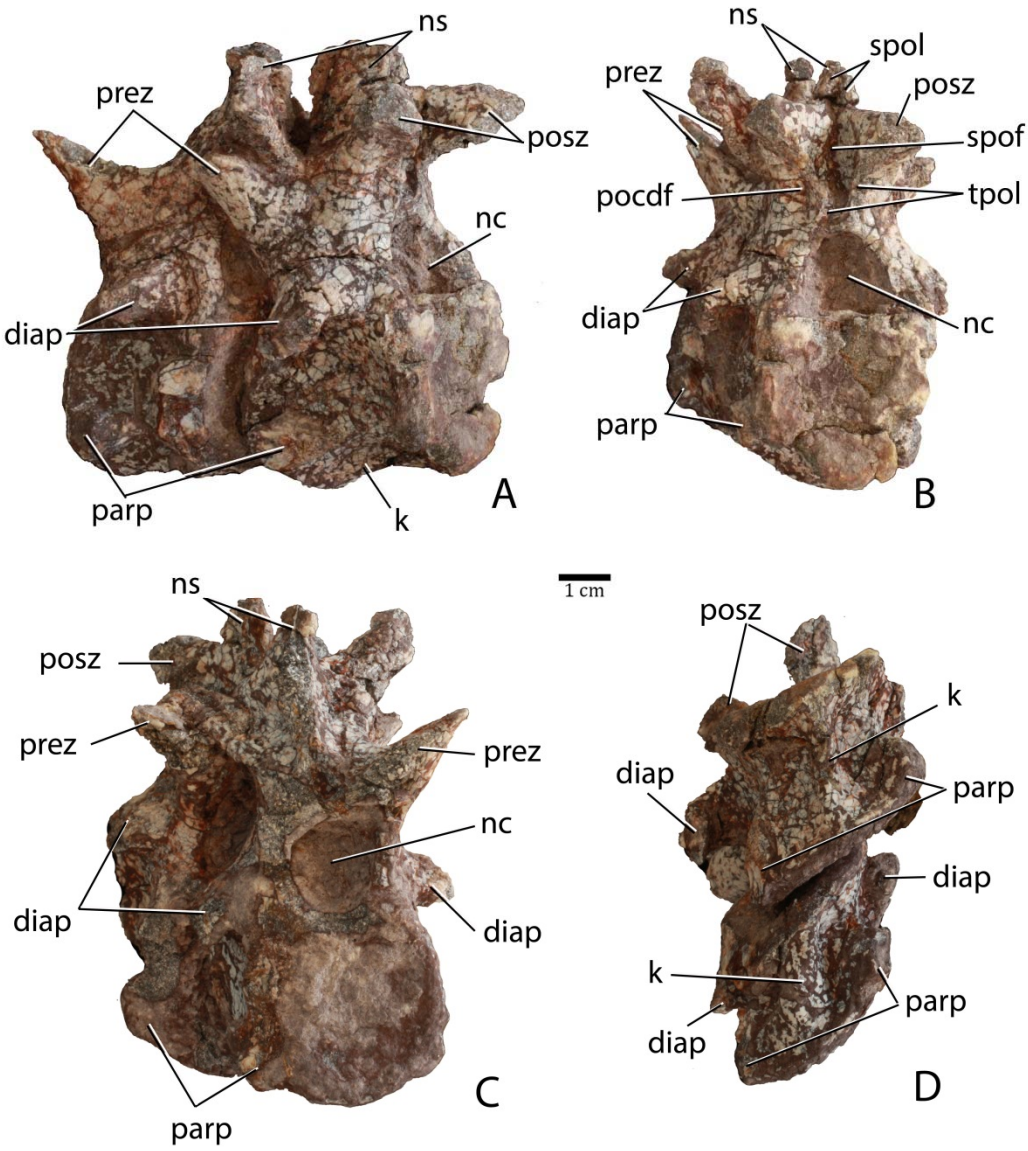

Figure 5.10. Articulated anterior post-axial vertebrae of *Scutarx deltatylus* (PEFO 31217) in posterolateral (A), posterior (B), anterior (C), and ventral (D) views. Scale bar equals 1 cm. Abbreviations: diap, diapophysis; k, keel; nc, neural canal; ns, neural spine; parp, parapophysis; pocdf, postzygapophyseal centrodiapophyseal fossa; posz, postzygapophysis; prez, prezygapophysis; spof, spinopostzygapophyseal fossa; spol, spinopostzygapophyseal lamina; tpol, intrapostzygapophyseal lamina.

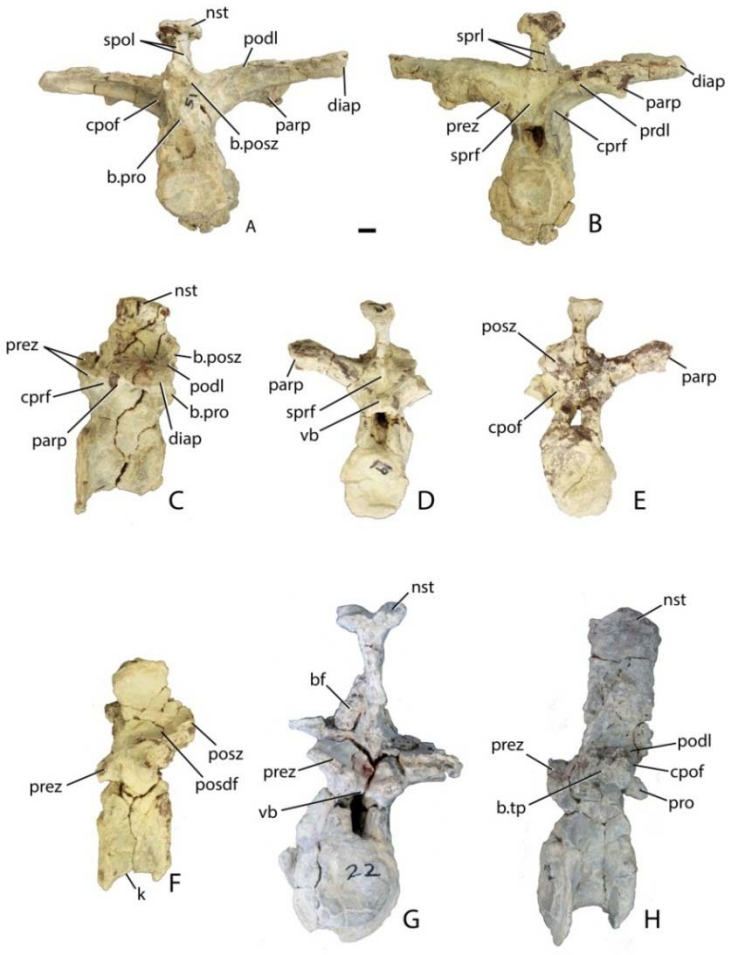

Figure 5.11. Trunk vertebrae of *Scutarx deltatylus*. A-C, PEFO 34045/FF-51, mid-trunk vertebra in posterior (A), anterior (B), and lateral (C) views. D-F, PEFO 34045/19, Anterior trunk vertebra in anterior (D), posterior (E), and lateral (F) views. G-H, PEFO 34045/22, Posterior trunk vertebra in anterior (G) and lateral (H) views. Scale bar equals 1 cm. Abbreviations: b., broken designated element; bf, bone fragment; cpof, centropostzygapophyseal fossa,; cpfr, centroprezygapophyseal fossa; diap, diapophysis; k, keel; nst, neural spine table; parp, parapophysis; podl, postzygodiapophyseal lamina; posdf, postzygapophyseal spinodiapophyseal fossa; posz, postzygapophysis; prez, prezygapophysis; pro, projection; sprf, spinoprezygapophseal fossa; spol, spinopostzygapophyseal lamina; tp, transverse process; vb, ventral bar.

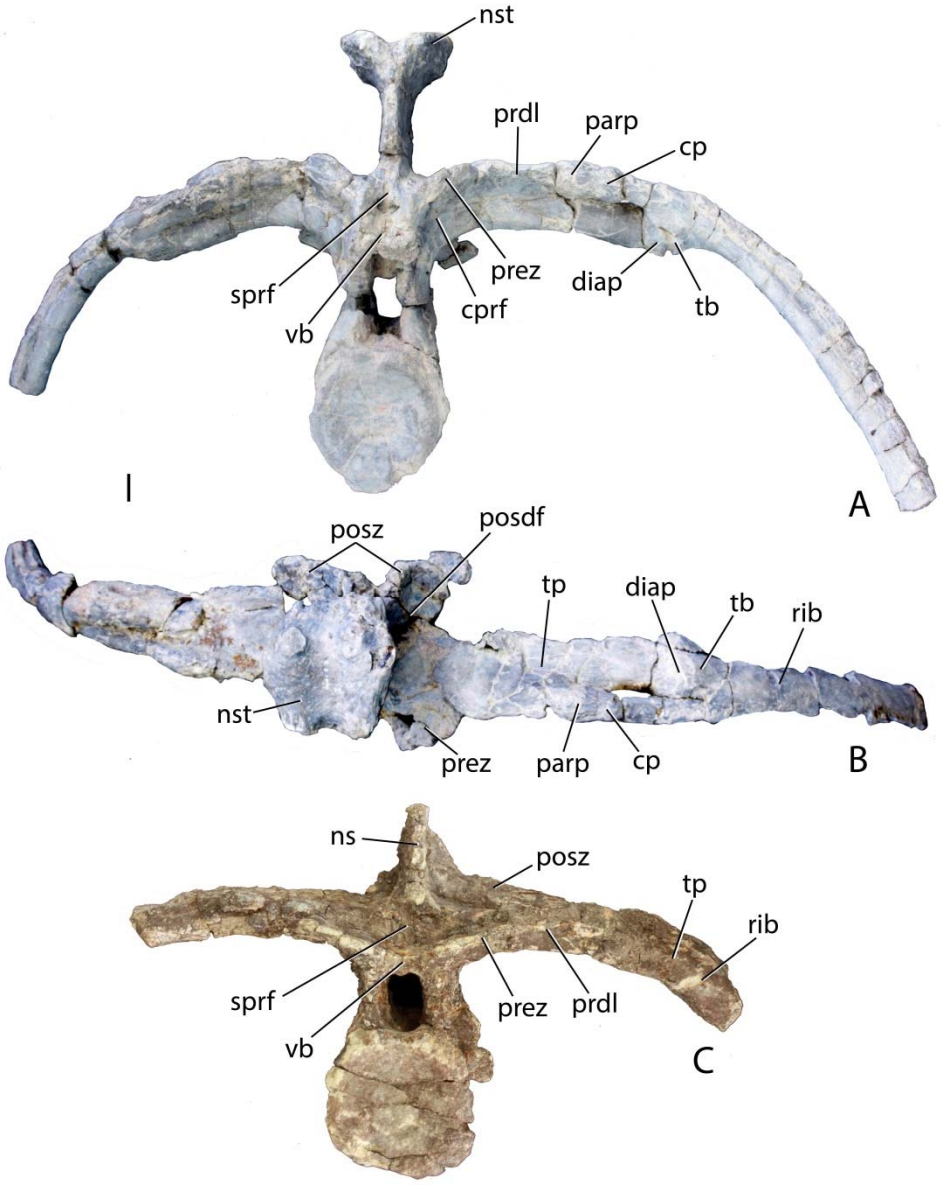

Figure 5.12. Posterior trunk vertebrae of *Scutarx deltatylus*. A-B, PEFO 34045 in anterior (A) and dorsal (B) view. C, PEFO 31217 in anterior view. Scale bar equals 1 cm. Abbreviations: cp, capitulum; cprf, centroprezygapophyseal fossa; diap, diapophysis; ns, neural spine; nst, neural spine table; parp, parapophysis; prdl, prezygadiapophyseal lamina; posdf, postzygapophyseal spinodiapophyseal fossa; posz, postzygapophysis; prez, prezygapophysis; sprf, spinoprezygapophyseal fossa; tb, tuberculum; tp, transverse process; vb, ventral bar.

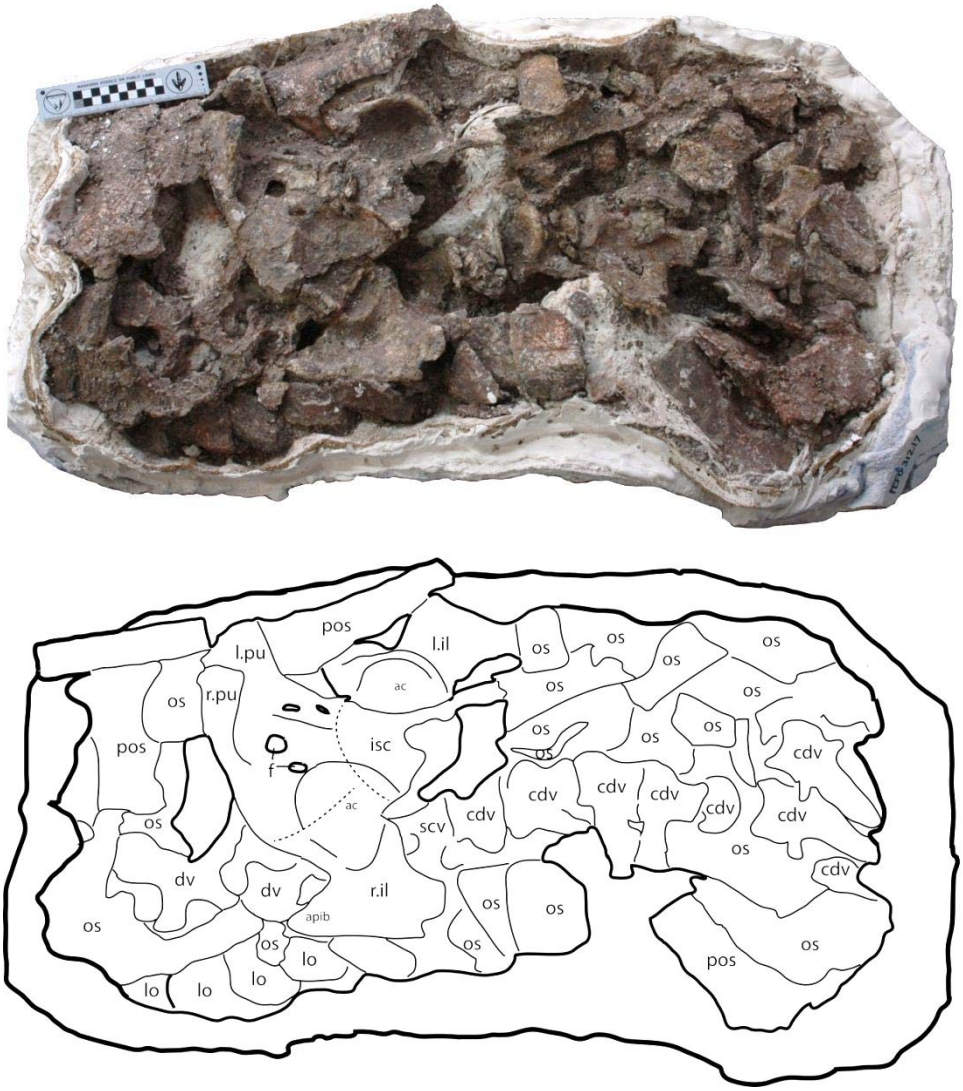

Figure 5.13. Photo and interpretive sketch of a partially articulated sacrum and anterior portion of the tail of *Scutarx deltatylus* (PEFO 31217). Scale bar equals 10 cm. Abbreviations: ac, acetabulum, apib, anterior process of the iliac blade; cdv, caudal vertebra; dv, trunk vertebra; f, foramen; isc, ischia; l.il, left ilium; l.pu, left pubis; lo, lateral osteoderm; os, osteoderm; pos, paramedian osteoderm; r.il, right ilium; r.pu, right pubis; scv, sacral vertebra.

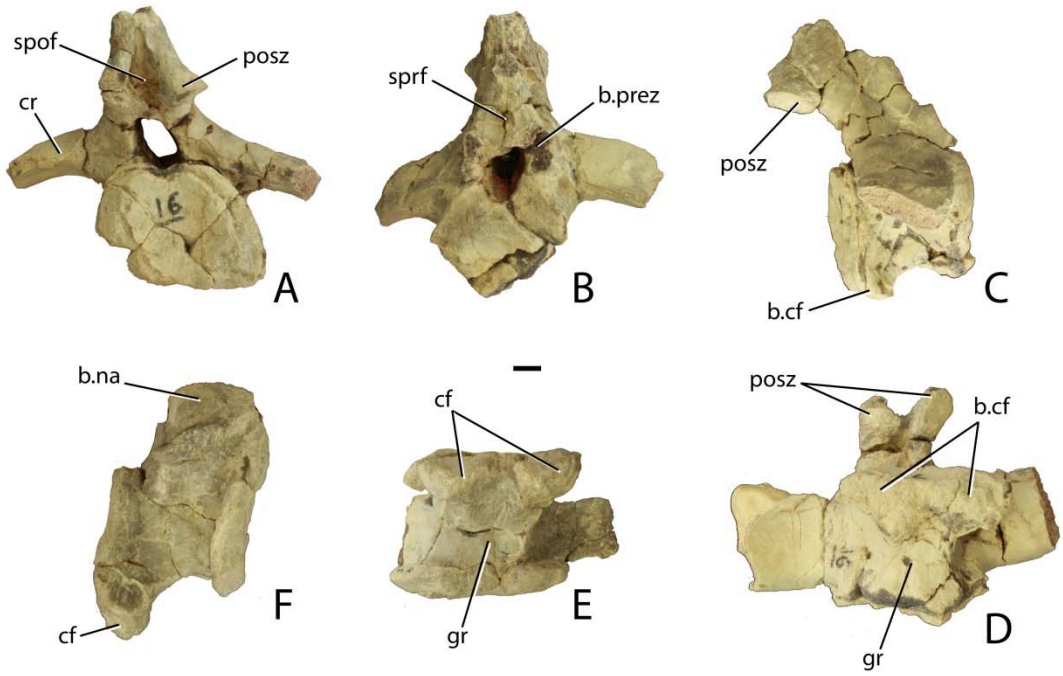

Figure 5.14. Anterior caudal vertebrae of *Scutarx deltatylus* (PEFO 34045). A-D, anterior caudal in posterior (A), anterior (B), lateral (C), and ventral (D). E-F, Anterior caudal vertebra in ventral (E) and lateral (F). Scale bar equals 1 cm. Abbreviations: b., broken designated element; cf, chevron facet; cr, caudal rib; gr, ventral groove; posz, postzygapophysis; prez, prezygapophysis; spof, spinopostzygapophseal fossa, ; sprf, spinoprezygapophseal fossa.

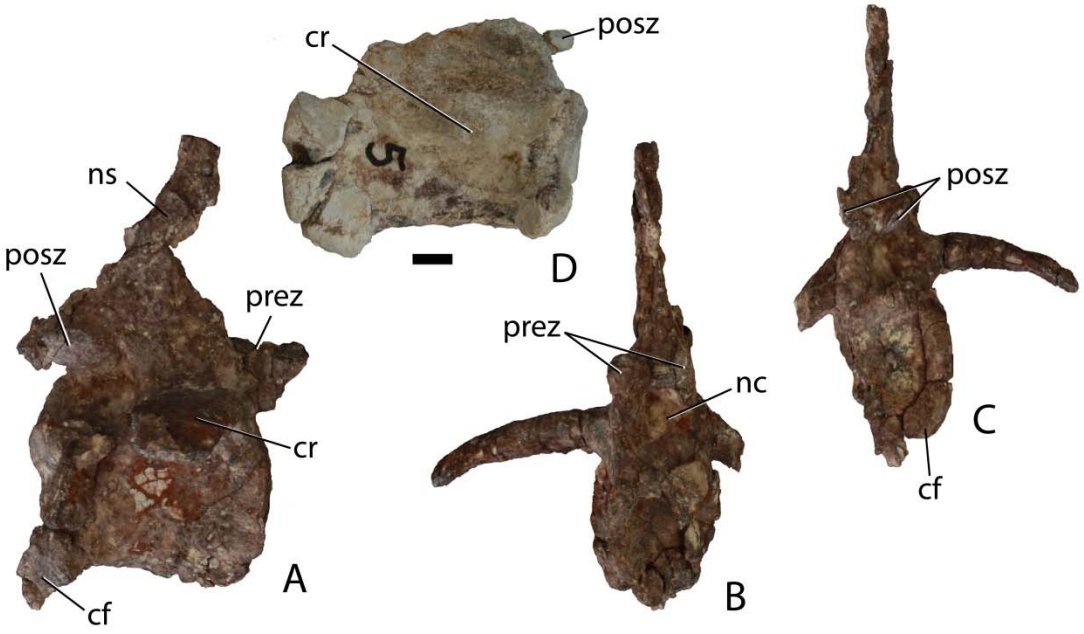

Figure 5.15. Mid-caudal vertebrae of *Scutarx deltatylus*. A-C, anterior mid-caudal vertebra (PEFO 34919) in lateral (A), anterior (B), and posterior (C) views. D, posterior mid-caudal vertebra (PEFO 34045) in lateral view. Scale bar = 1 cm. Abbreviations: cf, chevron facet; cr, caudal rib; ns, neural spine; prez, prezygapophysis; posz, postzygapophysis.

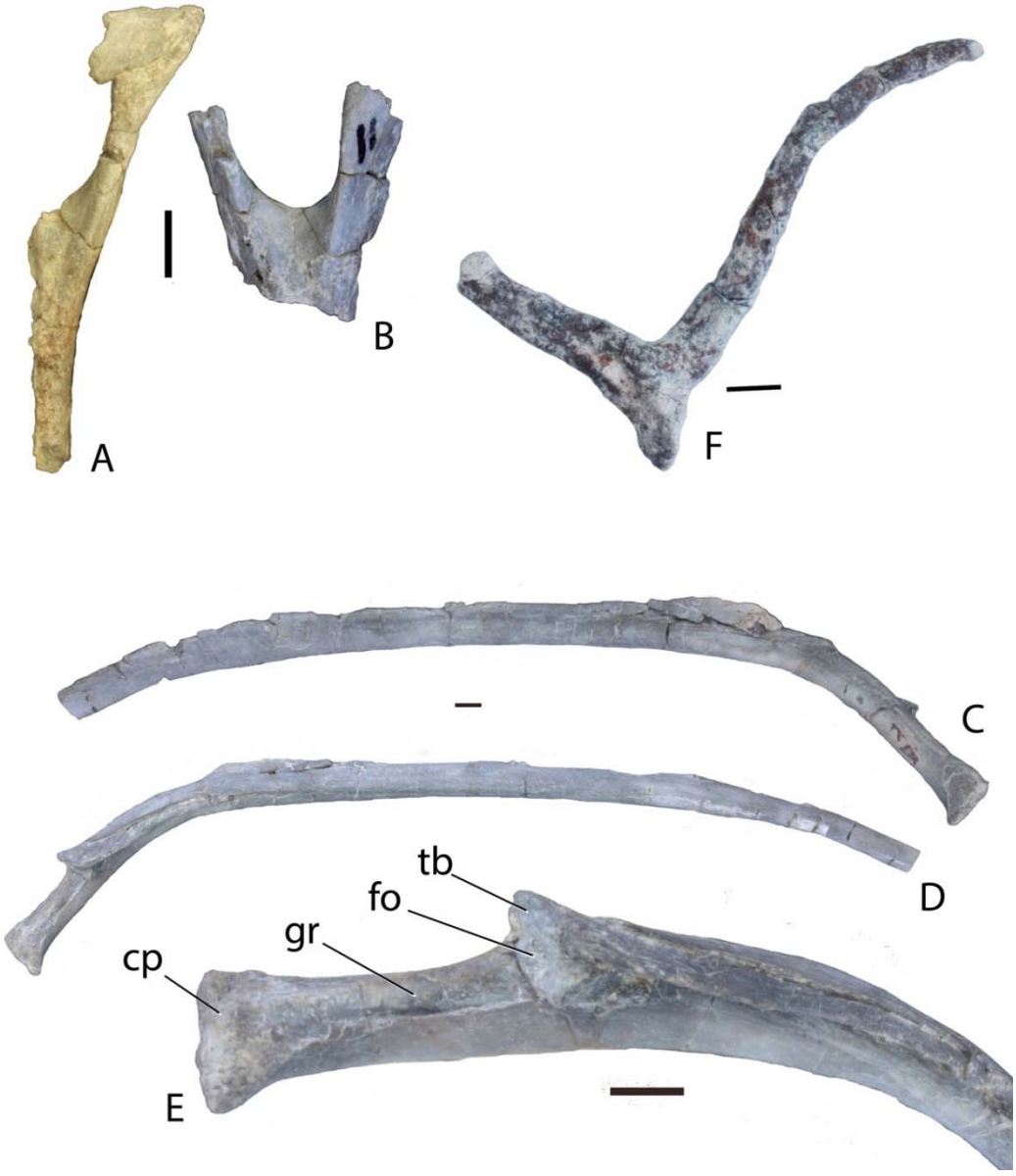

Figure 5.16. Chevrons and ribs of *Scutarx deltatylus*. A-B, partial anterior chevrons from PEFO 34045 in posterior view; C-D, left trunk rib from PEFO 34045 in posterior (C) and anterior (D) views. E, close-up view of head of trunk rib from PEFO 34045. F, paired gastral ribs from PEFO 34616. Scale bars equal 1 cm. Abbreviations: cp, capitulum; fo, fossa; gr, groove; tb, tuberculum.

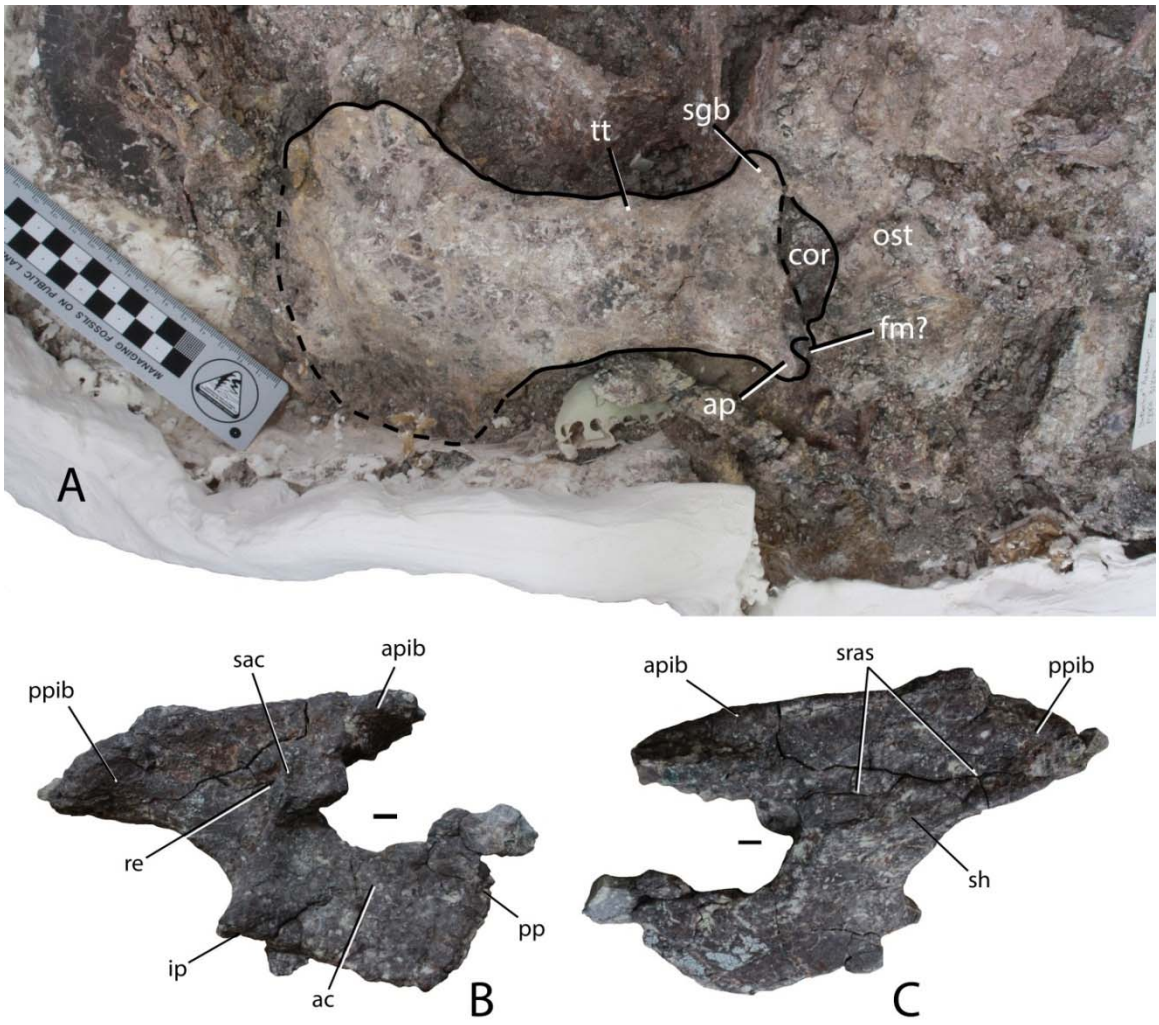

Figure 5.17. Girdle elements of *Scutarx deltatylus.* A, left scapulocoracoid of PEFO 31217 in lateral view. B-C, right ilium of PEFO 34919 in 'lateral' and 'medial' views (see text for discussion regarding anatomical direction of the ilium). Scale bars equal 10 cm (A) and 1 cm (B-C). Abbreviations: ac, acetabulum; ap, acromion process; apib, anterior process of the iliac blade; cor, coracoid; fm, foramen; ip, ischiadic peduncle; ost, osteoderms; pp, pubic peduncle; ppib, posterior process of the iliac blade; re, recess; sac, supraacetabular crest; sgb, supraglenoid buttress; sh, shelf; sras, sacral rib attachment surfaces; tt, triceps tubercle.

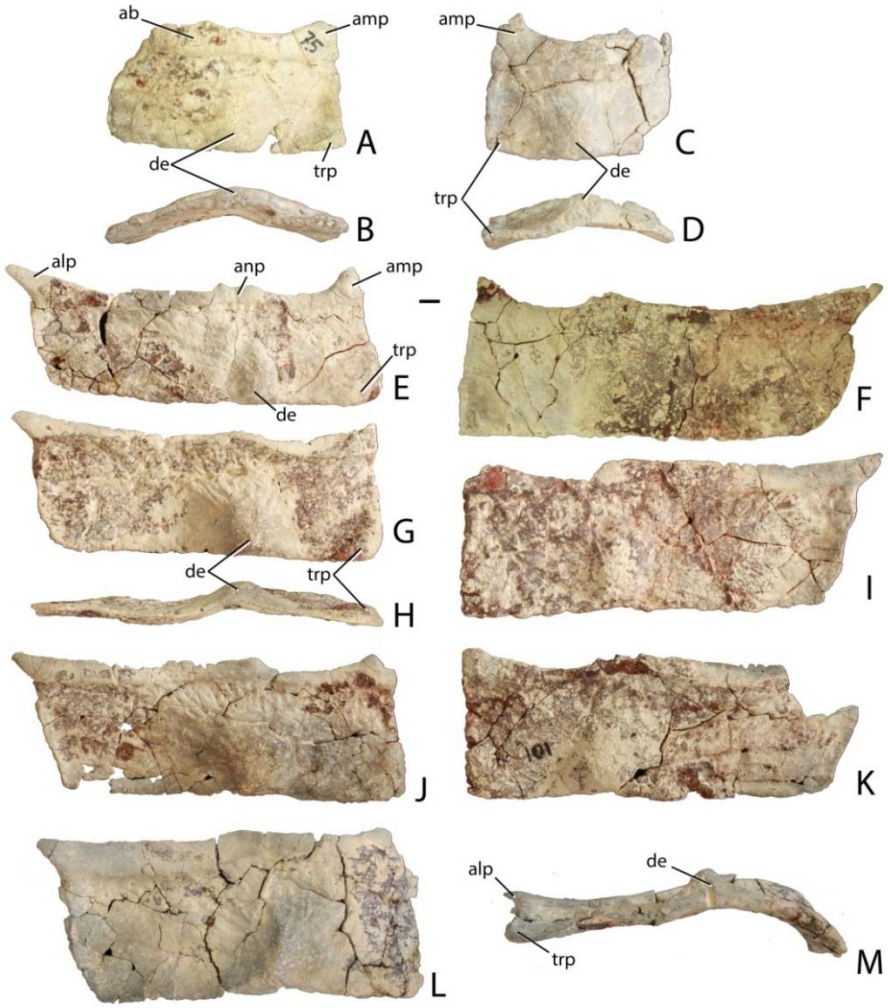

Figure 5.18. Cervical and dorsal trunk paramedian osteoderms of *Scutarx deltatylus* from PEFO 34045. A-B, left mid-cervical osteoderm in dorsal (A) and posterior (B) views. C-D, right mid-cervical osteoderm in dorsal (C) and posterior (D). E-F, left (E) and right (F) dorsal trunk osteoderms in dorsal view. G-I, left (G, H) and right (I) dorsal trunk osteoderms in dorsal (G, I) and posterior (H) views. J-K, left (J) and right (K) dorsal trunk osteoderms in dorsal view. L-M, posterior dorsal trunk osteoderm in dorsal (L) and posterior (M) views. Scale bar = 1 cm. Abbreviations: ab, anterior bar; alp, anterolateral process; amp, anteromedial process; anp, anterior process; de, dorsal eminence; trp, triangular protuberance.

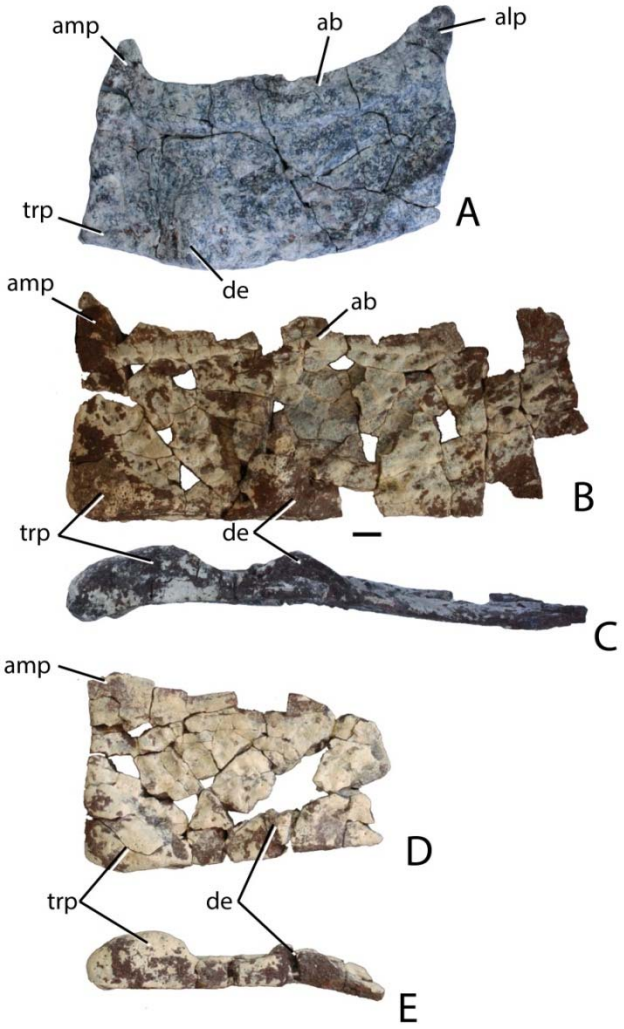

Figure 5.19. Holotype paramedian osteoderms of *Scutarx deltatylus* from PEFO 34616. A, posterior cervical osteoderm in dorsal view. B-C, right dorsal trunk paramedian osteoderm in dorsal (B) and posterior (C) views. D-E, partial right dorsal trunk paramedian osteoderm in dorsal (D) and posterior (E) views. Note the prominence of the triangular protuberance in the posterior views. Scale bar equals 1 cm. Abbreviations: ab, anterior bar; alp, anterolateral process; amp, anteromedial process; de, dorsal eminence; trp, triangular protuberance.

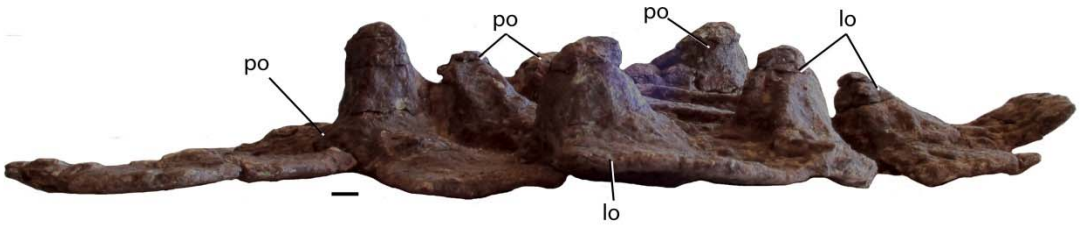

Figure 5.20. Fused semi-articulated anterior dorsal caudal paramedian and dorsal caudal lateral osteoderms of *Scutarx deltatylus* (PEFO 34919) in a lateral view showing extreme development of the dorsal eminences. Scale bar equals 1 cm. Abbreviations: lo, lateral osteoderm; po, paramedian osteoderm.

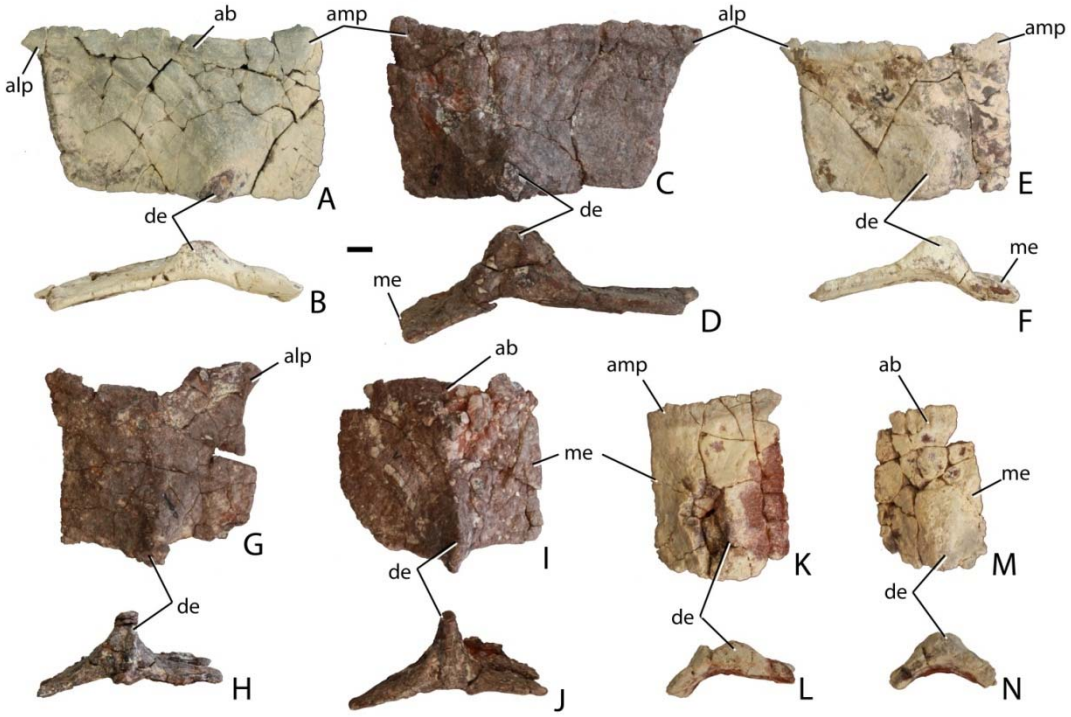

Figure 5.21. Dorsal caudal paramedian osteoderms of *Scutarx deltatylus*. A-B, left anterior mid-caudal osteoderm (PEFO 34045) in dorsal (A) and posterior (B) views. C-D, right anterior mid-caudal osteoderm (PEFO 34919) in dorsal (C) and posterior (D) views; E-F, left mid-caudal osteoderm (PEFO 34045) in dorsal (E) and posterior (F) views. G-H, right mid-caudal osteoderm (PEFO 34919) in dorsal (G) and posterior (H) views. I-J, left mid-caudal osteoderm (PEFO 34919) in dorsal (I) and posterior (J) views. K-L, right posterior caudal osteoderm (PEFO 34045) in dorsal (K) and posterior (L) views. M-N, left posterior caudal osteoderm (PEFO 34045) in dorsal (M) and posterior (N) views. Scale bar equals 1 cm. Abbreviations: ab, anterior bar; alp, anterolateral process; amp, anteromedial process; de, dorsal eminence; me, medial edge.

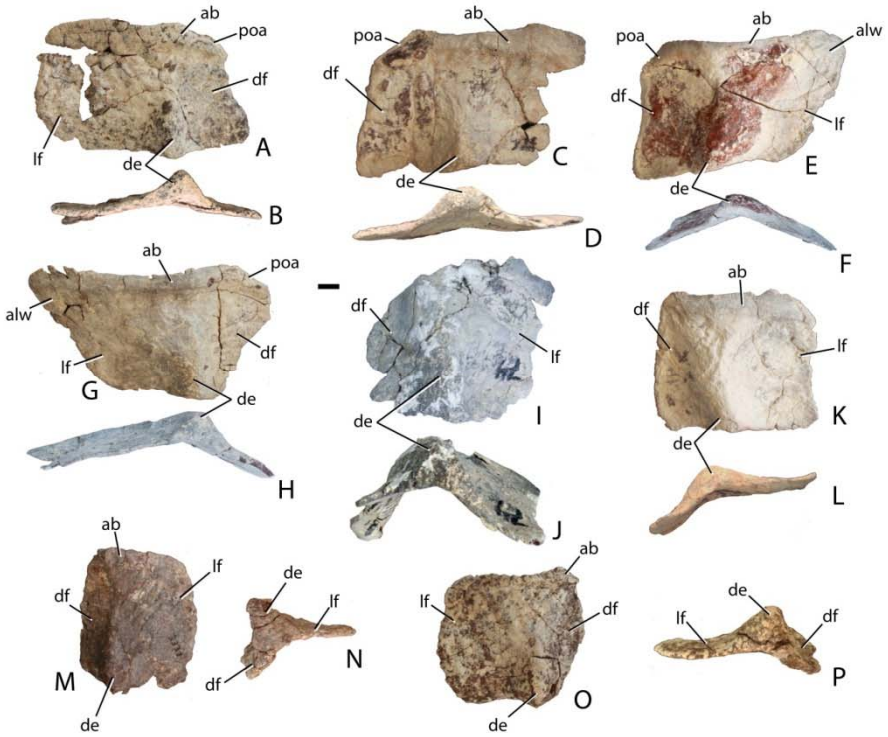

Figure 5.22. Lateral osteoderms of *Scutarx deltatylus*. A-B, left anterior trunk osteoderm (PEFO 34616) in dorsal (A) and posterior (B) views; C-D, right anterior trunk osteoderm (PEFO 34045) in dorsal (C) and posterior (D) views; E-F, right posterior mid-trunk osteoderm (PEFO 34045) in dorsal (E) and posterior (F) views; G-H, left posterior mid-trunk osteoderm (PEFO 34045) in dorsal (G) and posterior (H) views; I-J, right posterior trunk osteoderm (PEFO 34045) in dorsal (I) and posterior (J) views; K-L, right anterior dorsal caudal osteoderm (PEFO 34045) in dorsal (K) and posterior (L) views; right posterior dorsal mid-caudal osteoderm (PEFO 34919) in dorsal (M) and posterior (N) views; O-P, left dorsal mid-caudal osteoderm (PEFO 34616) in dorsal (O) and posterior (P) views. Scale bar equals 1 cm. Abbreviations: ab, anterior bar; alw, anterolateral wing; de, dorsal eminence; df, dorsal flange; mf, medial flange; poa, paramedian osteoderm articular surface.

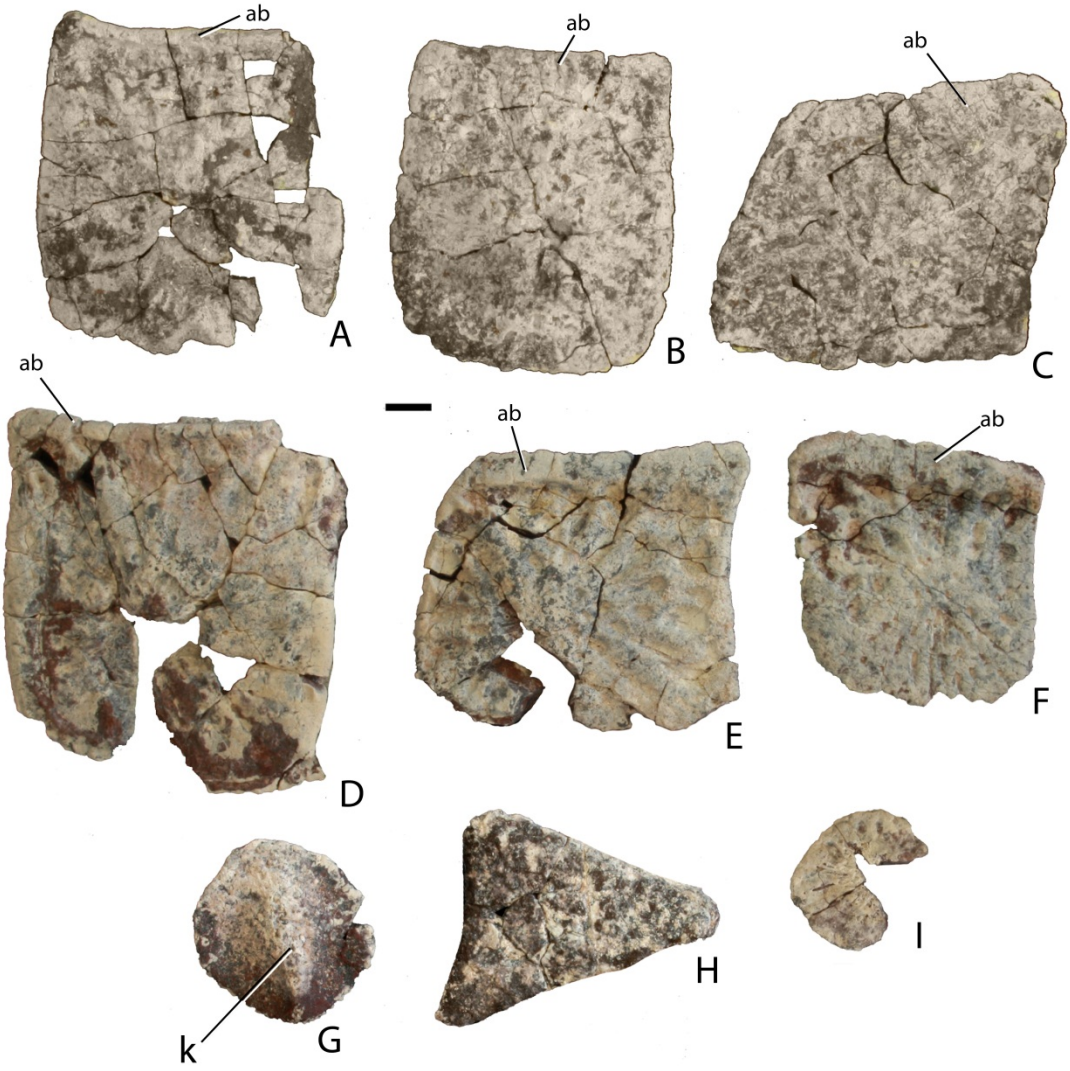

Figure 5.23. Ventral trunk and appendicular osteoderms of *Scutarx deltatylus* from PEFO 34616. A-F, square ventral osteoderms. G, round, keeled appendicular osteoderm. H, triangular ventral or appendicular osteoderm. I, round, ornamented appendicular osteoderm. Scale bar equals 1 cm. Abbreviations: ab, anterior bar; k, keel.

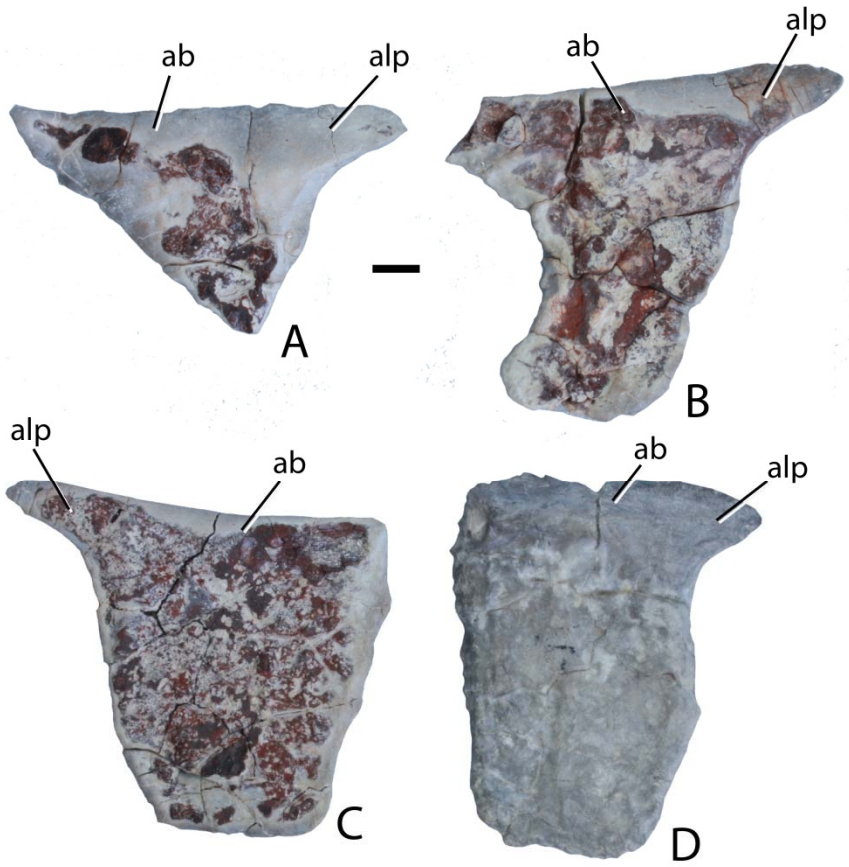

Figure 5.24. Incompletely formed trunk paramedian osteoderms from PEFO 34045. A-B, right osteoderms in dorsal view; C, left osteoderm in dorsal view; D, right osteoderm in dorsal view. Scale bar equals 1 cm. Abbreviations: ab, anterior bar; alp, anterolateral process.

CHAPTER 6: PHYLOGENETIC ANALYSIS

INTRODUCTION

The general goal of phylogenetic systematics is to determine phylogenetic relationships of organisms based on homologous character states, and to use this information to interpret the evolutionary histories of clades, or monophyletic lineages of organisms and the histories of evolutionary character transformations. This presents special challenges for vertebrates with dermal armor like aetosaurians and ankylosaurids, which possess extensive carapaces comprising hundreds of individual osteoderms. Whereas the osteoderms may be common in the fossil record, they are generally dissociated from the rest of the skeleton prior to burial. It has been asserted that osteoderms provide an exhaustive source of phylogenetically informative character data above and beyond that provided by the underlying skeleton (e.g., Heckert and Lucas, 1999a), but it has also been asserted that these data are plagued with phylogenetically confounding homoplasy (Parker, 2007, 2008a). The specific goal of this chapter is to confront these assertions analytically, by undertaking a phylogeny of aetosaurian archosaurs based on the largest taxonomic sample yet assembled, and using a suite of characters that samples both osteoderms and endoskeletal characters.

Historical Background

When Long and Ballew (1985) first proposed a taxonomy of aetosaurs based exclusively on osteoderm characters they considered only five taxa. Much new work and many new specimens revealed that the particular osteoderm character combinations proposed by Long and Ballew (1985) in fact can occur in many other unique

combinations, resulting in the creation of many new taxa (e.g., Zeigler et al., 2003; Martz and Small, 2006; Spielmann et al., 2006; Lucas et al., 2007a, Parker et al., 2008; Heckert et al., in press). Furthermore, it has recently been shown that aetosaurs with nearly identical osteoderm character combinations differ significantly in the other portions of the skeleton, especially in the cranial elements, indicating even more potential taxonomic variation (Desojo and Báez, 2005, 2007; Desojo and Ezcurra, 2011). Finally, aetosaurian osteoderm characters are not intraorganisimally homogeneous (i.e. characters can differ depending on position within the same carapace) and capturing this variation in the construction of phylogenetically informative characters is challenging (Harris et al., 2003a).

Although early studies did focus on character change across broadly defined carapace regions such as the cervical and caudal regions (e.g., Long and Ballew, 1985; Heckert and Lucas, 1999a), more recent studies have sought to detail variation within those subregions as well, in some cases almost osteoderm row by osteoderm row (Martz, 2002; Parker, 2003; 2008b; Schoch, 2007; Parker and Martz, 2011; Heckert et al., in press). Potentially complicating this situation further is our general lack of data regarding character transformations affected by ontogenetic variation as well as differences caused by individual and sexual dimorphism. Overall though, the rich source of character data present in aetosaurian osteoderms provides the systematist with a broad canvas on which to construct a detailed phylogenetic hypothesis, presuming of course that the changes in osteoderm characters are indeed phylogenetically informative (Parker, 2007) and that the homology of these characters can be determined (e.g., Harris et al., 2003a).

At present we do not have an appropriate sample size to capture all of intraorganisimal character variation that occurs across the aetosaurian carapace. Indeed, many taxa are currently only known by a handful of associated osteoderms, where the current challenge simply lies in determining the proper position of these osteoderms in the carapace (Lucas et al., 2003a; Martz and Small, 2006; Spielmann et al., 2006; Parker, 2007; Lucas et al., 2007a). Presumably as more discoveries are made, particularly of associated and articulated specimens, our increased understanding of positional variation will allow for more precise placement of isolated osteoderms leading to stronger determinations of homology (Parker and Martz, 2010; Heckert et al., in press).

For this study I reviewed all previously published characters used for aetosaurian systematics (Parrish, 1994; Heckert et al., 1996; Heckert and Lucas, 1999a; Parker, 2007; Desojo et al., 2012; Heckert et al., in press). I discarded characters if I found them to be generally uninformative or ambiguously scored. The characters I have retained as well as new characters have been rewritten to be more descriptive and thus hopefully more comprehensible. Although the retention and construction of many characters and associated character states would presumably lead to better resolution and clade support (Hillis et al., 1994), the goal of any phylogenetic analysis is accuracy, and this should not come at the expense of artificial resolution (Slowinski, 1993). Thus, the overarching goal of this project was to recover phylogenetic trees that 'make sense' given our anatomical understanding of aetosaurians, rather than highly resolved and supported trees that appear problematic and nonsensical in these regards. The matrix of Parker (2007), which is currently used as the basis for current phylogenetic analyses (Parker et al., 2008; Desojo

et al., 2012, Heckert et al., in press), is dominated in number by osteoderm characters, which is considered to be problematic given the past determinations of large amounts of homoplasy in this dataset (Parker, 2007; Desojo et al., 2012) as well as the major assumption that osteoderm characters provide a true phylogenetic signal irrespective of character states occurring throughout the rest of the skeleton (Parker, 2007, 2008b) Therefore this study sought to increase the number of non-osteoderm characters as suggested by Desojo (2005) and Desojo et al. (2012). This was challenging because of the relative rarity of aetosaurian postcranial remains, which are lacking for many taxa or covered by complete carapaces. The best source for aetosaurian postcranial bones is the *Placerias* Quarry in northeastern Arizona (Long and Murry, 1995). Owing to a lack of association with diagnostic osteoderm material, most of these postcranial elements cannot be referred to species-level groups unequivocally (Parker, 2005a; *contra* Long and Murry, 1995). However, another goal of this study is to use field numbers and quarry maps from the *Placerias* Quarry to try to establish association of the postcranial elements with apomorphic osteoderms. The results were equivocal for most elements (see Chapter 4). Fortunately, there is cranial material preserved for many aetosaurian taxa and almost every known skull, with the exception of some elements from the *Placerias* Quarry and the Post Quarry (Texas) are unambiguously associated with osteoderms. Thus the present analysis was able to significantly expand the number of cranial characters.

The basis for aetosaurian phylogenetic characters and character transformations is a table in Long and Ballew (1985:58) where comparisons are provided between various North American taxa, establishing the first character-based taxonomic scheme for

aetosaurians. Several of these characters are still utilized in current analyses. The first computed phylogenetic analysis of aetosaurians (Parrish, 1994) examined 15 characters (six osteoderm, nine non-osteoderm) and eight taxa. Nine of those characters were parsimony-uninformative for the in-group and there several incorrect scorings and typographical errors that affect the analysis; thus the published tree is neither well-resolved nor accurate in its character state distributions (Harris et al., 2003a). Heckert et al. (1996) expanded on Parrish's (1991) work, inflating the matrix to nine taxa and 22 (potentially 23) characters (17 armor, five non-armor). That study was affected by some scoring errors and the lack of a non-aetosaurian outgroup (Harris et al., 2003a). But it included many new characters that are still staples of aetosaurian phylogenetic studies to date and have been further corroborated in the present study. Furthermore that study was the first to unambiguously recover the major clades Desmatosuchinae and Typothoracisinae (*sensu* Parker, 2007).

Heckert and Lucas (1999a) aimed to expand the matrix of Heckert et al. (1996), in part to determine the phylogenetic relationships of a new taxon, *Coahomasuchus kahleorum*. Their published matrix consists of 13 in-group taxa and 60 characters. However, 26 of these characters are parsimony uninformative and as noted by Harris et al. (2003a) the published matrix included several typographical errors. When corrected, produced a tree different from the one published. Harris et al. (2003a) were critical of several other aspects of this study, including the ad hoc deletion of taxa from the matrix, when safe taxon deletion tests are available (Wilkinson, 1995a) and character constructions that inflated seemingly non-independent character suites that biased the

resulting tree (composite versus reductive coding, Rowe, 1988; Wilkinson, 1995b). However, the study by Heckert and Lucas (1999a) built further upon the character list of Heckert et al. (1996) and represents a very important progression in our understanding of aetosaurian systematics.

The most recent phylogenetic analysis (Parker, 2007) focused on the lateral osteoderms of aetosaurians, whereas previously studies had focused more on characters of the paramedian osteoderms (Heckert et al., 1996; Heckert and Lucas, 1999a). Parker (2007) noted that aetosaurians could roughly be divided into three groups based on the overall anatomy of the lateral osteoderms. This translated into a phylogenetic analysis (16 in-group taxa, 37 characters) that recovered three distinct clades; Aetosaurinae, Desmatosuchinae (Heckert and Lucas, 2000) and Typothoracinae. Whereas support for Desmatosuchinae and Typothoracinae was strong, especially for Paratypothoracini, Aetosaurinae was generally unresolved or weakly supported. This became especially apparent when other taxa were added to the matrix causing significant differences in tree topology and character support (Parker et al., 2008; Desojo et al., 2012). Indeed, a recent study (Desojo et al., 2012) failed to recover Aetosaurinae as a more inclusive clade, with *Aetosaurus ferratus* as the only member. Nonetheless Typothoracinae remains well-supported and resolved, and although Desmatosuchinae is always recovered and well-supported, the constituent taxa are not always fully resolved (Parker et al., 2008). Criticisms of this dataset include the lack of endoskeletal characters as well as scoring errors (Desojo and Ezcurra, 2011; Desojo et al., 2012; Heckert et al., in press).

Materials and Methods

In order to test these questions about taxon sampling, character independence, and tree topology, in this study I have expanded previous matrices to include more taxa and characters. Thus, it was quickly recognized that an expanded study was necessary to create a robust matrix to not only potentially clarify all in-group relationships, but also to create a baseline matrix that would remain stable for future additions of new taxa and specimens. The matrix utilizes 83 characters for 26 in-group taxa. The characters are well-divided between anatomical regions, with endoskeletal characters constituting the majority (34 cranial, 16 axial/appendicular, 33 osteoderm).

The 26 in-group taxa include the majority of aetosaurian taxa currently considered valid (Desojo et al., 2013; Heckert et al., in press; Roberto-Da-Silva et al., 2014). They are listed in the next section below and the present study is the first to investigate to phylogenetic positions of *Adamanasuchus eisenhardtae*, *Apachesuchus heckerti*, *Stagonolepis olenkae*, and *Redondasuchus rineharti*. Furthermore, it scores a new taxon, *Scutarx deltatylus*, and rescores some other taxa (e.g, *Coahomasuchus kahleorum*) based on new material.

Taxa excluded from the analysis include *Acaenasuchus geoffreyi* Long and Murry, 1995; *Redondasuchus reseri* Hunt and Lucas, 1991; *Typothorax antiquum* Lucas et al., 2003a; and *Chilenosuchus forttae* Casimiquela 1980. *Acaenasuchus* and *Chilenosuchus* were excluded because the holotype and referred specimens are poorly preserved and not morphologically informative. *Chilenosuchus* scores as a taxonomic equivalent of *Typothorax coccinarum* (Wilkinson, 1995a) and newly recognized material

of *Acaenasuchus* casts doubt on its aetosaurian identify (Parker, unpublished data). *Redondasuchus reseri* is poorly known and scores as a taxonomic equivalent of *Redondasuchus rineharti*. *Typothorax antiquum* probably represents an ontogenetic stage of *Typothorax coccinarum* (Parker, 2006; Parker and Martz, 2011).

Revueltosaurus callenderi is included in the analysis as an outgroup because it is the sister taxon of Aetosauria according to Nesbitt (2011). Furthermore, it is known from several specimens, which preserve nearly the entire skeleton. *Postosuchus kirkpatricki* is utilized as an outgroup because it is relatively complete, well-described and illustrated (Weinbaum, 2011, 2013). Furthermore, it represents a more nested clade (Paracrocodylomorpha) within Pseudosuchia providing deeper optimization of character states than can be provided by *Revueltosaurus*. Both of these taxa have been utilized as outgroups in past phylogenetic studies of the Aetosauria (e.g., Heckert and Lucas, 1999a; Parker, 2007; Desojo et al., 2012; Heckert et al., in press). Unfortunately neither *Postosuchus* nor *Revueltosaurus* can presently be scored for lateral osteoderm characters and therefore have been scored as inapplicable for these taxa. Furthermore, most of the paramedian osteoderm characters were scored as inapplicable for *Postosuchus* because even though *Postosuchus* possesses dorsal osteoderms, the homology of characters such as ornamentation pattern and presence of certain processes cannot be determined.

A previous work (Parker, 2007) incorporated many scorings from past studies (Parrish, 1994; Heckert et al., 1996; Heckert and Lucas, 1999a) some of which were determined to be erroneous (Schoch, 2007; Desojo and Ezcurra, 2011; Desojo et al., 2012). For this study the matrix was scored from scratch and the scorings completed from

carefully studying actual materials for most taxa, and using photos and the literature for any not studied first-hand (*Stagonolepis olenkae*, *Aetosaurus ferratus*, SMNS 19003, *Stenomyti huangae*, *Redondasuchus rineharti*, NCSM 21723, *Polesinesuchus aurelioi*). Errors in scoring based on misinterpretation of character states and materials probably exist, but much effort has gone into detecting and fixing typographic errors, which can have a major effect on the final tree topologies (Harris et al., 2003a). Taxon scoring completeness is shown in Table 1 for each taxon, compiled by counting the number of characters scored to determine the percentage of completetion. Inapplicable characters were counted as scored. Completeness scores range from 98% (80 of 82) for *Desmatosuchus smalli*, which is known from several skulls and skeletons; to 22% for *Apachesuchus heckerti* (18 of 82), which is known only from five paramedian osteoderms. The average completeness score was 60%. The biggest factor for incompleteness is the lack of skull material which affected all taxa that scored lower than 50%. Because aetosaurians are generally identified by armor characters, there are no taxa that consist solely of cranial material in contrast with many other groups (e.g., synapsids, dinosaurs).

Institutional abbreviations – **AMNH**, American Museum of Natural History, New York, USA; **ANSP**, Academy of Natural Sciences of Drexel University, Philadelphia, Pennsylvania, USA; **CPE2**, Coleção Municipal, São Pedro do Sul, Brazil; **DMNH**, Perot Museum of Natural History, Dallas, Texas, USA; **DMNH**, Denver Museum of Nature and Science, Denver, Colorado, USA; **FMNH**, Field Museum, Chicago, IL, USA; **FR**,

Frick Collection, American Museum of Natural History, New York, USA; **MCCDP**, Mesalands Community College Dinosaur Museum, Tucumcari, New Mexico, USA; **MCSNB,** Museo Civico di Scienze Naturali Bergamo, Bergamo, Italy; **MCP**, Museo de Ciencias e Tecnología, Porto Alegre, Brazil**;** **MCZ**, Museum of Comparative Zoology, Harvard University, Cambridge, Massachusetts, USA; **MCZD**, Marischal College Zoology Department, University of Aberdeen, Aberdeen, Scotland, UK; **NCSM**, North Carolina State Museum, Raleigh, North Carolina, USA; **NHMUK**, The Natural History Museum, London, United Kingdom; **NMMNH**, New Mexico Museum of Natural History and Science, Albuquerque, New Mexico, USA; **MNA**, Museum of Northern Arizona, Flagstaff, Arizona, USA; **PEFO**, Petrified Forest National Park, Petrified Forest, Arizona, USA; **PFV**, Petrified Forest National Park Vertebrate Locality, Petrified Forest, Arizona, USA; **PVL**, Paleontología de Vertebrados, Instituto 'Miguel Lillo', San Miguel de Tucumán, Argentina; **PVSJ,** División de Paleontologia de Vertebrados del Museo de Ciencias Naturales y Universidad Nacional de San Juan, San Juan, Argentina, **SMNS**, Staatliches Museum für Naturkunde, Stuttgart, Germany; **TMM**, Texas Memorial Museum, Austin, Texas, USA; **TTUP**, Museum of Texas Tech, Lubbock, Texas, USA; **UCMP**, University of California, Berkeley, California, USA; **ULBRA PVT**, Universidade Luterana do Brasil, Coleção de Paleovertebrados, Canoas, Rio Grande do Sul, Brazil; **UMMP**, University of Michigan, Ann Arbor, Michigan, USA; **USNM**, National Museum of Natural History, Smithsoniam Institution, Washington, D.C., USA; **VPL**, Vertebrate Paleontology Lab, University of Texas at Austin, Austin, Texas, USA; **YPM**, Yale University, Peabody Museum of Natural History, New Haven,

Connecticut, USA; **VRPH**, Sierra College, Rocklin, California, USA; **ZPAL,** Institute of Paleobiology of the Polish Academy of Sciences in Warsaw, Warsaw; Poland.

TERMINAL TAXA

The phylogenetic analysis by Nesbitt (2011) is currently the most thorough study of archosauriform relationships. I follow the format used in that study for the listing of terminal taxa and characters to make this work compatible.

Adamanasuchus eisenhardtae

Holotype – PEFO 34638, partial skeleton including paramedian and lateral osteoderms, several vertebral centra, and a partial femur (Lucas et al., 2007a).

Referred Material – PEFO 35093, osteoderm fragments, nasal fragment; PEFO 36806, osteoderm fragments.

Remarks -- Lucas et al. (2007a) refer a lateral osteoderm (UCMP 126867) to *Adamanasuchus eisenhardtae* without explanation other than noting a 2007 personal communication from A. Heckert. They neither figure nor describe the specimen, but list its provenance as the *Placerias* Quarry near St. Johns, Arizona and attribute it as another Adamanian record of *Adamanasuchus eisenhardtae*. Examination of UCMP 126867

confirms the identification of the element as an aetosaurian lateral plate; however, the specimen was collected from PFV 075 (Karen's Point) in Petrified Forest National Park and not from the *Placerias* Quarry. PFV 075 is in the Martha's Butte beds of the Sonsela Member, which are Revueltian in age (Parker and Martz, 2011), thus this would represent a range extension of this taxon up into the Sonsela Member and into the Revueltian biozone. This specimen differs from the holotype of *Adamanasuchus eisenhardtae* in possessing an extremely reduced dorsal flange and a dorsal eminence that forms a broadly triangular "spine" that projects dorsally. The outer surface of the lateral flange and the dorsal eminence bear an elongate ridge, which is located very close to the plate margin. Curiously the osteoderm lacks an anterior bar so it cannot be determined if this margin is the anterior or posterior edge. In *Adamanasuchus eisenhardtae*, the lateral osteoderms are more symmetrical with nearly equal lateral and dorsal flanges, and the eminence does not form a projected spine (PEFO 34638). Because of these anatomical differences and the discrepancy in the stratigraphic and locality data, the referral of this specimen to *Adamanasuchus eisenhardtae* is not supported.

PEFO 35093 includes osteoderm fragments that possess the unique surface ornamentation of a faint background, radial pattern, incised by deep randomly developed pits characteristic of *Adamanasuchus eisenhardtae*. An associated fragment of a nasal most likely belongs to the same specimen as it has an identical preservation and no other aetosaur specimens were recovered from the immediate area. Unfortunately the nasal fragment is too incomplete to provide more information. PEFO 36806 is another specimen and consists solely of osteoderm fragments. Both PEFO 35093 and PEFO

36806 were recovered from the upper part of the Blue Mesa Member at about the same stratigraphic horizon as the holotype specimen of *Adamanasuchus eisenhardtae*.

Age – Late Triassic, early to middle Norian, Adamanian (Ramezani et al., 2011; Parker and Martz, 2011).

Occurrence – upper Blue Mesa Member, Chinle Formation, Petrified Forest National Park, Arizona, U.S.A. (Lucas et al., 2007a; Parker and Martz, 2011).

Remarks – Lucas et al. (2007a) named *Adamanasuchus eisenhardtae* for a partial skeleton collected from the Blue Mesa Member (Chinle Formation) in Petrified Forest National Park in 1996 (Hunt, 1998; Parker, 2006). Parker (2006) incorrectly assigned this specimen to *Typothorax antiquum* based on the interpretations made by Hunt (1998) regarding this specimen. In 2010 park staff revisited the type locality and finished the excavation; several paramedian and lateral osteoderms had been covered and left by the original workers and these materials were not included in the original description. The diagnosis provided by Lucas et al. (2007a) does not adequately differentiate *Adamansuchus eisenhardtae* from other known aetosaurians, in particular from *Calyptosuchus wellesi*; however, key characters found in *Adamanasuchus eisenhardtae* to the exclusion of *Calyptosuchus wellesi* is the strongly sigmoidal lateral edge, that results is a ventrolateral corner of the osteoderm that appears to have been sheared-off (J. Martz, pers. com. 2013), and a triangular patch in the posteromedial corner of the paramedian

plate surface that is smooth and devoid of ornamentation. The first character state also occurs in paratypothoracins and the second is found in *Scutarx deltatylus*, except that in the latter taxon the triangular area is strongly raised.

Key References – Lucas et al. (2007a).

Aetobarbakinoides brasiliensis

Holotype – CPE2 168, partial postcranial skeleton (Desojo et al., 2012). A cast of this specimen is in the Petrified Forest National Park collections.

Referred Material – none.

Age – Late Triassic, late Carnian – earliest Norian, *Hyperodapedon* Assemblage Zone (Langer et al., 2007; Martinez et al., 2011).

Occurrence – Sequence 2, Santa Maria Supersequence, Rio Grande Do Sul, Brazil (Desojo et al., 2012).

Remarks – The holotype (CPE2 168) of *Aetobarbakinoides brasiliensis* is a fragmentary postcranial skeleton of a small aetosaurian that was originally referred to *Stagonolepis robertsoni* (=*Aetosauroides* in their hypothesis) by Lucas and Heckert (2001). The lack of

open neurocentral sutures in the cervical and dorsal vertebrae suggests that CPE2 168 represents a skeletally mature individual (Irmis, 2007). Despite the fragmentary preservation of the holotype, Desojo and Ezcurra (2011) were readily able to distinguish this material from that of other South American aetosaurs, based on the presence of discrete vertebral laminae in the dorsal series, a character lacking in taxa such as *Aetosauroides scagliai* and *Neoaetosauroides engaeus*. Furthermore, *Aetobarbakinoides* is the only South American aetosaurian specimen with dorsal vertebrae that bear accessory articular structures (i.e. hyposphene), a feature recognized previously only in desmatosuchines (Parker, 2008b). Determining the phylogenetic position of this taxon is difficult because it is represented almost exclusively by endoskeletal (non-osteoderm) material. A few osteoderms are present, but the surface ornamentation is poorly preserved. Lateral osteoderms, which have been key to phylogenetic placement, are not preserved. Furthermore, the preserved paramedian osteoderms lack their lateral edges, which, if preserved, would have provided information about the medial edges of the lateral osteoderms allowing for the scoring of some characters. Desojo et al. (2012) recovered *Aetobarbakinoides brasiliensis* as the sister taxon of the clade Desmatosuchinae + Typothoracinae; however, Heckert et al. (in press) considered it to be a 'wildcard' (unstable) taxon in their analysis and pruned it *a posteriori* from their published tree. It performed as a wildcard taxon in this analysis as well, which is discussed in more detail below.

Key References – Desojo et al. (2012).

Aetosauroides scagliai

Holotype – PVL 2073, postcranial skeleton including the majority of the carapace, vertebral column, and sacrum in articulation (Casimiquela, 1961).

Referred Material – see Desojo and Ezcurra (2011).

Age – Late Triassic, Carnian, *Hyperodapedon* Assemblage Zone (Rogers et al., 1993; Furin et al., 2006; Martinez et al., 2011).

Occurrence – Cancha de Bochas Member, Ischigualasto Formation, Argentina; Sequence 2, Santa Maria Supersequence, Rio Grande do Sul State, Brazil (Casimiquela, 1961; Desojo and Ezcurra, 2011).

Remarks – Aetosauroides scagliai was originally described by Casimiquela (1960, 1961) based on well-preserved cranial and postcranial material from the lower part of the Ischigualasto Formation of Argentina. Further material was assigned by Casimiquela (1967) who redescribed the specimens in light of the monograph on *Stagonolepis robertsoni* by Walker (1961). Strong similarities have been noted between *Aetosauroides* and *Stagonolepis* as well as *Aetosaurus* and based on element size *Aetosauroides* was considered to be somewhat morphologically transitional between the two European taxa (Casimiquela, 1967). In an unpublished masters thesis, Zacarias (1982) erected a second

species of *Aetosauroides* ("*Aetosauroides* subsulcatus") for material from the Upper Triassic of Brazil. All of this material has been briefly redescribed, the majority of it assigned to *Stagonolepis robertsoni* (Lucas and Heckert, 2001; Heckert and Lucas, 2002a). Those authors argued that only superficial differences could be found between all of these specimens and that assignment of the South American material strengthened previously proposed biostratigraphic correlations between Brazil, Argentina, and the U.K., as well as to the southwestern United States. In contrast, Desojo and Ezcurra (2011) assigned the Brazilian material to *Aetosauroides scagliai* based on the presence of well-developed fossae on the lateral sides of the dorsal vertebrae and the exclusion of the maxilla from the external naris in the skull of *Aetosauroides scagliai*, a character first noted by Casimiquela (1967). A phylogenetic analysis recovered *Aetosauroides scagliai* as the sister taxon to all other aetosaurs (Stagonolepididae) (Desojo et al., 2012). Those authors are presently working on a full redescription of the Argentinian material.

Cerda and Desojo (2011) provide details of the osteoderm histology of *Aetosauroides scagliai*, although using referred specimens rather than the holotype. This is the second published report on bone histology for an aetosaurian; the first is for *Sierritasuchus macalpini* (Parker et al., 2008). It is possible that once histological features and their relationships with ontogenetic maturity at time of death and potential environmental effects are better known, that histological characters can be incorporated in phylogenetic analyses of the Aetosauria.

Key References – Casimiquela, 1960, 1961, 1967; Heckert and Lucas, 2002a; Desojo and Ezcurra, 2011; Cerda and Desojo, 2011.

Aetosaurus ferratus

Lectotype – SMNS 5770, specimen XVI (16) (Schoch, 2007).

Referred Material – SMNS 5770, at least 24 specimens recovered in the same block as the lectotype; SMNS 18554, articulated skeleton lacking the skull and pectoral girdle; SMNS 14882, articulated caudal segment; SMNS 12670, dorsal and ventral osteoderms; MCZ 22/92G, partial skull, limb bones and vertebrae, osteoderms; MCSNB 4864, dorsal osteoderms.

Age – Late Triassic, middle Norian to early Rhaetian, Revueltian (Deutsche Stratigraphische Kommission, 2005; Lucas, 2010).

Occurrence – Lower and Middle Stubensandstein, Löwenstein Formation, Germany; Calcare de Zorzino Formation, Italy; Ørsted Dal Member, Fleming Fjord Formation, eastern Greenland (Wild, 1989; Jenkins et al., 1994; Schoch, 2007).

Remarks – The genus *Aetosaurus* originally included two species, *Aetosaurus ferratus* and *Aetosaurus crassicauda*. *Aetosaurus crassicauda* is presently understood to represent

a larger specimen of *Aetosaurus ferratus* (Schoch, 2007). Specimens of *Stegomus arcuatus* from eastern North American have been assigned to *Aetosaurus* (Lucas et al., 1998); however, the majority of this material consists of natural molds that do not preserve the surface ornamentation. These specimens are assignable to *Aetosaurus* only on the basis of "aetosaurine" (*sensu* Parker, 2007) synapomorphies such as a sigmoidal lateral margin of the paramedian osteoderms with a pronounced anterolateral projection, as well as their small size. Small osteoderms (e.g., NMMNH P-17165) from the Bull Canyon Formation of New Mexico referred to *Stegomus* (*Aetosaurus*) *arcuatus* by Heckert and Lucas (1998) possess an anterior bar, radial pattern, offset dorsal eminence, and an anterolateral projection, which are "aetosaurine" characters and not diagnostic of a less inclusive taxon Several authors consider the lack of dorsal ornamentation, including a dorsal eminence (boss) in the osteoderms of *Stegomus* (*Aetosaurus*) *arcuatus* to be diagnostic of the taxon (e.g., Heckert and Lucas, 2000; Heckert et al., 2001; Spielmann and Lucas, 2012); however, the lack of ornamentation is because the type and key referred specimens consist solely of natural molds of the ventral surfaces of the osteoderms which are typically smooth and unornamented in aetosaurs.

Purported specimens of *Aetosaurus ferratus* from the Chinle Formation of Colorado (Small, 1998) are now considered to represent a distinct taxon, *Stenomyti huangae* (Small and Martz, 2013). *Aetosaurus* has also been recognized from Greenland and Italy. The Greenland material consists of a partial skull, postcranial skeleton and osteoderms (MCZ 22/92G; Jenkins et al., 1994). This skull possesses the following characteristics of *Aetosaurus ferratus*; an anteroposteriorly short jugal, a round

supratemporal fenestra; and an antorbital fossa that covers the majority of the lacrimal (Schoch, 2007). The Italian material (MCSNB 4864) consists of a short series of articulated dorsal paramedian and lateral osteoderms that possess an identical surface ornamentation to *Aetosaurus ferratus* (Wild, 1989). This specimen is significant as it was recovered from marine sediments of Norian age and represents a potential tie point to the marine biostratigraphic record for the Late Triassic (Lucas, 1998a, Irmis et al., 2010).

In summary, *Aetosaurus ferratus* is presently known from Greenland, Germany, and Italy, and purported North American occurrences cannot be substantiated (Schoch, 2007; Small and Martz, 2013). For this study *Aetosaurus ferratus* is scored only from the German lectotype and referred material.

Key References – Wild, 1989; Jenkins et al., 1994; Schoch, 2007.

Apachesuchus heckerti

Holotype – NNMNH P-31100, left dorsal paramedian osteoderm.

Referred material – NMMNH P-63427, left cervical paramedian osteoderm; NMMNH P-63426, right caudal paramedian osteoderm. Both of these specimens were originally included in NMMNH P-31100 (Heckert et al., 2001; Spielmann and Lucas, 2012:fig. 70e), but have been renumbered. Spielmann and Lucas (2012) also report that much more complete material of this taxon, including postcrania, is currently under study by Axel

Hungerbühler at the Mesalands Dinosaur Museum in Tucumcari, New Mexico. This new material is also from the Redonda Formation of New Mexico; however, the new material referable to *Apachesuchus heckerti* only consists of a few more paramedian osteoderms, whereas the rest of the material is actually referable to *Redondasuchus rineharti* (J. Martz, pers. comm., 2013).

Age – Late Triassic, late Norian-Rhaetian, Apachean (Spielmann and Lucas, 2012).

Occurrence – Quay Member, Redonda Formation, Dockum Group, New Mexico, U.S.A (Spielmann and Lucas, 2012).

Remarks – The holotype and paratype (referred) osteoderms were recovered in a microvertebrate assemblage found within a very large phytosaur skull and were originally assigned to *Neoaetosauroides* sp. because of the lack of surface ornamentation of the paramedian osteoderms (Heckert et al., 2001). However, *Neoaetosauroides* does have a surface orientation of radial grooves and ridges (see Chapter 2) and therefore NMMNH material cannot be assigned to that taxon. The lack of surface ornamentation in the type material of *Apachesuchus heckert*i appears to be a real feature and is considered an autapomorphy of the taxon (Spielmann and Lucas, 2012; J. Martz, pers. comm., 2013). *Apachesuchus heckerti* is considered to possess a low width/length ratios (> 0.3) of the paramedian osteoderms; which was obtained by comparing the length of the lateral edge to the total plate length (Heckert et al., 2001; Spielmann and Lucas, 2012). However, the

lateral edge of NMMNH P-31100 is greatly expanded anteroposteriorly than the rest of the osteoderm strongly skewing this ratio. The length at the center of the osteoderm is 32 mm, compared to an overall width of 104 mm. This provides a width/length ratio of 3.25, compared to the ratio of 2.5 provided by Spielmann and Lucas (2012). It is important to standardized areas of measurements for determining ratios of aetosaur osteoderms as simply using maximum length can skew results in plates with abnormal shapes. This is also true for osteoderms with elongate anterolateral processes of the anterior bars (e.g., *Scutarx deltatylus*). In these cases osteoderm lengths should be taken from the main osteoderm body and not from the anterior bar. Furthermore, an unnumbered referred anterior dorsal paramedian osteoderm in the Mesalands Community College Dinosaur Museum (MCCDM) collection (field number 20080618RET002RRB) has a width of 110 mm and a median length of 28 mm for a W/L ratio of 3.92. This is comparable to typothoracin aetosaurs such as *Typothorax coccinarum* (Long and Murry, 1995; Heckert et al., 2010).

Key References – Heckert et al., (2001); Spielmann and Lucas (2012).

Calyptosuchus wellesi

Holotype – UMMP 13950, articulated dorsal carapace from the posterior dorsal and caudal regions, associated with a portion of the vertebral column and the sacrum (Case, 1932; Long and Murry, 1995).

Referred Material – UMMP 7470, two dorsal paramedian osteoderms, three dorsal vertebrae, mostly complete, articulated sacrum; UCMP 27225, paramedian, lateral, and ventral osteoderms, partial right dentary. Numerous specimens from the *Placerias* Quarry from the UCMP and the MNA collections, as well as specimens from Petrified Forest National Park are listed in the main description of this taxon in Chapter 4.

Age – Late Triassic, early-middle Norian, early Adamanian (Ramezani et al., 2011; Parker and Martz, 2011).

Occurrence – upper Blue Mesa Member, Chinle Formation, Arizona, U.S.A.; Tecovas Formation, Dockum Group, Texas, U.S.A (Long and Murry, 1995; Parker and Martz, 2011).

Remarks – Case (1932) described a posterior portion of a carapace and associated pelvis and vertebral column of what he believed to be a phytosaur from the Upper Triassic of Texas. Although he discussed possible taxonomic affinities he was thoroughly perplexed by the material and thus did not assign the specimen to an existing taxon or coin a new taxonomic name. Mainly this is because of the common association of aetosaurian osteoderms with phytosaur remains (e.g., *Nicrosaurus kapffi*, Case, 1929) and because the osteoderms of UMMP 13950 possessed a radial surface ornamentation more similar to the osteoderm material then assigned to "*Phytosaurus*" *kapffi* (now the holotype of the

aetosaurian *Paratypothorax andressorum* Long and Ballew, 1985). This is unlike the surface ornamentation found in *Desmatosuchus spurensis*, the other aetosaurian Case was familiar with (Case, 1922). Indeed, Case (1932) tentatively suggested that UMMP 13950 may belong to the genus *Phytosaurus*. Gregory (1953a) recognized that the specimen was probably more closely related to *Typothorax* than to phytosaurs and hence most likely a pseudosuchian (aetosaur), but still considered the purported close similarity of the rectangular osteoderms with those assigned to some phytosaurs to be problematic for taxonomic resolution of the material.

This problem was finally resolved by Long and Ballew (1985) who correctly determined that all of the material with broad, rectangular osteoderms was referable to aetosaurians. Those authors also listed UMMP 13950 as the holotype of a new genus, *Calyptosuchus wellesi*. They did not redescribe Case's specimen, but instead discussed the new taxon in terms of referred material from the Triassic of Arizona. The most recent description of the taxon is by Long and Murry (1995) who mainly described referred material from the *Placerias* Quarry of Arizona. Elsewhere I have questioned the referrals of material to *Calyptosuchus wellesi* by Long and Murry (1995) mainly because of the recognition that the cervical lateral osteoderms assigned to *Calyptosuchus wellesi* by Long and Ballew (1985) and Long and Murry (1995) actually belong to a paratypothoracin aetosaur demonstrating the presence of a third aetosaur taxon in the *Placerias* Quarry (Parker, 2005a, 2007).

For this study I carefully sorted the *Placerias* Quarry material based on field numbers and use resulting associations as well as apomorphic comparisons to test these

assignments. I redescribe and figure known elements of *Calyptosuchus wellesi* elsewhere (Chapter 4) and score this taxon in the phylogenetic analysis based on the holotype and referred specimens. This anatomical work in association with detailed biostratigraphic work of the Chinle Formation (Parker and Martz, 2011) has also determined that *Calyptosuchus wellesi* is presently restricted to the upper part of the Blue Mesa Member and that specimens of *Calyptosuchus* noted from the Sonsela Member (e.g., Parker and Martz, 2011) belong to a new taxon, *Scutarx deltatylus*.

Key References – Case, 1932; Long and Ballew, 1985; Long and Murry, 1995.

Coahomasuchus kahleorum

Holotype – NMMNH P-18496, much of an articulated, but crushed skeleton (Heckert and Lucas, 1999a).

Referred Material – TMM 31100-437, partial skull, paramedian, lateral, and ventral osteoderms, vertebrae, limb, and girdle material (this study); NCSM 23168, much of a carapace (Heckert et al., in press).

Age – Late Triassic, Carnian?, Otischalkian (Lucas, 2010).

Occurrence – Colorado City Formation, Dockum Group, west Texas, U.S.A.; Pekin Formation, Newark Supergroup, North Carolina, U.S.A (Heckert and Lucas, 1999a; Heckert et al., in press).

Remarks – The holotype of *Coahomasuchus kahleorum* is distinctive, but poorly preserved, consisting of a flattened carapace concealing the majority of the vertebrae, the posteroventral corner of the skull, the posterior portion of the mandible, and a poorly preserved braincase, as well as articulated limb and girdle material (Heckert and Lucas, 1999a; Desojo and Heckert, 2004). Past phylogenetic analyses have recovered *Coahomasuchus kahleorum* as the sister taxon of *Typothorax coccinarum* and *Redondasuchus reseri* (Harris et al., 2003a correction of Heckert and Lucas, 1999a dataset), as the sister taxon of an unresolved clade containing *Aetosauroides*, *Calyptosuchus*, *Aetosauroides*, and *Aetosaurus* (Parker, 2007), and in an unresolved position closer to the base of Stagonolepididae (Desojo et al., 2012). Moreover, the latter authors pruned *Coahomasuchus* from their final tree to achieve better resolution, thus the phylogenetic relationships of this taxon are far from resolved. However, a more recent analysis by Heckert et al. (in press), utilizing a modified version of the dataset in Parker (2007) and Desojo et al. (2012), recovered *Coahomasuchus* as a non-stagonolepidid aetosaur at the base of Aetosauria. In this analysis *Coahomasuchus kahleorum* is coded from the holotype as well as a newly referred specimen from the Dockum Group of Texas (TMM 31100-437) formally referred to as the 'carnivorous form' (Murry and Long, 1996), which was recovered from the same geographical area and stratum as the

type specimen (Lucas et al., 1993). Fraser et al. (2006) documented the first occurrence of *Coahomasuchus* in the Pekin Formation of North Carolina providing a biostratigraphic correlation with the lower part of the Dockum Group of west Texas.

It was suggested that the holotype of *Coahomasuchus kahleorum* may represent a skeletally immature individual (Parker, 2003). However, histological sampling of the referred specimen TMM 31100-437, which is in the same size class, indicates that TMM 31100-437 is close to skeletal maturity (S. Werning, pers. comm., 2014). These findings will be presented elsewhere.

Key References – Heckert and Lucas (1999a); Desojo and Heckert (2004).

Desmatosuchus spurensis

Holotype – UMMP 7476, skull, nearly complete carapace, articulated cervical and dorsal vertebral column, ilium (Case, 1922).

Referred Material – see Parker, 2008b.

Age – Late Triassic, early to middle Norian, Adamanian (Ramezani et al., 2011; Parker and Martz, 2011).

Occurrence – Tecovas Formation, Dockum Group, Texas, U.S.A., Los Esteros Member, Santa Rosa Formation, Dockum Group, New Mexico, U.S.A., upper Blue Mesa Member, Chinle Formation, Arizona, U.S.A (Long and Murry, 1995; Parker, 2008b).

Remarks – First described from much of a carapace, and associated vertebral column as well as a skull, *Desmatosuchus spurensis* is a well-known aetosaurian from the Upper Triassic of the southwestern United States. Despite this confusion exists regarding characters of the dorsal armor for referral of specimens. For example all of the specimens listed by Long and Ballew (1985) from Petrified Forest National Park actually pertain to paratypothoracins and the osteoderm of *Desmatosuchus haplocerus* figured by Lucas and Connealy (2008:26) for the Dawn of the Dinosaurs exhibit at the New Mexico Museum of Natural History and Science is actually referable to *Calyptosuchus wellesi*.

Gregory (1953a) synonymized *Desmatosuchus spurensis* with *Episcoposaurus haplocerus*, a form described by Cope (1892), and the taxon was known as *Desmatosuchus haplocerus* for several decades, until it was determined that *Episcoposaurus haplocerus* was actually a *nomen dubium* (Parker, 2008b; 2013) although this has not been accepted by all workers (e.g., Heckert et al., 2012). New material from the Chinle Formation of Arizona demonstrated that previous carapace reconstructions for *Desmatosuchus spurensis* were erroneous and the body was broader than previous believed (Parker, 2008b).

Limb and pectoral girdle for *Desmatosuchus spurensis* is not known from the two best preserved specimens (UMMP 7476, MNA V9300), but Long and Murry (1995)

assigned isolated material from the *Placerias* Quarry to the taxon, which has been utilized for studies including bone histology (de Ricqlés et al., 2003). Unfortunately Long and Murry (1995) did not discuss the evidence for these referrals, which have been questioned (Parker, 2005a, 2008b); however, utilizing field numbers from the *Placerias* Quarry it may possible to refer some of this material to *Desmatosuchus spurensis*. For this analysis *Desmatosuchus spurensis* is coded from UMMP 7476 and MNA V9300.

Key References – Case, 1920, 1922; Long and Ballew, 1985; Long and Murry, 1995; Parker, 2008b.

Desmatosuchus smalli

Holotype – TTU P-9024, almost complete skull and right mandible, partial pelvis, femora, nearly complete cervical armor and numerous plates from the rest of the carapace (Parker, 2005c).

Referred Material – see Parker (2005c) and Martz et al. (2013).

Age – Late Triassic, mid-Norian, latest Adamanian and possibly earliest Revueltian (Ramezani et al., 2011; Martz et al., 2013).

Occurrence – Middle section of the Cooper Canyon Formation, Dockum Group, Texas, U.S.A. ; ?Martha's Butte beds, Sonsela Member, Chinle Formation, Arizona, U.S.A (Parker, 200c; Martz et al., 2013).

Remarks – Small (1985, 2002) described new material of *Desmatosuchus* from the Cooper Canyon Formation of Texas. Although he noted differences in the cranial material of the new material from the holotype of *Desmatosuchus spurensis* (UMMP 7476), he did not feel they were of taxonomic significance. In a revision of the genus *Desmatosuchus*, significant differences in the lateral armor were noted between the Cooper Canyon specimens and the type of *Desmatosuchus spurensis* (Parker, 2003). Combined with the cranial differences noted by Small (2002) the Cooper Canyon Formation material was assigned to a new species (Parker, 2005c). Further comments regarding this taxon including a novel reconstruction of the lateral cervical armor were provided by Martz et al., (2013). One of the problems in utilizing the non-osteoderm postcranial material of *Desmatosuchus smalli* is that some of it may actually pertain to an undescribed specimen of *Paratypothorax* from the quarry (Martz, 2008). A detailed apomorphy-based study of the aetosaurian material from the Post Quarry is needed along with field note reinvestigation to clarify some of the taxonomic assignments of the material (Martz, 2008).

Other than the Texas material, *Desmatosuchus smalli* is known from only one single referred lateral osteoderm from the Chinle Formation of Arizona (MNA V697), which had been assigned to *Desmatosuchus* by Long and Ballew (1985) as a cervical

lateral osteoderm. MNA V697 actually represents a dorsal lateral osteoderm and is assigned to *Desmatosuchus smalli* based on the ventrally recurved spine tip, which is an autapomorphy of *Desmatosuchus smalli* and does not occur in *Desmatosuchus spurensis* (Parker, 2005c). Although MNA V697 is listed as originating from a locality in the upper part of the Sonsela Member near Petrified Forest National Park (Long and Ballew, 1985), the locality data for this specimen are ambiguous. However, if correct this would represent the only Revueltian occurrence of *Desmatosuchus* (Parker and Martz, 2011).

The holotype of *Desmatosuchus* (=*Episcoposaurus*) *haplocerus* (ANSP 14688; Cope, 1892) consists chiefly of lateral and paramedian osteoderms of the cervical and anterior dorsal regions (Gregory, 1953a, Parker, 2013). Unfortunately the tips of the spines on all of the dorsal lateral osteoderms are broken away so the material cannot be differentiated between *Desmatosuchus spurensis* and *Desmatosuchus smalli*. Interestingly, the shape of the cervical lateral osteoderms as well as the ornamentation of the dorsal paramedian osteoderms are more reminiscent of *Desmatosuchus smalli* rather than *Desmatosuchus spurensis*, but the data are not conclusive and therefore *Desmatosuchus haplocerus* is considered a *nomen dubium* (Parker, 2008b, 2013).

Key References – Small, 1985, 2002; Parker, 2005c; Martz et al., 2013.

Longosuchus meadei

Lectotype – TMM 31185-84b, skull and much of a postcranial skeleton (Sawin, 1947). See Parker and Martz (2011) for detailed discussion of the status of the type materials.

Referred Material – TMM 31185-84a, partial skull and postcranial skeleton. See Long and Murry (1995) for a complete list.

Age – Late Triassic, ?Carnian, Otischalkian (Lucas, 2010).

Occurrence – Colorado City Formation, Dockum Group, Texas, U.S.A (Hunt and Lucas, 1990).

Remarks – The Works Progress Administration program in the 1930s made vast collections of vertebrate fossils from a series of quarries in strata of the Dockum Group in Howard County, Texas. This included several skeletons of an aetosaurian that Sawin (1947) described as a new species of *Typothorax*, *Typothorax meadei*. Several subsequent authors recognized the distinctiveness of this material (Long and Ballew, 1985; Small, 1989; Murry, 1989) and the species was placed in a new genus, *Longosuchus*, by Hunt and Lucas (1990). Sawin's original description is thorough but affected by a lack of good comparative material as well as a poor historical understanding of the taxonomic make-up of the Aetosauria. Thus he incorrectly reconstructed the incomplete lower jaw and pelvis, which confused aetosaur in-group relationships until these details were corrected by Walker (1961).

Most of the Otis Chalk material remains unprepared and numerous specimens, including partial skeletons, referable to *Longosuchus meadei* are in the Vertebrate Paleontology Lab (VPL) collections at the University of Texas (Austin) awaiting preparation.

An isolated fragment of a paramedian plate from the Salitral Shale (Chinle Formation) of New Mexico, assigned to *Longosuchus meadei* by Hunt and Lucas (1990), possesses a beveled posterior edge and a radial ornament pattern and is more likely referable to Paratypothoracini, in particular *Tecovasuchus* (Irmis, 2008). Lateral osteoderms from the Argana Group of Morocco assigned to *Longosuchus meadei* by Lucas (1998) appear to also represent a paratypothoracin as they are strongly dorsoventrally compressed and slightly recurved (Parker and Martz, 2010). Unfortunately this cannot be tested as these specimens have been reported as lost (S. Nesbitt, pers. comm. 2013). Character state scorings for this study were made solely using the TMM material.

Key References – Sawin, 1947; Hunt and Lucas, 1990; Long and Murry, 1995; Parker and Martz, 2010.

Lucasuchus hunti

Holotype – TMM 31100-257, posterior dorsal paramedian osteoderm (Long and Murry, 1995).

Referred Material – see Parker and Martz (2010) and Long and Murry (1995).

Age – Late Triassic, Carnian?, Otischalkian (Lucas, 2010).

Occurrence – Colorado City Formation, Dockum Group, Texas, U.S.A.; Pekin Formation, Newark Supergroup, North Carolina, U.S.A (Long and Murry, 1995; Parker and Martz, 2010).

Remarks – Long and Murry (1995) recognized the presence of two distinct large aetosaurian morphotypes in material from the Otis Chalk quarries in Howard County, Texas, the first being *Longosuchus meadei* and a second for which they coined a new taxon, *Lucasuchus hunti*. Sawin (1947) had also recognized the presence of this second aetosaurian, which he erroneously assigned to *Typothorax coccinarum*. Hunt and Lucas (1990) overlooked Sawin's (1947) separation of the material when they reassigned all of the material to *Longosuchus meadei*. Separated out again by Long and Murry (1995), the presence of two distinct taxa was disputed by some workers (e.g., Heckert and Lucas, 1999a, 2000) until Parker and Martz (2010) presented the differences in greater detail (Heckert et al., in press).

The holotype of *Lucasuchus hunti* is a single paramedian plate, but Long and Murry (1995) assigned numerous postcranial elements to the taxon. However, lack of preparation of much of this material, questions regarding associated with apomorphic

osteoderms, as well as apparent similarities with *Longosuchus meadei* makes many of these referrals questionable. Nonetheless there is still much unprepared material at the VPL that is almost certainly represents *Lucasuchus hunti*. A recently prepared partial skull (TMM 31100-531) from Howard County, Texas differs in some ways from the lectotype skull of *Longosuchus meadei* and could represent *Lucasuchus hunti* (Martz and Parker, unpublished data).

Osteoderms previously referred to *Desmatosuchus* and *Longosuchus* from the Pekin Formation of North Carolina actually pertain to *Lucasuchus* providing an important biostratigraphic correlation (Parker and Martz, 2010; Heckert et al., in press).

Key References – Long and Murry, 1995; Parker and Martz, 2010; Heckert et al., in press.

Unnamed taxon NCSM 21723

Holotype – NCSM 21723, a large portion of the cervical and anterior dorsal carapace.

Referred Material – none.

Age – Late Triassic, Carnian?, Otischalkian (Huber et al., 1993).

Occurrence – Upper portion of the Pekin Formation, Newark Supergroup, North Carolina, U.S.A. (Heckert et al., in press).

Remarks – NCSM 21723 consists solely of the anterior portion of the dorsal carapace of a desmatosuchine aetosaur. Similar in overall anatomy to *Longosuchus meadei* and *Lucasuchus hunti*, NCSM 21723 differs from these two taxa, and all other desmatosuchines, mainly in the possession of cervical paramedian osteoderms that are wider than long.

Key References – Schneider et al., 2011; Heckert et al., in press.

Neoaetosauroides engaeus

Holotype – PVL 3525, skull and postcranial skeleton (Bonaparte, 1969).

Referred Material – see Desojo and Báez (2007).

Age – Late Triassic, middle Norian, early Revueltian (Santi Malnis et al., 2011; Martinez et al., 2013).

Occurrence – Upper part of the Las Colorados Formation, Argentina (Desojo and Báez, 2005). Lucas (1998a) considered the Los Colorados Formation equivalent to his Apachean 'Land Vertebrate Faunachron' and therefore Rhaetian or at least latest Norian based on the presence of sauropodomorph dinosaurs and crocodyliform pseudosuchians. However, recent reexamination of strata in the Ischigualasto Basin, including a detailed

paleomagnetic study, suggests instead that the vertebrate bearing portion of the Los Colorados may in fact be equivalent to the upper portion of the Sonsela Member of the Chinle Formation and thus Revueltian in age (Santi Malnis et al., 2011; Martinez et al., 2013).

Remarks – The holotype of *Neoaetosauroides engaeus* was diagnosed by Bonaparte (1969) and first described in detail by Bonaparte (1972). Poorly understood for the purpose of prior phylogenetic analyses the holotype and several referred skulls were recently redescribed by Desojo and Báez (2005, 2007). Heckert and Lucas (2000) considered the paramedian osteoderms almost completely devoid of ornamentation and this lack of ornamentation to be an autapomorphy of the taxon. However, personal examination of the type specimens shows that *Neoaetosauroides engaeus* possesses a clear radial ornamentation of the dorsal osteoderms (also see Desojo and Báez, 2005). Indeed, the ornamentation is indistinguishable from that of the Ischigualasto taxon *Aetosauroides scagliai*. Portions of the holotype carapace are devoid of ornamentation, but this is clearly the result of overpreparation of the material. Nonetheless, three small osteoderms from the Redonda Formation (Dockum Group) of New Mexico were assigned to *Neoaetosauroides* based upon a lack of distinct ornamentation (Heckert et al., 2001). These osteoderms subsequently became the holotype of a new taxon *Apachesuchus heckerti* (Spielmann and Lucas, 2012). Character state scorings for *Neoaetosauroides engaeus* are from the type and referred materials.

Key References – Bonaparte, 1969, 1972; Desojo and Báez, 2005, 2007.

Paratypothorax andressorum

Holotype – SMNS unnumbered, left dorsal paramedian osteoderm (labeled L18 on red sticker) (Long and Ballew, 1985).

Paratypes – SMNS unnumbered, partial disarticulated carapace that includes the holotype osteoderm.

Referred Material – NHMUK R38070, posterior dorsal vertebra (Meyer, 1865:pl. XXVII, figs. 1-3); NHMUK R38083, left dorsal paramedian osteoderm; NHMUK R38085, partial right dorsal paramedian osteoderm (Meyer, 1865:pl. XXVIII, figs. 4-6); NHMUK R38086, partial right paramedian osteoderm; NHMUK R38087, pathologic left mid-caudal paramedian osteoderm (Meyer, 1865:pl. XXVIII, figs. 7-9; NHMUK R38090, right dorsal paramedian osteoderm, partial left dorsal paramedian osteoderm, three partial right paramedian osteoderms, partial left lateral osteoderm, left lateral osteoderm, two partial paramedian osteoderms; SMNS 3285, partial paramedian osteoderm; SMNS 2958, three pathologic paramedian osteoderms (Lucas, 2000); SMNS 4345 left dorsal lateral osteoderm; SMNS 4386, right dorsal lateral osteoderm (Meyer, 1861: pl. XLIII, fig. 1). ; SMNS 5721 right paramedian osteoderm (Meyer, 1865: Pl. XXVIII, figs. 1-3); YPM 3694, right dorsal lateral osteoderm (Gregory, 1953b).

Age – Late Triassic, Norian, Revueltian (Deutsche Stratigraphische Kommission, 2005; Lucas, 2010).

Occurrence – Lower Stubensandstein, Löwenstein Formation, Baden-Württemberg, Germany (Long and Ballew, 1985).

Remarks – The SMNS collections possess numerous osteoderms including much of what appears to be a carapace of a single individual that have had a confusing taxonomic history. The osteoderms were collected with and considered to belong to the phytosaur *Nicrosaurus* (=*Belodon* = *Phytosaurus*) until the mid-1980s (Long and Ballew, 1985). This belief caused significant confusion regarding the taxonomy of phytosaur and aetosaur material (Case, 1932; Gregory, 1962; Gregory and Westphal, 1969). The issue was finally sorted out when Long and Ballew (1985) recognized that all of the broad rectangular osteoderms belonged to aetosaurs and coined the name *Paratypothorax addressed* for the German osteoderms originally assigned to *Nicrosaurus*. The species epithet was correctly amended to *Paratypothorax andressorum* by Lucas and Heckert (1996). Long and Ballew (1985) also noted material from southwestern North America that is referable to *Paratypothorax* although they were unsure that it represented the same species as the European material. This has led to two views regarding the assignment of the North American material; 1) that it is referable to *Paratypothorax andressorum* (Hunt and Lucas, 1992; Heckert and Lucas, 2000; Lucas et al., 2006b), or that it may represent

a new taxon (Long and Ballew, 1985; Long and Murry, 1995). This is not yet resolved and I treat them here as two separate taxa.

The German material has never actually been fully described and the present concept of *Paratypothorax* (*sensu* Long and Murry, 1995) is actually based on the referred North American material. There is also some confusion regarding the type specimens of *Paratypothorax andressorum*, with some workers treating a well preserved carapace (SMNS unnumbered) as the holotype or as a syntype series for the taxon (e.g., Hunt and Lucas, 1992, Lucas et al., 2006b) However, Long and Ballew (1985:57) clearly identify a single osteoderm as the holotype so the other osteoderms in this specimen can be no more than paratypes (Heckert and Lucas, 2000).

An impression of a partial dorsal paramedian osteoderm (MCZ field No. 23/92G) from Greenland was assigned to *Paratypothorax andressorum* (Jenkins et al., 1994). Although the specimen clearly possesses a raised anterior bar, radial pattern of pits and grooves, a dorsal eminence that contacts the posterior osteoderm margin, characteristic for paratypothoracins, the beveled posterior edge delineated by a distinct ridge is not a clear autapomorphy of *Paratypothorax andressorum* and thus this specimen should be assigned to Paratypothoracini (Martz and Small, 2006; Desojo et al., 2013). I have not examined the other three osteoderms mentioned by Jenkins et al. (1994) and assigned to *Paratypothorax andressorum*.

Key References – Long and Ballew, 1985.

***Paratypothorax* sp.**

Referred Material – PEFO 3004, associated osteoderms and vertebrae from the posterior dorsal and anterior caudal regions (Long and Murry, 1995); FMNH PR1610, partial paramedian osteoderm (same specimen as PEFO 3004); DMNH 9942; partial postcranial skeleton (Long and Murry, 1995); VRPH2, numerous paramedian and lateral osteoderms; see Martz et al. (2013) for additional specimens.

Age – Late Triassic, Adamanian-Revueltian, mid-Norian (Ramezani et al., 2011; Parker and Martz, 2011).

Occurrence – Chinle Formation, Arizona and New Mexico, U.S.A.; Dockum Group, Texas, U.S.A (Long and Murry, 1995; Parker and Martz, 2011; Martz et al., 2013).

Remarks – the presence of *Paratypothorax* material in North America was first recognized by Long and Ballew (1985) although they were unsure of its exact relationship with the German material they named *Paratypothorax andressorum*. Since that time numerous specimens referable to *Paratypothorax* sp. or Paratypothoracini have been collected from the Upper Triassic Chinle Formation and Dockum Group (see Long and Murry, 1995; Parker and Martz, 2011; Martz et al., 2013 for lists). This includes lateral osteoderms from the *Placerias* Quarry of Arizona that were identified by Long and Ballew (1985) as cervical laterals of *Calyptosuchus wellesi* (Parker, 2005a). The best

preserved specimen (PEFO 3004) is an associated set of posterior dorsal and anterior caudal osteoderms and vertebrae of a single individual from the Chinle Formation of Arizona. First mentioned by Long and Ballew (1985), but described by Hunt and Lucas (1992), the latter authors assigned PEFO 3004 to *Paratypothorax andressorum*. This assignment was followed by Heckert and Lucas (2000) and Lucas et al. (2006b). However, differences between the North American and European material were noted by Long and Murry (1995) based on a specimen from the Dockum Group of Texas (DMNH 9942). Therefore the North American material is treated separately for this study. *Paratypothorax* sp. is known almost solely from osteoderms and vertebrae (Hunt and Lucas, 1992; Long and Murry, 1995). However, DMNH 9942 contains some forelimb material (Long and Murry, 1995). Long and Murry (1995) also questionably referred an ilium from the Post Quarry of Texas to the taxon, but this assignment is ambiguous. Martz et al. (2013) figure a fibula (TTU P-09416) they assign to *Paratypothorax* sp. A dentary of *Paratypothorax* was mentioned by Small (1989); however, the specimen is now considered a lateral osteoderm (Martz et al., 2013). It is possible that cranial material referred by Small (2002) to *Desmatosuchus* actually represents *Paratypothorax* sp. (Martz et al., 2013), but this has not yet been fully demonstrated.

Key References – Hunt and Lucas, 1992; Small, 1989; Long and Ballew, 1985; Long and Murry, 1995; Martz et al., 2013.

Polesinesuchus aurelioi

Holotype—ULBRA PVT003, parietal and braincase fragments, much of a postcranial skeleton (Roberto-da-Silva et al., 2014).

Age – Late Triassic, late Carnian – earliest Norian, *Hyperodapedon* Assemblage Zone (Langer et al., 2007; Martinez et al., 2011).

Occurrence – Sequence 2, Santa Maria supersequence, Rio Grande Do Sul, Brazil (Desojo et al., 2012).

Remarks— *Polesinesuchus aurelioi* was erected for mainly the endoskeletal material of a skeletally immature aetosaurian from the Upper Triassic of Brazil (Roberto-da-Silva et al., 2014). The taxon was not diagnosed by any recognized autapomorphies, but rather from a unique combination of characters that differentiates it from all known South American aetosaurians. Overall the material is most similar to that of *Aetosauroides scagliai*, but lacks the deep lateral fossae found in the cervical and dorsal vertebrae of that taxon. The vertebrae of *Polesinesaurus aurelioi* are notable in that they appear to lack vertebral laminae, which may be an autapomorphy of the taxon. However, the laterally expansive prezygapophyses listed as a defining character of the taxon may actually represent prezygadiapophyseal laminae (*sensu* Wilson, 1999), as these laminae form a similar structure in the presacral vertebrae of *Scutarx deltatylus* (PEFO 31217). The skeletally immature status of the material is problematic because our present understanding of character variation and transformation through ontogeny is poor and these unique characteristics may simply be the result of the ontogenetic immaturity at

time of death. Indeed, *Polosinesuchus aurelioi* appears to represent the well-preserved, but relatively unremarkable remains of a skeletal immature aetosaurian. Future histological studies of this taxon and others across will provide needed information on the timing of the appearance of key osteological landmarks in aetosaurian clades.

A phylogenetic analysis recovered *Polesinesuchus* as the sister taxon to *Aetobarbakinoides* in a clade that is sister taxon to Desmatosuchinae plus Typothoracinae, but this could be an artifact of missing data, especially from the paramedian and lateral osteoderms (Roberto-da-Silva et al., 2014).

Key Reference – Roberto-da-Silva et al., 2014.

Postosuchus kirkpatricki

Holotype – TTU P-9000, almost complete skull and partial skeleton (Chatterjee, 1985).

Paratype – TTU P-9002, almost complete skull and partial skeleton (Chatterjee, 1985).

Age – Late Triassic, early to middle Norian, Adamanian (Martz et al., 2013).

Occurrence – Cooper Canyon Formation, Dockum Group, Texas, U.S.A (Martz et al., 2013).

Remarks – *Postosuchus kirkpatricki* is a well-known rauisuchid archosaurs represented by excellent material from the Post Quarry of Texas. The type materials were recently redescribed in detail by Weinbaum (2011, 2013).

Key References – Chatterjee, 1985; Weinbaum, 2011, 2013.

Redondasuchus rinehardti

Holotype – NMMNH P-43312, partial right dorsal paramedian osteoderm (Spielmann et al., 2006).

Referred Material – see Spielmann et al., 2006. With permission I also score unpublished material currently under study by Jeffrey Martz and Axel Hungerbühler at Mesalands Dinosaur Museum in Tucumcari, New Mexico.

Age – Late Triassic, late Norian to Rhaetian, Apachean (Spielmann and Lucas, 2012).

Occurrence – Redonda Formation, Dockum Group, New Mexico, U.S.A (Spielmann and Lucas, 2012).

Remarks – A fair amount of aetosaurian osteoderm material has been recovered from the Upper Triassic Redonda Formation of New Mexico, most of which appears to be from at least one typothoracine. *Redondasuchus reseri* was named by Hunt and Lucas (1991) for a small typothoracine aetosaurs that reportedly lacked lateral osteoderms, and instead used flexion of the dorsal paramedians to cover the flank of the animal (Heckert et al.,

1996). However, the holotype osteoderm was interpreted backwards by those authors, and there is no evidence that *Redondasuchus reseri* differed from all other aetosaurs in lacking lateral osteoderms (Martz, 2002). Furthermore, Martz (2002) could not distinguish the osteoderms of *Redondasuchus reseri* from those of *Typothorax coccinarum* in any characteristic other than size. Spielmann et al. (2006) argued that *Redondasuchus reseri* was indeed distinct and named a second species, *Redondasuchus rineharti*, for isolated osteoderms and a proximal femur head from a larger aetosaurian. Those authors differentiated the new species from *Redondasuchus reseri* based on larger size and the presence of a dorsal eminence. This is problematic as no ontogenetic study has been made for *Redondasuchus* to refute the idea that *Redondasuchus reseri* is simply a skeletally immature specimen of another typothoracine. Moreover, in *Typothorax coccinarum*, the more anterior dorsal paramedian osteoderms lack dorsal eminences. Furthermore, strong flexion of paramedian osteoderms occurs in several aetosaur taxa including *Typothorax coccinarum* (PEFO 23388), *Paratypothorax* sp. (PEFO 3004), *Sierritasuchus macalpini* (UMMP V60817), and *Calyptosuchus wellesi* (UCMP 136744). Thus *Redondasuchus reseri* lacks clear autapomorphies or even a unique combination of characters and I do not include it in this study pending future reexamination. However, there are some fundamental differences between *Redondasuchus rineharti* and *Typothorax coccinarum* including the more closely packed and deep pits in *Redondasuchus rineharti*, as well as the oblong pits in the transverse trough posterior to the anterior bar and I include it in the present analysis, including scorings from new undescribed material from New Mexico (J. Martz, pers. comm. 2013).

Key References – Spielmann et al., 2006; Spielmann and Lucas, 2012.

Revueltosaurus callenderi

Holotype – NMMNH P-4957, nearly complete premaxillary tooth.

Referred Material – PEFO 33787, partial skeleton and skull; PEFO 33788, partial skull; PEFO 34269, partial skeleton and skull; PEFO 34561, nearly complete skeleton and skull; PEFO 36875, nearly complete skeleton and skull; PEFO 36876, partial skeleton and skull (Parker and Martz, 2011; Nesbitt, 2011; Parker et al., 2007, in prep).

Age – Late Triassic, mid to late Norian, Revueltian (Ramezani et al., 2011; Parker and Martz, 2011).

Occurrence – Petrified Forest Member, Chinle Formation, Arizona, U.S.A.; Bull Canyon Formation, Dockum Group, New Mexico, U.S.A (Hunt, 1989; Parker et al., 2005).

Remarks – Originally known from only isolated teeth that were assigned to ornithischian dinosaurs (Hunt, 1989; Padian, 1990; Heckert, 2003), *Revueltosaurus callenderi* is currently one of the most completely documented pseudosuchians based on an as of yet undescribed series of skeletons recovered from the Chinle Formation of Petrified Forest

National Park in Arizona (Parker et al., 2005, 2007). A current phylogenetic analysis of the Archosauriformes recovers *Revueltosaurus callenderi* as the sister taxon of Aetosauria (Nesbitt, 2011).

Key References – Heckert, 2002; Parker et al., 2005, 2007; Nesbitt, 2011.

Rioarribasuchus chamaensis

Holotype – NMMNH P-32793, right anterior caudal paramedian osteoderm (Zeigler et al., 2003).

Referred Material – see Parker, 2007.

Age – Late Triassic, mid-late Norian, Revueltian (Irmis et al., 2011).

Occurrence – Petrified Forest Member, Chinle Formation, New Mexico, U.S.A.; Marthas Butte beds, Sonsela Member, Chinle Formation, Arizona, U.S.A (Zeigler et al., 2003; Parker and Martz, 2011).

Remarks – *Rioarribasuchus chamaensis* was first described as a new species of *Desmatosuchus* by Zeigler et al. (2003) based on isolated paramedian and lateral osteoderms from the Revueltian Snyder Quarry in New Mexico. Parker (2003)

demonstrated with a phylogenetic analysis that "*Desmatosuchus*" *chamaensis* was closer to *Paratypothorax* rather than *Desmatosuchus*, a finding opposed by Heckert et al. (2003) who argued that the taxon was more like *Desmatosuchus* than *Paratypothorax*. Parker and Irmis (2005) and Parker (2006) argued that "*Desmatosuchus*" *chamaensis* should be assigned to a new genus, differing from studies such as Lucas et al. (2005) and Heckert et al. (2005a, b) who continued to assign the species to the genus *Desmatosuchus*. Subsequently two names were coined for the taxon almost simultaneously, *Heliocanthus* Parker 2007 and *Rioarribasuchus* Lucas, Hunt, and Spielmann 2006a; however, the paper by Lucas et al., 2006a was published earlier and thus the name *Rioarribasuchus* has priority. The status of the taxonomic name is considered controversial (e.g., Dalton, 2008), but was resolved by Irmis et al. (2007a), who as first reviser, used the name *Rioarribasuchus chamaensis* and accordingly *Heliocanthus* is the junior objective synonym of *Rioarribasuchus*. The close relationship between *Rioarribasuchus* and *Paratypothorax* has been recovered by all current phylogenetic analyses of the Aetosauria (Parker, 2007; Desojo et al., 2012; Heckert et al., in press). Indeed *Rioarribasuchus chamaensis* possesses no desmatosuchine apomorphies (Parker, 2007).

Parker (2007) also provided a novel reconstruction of *Rioarribasuchus chamaensis* in which the sacral and anterior caudal paramedian osteoderms possess dorsal eminences that have the form of an elongate, anterior medially directed, curved spine. The presence of these eminences is an autapomorphy of the taxon. The anterior paramedians and all of the lateral osteoderms are identical to *Paratypothorax*, and originally were thought to represent that taxon by the discoverers (Heckert and Zeigler,

2003). *Rioarribasuchus chamaensis* is currently known from the Snyder and Hayden quarries in the Chama Basin of New Mexico and from Petrified Forest National Park in Arizona. All three of these localities are in Revueltian strata of the Chinle Formation (Heckert et al., 2005b; Irmis et al., 2007a; Parker and Martz, 2011).

Rioarribasuchus chamaensis is currently known mainly from osteoderms, although Heckert et al., (2003) referred two astragali (NMMNH P-33927, NMMNH P-33932) and a calcaneum (NMMNH P-33931) from the Snyder Quarry. Those authors did not list any apomorphies or provide any comparisons to other taxa for the astragali and thus this referral is ambiguous given the co-occurrence of *Typothorax coccinarum* in the quarry. However, they did note that the referred calcaneum is not as dorsoventrally compressed as the calcaneum of *Typothorax coccinarum* (presumably AMNH FR 2713). Unfortunately there are no recognized paratypothoracin distal tarsals to use for a comparison to help verify these assignments. An isolated anterior aetosaurian caudal vertebrae (GR 174) from the Hayden Quarry bears caudal ribs that originate close to the base of the centrum rather than at the base of the neural arch. This character only occurs in *Paratypothorax* sp. (PEFO 3004) and not in *Typothorax* (Martz, 2002) so I consider the Hayden Quarry vertebra to represent a paratypothoracin, most likely *Rioarribasuchus chamaensis*.

Key References – Zeigler et al., 2003; Heckert et al., 2003; Parker, 2007.

Scutarx deltatylus

Holotype – PEFO 34616, partial skull, cervical paramedian and lateral osteoderms.

Referred Material – PEFO 31217, much of a postcranial skeleton including vertebrae, ribs, pectoral and pelvic girdles, osteoderms; PEFO 34919, much of a postcranial skeleton including vertebrae, ribs, osteoderms, ilium; PEFO 34045, much of a postcranial skeleton including vertebrae, ribs, and osteoderms; TTU P-09420, two paramedian osteoderms; UCMP 36656, paramedian and lateral osteoderms. The last two specimens were previously referred to *Calyptosuchus wellesi* (Long and Murry, 1995; Martz et al., 2013).

Age – Late Triassic, middle Norian, late Adamanian (Ramezani et al., 2011; Parker and Martz, 2011; Martz et al., 2013).

Occurrence – lower part of the Sonsela Member, Chinle Formation, Arizona, U.S.A.; middle part of the Cooper Canyon Formation, Dockum Group, Texas, U.S.A (Parker and Martz, 2011).

Remarks – Aetosaurian material referable to *Calyptosuchus* occurs through Adamanian-age deposits in Arizona, New Mexico, and Texas. In Arizona, specimens from the Sonsela Member previously referred to *Calyptosuchus wellesi* (e.g, Long and Murry, 1995; Parker and Irmis, 2005; Parker, 2005a, 2006; Parker and Martz, 2011; Martz et al.,

2013) possess a distinctive raised triangular boss on the posteromedial corner of the dorsal surface of the paramedian osteoderms. Detailed comparison demonstrates that this character is not present in the holotype of *Calyptosuchus wellesi* (UMMP 13950) or in referred material of that taxon from the *Placerias* Quarry. Thus this feature is autapomorphic of a new taxon, *Scutarx deltatylus* (described above). In this analysis, *Scutarx deltatylus* is coded from four new, partial skeletons from Petrified Forest National Park in Arizona. Newly recognized osteoderms of *Calyptosuchus* (TTU P-09420) from the Post Quarry of Texas also possess the diagnostic triangular boss and thus are actually referable to *Scutarx deltatylus* and not *Calyptosuchus wellesi* (differing from the interpretation by Martz et al., 2013). This occurrence supports correlation of the Post Quarry (middle Cooper Canyon Formation) to the lower part of the Sonsela Member of Arizona as suggested by Martz et al. (2013). Thus is may be possible to subdivide the Adamanian biozone utilizing *Calyptosuchus* and *Scutarx*.

Key References – This study; Parker and Irmis, 2005; Martz et al., 2013.

Sierritasuchus macalpini

Holotype – UMMP V60817, partial postcranial skeleton consisting of vertebrae and osteoderms (Parker et al., 2008).

Referred Material – TTU P-10731, left lateral osteoderm.

Age – Late Triassic, early to mid-Norian, Adamanian (Ramezani et al., 2011; Lucas, 2010).

Occurrence – Tecovas Formation, Dockum Group, Texas, U.S.A (Long and Murry, 1995; Parker et al., 2008).

Remarks – The holotype (UMMP V60817) of *Sierritasuchus macalpini* was collected in 1939 from the Tecovas Formation of Texas by the late Archie J. MacAlpin (University of Notre Dame), who at the time was a student of Ermine C. Case of the University of Michigan. The specimen, which consists of vertebrae and osteoderms from the cervical and dorsal regions, was originally referred to *Desmatosuchus haplocerus* by Long and Murry (1995). Parker (2002) questioned this referral and considered the possibility that UMMP V60817 represented a skeletally immature specimen of *Longosuchus meadei* even though it was from a higher stratigraphic position.

Redescribed by Parker et al. (2008), this was the first aetosaurian specimen to have osteoderms histologically sampled to help determine the ontogenetic stage of the specimen. Histological analysis suggested that although it is not a full grown adult, the specimen has no indicators of skeletal immaturity either (Parker et al., 2008). Within Desmatosuchinae *Sierritasuchus macalpini* shares more characters with *Longosuchus meadei* than *Desmatosuchus spurensis*, but differs from the former in possessing dorsoventrally flattened, non- faceted, recurved spines on the lateral osteoderms. Parker

et al. (2008) listed an additional difference, the lack of radial pattern on the dorsal paramedian osteoderms, but subsequent examination of the type materials of *Longosuchus meadei* demonstrate a random not radial pattern (Parker and Martz, 2010). *Longosuchus meadei* was scored as having a radial pattern in existing phylogenetic analyses (Heckert et al., 1996; Heckert and Lucas, 1999a), and this scoring was repeated in subsequent analyses (Parker, 2007; Parker et al., 2008). Determining the exact position of *Sierritasuchus macalpini* within Desmatosuchinae has been problematic (Parker, 2007; Parker et al., 2008); but Desojo et al. (2012) recovered *Sierritasuchus macalpini* as the earliest branching member of the Desmatosuchinae.

Key References – Parker et al., 2008; Desojo et al., 2012.

Unnamed taxon SMSN 19003

Age – Late Triassic, Norian, Revueltian (Deutsche Stratigraphische Kommission, 2005; Lucas, 2010).

Occurrence – Lower and middle Stubensandstein, Löwenstein Formation, Germany (Desojo et al., 2013).

Remarks – SMNS 19003 represents an almost complete, articulated skeleton of a paratypothoracin aetosaur from the Upper Triassic of Germany. The specimen includes a

beautifully preserved skull, which is the only unambiguous, non-braincase skull material known for a paratypothoracin. Desojo et al. (2013) refer the specimen as *Paratypothorax andressorum*, but the material has yet to be described and is currently under study by Rainer Schoch and Julia Desojo. However, some details of the skull were presented by Sulej (2010). One notable characteristic of the skull is that the apex of the premaxilla lacks the transverse expansion found in aetosaurs such as *Desmatosuchus* and *Stagonolepis* (pers. obs.). *Typothorax coccinarum* (YPM 58121) also lacks this expansion, suggesting that this may be an apomorphy for Typothoracinae.

Key References – Sulej, 2010; Desojo et al., 2013.

Stagonolepis robertsoni

Holotype – EM 27 R, impression of a segment of the ventral carapace (Agassiz, 1844).

Referred Material – see Walker (1961) for a full list; particularly important is MCZD 2, an articulated partial skeleton including much of the skull with a well preserved braincase and articulated nuchal and cervical paramedian osteoderms.

Age – Late Triassic, ?Carnian (Lucas, 2010).

Occurrence – Lossiemouth Sandstone Formation, Scotland, U.K (Walker, 1961).

Remarks – Originally described by Agassiz (1844) as a fish from what was thought to be the Old Red Sandstone in Scotland, Charles Lyell first raised suspicions that *Stagonolepis* might instead be a reptile more closely related to *Mystriosuchu*s (Huxley, 1859). Reexamination the material showed it to be a parasuchian reptile and provided the first solid evidence that the Lossiemouth Sandstone Formation was Triassic in age (Huxley, 1859, 1875, 1877). Unfortunately much of the collected material consists of natural molds, which has made study of the specimens difficult and only possible through the making of casts (Huxley, 1859, 1877). *Stagonolepis robertsoni* was fully described by Walker (1961) who developed a new technique of creating flexible PVC casts to recover additional details from the deeper portions of the molds than was available to Huxley. Walker (1961) also had the benefit of new specimens, most importantly an actually articulated body fossil (MCZD 2), which represents a nearly complete skull and the anterior cervical armor (Walker, 1961; Gower and Walker, 2002). This specimen allowed for detailed reconstruction of the skull and braincase and demonstrated clearly that *Stagonolepis robertsoni* was an aetosaurian rather than a phytosaur as previously believed (e.g., Camp, 1930).

Although Walker's (1961) reconstruction of *Stagonolepis robertsoni* relied significantly on observations made from *Aetosaurus ferratus*, examination of the MCZD specimen and the NHMUK casts show that Walker's work is extremely reliable for comparisons; however, character scorings for this analysis are taken from the fossils and casts, not from the published reconstruction. And, of course, this is based on the

assumption that only a single taxon is present in the Scottish quarries. Walker did note the presence of two different size catagories in the specimens, but determined any anatomical differences between the two to represent sexual dimorphism. There is currently no evidence to refute this hypothesis, the most notable difference is in the coverage of ornamentation on the dorsal paramedian osteoderms where in the smaller individuals the posterior portions of the dorsal surfaces are devoid of any ornamentation. Unfortunately all of the quarries where all of the *Stagonolepis robertsoni* material originates have been closed and grown over, and it is unlikely that more material of *Stagonolepis robertsoni* will be found in the immediate future.

What is clear from examination of the Scottish material is that *Stagonolepis robertsoni* is anatomically distinct from *Calyptosuchus* from North America, and *Aetosauroides scagliai* from South America (Parker and Martz, 2011; Desojo and Ezcurra, 2011; differing from Lucas and Heckert, 2001 and Heckert and Lucas, 2002a). Although all share a basic radial patterning and a medially offset dorsal eminence, there are key differences in the osteoderms and especially in the cranial material of these taxa, all of which are discussed in detail in Chapter 2. Therefore all are treated as separate terminal taxa in this analysis.

Key References – Huxley, 1877; Walker, 1961; Gower and Walker, 2002.

Stagonolepis olenkae

Holotype –ZPAL AbIII/466/17, skull roof (Sulej, 2010).

Referred Material – see Sulej (2010).

Age – Late Triassic, late Carnian (Dzik and Sulej, 2007).

Occurrence – Drawno beds, Krasiejów, Opole Silesia, Poland (Sulej, 2010).

Remarks – *Stagonolepis olenkae* was described by Sulej (2010) for remarkably well preserved aetosaur material from the Krasiejów quarry in Poland (Dzik, 2001; Dzik and Sulej, 2007). The original description of the holotype (Sulej, 2010) is based mainly on the skull material; unfortunately much of the descriptive text is identical to that of Walker (1961) so it is not clear if the Polish material is accurately described. Sulej (2010) provides some obscure references to postcranial material (e.g., mentioning of a tibia in the diagnosis), but other than some of this material being mentioned and partly figured by Dzik (2001), Lucas et al. (2007d) have provided the only descriptions and photographs of this material, but assigned it to *Stagonolepis robertsoni* based mainly on the ornamentation of the dorsal paramedian osteoderms.

Key References – Sulej, 2010; Lucas et al., 2007d.

Stenomyti huangae

Holotype – DMNH 60708, skull with lower jaws, partial postcranial skeleton including well-preserved ventral armor (Small and Martz, 2013).

Referred Material – DMNH 61392, partial skull with lower jaws, osteoderms, ribs, and vertebrae; DMNH 34565, maxilla, scapula, pubis, ribs and osteoderms.

Age – Late Triassic, middle – late Norian, Revueltian (Ramezani et al., 2011; Small and Martz, 2013).

Occurrence – "red siltstone" member, Chinle Formation, Eagle County, Colorado (Small and Martz, 2013).

Remarks – *Stenomyti huangae* is a well-documented small-sized aetosaurian that, when originally discovered, was presented as the first good evidence for the presence of *Aetosaurus* in western North America (Small, 1998). Subsequent preparation and study revealed that it was anatomically distinct (Small and Martz, 2013). *Stenomyti huangae* possesses a unique ventral armor arrangement, which instead of rows of articulated square osteoderms, consists of an arrangement of oval and irregularly shaped osteoderms that do not contact each other. The removal of these specimens from the genus

Aetosaurus eliminates a proposed biochronological correlation between Europe and eastern North America, with western North America (Lucas et al., 1998).

Key References – Small, 1998; Small and Martz, 2013.

Tecovasuchus chatterjeei

Holotype – TTU P-00545, paramedian and lateral osteoderms of the dorsal region, braincase, partial vertebra (Martz and Small, 2006).

Referred Material – UMMP 9600, right dorsal paramedian osteoderm; TTU P-09222, left dorsal paramedian osteoderm; TTU P-07244, dorsal paramedian osteoderm; NMMNH P-25641, left (?) dorsal lateral osteoderm; TMM 31173-54, partial left paramedian osteoderm; MNA V3202, partial right paramedian osteoderm, three right dorsal lateral osteoderms, one ?left dorsal lateral osteoderm fragment (Parker, 2005a); MNA V3000, left dorsal lateral osteoderm; MNA V2898, left dorsal lateral osteoderm (Heckert et al., 2007b).

Age – Late Triassic, early to middle Norian, Adamanian (Lucas, 2010).

Occurrence – Tecovas Formation, Dockum Group, Texas, U.S.A.; ?Bluewater Creek Member, Chinle Formation, New Mexico, U.S.A.; upper Blue Mesa Member, Chinle

Formation, Arizona, U.S.A (Parker, 2005a; Martz and Small, 2006; Heckert et al., 2007b).

Remarks – The holotype (TTU P-00545) was collected in the 1950s by Wann Langston Jr. from the Tecovas Formation near Potter County, Texas. A referred specimen (UMMP 9600) was collected near the same area in 1925 by William Buettner of the University of Michigan. TTU P-00545 was assigned to *Typothorax coccinarum* by Small (1985:8) and TTU P-00545, TTU P-09222, and UMMP 9600 were assigned to *Paratypothorax* sp. by Long and Murry (1995). Lucas et al. (1995) recognized the distinctness of the UMMP osteoderm, but hesitated to erect a new taxonomic name based on a single osteoderm and were apparently unaware of the Texas Tech specimen. The TTU material was later described under the name *Tecovasuchus chatterjeei* (Martz and Small, 2006).

Parker (2005a) and Heckert et al. (2007b) referred material from the lower part of the Chinle Formation, including MNA V3202, which had previously used as support for the presence of cervical spines in *Calyptosuchus wellesi* (Long and Ballew, 1985; Long and Murry, 1995). However, the lateral osteoderms of MNA V3202 possess apomorphies of Paratypothoracini most notably the greatly reduced triangular dorsal flange. The preserved paramedian osteoderm in MNA V3202 appears to have a high width/length ratio and the posterior edge is distinctly beveled, which is an autapomorphy of *Tecovasuchus chatterjeei* (Parker, 2005a; Martz and Small, 2006). *Tecovasuchus chatterjeei* has been postulated as an index taxon for the early Adamanian (Heckert et al., 2007b). These authors also assigned additional material from the NMMNH collections

(Heckert et al., 2007b:fig. 3) to *Tecovasuchus*; however, no apomorphies of that taxon are apparent in the published figures or listed in the text so I do not include those specimens here.

Key References – Lucas et al., 1995; Parker, 2005a; Martz and Small, 2006; Heckert et al., 2007b.

Typothorax coccinarum

Lectotype – USNM 2585, five paramedian osteoderm fragments.

Referred Material – Numerous specimens, see Long and Murry, 1995; Hunt, 2001; Martz, 2002; and Parker and Martz, 2011 for lists. Notable referred specimens include AMNH FR 2709, paramedian osteoderms, left femur; AMNH FR 2710, right femur (probably same specimen as AMNH FR 2709); AMNH FR 2713, lateral osteoderms, right femur, left calcaneum, caudal vertebra (lectotype of *Episcoposaurus horridus*); NMMNH P- 56299, articulated carapace missing the skull; NMMNH P-12964, nearly complete skeleton with skull (mostly destroyed); TTU P-09214, osteoderms, vertebrae, braincase, dentary; UCMP 34227, numerous dorsal paramedian osteoderms; UCMP 34255, articulated tail, limb and girdle material; YPM 58121, associated skeleton with complete skull; partial skeleton with skull (still in preparation).

Age – Late Triassic, middle to late Norian, latest Adamanian and Revueltian (Ramezani et al., 2011; Irmis et al., 2011).

Occurrence – Sonsela and Petrified Forest members, Chinle Formation, Arizona, U.S.A.; middle part of the Cooper Canyon Formation, Dockum Group, Texas, U.S.A.; Bull Canyon Formation, Dockum Group, New Mexico, U. S. A. (Long and Ballew, 1985; Heckert et al., 2010; Parker and Martz, 2011; Martz et al., 2013).

Remarks – Fossils of *Typothorax coccinarum* are extremely common in Revueltian rocks across the southwestern United States, but despite the large amount of available material most specimens have only been superficially or not described. An exception is a nearly complete skeleton (NMMNH P-56299) described by Heckert et al. (2010), which provides key information on the lateral osteoderms and especially the ventral armor. Some of the best figured materials are from the Canjilon Quarry (Martz, 2002), which forms the basis of much of the description by Long and Murry (1995) as well as our understanding of the taxon.

To date the best cranial material was a complete skull (NMMNH P-12964) from the Bull Canyon Formation (Dockum Group) of New Mexico. This skull was very preliminarily described by Hunt et al. (1993) and later figured, but not described by Heckert et al. (2010). Unfortunately this specimen was badly damaged during molding and is currently only visible in a cast (NMMNH C-4638) that is on exhibit at the New Mexico Museum of Natural History and Science (Heckert et al., 2010:628). Fieldwork by

Yale University in the Petrified Forest Member (Chinle Formation) of Petrified Forest National Park in the summer of 2008 resulted in the discovery of two skeletons of *Typothorax coccinarum* including a well-preserved skulls (YPM 58121). One of these skulls was used to code *Typothorax* for this study, but unfortunately the braincase is not exposed in that specimen. The second skull is still in preparation (M. Fox, pers. comm, 2014).

The type material of *Typothorax coccinarum* consists of only a few fragments of paramedian osteoderms and most descriptions and referrals have been made using better preserved material such as AMNH FR 2709, AMNH FR 2710, or UCMP 34227. The type material is not diagnostic above the level of Typothoracinae and accordingly *Typothorax coccinarum* is most likely a *nomen dubium* (Parker, 2013). Note that, following discussion by Parker (2006) and Parker and Martz (2013), I do not consider *Typothorax antiquum* Lucas, Heckert, and Hunt, 2003 a valid taxon, but rather a skeletally less mature specimen of *Typothorax coccinarum*. The occurrence (NMMNH P-25745) of the Revueltian phytosaur *Machaeroprosopus* (=*Pseudopalatus*) at the type locality for *Typothorax antiquum* also necessitates a detailed review of the stratigraphic position of this material, which is purportedly Adamanian in age (Lucas et al., 2003; Hunt et al., 2005).

Key References – Cope, 1875, 1877, 1887; Long and Ballew, 1985; Long and Murry, 1995; Martz, 2002; Heckert et al., 2010; Parker, 2013.

DESCRIPTION OF CHARACTERS

Many of these characters are taken from earlier phylogenetic studies by Parrish (1994), Heckert et al., (1996), and Heckert and Lucas (1999a), although some have been modified to incorporate more recent understanding of aetosaurian anatomy. Thus, these are considered framework studies in addition to the phylogenetic work of Parker (2007), with each study building on the former as our knowledge of aetosaur anatomy and taxonomy has increased. Therefore, in this section rather than repeating all of the citations for every character, I only list the initial analysis where a character first appeared in its original form.

Cranial Characters

1. Premaxilla, anterior portion in dorsal view: tapers anteromedially (0); laterally expanded (1). Modified from Parrish, 1994: character 3 (in part). Figures 6.1a, c, d, f.

In aetosaurians such as *Stagonolepis robertsoni* (Walker, 1961) and *Desmatosuchus smalli* (TTU P-9024) the anterior end of the premaxilla is mediolaterally wide and maintains a nearly constant width until the apex, which is an inclined and mediolaterally expanded, described as a "shovel" by previous workers (e.g., Parrish, 1994). This expanded apex was considered to be present in all aetosaurs for which a premaxilla was preserved, therefore in earlier phylogenetic analyses the character was an autapomorphy of Aetosauria and parsimony uninformative (Parrish, 1994; Heckert and Lucas, 1999a. Parker (2007) noted that an expanded apex was not present in *Aetosaurus*

(SMNS 5770, S-16) and SMNS 19003. In these taxa the premaxillae gradually decrease in width anteriorly and bear flattened lateral margins (Small and Martz, 2013). The premaxillae of *Typothorax coccinarum* (YPM 58121), *Stenomyti huangae* (Small and Martz, 2013), and *Aetosauroides scagliai* (PVL 2073) also taper and lack the expanded apex.

2. Premaxilla, contact of posterior process with nasal: present, excludes maxilla from the margin of the external naris (0); absent, maxilla participates in the posterior margin of the external naris (1). Modified from Heckert and Lucas (1999a), character 13. Figures 6.1a, g.

Contact between the nasal and premaxilla, excluding the maxilla from participation in the margin of the external naris is an apomorphy of Archosauriformes (Nesbitt, 2011). However, with the exception of *Aetosauroides scagliai* (PVL 2073), this contact is not present in aetosaurians and the maxilla forms a portion of the posterior and posteroventral borders of the external naris. In the referred skull of *Aetosauroides scagliai* (PVL 2073) the posterior process of the premaxilla underlies the entire length of the external naris contacting the ventral process of the nasal and excluding the maxilla from the border of naris (Casimiquela, 1961; Desojo and Ezcurra, 2011). Conversely, Heckert and Lucas (2002a) considered figures by Casimiquela (1961, 1967) to be inconclusive (see below) and that the maxilla bounded a portion of the naris as in *Stagonolepis robertsoni* (Walker, 1961). My examination of PVL 2059 and PVL 2052 found that the maxilla is definitely excluded. Heckert and Lucas (1999a) introduced this

character and because they were unsure of the condition in *Aetosauroides scagliai*, scored it as unknown. Parker (2007) excluded this character without explanation; however, it is reintroduced here.

3. Premaxilla, tooth arrangement: teeth present along ventral surface of entire element (0); teeth present, but restricted to posterior half of the element (1); teeth absent (i.e., premaxilla edentulous) (2). Modified from Heckert et al. (1996), character 21. Figures 6.1a, d, h.

Non-aetosaurian aetosauriforms such as *Revueltosaurus callenderi* have premaxillae with five alveoli present along the entire length of the element. At present, in all known aetosaurians with preserved premaxillae either the anterior portion (e.g, *Aetosaurus ferratus, Stagonolepis robertsoni*) or the entire element (*Desmatosuchus smalli*) lacks teeth. It was previously alleged that the premaxilla of *Typothorax coccinarum* is completely edentulous (e.g., Heckert et al., 1996) and was coded as such in all subsequent analyses (Heckert et al., 1999a; Parker, 2007; Desojo et al., 2012); however, new specimens (e.g., YPM 58121) demonstrate that there are a minimum of four teeth present in the premaxilla of *Typothorax coccinarum*.

4. Premaxilla, tooth count (single ramus): 4 or more tooth positions (0); 3 tooth positions (1); edentulous (2). [Ordered] New character. Figures 6.1c, f.

In prior analyses all known aetosaurs either had edentulous premaxillae (e.g., *Desmatosuchus smalli*) or when teeth were present they numbered between 4 and 5 tooth

positions (e.g., *Neoaetosauroides engaeus*, *Stagonolepis robertsoni*). However, the recently described *Stenomyti huangae* possesses only three premaxillary teeth (Small and Martz, 2013).

5. Premaxilla, dorsal surface of posterior process: smooth (0); with prominent dorsal tubercle that extends dorsally into the external naris (1). Small (2002). Figure 6.1a.

The presence of a tubercle on the dorsal surface of the premaxilla that projects into the naris of *Stagonolepis robertsoni* was briefly mentioned by Walker (1961); however, its possible phylogenetic significance was first recognized by Small (2002). In some taxa, such as *Stenomyti huangae*, the protuberance is weakly developed (Small and Martz, 2013); however it is still scored as present for this study.

6. External naris, anteroposterior length: less than the anteroposterior length of the antorbital fenestra (0); length is greater than or equal to that of the antorbital fenestra (1). Heckert and Lucas (1999a), character 8. Figures 6.1g, h.

In *Postosuchus kirkpatricki* the anteroposterior length of the external naris is less than that of the antorbital fenestra (Weinbaum, 2011); however, it is longer in all known aetosaurians so presently this character is parsimony uninformative within Aetosauria as the extreme length found in aetosaurians is an autapomorphy of that group (Parker, 2007).

7. Maxilla, lateral surface, longitudinal ridge: present, rounded and bulbous (0); present,

sharp (1); absent, lateral surface is smooth (2). Modified from Nesbitt (2011), character 26. Figures 6.1d; 6.2a.

Character state 2 refers to specimens with a smooth lateral surface of the maxilla ventral to the antorbital fenestra, as well as specimens that possess an antorbital fossa where the fossa rim is not raised above the surface of the maxilla (Nesbitt, 2011). Specimens with a fossa rim that is raised above the surface of the maxilla are scored as 1. A third character state where the raised ridge was bulbous (0) is only found in the outgroup taxon *Postosuchus kirkpatricki* (Nesbitt, 2011).

8. Maxilla, ventral portion of antorbital fossa in lateral view: dorsoventrally deep, more than 1/3 of the total element height (0); dorsoventrally shallow, less than 1/3 of the total element height, or absent (1). New character. Figures 6.1a; 6.2a.

Some aetosaurs (e.g., *Stagonolepis robertsoni*) possess a dorsoventrally deep antorbital fossa ventral to the antorbital fenestra; whereas in others (e.g., *Desmatosuchus spurensis*) the ventral portion of the fossa is extremely shallow.

9. Nasal, shape of anterior margin in dorsal view: tapering (0); maintains an equal width (1).New character. Figures 6.1b, e; 6.2b.

In some aetosaurians (e.g., *Stenomyti huangae*) the nasals reduce in transverse width anteriorly, tapering to a point dorsal to the premaxilla (Small and Martz, 2013). In others such as *Desmatosuchus smalli* (TTU P-9024), the nasals maintain a nearly

constant width along the entire anterior portion, contacting the posterior margin of the premaxillae.

10. Nasal, lateral margin: does not form part of the dorsal border of the antorbital fossa (0); forms part of the dorsal border of the antorbital fossa (1). Nesbitt (2011), character 37. Figures 6.1a, g; 6.2a.

In taxa without an extensive antorbital fossa, the ascending process of the maxilla and the anterior portion of the lacrimal meet to exclude the nasal from bordering the antorbital fossa (Nesbitt, 2011).

11. Nasals, posterior portion of the midline suture area: triangular depression (formed at the midline) (0); flat or convex (1). New character. Figures 6.1b, e; 6.2b.

In *Stenomyti huangae* the lateral margins of the nasals are raised and this raised area widens anteriorly, causing a triangular depression to form on the posteromedial portion of the nasals (Small and Martz, 2011: fig. 11c). This triangular depression is also apparent in *Aetosaurus ferratus* (Schoch, 2007: fig. 8c), *Aetosauroides scagliai* (PVL 2059), and *Longosuchus meadei* (TMM 31185-97). In contrast, the nasals of *Stagonolepis olenkae* (AbIII/2000) lacks this depression, as do the nasals of *Desmatosuchus* (e.g., UMMP 7476).

12. Jugal, lateral view: ventral margin is nearly horizontal (0); ventral margin is strongly

posteroventrally inclined (1). Modified from Nesbitt (2011), character 74, and Heckert and Lucas (1999a), character 14. Figures 6.1a, d.

In lateral view the ventral margin of the jugal is oriented nearly horizontally in most archosauriforms (Nesbitt, 2011), including aetosaurians such as *Aetosaurus ferratus* (Schoch, 2007) and *Stenomyti huangae* (Small and Martz, 2013). In other aetosaurians such as *Desmatosuchus spurensis* (UMMP 7476) and *Longosuchus meadei* (TMM 31185- 97) the jugal is strongly inclined anterodorsally so that the quadrate condyle is situated ventrally to the maxillary tooth row. *Stagonolepis olenkae* has a nearly horizontal ventral margin of the jugal; however, the jugal and quadratojugal are unknown for that taxon and were reconstructed using bones from *Neoaetosauroides* and *Desmatosuchus* (Sulej, 2010:867, 869). Likewise the jugals are missing in the skull of *Aetosauroides scagliai* (PVL 2059) and *Scutarx deltatylus* (PEFO 34616). A referred specimen of *Aetosauroides scagliai* (PVL 2052) preserves the anterior portion of the jugal; however, not enough is preserved to determine if it was inclined or nearly horizontal.

13. Jugal, anterior process: excluded from the border of the antorbital fenestra by contact between the lacrimal and maxilla (0); contributes to the border of the antorbital fenestra. (1). New character. Figures 6.1a, d.

In *Stenomyti huangae* (Small and Martz, 2013) the posterior portions of the lacrimal and maxilla contact each other, excluding the anterior portion of the jugal from contributing to the border of the antorbital fossa. In *Desmatosuchus smalli* (Small, 2002)

the posterior portions of the lacrimal and maxilla are separated from each other by the forward projection of the jugal into the margin of the antorbital fenestra.

14. Postfrontal, contact with parietal: absent (0); restricted by a posterolateral process of the frontal (1); extensive (2). [Ordered]. Desojo (2005), character 12. Figures 6.1b, e.

In some taxa (e.g., *Aetosaurus ferratus, Stenomyti huangae*), the postfrontal and parietal share an extensive border along the anterolateral margin of the parietal (Schoch, 2007; Small and Martz, 2013). In *Stagonolepis robertsoni*, this shared border is greatly restricted by a posterolateral process of the frontal that nearly contacts the anterodorsal corner of the dorsal process of the postorbital (Walker, 1961). In *Desmatosuchus smalli*, the postfrontal and parietal are separated from each other by a strong contact between the postorbital and the frontal (Small, 2002).

15. Postorbital: contact with quadratojugal - absent (0); present (1). Nesbitt (2011), character 64. Figures 6.1d, h.

In the majority of aetosaurians the postorbital and quadratojugal are separated from each other by an anterior process of the squamosal. However, in SMNS 19003 the squamosal process is reduced and there is extensive contact between the postorbital and quadratojugal. Schoch (2007) noted contact between the two bones in some specimens of *Aetosaurus ferratus*, and following Nesbitt (2011), *Aetosaurus ferratus* is coded as possessing character state 1.

16. Quadratojugal, anterior process: absent (0); forms ventral margin of lateral temporal fenestra (1); underlies jugal and is excluded from the lateral temporal fenestra (2). New character. Figure 6.1h.

In most aetosaurians, an anterior projection of the quadratojugal separates the dorsal portion of the posterior process of the jugal from the lateral temporal fenestra. However, in SMNS 19003, the posterior process of the jugal overlies the anterior process of the quadratojugal forming the entire fenestra border. *Neoaetosauroides* has a similar condition (state 1: Desojo and Báez, 2007); however, of the two referred skulls, one has had the lateral temporal fenestra artificially enlarged and the other is actually impressions of the bones in soft tissue, thus it is difficult to tell the actual condition and I score it as unknown. In *Stagonolepis robertsoni* the anterior projection of the quadratojugal forms the ventral margin of the lateral temporal fenestra; however, this reconstruction is based on *Aetosauroides ferratus* (Walker, 1961: 127). The jugal and quadratojugal are unknown for *Stagonolepis olenkae* (Sulej, 2010).

17. Quadratojugal, anterior margin: lacks dorsal anteroprocess between the posterior process of the jugal and the lateral temporal fenestra (0); distinct anterior facing notch in the middle of the anterior margin for reception of posterior process of the jugal (1). New character. Figure 6.1a, h.

In *Revueltosaurus callenderi* (PEFO 34561) and some aetosaurians such as *Coahomasuchus kahleorum* (TMM 31100-437) the anterior margin of the quadratojugal bears a distinct anteriorly opening notch for reception of a posterior process of the jugal.

Other aetosaurs such as *Stenomyti huangae* lack this notch and the posterior process of the jugal underlies the quadratojugal (Small and Martz, 2013).

18. Quadrate foramen, position: between the quadrate and the quadratojugal (0); completely within the quadrate (1). Modified from Nesbitt (2011), character 79. Figure 6.1a.

In *Stagonolepis robertsoni* the quadrate foramen is situated between the quadratojugal and the quadrate (Walker, 1961: 122). In *Coahomasuchus kahleorum* (TMM 31100-437) the foramen is entirely within the quadrate body.

19. Parietals/ frontals - transverse width at anteroposterior mid-points: parietal wider (0); frontal wider (1). New character. Figures 6.1b, e; 6.2b.

In *Aetosaurus ferratus* (Schoch, 2007) and *Stenomyti huangae* (Small and Martz, 2013) the transverse width of the parietals at their midpoint is greater than that of the frontals at their midpoint. In *Desmatosuchus smalli* (Small, 2002) and *Stagonolepis robertsoni* (Walker, 1961) the frontals are wider than the parietals at mid-point.

20. Supratemporal fenestra, position: only exposed in dorsal view (0); dorsolaterally or laterally oriented and visible in lateral view (1). Modified from Heckert and Lucas (1999a), character 10. Figures 6.1a, h.

In *Revueltosaurus callenderi* (PEFO 34561) the supratemporal fenestra are exposed dorsally which is the typical archosauriform condition; however, in aetosaurians

the squamosal and the postorbital-squamosal bar have shifted ventrally and the supratemporal fenestra is broadly exposed in lateral view. All aetosaur taxa that can be scored for this character have laterally exposed supratemporal fenestra so presently the character offers no in-group resolution (Parker, 2007). The supratemporal fenestra is completely exposed laterally in *Aetosauroides scagliai* (PVL 2073), a potential autapomorphy of that taxon.

21. Supratemporal fenestra, shape in lateral view: horizontal orientation of parietal forms a round or oval fenestra (0); strong posteroventral orientation of the posterior portion of the parietal forms a triangular fenestra (1). New character. Figures 6.1d, g.

The shape of the supratemporal fenestra is variable within Aetosauria and formed by the orientation of the parietal. *Desmatosuchus spurensis* (UMMP 7476) has a round fenestra, whereas it is triangular in SMNS 19003. In *Neoaetosauroides engaeus* (PVL 5698) the fenestra is strongly oval.

22. Supratemporal fenestra, anteroposterior diameter: larger than or nearly the same diameter as orbit (0); roughly half the size of the orbit (1); less than half the diameter of the orbit (2). [Ordered]. New character. Figures 6.1a, d, g.

The size of the supratemporal fenestra is variable in aetosaurs. It is nearly the size of the orbit in *Desmatosuchus spurensis* (UMMP 7476), roughly half the size of the orbit in *Neoaetosauroides engaeus* (PVL 5698), and much smaller than the orbit in SMNS 19003.

23. Post-temporal fenestra: present (0); absent (1). New character. Figures 6.1b, e.

In aetosaurs the posttemporal fenestra is a broad slit-like opening in the back of the skull between the ventral portion of the posteroventrally sloping flange (*sensu* Walker, 1961:114) of the parietal and the dorsal margin of the paroccipital process of the opisthotic. This fenestra is present in *Stagonolepis olenkae* (Sulej, 2010) and *Scutarx deltatylus* (PEFO 34616). Conversely, the fenestra is not present in *Desmatosuchus spurensis* (Case, 1922). This character is difficult to score in articulated specimens where the nuchal and anterior cervical paramedian osteoderms cover the back of the skull (e.g., *Aetosaurus ferratus*).

24. Basicranium, basal tubera: nearly or completely connected medially (0); clearly separate (1). Modified from Nesbitt (2011), character 104. Figures 6.3a-c.

In *Aetosauroides scagliai* (PVSJ 326) the basal tubera are distinctly separated by a broad anteroposterior trough between the occipital condyle neck and the basisphenoid recess. In *Scutarx deltatylus* (PEFO 34616) the basal tubera contact each other along the midline. In *Desmatosuchus spurensis* (UMMP 7476) are situated very closely together and are connected by a medial ridge. This latter condition is scored the same as a midline contact.

25. Basioccipital, distance between basal tubera and basipterygoid processes: widely separated anteroposteriorly (0); closely situated or nearly touching (1). Similar to Nesbitt (2011), character 103. Figures 6.3a-c.

In *Aetosauroides scagliai* (PVSJ 326) and *Stagonolepis robertsoni* (MCZD 2) the basal tubera and basipterygoid processes are widely separated anteroposteriorly the result of elongation of the parabasisphenoid. In *Desmatosuchus spurensis* (UMMP 7476) and *Scutarx deltatylus* (PEFO 34616), the basal tubera and basipterygoid processes are very closely situated anteroposteriorly, and this results in a foreshortened parabasisphenoid. This distance is the best way to quantify the differences in relative length of the parabasisphenoid between aetosaurians.

26. Dentary, dorsal and ventral posterior processes in lateral view: roughly equal lengths (0); upper process more elongate (1); lower process more elongate (2). New character. Figures 6.1a, d, h.

In most aetosaurians the posterior portion of the dentary splits into two posterior processes that are situated dorsal and ventral to the lateral mandibular fenestra. In lateral view these two processes are of roughly equal length in *Neoaetosauroides engaeus* (PVL 3525); however, in *Stagonolepis olenkae* (ZPAL AbIII/573) the dorsal process is much more elongate than the lower process. The reverse is found in *Desmatosuchus smalli*, where the ventral process in longer than the dorsal process (Small, 2002). The dentary of *Coahomasuchus kahleorum* (TMM 31100-437) also bears a median posterior (third)

process as in *Revueltosaurus callenderi* (PEFO 34561), but for this character they are both scored as 0 as all of the processes are of equal length.

27. Dentary, tooth count: 9 or more (0); fewer than 9 (1). Parker (2007), character 9; modified from Heckert and Lucas (1999a), character 16. Figures 6.1a, g.

Dentary tooth counts are variable across Aetosauria; however, the range of alveoli present seems to border on nine, with *Desmatosuchus smalli*, *Neoaetosauroides engaeus*, *Aetosaurus ferratus*, and *Longosuchus meadei* possessing between six and eight dentary tooth positions and *Aetosauroides scagliai* and *Stagonolepis robertsoni* having nine or ten. The original character of Heckert and Lucas (1999a) used 10 positions as the division between character states, but Parker (2007) changed it to nine without discussion. I retain the use of nine teeth here as *Stagonolepis robertsoni* has nine or 10 teeth (Walker, 1961). Furthermore, *Stenomyti huangae* has a minimum of nine positions in an incomplete lower jaw (Small and Martz, 2013) so the choice of nine as the division simplifies these character state codings. There are seven to nine positions in *Stagonolepis olenkae* (Sulej, 2010), but I use the average value and code it as state 1. Parker (2007) followed Heckert and Lucas (1999a) scored *Aetosaurus ferratus* as state 0; but despite that these teeth are poorly exposed in all known specimens, *A. ferratus* apparently has only seven or eight dentary tooth positions (Walker, 1961; Schoch, 2007). *Typothorax coccinarum* has more than nine dentary teeth based on YPM 58121. *Coahomasuchus kahleorum* can also be scored as 0 based on specimen TMM 31100-437.

28. Dentary, anterior half of dorsal margin: with teeth/alveoli (0); edentulous (1). Parrish (1994), character 9. Figures 6.1a, g, h.

In all aetosaurians with preserved dentaries, the anterior portions are edentulous, so this character is presently parsimony uninformative with respect to in-group relationships (Parker, 2007). However, *Revueltosaurus callenderi*, which is the sister taxon of Aetosauria (Nesbitt, 2011), bears alveoli for the entire length of the dentary so the possibility exists for an aetosaurian to possess the plesiomorphic character state. Earlier analyses (Parrish, 1994; Heckert et al., 1996; Heckert and Lucas, 1999a) scored *Aetosaurus ferratus* as having teeth in the anterior portion of the dentary, but Walker (1961) noted that the anterior portion of the dentary was edentulous. This was also noted by Schoch (2007).

29. Mandibular ramus, ventral margin in lateral view: The ventral margin of the ramus is gradually convex (0); a 'chin' is present, formed by a ventral inflexion of the splenial, which is exposed ventral to the dentary (1); A 'chin' is present, formed by a ventral inflexion of the dentary, which covers the splenial (2). New character. Descriptive terminology after Desojo and Ezcurra (2011). Figures 6.1a, d, g, h.

A classic character of aetosaurians is the ventral inflexion of the mandibular ramus in some taxa forming a prominent ‘chin’, which is part of Walker’s (1961) description of the element as ‘slipper-shaped’ (see discussion below). When present, this ‘chin’ is usually formed by the ventral inflexion of the splenial, extending below the concave ventral margin of the dentary. In this arrangement the ventral portion of the

splenial is visible in lateral view. *Stenomyti huangae* possesses a different arrangement, where the ventral inflexion is actually on the dentary and the splenial is not visible in lateral view (Small and Martz, 2013). This may also be the case in *Neoaetosauroides engaeus* (Small and Martz, 2013). Examination of PVL 3525, a right mandibular ramus, shows that the anterior portion is mostly reconstructed in plaster, but there is a slight ventral inflexion of the dentary where the bone ends. A referred specimen of *Neoaetosauroides engaeus* (PULR 108) also shows that the ventral margin of the dentary bears the ventral inflexion (Desojo and Báez, 2007; Desojo and Vizcaíno, 2009).

30. Dentary, anterior end in lateral view: rounded (0); tapers to an acute point (1). Modified from Heckert and Lucas (1999a), character 15. Figures 6.1a, d, g-h.

Walker (1961) was the first to describe the acute termination of the anterior portion of the dentary as contributing to the 'slipper-shape' of the mandibular ramus. The presence or absence of this shape was used as a phylogenetic character by Heckert and Lucas (1999a) and Parker (2007), although all aetosaurians with preserved dentaries were scored as possessing that character so it was parsimony uninformative. I have separated the 'slipper-shape' into two distinct characters (also see Character 29). Desojo and Ezcurra (2011) noted that the dentary of *Aetosauroides scagliai* was slender, lacking the ventral inflexion found *Stagonolepis robertsoni* (Walker, 1961), and therefore was not 'slipper-shaped.' Furthermore, although the anterior end of the dentary of *Aetosaurus scagliai* (PVL 2059) is distorted, it clearly was not acute and accordingly should be scored as bearing the 0 state (Desojo et al., 2012).

31. Surangular, dorsal margin: smooth (0); prominent rounded tuber (1). New character. Figure 6.4.

The surangular of *Stagonolepis olenkae* (ZPAL AbIII/578/34) bears a distinct rounded tuber on the dorsal surface dorsal to the lateral mandibular fenestra. A similar tuber is also present *in Stagonolepis robertsoni*, which Walker (1961) attributed to muscle or tendon attachment, most probably the *musculus adductor mandibulae externus* (Desojo and Vizcaíno, 2007). This tuber is absent in other specimens such as *Aetosaurus ferratus* (Schoch, 2007).

32. Articular, retroarticular process: height is greater than or equal to the length (0); longer than high (1). Desojo (2005), character 11. Figures 6.1a, 6.4.

In *Longosuchus meadei* (TMM 31185-84B) the retroarticular process of the articular is anteroposteriorly short and dorsoventrally tall. In contrast, the retroarticular process of *Desmatosuchus spurensis* (MNA V9300) is more elongate so that its anteroposterior length is greater than the dorsoventral height (Parker, 2008b).

33. Articular, dorsolateral surface: smooth (0); dorsally projecting tuber (1). New character. Figures 6.1a, d; 6.4.

The articular of *Stagonolepis olenkae* bears a pronounced dorsally projecting tuber (=articular projection) that is readily visible in lateral and medial views (Sulej, 2010:figs. 6, 7). It is also present in *Coahomasuchus kahleorum* (TMM 31100-437) and

Longosuchus meadei (TMM 31185-98). This tuber is absent in *Desmatosuchus spurensis* (MNA V9300) where the dorsal surface of the articular is smooth. There is a mound in *Desmatosuchus smalli* (TTU P-9023) but not the sharp, well-developed tuber found in other taxa.

34. Tooth, maxillary, root and crown base shape in occlusal view: narrow, mediolaterally compressed (0); oval, but not strongly mediolaterally compressed (1); conical (2). [Ordered] Modified from Parrish (1994), character 8. Figure 6.5.

The teeth of *Postosuchus kirkpatricki* (e.g., TTU P-9000) are mediolaterally compressed in occlusal view. No aetosaurian possesses teeth that are as medially compressed. The teeth of SMNS 19003 are oval in occlusal view, but not mediolaterally compressed, whereas in other aetosaurians the teeth are conical or round in occlusal view (e.g., *Desmatosuchus smalli*, TTU P-9023).

35. Tooth, maxillary, crown shape in labial/lingular view: fully recurved, anterior edge is convex and posterior edge is straight or concave (0); bulbous and partly recurved, anterior edge is concave, posterior edge straight (1); bulbous with pointed or slightly recurved tips (2). Figures 6.5a-d.

Aetosaurian teeth are quite variable in their anatomy, even within an individual skull, and this variability is difficult to capture as discrete states for a phylogenetic character. The first study to try to capture this was Parrish (1994), who divided aetosaurian tooth form into two states, recurved or conical. Heckert and Lucas (1999a)

retained Parrish's original character and added a second character: teeth unreduced, mediolaterally compressed, or reduced in size, nearly conical. However, this essentially was a duplication of Parrish's character and indeed all taxa coded for these characters were coded similarly with the exception of *Aetosaurus ferratus*.

In each of these analyses *Aetosaurus ferratus* was coded as possessing recurved teeth (Parrish, 1994) and recurved conical teeth (Heckert and Lucas, 1999a). The only other taxon coded for recurved, mediolaterally compressed teeth in the Heckert and Lucas (1999a) analysis was the rauisuchid *Postosuchus kirkpatricki.* However, Walker (1961) had noted earlier that the teeth of *Aetosaurus ferratus* were actually conical, with a bulbous base of the crown, and that only the apices were recurved. Parker (2007) tried to capture this variation with three character states; 1) mediolaterally compressed and recurved; 2) bulbous and conical with recurved tips; and 3) bulbous and conical lacking recurved tips, but this actually describes two non-homologous characters.

Since that time Schoch (2007) published a full description of *Aetosaurus ferratus*, including the dentition. He noted that none of the teeth of *Aetosaurus ferratus* were recurved and that they were conical and more similar to the teeth of other aetosaurs, but they all had a well-curved anterior edge unlike other aetosaurians except for *Stenomyti huangae* and SMNS 19003. However, I have also had the opportunity to study the material of *Aetosauroides scagliai* and the "carnivorous aetosaur" (=*Coahomasuchus kahleorum*) of Long and Murry (1996). Both have conical teeth that are fully recurved unlike the mediolaterally compressed, recurved teeth of *Postosuchus kirkpatricki*. Thus, I have divided these states between two distinct characters, one (character 33) describing

the tooth shape in occlusal view, and the other (character 34) describing crown shape in labio-lingular view.

Postcranial Characters

36. Cervical centra, ventral surface, at midline: keeled (0); smooth (1). Heckert and Lucas (1999a), character 20. Figure 6.6b, c, f.

Many archosauriforms have prominent anteroposteriorly sharp flanges of bone (keels) on the ventral surface of the cervical centra (Nesbitt, 2011). However, some aetosaurs (e.g., *Desmatosuchus spurensis*) have smooth ventral surfaces (Parker, 2008b).

37. Cervical vertebrae, length: anteroposteriorly shorter (more than 50%) than dorsoventrally tall (0); anteroposteriorly shorter (less than 50%) than dorsoventrally tall (1). New character. Figures 6.6b, e.

Aetosaurians differ from many archosauriforms in possessing cervical centra that are much shorter anteroposteriorly, than they are tall. However, some aetosaurians have cervical centra that are even anteroposteriorly shorter such as *Typothorax coccinarum* (Long and Murry, 1995).

38. Cervical vertebrae, centrum, shape of articular face: transversely oval (0); circular (1); subrectangular (2). Desojo (2005), character 17. Figures 6.6a, d.

The shape of the anterior articular face of the cervical centrum is variable in aetosaurians, circular in *Aetobarbakinoides brasiliensis* (CPE2 168), *Sierritasuchus*

macalpini (UMMP V60817), and *Stagonolepis robertsoni* (Walker, 1961); a shallow, wide oval in *Neoaetosauroides engaeus* (PVL 3525) and *Calyptosuchus wellesi* (UCMP 27225); and sub-rectangular in *Desmatosuchus spurensis* (MNA V9300; Desojo et al., 2012).

39. Cervical and trunk vertebrae, lateral surfaces of centra: concave or flat (0); concave with deep fossae (1). Desojo and Ezcurra, 2011. Figures 6.6e; 6.7d.

The cervical and trunk vertebrae of *Aetosauroides scagliai* bear prominent lateral fossae that cover much of the lateral surface of the centrum (Desojo and Ezcurra, 2011).

40. Trunk vertebrae, transverse processes: short, less than twice as wide as the centrum (0); elongate, more than twice as wide as the centrum (1). Heckert and Lucas (1999a), character 18. Figures 6.7b, c, f.

The mid-trunk vertebrae of *Paratypothorax* sp. (TTU P-9169) and *Typothorax coccinarum* (e.g., TTU P-9214) have elongate transverse processes. The transverse process width is 2.5 times the centrum width in TTU P-9214 (Martz, 2002). These elongate transverse processes appear to coincide with the more discoidal carapace in *T. coccinarum* and *Paratypothorax*. Long and Murry (1995) considered the transverse processes of *Calyptosuchus wellesi* to be extremely long; however, they were examining the posterior dorsal vertebrae, which have ribs fused to the transverse processes and *Calyptosuchus wellesi* should be coded as having short transverse processes because the mid-dorsals less than twice the width of the centrum (Parker, 2007). In the specimen of

Calyptosuchus wellesi with the longest transverse processes (UMMP 7470) the process is about 1.9 times the width of the centrum.

41. Mid-trunk vertebrae, neural spine height (from the base of the spine): greater than the height of the centrum (to the neurocentral suture) (0); equal to or less than the height of the centrum (1). Heckert and Lucas (1999a), character 19. Figures 6.7b, c, f.

In *Desmatosuchus* (e.g., MNA V9300) and *Typothorax coccinarum* (e.g., TTU P-9124) the heights of the neural spines of the presacral vertebrae are less than the height of the centrum. In contrast, *Stagonolepis robertsoni* (Walker, 1961) and *Neoaetosauroides engaeus* (Desojo and Báez, 2005) have tall neural spines that are more than the height of the centrum. This character is restricted to the mid-trunk series because in *Scutarx deltatylus*, the anterior and mid-trunk vertebrae have neural spines that are shorter than the centrum. However, around the position of the 13th trunk vertebra the neural spine and centrum heights transition to be roughly equal and in the more posterior vertebrae the neural spine becomes taller than the centrum. This variation does not occur in other specimens with short neural spines such as *Desmatosuchus spurensis*, as the ratio remains constant through the entire vertebral column (Parker, 2008b).

42. Trunk vertebrae, zygadiapophyseal laminae, connecting the diapophysis to the zygapophyses: present (0); absent (1). Desojo (2005), character 19. Figures 6.7a, b, d.

The cervical and trunk vertebrae of some aetosaurians (e.g., *Desmatosuchus spurensis*, MNA V9300) bear distinct vertebral laminae (Parker, 2008b). Four sets are

present in the cervical vertebrae of *Desmatosuchus spurensis*, following the terminology of Wilson (1999) they are the 1) the acdl, anterior centrodiapophyseal lamina, which originates on the diapophysis and terminates on the anterior margin of the neurocentral suture; 2) the pcdl, posterior centrodiapophyseal lamina, which originates on the diapophysis and terminates on the posterior margin of the neurocentral suture; 3) the podl, the postzygadiapophyseal lamina, which originates on the diapophysis and terminates on the postzygapophysis; and the 4) prezygadiapophyseal lamina, which originates on the diapophysis and terminates at the prezygapophyses. Furthermore, the trunk vertebrae of *Desmatosuchus spurensis* possess an additional two spinozygapophyseal laminae (*sensu* Wilson, 1999); 1) the spol, spinopostzygapophyseal lamina, which originates on the postzygapophysis and terminates on the posterior face of the neural spine; and 2) the sprl, the spinoprezygapophyseal lamina, which originates on the prezygapophysis and terminates on the anterior face of the neural spine. The presacral vertebrae of *Typothorax coccinarum* (TTU P-9214) and *Paratypothorax andressorum* (NHMUK 38070) possess all four laminae and the zygadiapophyseal laminae are extremely robust and confluent with the pre- and postzygapophyses.

A pair of laminae previously unrecognized in aetosaurs is present in the cervical vertebrae of *Scutarx deltatylus*. These laminae originate on the posteroventral surface of the postzygapophyses and form two sharp ridges that meet at the dorsomedial margin of the neural canal. These appear to be homologous to the intrapostzygapophyseal laminae (tpol) of Wilson (1999) found in saurischian dinosaurs.

Aetosaurian vertebrae generally tend to be poorly preserved, crushed and broken, or often are covered by the carapace and inaccessible. Furthermore, delicate portions of the bone such as accessory processes and laminae are often broken away making determination of their presence/absence difficult. Nonetheless, all known aetosaurians have presacral vertebrae with zygadiapophyseal laminae (except possibly *Polesinesuchus aurelioi*, Roberto-da-Silva et al., 2014) suggesting the presence may be an aetosaurian apomorphy. Future versions of this character may focus on the presence or absence of specific laminae (e.g., intrapostzygapophyseal laminae) once the presence or absence of general laminae have been demonstrated for most aetosaurians.

43. Trunk vertebrae, well-developed intervertebral articulations (hyposphene/hypantrum): present (0); absent (1). Figure 6.7f.

Desmatosuchus spurensis (e.g., MNA V9300) possesses a well-developed hyposphene and hypantrum in the trunk vertebrae (Parker, 2008b). Presently the only other known taxon with well-developed processes is *Aetobarbakinoides brasiliensis* (Desojo et al., 2012). TTU-P09416, a posterior presacral vertebra of *Paratypothorax* sp., has a very slight posterior projection at the base of the postzygapophyses (Figure 6.8b) that may represent an incipient hyposphene as it corresponds to a slight indentation in the ventral bar between the prezygapophyses, but this is not the same as the extremely well-developed processes in *Desmatosuchus* and *Aetobarbakinoides* and therefore is scored as 0. However if this feature is found to be present in more aetosaurian specimens, a new state could be added for this character.

44. Posterior trunk vertebrae (positions 14-16), ventral surface: smooth, rounded (0); lateral faces meet to form sharp edge or keel (1). New character. Figure 6.8a.

In the posterior trunk vertebrae of *Paratypothorax* sp., the lateral surfaces of the centrum meet to form a sharp ventral keel on the ventral surface of the centrum. This is best demonstrated by TTU P-09416, a posterior dorsal vertebra from the Post Quarry of Texas (Figure 6.8a). A ventral keel is present but weakly formed in NHMUK 38070, a posterior trunk vertebra of *Paratypothorax andressorum*.

45. Anterior caudal vertebrae (positions 1-12), origin point of caudal ribs: at the level of neural arch (0); near the base of the centrum (1). New character. Figure 6.7e, g.

In most aetosaurians the caudal ribs originate from the neural arch (e.g., *Desmatosuchus spurensis*, MNA V9300), but in *Paratypothorax* sp. (PEFO 3004) the caudal ribs originate low down on the centrum. An isolated caudal vertebra (GR 174) from the Hayden Quarry at Ghost Ranch New Mexico possesses caudal ribs situated low on the centrum and is most likely referable to *Rioarribasuchus chamaensis*, which occurs in the quarry (Irmis et al., 2007a).

46. Coracoid, posterolateral thickening below genoid lip that divides coracoid into posterior and lateral faces ('subglenoid pillar'): present (0); absent (1). Desojo (2005), character 20. Figures 6.9a-b.

Walker (1961:145) described the subglenoid region of the coracoid of *Stagonolepis robertsoni* as bearing "a depressed area bounded in front by a stout pillar which makes a slight projection in the medial margin and thus divides the outer surface into two areas". The first area contains the coracoid foramen and receives the insertion of *M. supracoracoideus*; whereas the second area is the insertion area for *M. coracobranchialis* (Desojo, 2005). A subglenoid pillar is also present in *Typothorax coccinarum* (Long and Murry, 1995) and absent in *Aetosauroides scagliai* and *Longosuchus meadei* (Desojo, 2005). A nearly complete scapulocoracoid of *Coahomasuchus kahleorum* (TMM 31100-437) lacks a prominent subglenoid pillar.

47. Humerus, distal end, lateral side of the ectepicondyle: proximodistally oriented groove present (0); proximodistally oriented foramen present (1). New character, but similar to Nesbitt (2011), character 234. Figures 6.9c-e.

The ectepicondylar foramen is present at the distal end of the humerus where it serves as a passage for the median (ulnar) nerve and the brachial artery (Landry, 1958). In stem- amniotes the opening is a foramen completely enclosed by bone in mature individuals (Romer, 1966). However; in some aetosaurs (e.g., *Aetosaurus ferratus*), the foramen is open laterally and thus a groove instead of a true foramen. A laterally open ectepicondylar groove is also found in *Revueltosaurus callenderi* (PEFO 34561), suggesting that this is the plesiomorphic state for aetosaurians. Nesbitt (2011) notes that a groove is also present in phytosaurs and some paracrocodylomorphs.

48. Humerus, proximal head: expanded medially, but lacks significant lateral expansion (0); broadly expanded transversely, with significant lateral expansion (1). New character. Figures 6.9d-e.

The proximal head of the humerus of *Aetosauroides scagliai* (PVL 2073) is moderately expanded (about one-third the element length), with almost all of the expansion medially, and almost no lateral expansion. In contrast, the humeral head of *Desmatosuchus smalli* (TTU P-9024) is nearly one-half the element length. Not only is the head expanded medially, but there is also a significant lateral expansion.

49. Ilium, orientation of acetabulum: opens fully or mostly ventrally (0); opens fully or mostly laterally (1). Modified from Desojo (2005), character 23. Figures 6.10a, c.

As noted by Desojo (2005) the orientation of the acetabulum can be difficult to determine because of crushing of preserved pelves and even more difficult in taxa only known from isolated ilia. Nonetheless various specimens demonstrate that the acetabulum opens ventrally in *Aetosauroides scagliai* (PVL 2073). *Scutarx wellesi* (UMMP 13950), *Scutarx deltatylus* (PEFO 31217), *Typothorax coccinarum* (PEFO 33967), and *Longosuchus meadei* (TMM 31100-236). The acetabulum opens mostly laterally in *Desmatosuchus spurensis* (MNA V9300) and in *Neoaetosauroides engaeus* (PVL 3525). The acetabulae of *Stagonolepis robertsoni* (Walker, 1961) and *Aetosaurus ferratus* (Schoch, 2007) to open ventrally (Desojo, 2005).

50. Pubis, proximal portion, number of 'obturator foramina': one (0); two (1).

Modified from Heckert and Lucas (1999a), character 25. Figure 6.10b.

Walker (1961) described two pubic foramina for *Stagonolepis robertsoni*, which differed from the condition in all other known aetosaurs. However, the pubis of *Scutarx deltatylus* (PEFO 31217) also has two foramina. This character was not considered by Parker (2007) who noted that two foramina were only known for a single taxon (*Stagonolepis robertsoni*) and thus the character was parsimony-uninformative; however, the discovery of that character state in a second taxon (*Scutarx deltatylus*) necessitates reinstatement of the character.

51. Pubis, symphysis length: long, more than one-half of the element length (0); short, less than one-half of the element length (1). New character. Figure 6.10c.

The pubis symphysis in *Aetosaurus ferratus* (Schoch, 2007) and *Typothorax coccinarum* (Long and Murry, 1995) is short, with the symphysis length less than half the length of the pubis. In contrast, the symphysis in *Desmatosuchus spurensis* (MNA V9300) is long, much more than half the element length (Parker, 2008b).

52. Osteoderms, dorsal carapace, transverse smooth strip along anterior edge of osteoderm (= anterior bar): absent (0); present but strongly raised (deliminated from remainder of osteoderm by a distinct trough) (1); present, but weakly raised (2); absent, depressed lamina present instead (3). Modified from Long and Ballew (1985): Table 1. Figure 6.11a, c-d, f-g, i.

Aetosaurians possess a smooth, narrow, transverse area along the anterior edge of osteoderms that represent the articular surface for slight overlap of the next anteriorly situated osteoderm. When this area is raised it is termed an "anterior bar" (Long and Ballew, 1985). According to those authors, a fully (strongly) raised anterior bar is delimited by a distinct trough along the posterior margin of the smooth area. In *Paratypothorax*, this distinct trough is lacking and the anterior bar is considered to be only weakly raised (Long and Ballew, 1985). In *Desmatosuchus*, the smooth articular surface is depressed below the level of the rest of the ornament surface. This is considered to be an anterior 'lamina' rather than an anterior bar (Long and Ballew, 1985).

53. Paramedian osteoderms (any), patterning of dorsal surface: random, no observable pattern (0); radiate (1); reticulate (2); smooth or flat (3). Modified from Long and Ballew (1985): Table 1. Figures 6.11f-g, j, l.

Long and Ballew (1985) first clearly defined the utility of the surface ornamentation of paramedian osteoderms for aetosaurian taxonomy, and Heckert et al. (1996) were this first to quantify this as a phylogenetic character. Heckert and Lucas (1999a) divided this character into three based on discrete carapace regions (i.e., cervical, dorsal, lateral), but Harris et al., (2003a) noted that there was no difference in the patterns of these areas and thus reductive coding of this character improperly weighted its' significance in the analysis. Following this, Parker (2007) devised a composite coding, utilizing only a single character to capture this variation.

In past studies (Heckert et al., 1996; Heckert and Lucas, 1999a; Parker, 2007) the ornament patterns in *Desmatosuchus* and *Typothorax* have both been considered to be 'random' as they lack a clear radial patterning. However, the ornamentation pattern is very different between these taxa with the ornamentation in *Typothorax* consisting mainly of uniformly placed small pits, surrounded by a nearly symmetrical latticework of raised areas, and that of *Desmatosuchus* consisting of pits and grooves of various sizes, offset by raised ridges. The patterning in *Typothorax coccinarum* is described as reticulate or equally spaced, non-radiate pits (Desojo, 2005). Thus I have added a new character state, reticulate, to capture this variation and for scoring the nearly symmetrical pattern found in *Typothorax*.

54. Paramedian osteoderms, dorsal eminence (or center of ossification) position throughout the carapace does not contact the posterior margin of the osteoderm in most rows (0); contacts posterior margin of osteoderm in most osteoderm rows (1). Modified from Long and Ballew (1985), Table 1. Figures 6.11a-d, f-h, l.

In most aetosaurians the dorsal eminence contacts the posterior plate margin (e.g., *Calyptosuchus wellesi*); however, in *Desmatosuchus* (e.g., MNA V9300) the boss is just posterior to the center of the osteoderm. In *Paratypothorax*, the boss position varies from close to the center of the osteoderm as in *Desmatosuchus*, to just anterior of the posterior plate margin, to actually contacting the posterior plate margin. This variation is related to anteroposterior position within the carapace, with the bosses being smaller and more anteriorly situated in more anterior osteoderms. The boss migrates posteriorly

backwards through the carapace reaching the posterior edge in the anterior caudal/posterior dorsal trunk paramedians. Nonetheless a boss that does not contact the posterior plate margin is more common in dorsal trunk paramedians of *Paratypothorax*, so they are coded 1.

The more forward situated eminence in *Paratypothorax* has caused confusion with some workers attempting to assign incomplete osteoderms to specific taxa. For example, all of the paramedian osteoderms from Petrified Forest National Park assigned to *Desmatosuchus* by Long and Ballew (1985) are actually incomplete osteoderms of *Paratypothorax* sp. The key difference is that the dorsal eminence is strongly offset medially in *Paratypothorax*, whereas the boss is centralized in *Desmatosuchus*. In the osteoderms assigned by Long and Ballew (1985) the lateral edges of the osteoderms are missing, making it appear that the bosses are located more centrally than they actually are.

55. Paramedian osteoderms, posterior margin: osteoderm maintains similar thickness throughout posterior to the anterior bar (0); posterior margin bears a transverse, posteroventrally sloping flange (bevel) (1). New character. Figure 6.11b, i, l.

Dorsal trunk paramedian osteoderms of *Tecovasuchus chatterjeei* (TTU P-00545) and *Paratypothorax andressorum* (SMNS uncatalogued – L10) have a distinct beveling of the posterior plate margin, which is extremely well-developed in *Tecovasuchus chatterjeei* (Martz and Small, 2006).

56. Paramedian osteoderms, transverse anteroposterior thickening (ventral keel or strut) absent, ventral surface is flat (0); weakly developed (1); strongly developed (2). Modified from Heckert et al. (1996), character 11. Figures 6.12a-c.

Dorsal trunk paramedian osteoderms with a ventral keel or strut bear a prominent mediolateral thickening of the ventral surface. The keel is strongly developed in *Typothorax coccinarum* (e.g., AMNH FR 2709) where it more than doubles the thickness of the osteoderm. Indeed, the first descriptions of *Typothorax coccinarum* interpreted this strut as a dorsal rib (e.g., Cope 1887; Huene 1915). There is a reduced strut in *Calyptosuchus wellesi* (UCMP 136744; Martz, 2002), and in *Adamanasuchus eisenhardtae* (PEFO 34638). In other taxa, such as *Desmatosuchus spurensis* (MNA V9300), the ventral surface of the osteoderm is completely flat and there is no strut.

57. Paramedian osteoderms, dorsal to the cervical and anterior trunk vertebrae, relative dimensions: wider than long (0); longer than wide (1). Heckert et al. (1996), character 1. Figures 6.11a-b.

Aetosaurian cervical dorsal paramedian osteoderms are either rectangular (wider than long) or roughly square (longer than wide, with the anterolateral corner 'cut off'). Osteoderms that are longer than wide are a synapomorphy of Desmatosuchinae (Parker et al., 2008); however, the newly described NCSM 21723, which possesses many desmatosuchine characters, has cervical paramedian osteoderms that are wider than long (Heckert et al., in press).

58. Paramedian osteoderms, dorsal to the cervical vertebrae (=cervical paramedian osteoderms), ratio of number of osteoderms to number of cervical vertebrae: approximately 1:1 (0); significantly less than 1:1 (1). New character.

Traditionally it was thought that aetosaurians with wider than long cervical paramedian osteoderms (character 56), possessed one osteoderm per cervical vertebra (generally nine), and that aetosaurians with longer than wide osteoderms only had about five or six osteoderms per for the nine vertebrae. However, *Typothorax coccinarum*, which possesses cervical paramedians that are wider than long, only had about five sets of osteoderms covering the entire cervical series (Heckert et al., 2010). This is similar to the counts in *Desmatosuchus* and *Longosuchus*, which have cervical paramedian osteoderms that are longer than wide and only five or six osteoderm sets over the cervical vertebrae.

59. Osteoderms dorsal to the cervical and anterior trunk vertebrae, articular surfaces: adjacent paramedian and lateral osteoderms are separate (0); adjacent paramedian and lateral osteoderms are often fully fused (1). New character. Figures 6.12c, d, g.

In *Desmatosuchus*, the dorsal and lateral cervical osteoderms are often completed fused (Parker, 2008b). This unrecognized fusion caused problems with the identification of some of these osteoderms in past studies (e.g., Brady, 1958:fig. 3; Long and Ballew, 1985: fig 6a). Fusion of the lateral and paramedian cervical osteoderms also occurs in *Longosuchus meadei* (Parker and Martz, 2010).

60. Paramedian osteoderms dorsal to the cervical and anterior trunk vertebrae, lateral edge articulation with lateral osteoderms: vertical 'flat' contact with some interdigitation (0); dorsoventrally thickened, angled contact, with deeply incised interdigitation (='tongue and groove') (1). Modified from Heckert and Lucas (1999a), character 46. Figure 6.11k.

The thickened and complex medial and lateral articular surfaces between osteoderms in *Desmatosuchus* was first described as ‘tongue and groove” by Long and Ballew (1985) and this has been followed by all subsequent workers. Long and Ballew (1985) described this articular surface as greatly thickened (dorsoventrally), strongly rugose and concave. This differs significantly from the thinner, vertical, and generally smoother articular surfaces found in other aetosaurs. This character is presently found only in both species of *Desmatosuchus*, *Longosuchus meadei*, *Lucasuchus hunti*, and *Sierritasuchus macalpini* and was considered a synapomorphy of Desmatosuchinae (Parker et al., 2008). The recently described NCSM 21723 was described as potentially being closely related to Desmatosuchinae; however, the original describers (Heckert et al., in press) do not mention if the osteoderm articular surfaces have a ‘tongue and groove’ articular surface, so I have coded it as unknown.

61. Paramedian osteoderms dorsal to the cervical vertebrae, dorsal eminence shape: smooth, not raised above osteoderm surface (0); low, pyramidal or rounded boss or elongate keel (1); tall, cone-shaped in posterior view (2). New character. Figure 6.11a.

Longosuchus meadei (TMM 31185-97), *Desmatosuchus smalli* (TTU P-9024), and *Lucasuchus hunti* (e.g., TMM 31185-60) have cervical paramedian osteoderms which bear prominent raised dorsal eminences. In contrast, in *Aetosauroides scagliai* (PVL 2073) and *Stagonolepis robertsoni* (Walker, 1961) have dorsal eminences that are barely visible and in *Typothorax coccinarum* (e.g., NMMNH P-56299), dorsal eminences are not visible until well into the dorsal trunk paramedian series (Heckert et al., 2010).

62. Osteoderms dorsal to the trunk vertebrae, articulation of lateral and paramedian osteoderms: the anterior edge of paramedian osteoderm overlaps the anterior edge of lateral osteoderm (0); the anterior edge of lateral osteoderm overlaps the anterior edge of paramedian osteoderm (1). Parker and Martz (2010). Figures 6.11g-h.

Aetosaurians have two distinct articulation patterns between the anterior edges of the paramedian osteoderm and the corresponding lateral osteoderm. In *Longosuchus meadei* (TMM 81185-84B) the anterolateral corner of the paramedian osteoderm has a dorsally facing articular facet that in articulation is overlapped by the anteromedial corner of the lateral osteoderm. In *Scutarx deltatylus* (e.g., PEFO 34616) the anteromedial corner of the lateral osteoderm is rounded and has a dorsally facing facet that receives the anteromedial projection of the paramedian osteoderm.

63. Paramedian osteoderms dorsal to the trunk vertebrae, “shape of the lateral edge in dorsal view: roughly straight or sigmoidal (0); sigmoidal with strongly posteromedially oriented posterolateral ("cut-off") corner (1). New character. Figures 6.11d, f-g, i.

Stagonolepis robertsoni (Walker, 1961), *Desmatosuchus spurensis* (MNA V9300), and *Aetosaurus ferratus* (Schoch, 2007) possess dorsal trunk paramedian osteoderms with roughly straight to sigmoidal lateral edges in dorsal view. *Paratypothorax* sp. (PEFO 3004) and *Adamanasuchus eisenhardtae* (PEFO 34638) possess strongly sigmoidal lateral edges in dorsal view, with a posterolateral corner that appears to have been sheared off. The strongly posteromedially oriented edge corresponds with a prominent triangular posterolateral projection of the lateral plate that fills the space voided by the 'cut-off corner' of the paramedian in the dorsal carapace.

64. Paramedian osteoderms dorsal to the trunk vertebrae, width/length ratio of widest osteoderms (rows 9-11) in series: less than 3.0 (0); 3.01-3.5 (1); 3.5 or more (2). Modified from Parrish (1994), character 15. Figures 6.11d, f-g.

As originally constructed by Parrish (1994) this character had two states, width/length ratio greater than or equal to 4.0 and width/length ratio less than 4.0 (Heckert et al., 1996; Heckert and Lucas, 1999a). Parker (2007) argued that only *Paratypothorax* possessed a width/length ratio greater than 4.0 so he reduced the division point to 3.5 to make the character more applicable. Heckert and Lucas (1999a) coded *Typothorax coccinarum* as possessing a maximum width/length ratio of greater than 4.0; however, I have not measured a paramedian osteoderm of *Typothorax* with that great of a ratio. The widest paramedian osteoderm from the UCMP Canjilion Quarry material has a ratio of about 3.88 and the Revuelto Creek *Typothorax* has a maximum of 3.5 (Heckert et al., 2010). Even the extremely large paramedian plate (PEFO 23388) discussed by Parker

and Irmis (2005) falls short of having a 4.0 ratio. However, referred material of *Redondasuchus rineharti* at the MCCDM (field number 2011RRBWKB#9) has a ratio of around 4.5 (J. Martz, pers. comm., 2013).

Most aetosaurs fall within the 3.01-3.5 ratio range; however a few have maximum ratios of less than 3.0. These include *Longosuchus meadei*, *Desmatosuchus spurensis*, *Stagonolepis robertsoni*, and *Aetobarbakinoides brasiliensis*.

65. Paramedian osteoderms dorsal to the trunk vertebrae; posteromedial surface of osteoderm ornamentation: lacking distinct transverse ridge between dorsal eminence and medial margin of the osteoderm. (0); distinct sharp raised mediolateral ridge extends medially from dorsal eminence to medial osteoderm margin (1). New character. Figures 6.11b, i.

The dorsal trunk paramedian osteoderms of *Tecovasuchus chatterjeei* (TTU P-545) bear a distinct mediolateral ridge that originates at the dorsal eminence and extends medially to contact the posteromedial plate margin. This ridge delineates the posterior beveled area in *Tecovasuchus chatterjeei*. This ridge is also present in *Paratypothorax* sp. (TTU P-9169), and although faint is also present in *Paratypothorax andressorum* (SMNS uncatalogued, R12).

66. Paramedian osteoderms dorsal to the trunk vertebrae, position of dorsal eminence relative to the center of the osteoderm centralized (0); moderately offset medially (1); strongly offset medially (2). Parker (2007), character 29. Figures 6.11f-g, j.

In *Desmatosuchus spurensis* (UMMP 7476) the dorsal eminence is situated centrally on the mediolateral axis of the paramedian osteoderm. It is shifted medially in *Stagonolepis robertsoni* (Walker, 1961), and it is shifted even further medially, almost to the medial edge of the osteoderm, in *Paratypothorax andressorum* (Long and Ballew, 1985)

67. Paramedian osteoderms dorsal to the trunk vertebrae, anterior margin of the anteromedial corner of the anterior bar in dorsal view: anteriorly directed triangular projection (0); straight (1). New Character. Figures 6.11d, g.

In aetosaurians such as *Stenomyti huangae* (Small and Martz, 2013), *Stagonolepis robertsoni* (Walker, 1961), and *Paratypothorax andressorum* (SMNS uncatalogued, L16) the anteromedial corner of the anterior bar bears a sharp triangular anterior projection. This projection is lacking in other aetosaurs such as *Desmatosuchus spurensis* (MNA V9300) where the anteromedial corner of the anterior bar is mediolaterally straight.

68. Paramedian osteoderms dorsal to the trunk vertebrae, lateral margin of the anterolateral corner of the anterior bar: distinct triangular lateral projection that barely extends beyond the lateral osteoderm margin (projection may be rounded distally (0); distinct triangular lateral projection that extends well beyond the lateral osteoderm margin (1); corner embayed for reception of the anteromedial projection of the lateral osteoderm (2). New character. Figures 6.11d, i, l.

Many non-desmatosuchine aetosaurs possess dorsal trunk paramedian osteoderms with anterior bars that bear an anterolateral projection that extends beyond that lateral margin of the main plate body. The length and distal end shape of the process are variable. *Aetosauroides scagliai* (PVL 2073) possesses a projection that is mediolaterally short with a pointed distal end. *Scutarx deltatylus* (PEFO 34616) also possesses a pointed process that is significantly more elongate. *Paratypothorax* sp. (PEFO 3004) has the shorter process, which instead of being pointed, it is gently rounded in dorsal view. This condition is coded the same as the short, pointed process as this character is based on process length and not process end shape. These anterolateral projections fill in a void in the anteromedial corner of the adjacent lateral osteoderm, slightly overlapping that portion of the lateral osteoderm.

69. Paramedian osteoderms dorsal to the trunk vertebrae, anterior margin of anterior bar/lamina on the medial side of the osteoderm: anteriorly concave ('scalloped") (0); straight (1). New character. Figures 6.11d, g, j.

The anterior bar in many aetosaurians bear a ‘scalloped-out’ anterior margin on the medial side of the dorsal trunk paramedian osteoderm. In plates with this character the anterior edge of the anterior bar is concave in dorsal view with the bar thinning anteroposteriorly in the center of the medial portion of the bar. Often this scalloping is associated with a triangular anterior process of the anterior bar that is directly anterior to the dorsal eminence. This character state is very prominent in the dorsal trunk paramedians of *Stagonolepis robertsoni* (Walker, 1961) and *Scutarx deltatylus* (PEFO

34045). It is absent in *Desmatosuchus spurensis* (MNA V9300) and *Longosuchus meadei* (TMM 31185-97). In *Typothorax coccinarum* (e.g., UCMP 34227), the medial portion of the anterior bar thins drastically, but the anterior projection anterior to the dorsal eminence does not appear to be present.

70. Paramedian osteoderms dorsal to the trunk vertebrae, posteromedial corner: flat with ornamentation (0); flat triangular area devoid of ornamentation (1); prominent raised triangular tuberosity devoid of ornamentation (2). [Ordered]. New character. Figures 6.11l, 6.12e-f.

An apparent autapomorphy of *Scutarx deltatylus* (e.g., PEFO 34616) is the presence of a large triangular protuberance in the posteromedial corner of the dorsal trunk paramedian osteoderms. However, although *Adamanasuchus eisenhardtae* (PEFO 34638) lacks the tuberosity, a triangular area in the same position is devoid of ornamentation, and this is considered a variation of this character.

71. Paramedian osteoderms dorsal to the anterior caudal vertebrae, dorsal eminence shape: absent, no dorsal eminence (0); low and pyramidal or rounded and knob-like (1); moderate, bulbous spike (2); tall, cone-shaped (3); tall anteriorly curved elongate spine (4). Modified from Long and Ballew (1985): Table 1. Figures 6.11c-e, g, j.

All aetosaurians, with the possible exception of *Redondasuchus reseri*, possess a raised dorsal eminence (boss) on the dorsal surface of the paramedian plates. In most taxa this boss takes the form of a low pyramidal or rounded knob, but in others the

eminence is dorsoventrally taller. Taller eminences take three distinct forms. In *Paratypothorax* they have the shape of a bulbous spike (although they tend to be larger in the German specimens). In *Lucasuchus hunti* (TMM 31100-361) , they are in the form of what Long and Murry (1995) described as an 'inverted ice-cream cone' in that they are extremely tall and conical with a broad rounded base. The third form is found in *Rioarribasuchus chamaensis* (e.g., NMMNH P-32793), where the dorsal eminence in the posterior trunk and anterior pelvic areas is an elongate, gracile, anteromedially recurved spine. Presently each of these tall forms is found in separate taxa. I do not combine them into a single 'tall' character because although the presence of the boss itself is homologous, it is not clear that a tall boss is homologous because it has taken so many unique forms.

72. Lateral osteoderms: absent (0); present (1). New character.

All known aetosaurs preserve lateral osteoderms with the exception of *Redondasuchus reseri* (Hunt and Lucas, 1991) and *Aetobarbakinoides brasiliensis* (Desojo et al., 2012); however, despite this absence, the evidence that they completely lacked lateral osteoderms is unequivocal. Lateral osteoderms are not present in *Postosuchus kirkpatricki* (Nesbitt, 2011; Weinbaum, 2013).

73. Lateral osteoderms, distribution within carapace; absent (0); only present in the sacral and anterior caudal region (1); present through the entire carapace (2). New character.

In all aetosaurians that preserve lateral armor this osteoderms extend through the entire carapace and even in taxa with incomplete carapaces there is no evidence to the contrary. There is unpublished data that shows that *Revueltosaurus callenderi* almost certainly had lateral osteoderms in the pelvic region (W. Parker, unpublished data).

74. Lateral osteoderms dorsolateral to the cervical vertebrae, form of the dorsal eminence: low keel or knob (0); moderate length dorsoventrally flattened slightly recurved spine (1); moderate length faceted, slightly recurved spine (2); greatly elongated horn (3). Figures 6.12g; 6.13h.

Taxa such as *Aetosaurus ferratus* (Schoch, 2007) and *Coahomasuchus kahleorum* (Heckert and Lucas, 1999a) possess cervical lateral osteoderms bearing dorsal eminences in the form of a low keel or knob. In other taxa such as *Longosuchus meadei* (TMM 31185-84B) and *Paratypothorax* sp. (VRPH 2) the eminence takes the form of a moderately elongate spine; however, in the former the spine is distinctly faceted. The facets, *sensu* Hunt and Lucas (1998), provide the spine with a trihedral cross-section (Lucas, 1998). The extreme is seen in *Desmatosuchus* (e.g., UMMP 7476) where the eminence is an enormous posteriorly recurved horn.

75. Lateral osteoderms dorsolateral to the anterior trunk vertebrae, dorsal eminence form knob or spine (0); large and hemispherical (1). Modified from Parker (2007), character 37. Figure 6.13e.

In *Desmatosuchus* the dorsal eminences on the first three dorsal trunk lateral osteoderms, situated just posterior to the large hornlike dorsal eminence of the posterior cervical laterals, are in the forms of a large, but low, ovate mounds (Brady, 1958:fig. 3; Long and Ballew, 1985:fig. 6a; Parker, 2008b:figs. 24a-c). Long and Ballew (1985) considered this shape for osteoderms of the pelvic region; however, the articulated specimen MNA V9300 demonstrated that they are instead from the anterior dorsal region (Parker, 2008b).

76. Lateral osteoderms dorsolateral to the trunk vertebrae, shape of dorsal flange: broad rectangle (0); triangular (1); highly reduced in size and a narrow triangle ("tongue-shaped") (2). [Ordered]. Parker (2007), character 36. Figures 6.13b-c, g, i-k.

The dorsal flange of the lateral osteoderms is the portion of the osteoderm that is medial to the dorsal eminence. The lateral flanges of many of the dorsal lateral osteoderms in *Calyptosuchus wellesi* (e.g., UCMP 27225) are distinctly triangular in dorsal view. This differs significantly from the dorsal flanges in *Tecovasuchus chatterjeei* (TTU P-545) and *Paratypothorax* sp. (PEFO 3004), which are much reduced and ‘tongue-like’ (Martz and Small, 2006), as well as the rectangular dorsal flanges of *Desmatosuchus spurensis* (MNA V9300) and *Longosuchus meadei* (TMM 31185-97). The triangular dorsal flange in *Calyptosuchus wellesi*, results from the elongate anterolateral process of the adjacent paramedian osteoderm projecting into the ‘space’ of the lateral osteoderm. Some of the lateral osteoderms of *Calyptosuchus wellesi* are sub-rectangular in dorsal view (e.g., UCMP 27225), however, these co-occur in the same

carapace with the triangular osteoderms and differ from taxa such as *Desmatosuchus spurensis* where all of the lateral osteoderms in the carapace bear rectangular flanges. Thus *Calyptosuchus wellesi* is scored for state 1, as at least some of the osteoderm lateral flanges are distinctly triangular.

Although the dorsal trunk lateral osteoderms of *Typothorax coccinarum* (e.g., NMMNH P-56299) share many characters with *Paratypothorax* sp., rather than *Calyptosuchus wellesi* (e.g., strongly acute angle of flexion, 'blade-like' flanges forming a curved spine in ventral view), the dorsal flange is clearly triangular in dorsal view and not 'tongue-like' as in *Paratypothorax*, thus I have scored *Typothorax coccinarum* as possessing state 1.

77. Lateral osteoderms dorsolateral to the trunk vertebrae, ventralmost 1/3 of the posterior face of the dorsal eminence (spine) ventral margin straight (0); distinct ventrally concave embayment ('emarginated') (1). Heckert and Lucas (1999a), character 48. Figures 6.12g; 6.13b, j.

In taxa where the dorsal eminence of the dorsal trunk lateral osteoderms forms a spine, there is a deep ventral, triangular emargination of the posterior face of the spine in some (e.g., *Longosuchus meadei*). This emargination is lacking in other taxa such as *Lucasuchus hunti* (Parker and Martz, 2010). This character is scored as inapplicable for taxa lacking a spine-like dorsal eminence, because absence of the spine is not the same as absence of the ventral emargination.

78. Lateral osteoderms dorsolateral to the mid-trunk region, form of the dorsal eminence: triangular boss or keel, not elongated (0); elongated flattened horn (1); conical spike (2). Parker (2007), character 30. Figures 6.13a-d, f-g, i-k.

A number of aetosaurians (e.g., *Calyptosuchus wellesi*, *Aetosaurus ferratus*) lack the extension of the dorsal eminence of the dorsal trunk lateral osteoderms into an elongate conical spike as in *Desmatosuchus spurensis* (UMMP 7476) and *Lucasuchus hunti* (TMM 31185-66). In *Typothorax coccinarum* (e.g., AMNH 2713) and *Paratypothorax andressorum* (SMNS uncatalogued, L18) the dorsal and lateral (ventral) flanges are mediolaterally elongate and meet along an extended transverse edge. This edge continues laterally and terminates in a slightly recurved point. Thus it is more like an elongate flattened horn than a conical spine.

79. Lateral osteoderms dorsolateral to the mid-trunk region, angle of flexion between dorsal and lateral flanges of the osteoderms obtuse (0); approximately 90 degrees (1); strongly acute (2). [Ordered] Modified from Heckert et al. (1996), character 14. Figures 6.14a, d, j.

This character is variable through the anteroposterior extent of the carapace and thus is restricted to the mid-lateral to posterior dorsal trunk lateral osteoderms. Aetosaurians with obtuse angles of flexion between the dorsal and lateral flanges include *Aetosaurus ferratus* (Schoch, 2007) and *Coahomasuchus kahleorum* (Heckert and Lucas, 1999a). Heckert and Lucas (1999a) considered the dorsal trunk lateral osteoderms of the holotype of *Coahomasuchus kahleorum* (NMMNH P-18496) to be completely flat with

not sign of a division into dorsal and lateral flanges. This would be autapomorphic for Aetosauria; however, in NMMNH P-18496, the lateral osteoderms have small, triangular dorsal flanges as in *Aetosaurus ferratus* and *Calyptosuchus wellesi* (UCMP 27225) and flattening of the carapace because of crushing has pushed the dorsal flanges downward and partially obscuring them. However, they can be seen in the holotype (Heckert and Lucas, 1999a: fig. 3) on the right side in the waist narrowing and anterior to it. Note also that the width of the lateral flange increases significantly anterior to the waist compared to the very reduced dorsal flange and this helps to create the illusion that these is no discrete dorsal flange. The presence of a discrete triangular flange and obtuse flexion of the lateral osteoderms is also confirmed by isolated osteoderms in TMM 31100-437. Specimens that possess an obtuse angle of flexion retain this through the entire carapace. *Calyptosuchus wellesi* has been described as possessing cervical laterals with an acute angle of flexion (Long and Ballew, 1985; Long and Murry, 1995); however, these are dorsal lateral osteoderms of a '*Tecovasuchus*-like' taxon (Parker, 2005a).

Desmatosuchus spurensis (e.g., MNA V9300) and *Longosuchus meadei* (TMM 31185-97) possess distinct dorsal and lateral flanges that meet at an angle of around 90 degrees. This varies little throughout the carapace. *Typothorax coccinarum* (e.g., NMMNH P-56299) and *Paratypothorax andressorum* (SMNS unnumbered, L18) have dorsal and lateral flanges that meet at an acute angle and are scored as such; however, other lateral osteoderms in these taxa are anteroposteriorly shorter and have flanges that meet at right angles (e.g., *Paratypothorax andressorum* (SMNS unnumbered, L9, R10). It is not entirely certain where in the carapace this character state occurs but scoring of

disarticulated, incomplete material needs to be done with caution. If a specimen possesses the acute angle in at least one osteoderm, I code the taxon as possessing that state even if the angle of flexion in other osteoderms in the same carapace may trend closer to 90 degrees. Completion of preparation and description of SMNS 19003 should reveal these changes in angle of flexion in an aetosaur with the acute osteoderm type.

80. Lateral osteoderms dorsolateral to the mid-trunk region, symmetry of dorsal and lateral flanges: weakly or strongly asymmetrical, with lateral flange the longest (0); strongly asymmetrical with dorsal flange longest (1). Modified from Heckert et al. (1996), character 15. Figures 6.14a,c, i.

This character considers size differences (symmetry) of the lateral and dorsal flanges of the dorsal trunk lateral osteoderms as divided by the axis of the dorsal eminence. No aetosaurian lateral osteoderm is perfectly symmetrical; however, in taxa where the symmetry is close the lateral flange is still larger than the dorsal flange (e.g., *Aetosauroides scagliai*). Where the flanges are strongly asymmetrical, some taxa such as *Coahomasuchus kahleorum* (NMMNH P-18496), have greatly reduced dorsal flanges where the dorsal flange is a small triangle and the lateral flange is a wide rectangle (see Heckert and Lucas, 1999a: fig. 3). In *Desmatosuchus spurensis* (MNV V9300), the mid-dorsal trunk lateral osteoderms possess elongate dorsal flanges, and reduced lateral flanges (Parker, 2008b).

81. Lateral osteoderms dorsolateral to the sacral and anterior caudal vertebrae, lateral flange shape: roughly rectangular and lateral to a sharp medially situated keel (0); roughly triangular in lateral view with a semicircular ventrolateral border and a hook-like eminence (1); rectangular and ventral to a well-developed spine (2). Parker (2007), character 28. Figures 6.13c, f, j.

This character attempts to capture the anatomical variation in the lateral flange of the pelvic and anterior caudal lateral osteoderms. A roughly triangular osteoderm with a semicircular ventrolateral border and a hook-like eminence is shared by several taxa including *Typothorax coccinarum* (NMMNH P-56299) and *Paratypothorax sp.*(PEFO 3004), and differs strikingly from the spiked plate found in *Desmatosuchus spurensis* (MNA V9300) and *Longosuchus meadei* (TMM 31185-84b). A somewhat similar form occurs in *Aetosaurus ferratus* (Schoch, 2007), *Stagonolepis robertsoni* (Walker, 1961), *Aetosauroides scagliai* (PVL 2073), and *Neoaetosauroides engaeus* (PVL 3525), but these plates are more rectangular rather than triangular (Parker, 2007).

82. Carapace, overall shape in dorsal view: presence of narrow waist anterior to sacrum (0); moderate spinose carapace (1); broad discoidal carapace (2). Modified from Heckert et al. (1996), character 16.

The aetosaur carapace comes in three general forms, a narrow carapace with a distinct narrowing (waist) just anterior to the pelvis (e.g., *Aetosaurus ferratus*), a broader carapace that lacks the narrow waist and is generally spinose (e.g., *Desmatosuchus*

spurensis), and a very broad discoid form (e.g., *Typothorax coccinarum*) (Desojo et al., 2013:fig. 1).

83. Osteoderms ventral to the trunk vertebrae, shape and arrangement: absent (0); irregular, non-touching (1); square, overlapping (2). New character.

Previous characters regarding the ventral osteoderms focused on number of rows or the type of ornament; however, these were difficult to score given the incomplete preservation of the ventral osteoderms in many taxa. Instead, this new character focuses on the shape and arrangement of the ventral osteoderms in light of the recent discovery of *Stenomyti huangae*, which has a unique arrangement of the ventral osteoderms (Small and Martz, 2013). In aetosaurians such as *Stagonolepis robertsoni* (Walker, 1961) and *Coahomasuchus kahleorum* (Heckert and Lucas, 1999a) the associated ventral osteoderms consists of rows and columns of overlapping, equant osteoderms. However, in *Stenomyti huangae* the ventral osteoderms are round to oval and non-overlapping (Small and Martz, 2013). Despite the recovery of several nearly complete skeletons of *Desmatosuchus* and *Longosuchus meadei*, no ventral osteoderms are known for the taxa and it is hypothesized here that these forms lacked ventral armor (Parker, 2008b).

PHYLOGENETIC ANALYSIS

The character matrix of 28 taxa and 83 characters was assembled and edited in Morphobank (O'Leary and Kaufman 2012) as matrix number 2617 of project number

1009, and exported as a NEXUS file (Appendix A). Submatrices (partitions) were edited using NEXUS Data Editor for Windows version 5.0 (Page, 2001). All matrices were analyzed in PAUP* (Version 4.0b10 for 32-bit Microsoft Windows, Swofford, 2003). *Postosuchus kirkpatricki* was constrained as the outgroup for the analysis. *Revueltosaurus callenderi* was utilized as a second outgroup, but unconstrained.

PAUP* determined three characters to be parsimony uninformative (39, 42, 72), which were excluded *a priori* to eliminate inflation of tree C.I. values (Kitching et al., 1998). The final matrix consists of 52 binary and 28 multi-state characters ten of which were treated as ordered if they were judged to form a morphocline (Slowinski, 1993)..

Branches were set to collapse and form polytomies if the maximum branch length was zero. This is the default setting for PAUP* and preferable to collapsing minimum branch lengths of zero for this small dataset as the latter method can be too strict for small datasets, eliminating possible topologies (Swofford and Begle, 1993; Coddington and Scharff, 1994). Nonetheless, I did a test run with the 'minbrlens' setting, but obtained the same results as 'maxbrlens', as there is support for all branches. The matrix was analyzed using the Branch and Bound ('bandb') search option and the resultant trees were rooted with the outgroup ('outroot=para').

A Permutation Tail Probability (PTP) test (Faith, 1991; Faith and Crandall, 1991) was conducted to test whether the data contain a signal that is more significant than random. The result of P=0.01 is demonstrative that the constructed dataset for this study (28 taxa, 83 characters) is significantly more structured than a random dataset (Faith and Crandall, 1991; Hillis and Huelsenbeck, 1992).

Results

The initial run of 27 in-group taxa and 83 characters (80 parsimony informative), with the settings given above, yielded 30 most parsimonious trees (MPTs) with a length of 203 steps; a reported Consistency Index (C.I.) of 0.5567, Homoplasy Index (H.I.) of 0.4433, a Retention Index (R.I.) of 0.7345, and a Rescaled Consistency Index (R.C.) of 0.4089. The strict consensus of these trees is provided in Figure 6.15a and features a large polytomy of at the base of the tree. An Adams consensus (Adams, 1972) of the 30 MPTs (Figure 6.15b) recovers *Aetobarbakinoides brasiliensis* at the base of this large polytomy and examination of the 30 MPTs demonstrates that this taxon occurs in 10 possible positions throughout the strict consensus tree including as the sister taxon to *Revueltosaurus callenderi,* the sister taxon to all aetosaurs, the sister taxon to the Desmatosuchinae, and the sister taxon to the Typothoracinae. A 50% Majority Rule consensus tree (Figure 6.15c) places *Aetobarbakinoides* in a polytomy with *Stagonolepis olenkae* and Desmatosuchinae in 70% of the recovered trees.

Coahomasuchus kahleorum is recovered in three positions in the strict consensus, as the sister taxon to *Aetosaurus ferratus*, the sister taxon to Typothoracinae, and as the sister taxon to *Aetosaurus ferratus* + Typothoracinae.

A reduced consensus tree (Figure 6.15d) was generated by pruning *Aetobarbakinoides brasilensis*. Thus, this final matrix has 27 taxa and 83 characters (80 are parsimony informative). The reduced consensus tree has a length of 201 steps, a C.I. of 0.5622, H.I. of 0.4378, a R.I. of 0.7373, and a R.C. of 0.4145.

The reduced consensus (Figure 6.16) features a nearly resolved topology with the exception of a clade with the unresolved polytomy that includes *Coahomasuchus kahleorum*, *Aetosaurus ferratus*, and Typothoracinae. Bremer support values were calculated for each node utilizing PAUP* by running repeated heuristic searches keeping trees one step longer in each iteration and noting which nodes collapse in strict consensus trees until no nodes remain. No nodes had a support value higher than four and many clades collapsed after a single additional step (Figure 6.16).

Bootstrap values were calculated using 600 replicates. Because of computational constraints I was unable to calculate bootstrap values using a higher number of replicates. Although using more replicates provides a better representation of confidence values, replicate numbers as low as 100, will provide a "rough but useful estimate" (Efron et al., 1996: 13432). Bootstrap values for this analysis are provided for all nodes in Figure 6.16. Bootstrap values higher than 70%, the minimum meaningful value according to Hillis and Bull (1993) are noted in black, values less than 70% are provided in red, with values lower than 50% interpreted as having very low confidence.

Aetosauroides scagliai was recovered at the base of the tree as a non-stagonolepidid aetosaurian, similar to the most recent analyses (Desojo et al., 2012; Heckert et al., in press; Roberto-da-Silva et al., 2014). Stagonolepididae (Heckert and Lucas, 2000) comprises two major clades, Aetosaurinae (Heckert and Lucas, 2000) and Stagonolepidoidea (clade nov.). The former includes Paratypothoracini (Parker, 2007) as the sister taxon to a clade consisting of *Typothorax coccinarum* and *Redondasuchus rineharti*. Paratypothoracini includes *Rioarribasuchus* (=*Heliocanthus*) *chamanensis*,

SMNS 19003 (*Paratypothorax* sp. of Sulej, 2010 and Desojo et al., 2013), *Tecovasuchus chatterjeei*, *Paratypothorax andressorum*, and *Paratypothorax* sp. (North American *Paratypothorax* specimens). This clade is well supported by six unambiguous synapomorphies (listed below), as well as a high decay index (+4) and bootstrap value (95%).

The sister taxon to that clade ((*Typothorax* + *Redondasuchus*) + Paratypothoracini)) is the recently described *Apachesuchus heckerti* Spielmann and Lucas 2012, which is known from only a handful of osteoderms, and is situated here based mainly on the presence of the synapomorphy that supports the clade, width/length ratio of widest paramedian osteoderms 3.5 or higher (character 64-2).

In this analysis Typothoracinae as defined by Parker (2007) would be equivalent to Aetosaurinae, so Typothoracinae is redefined with an additional specifier (*Aetosaurus ferratus*, see below). With the new definition Typothoracinae consists of *Apachesuchus heckerti*, Paratypothoracini, and *Typothorax coccinarum* + *Redondasuchus rineharti*. This clade is well supported by bootstrap values and decay indices (Figure 6.16).

As mentioned previously *Aetosaurus ferratus* and *Coahomasuchus kahleorum* form a polytomy with Typothoracinae (Figure 6.16). This close relationship is novel but not entirely unprecedented as these taxa were recovered as adjacent terminal taxa by Heckert et al. (in press) and Roberto-da-Silva et al., (2014). Nonetheless because of the polytomy support for this clade is not robust and these taxa may form other relationships in future analyses. *Stenomyti huangae* (Small and Martz, 2013) is recovered at the base of

Aetosaurinae, but this position is also very weakly supported and at present there can be little confidence in this position.

Stagonolepidoidea consists of two clades, Stagonolepidinae (Heckert and Lucas, 2000) and Desmatosuchinae (Heckert and Lucas, 2000). Stagonolepidinae consists of *Stagonolepis robertsoni* (by definition) and the newly described *Polesinesuchus aurelioi* (Roberto-da-Silva et al., 2014), however, this relationship is not very well supported with a decay index of +1 and a bootstrap value of 27% (Figure 6.16).

At the base of Desmatosuchinae lie *Stagonolepis olenkae* Sulej 2010 and *Neoaetosauroides engaeus* (Figure 6.16). *Neoaetosauroides* was previously recovered outside of Desmatosuchinae by Parker (2007) and Desojo et al., (2012), but within by Heckert and Lucas (1999a, 2000). Regardless these positions are not well supported with both branches having decay indices of +1 and bootstrap values under 10%.

Nested deeper in Desmatosuchinae is a clade consisting of *Calyptosuchus wellesi*, which is the sister taxon to *Adamanasuchus eisenhardtae* + *Scutarx deltatylus* (Figure 6.16). These clades are fairly well supported with decay indices of plus one and bootstrap values in the high 60th percentile nearly reaching the confidence threshold of 70% proposed by Hillis and Bull (1993). This is a novel position for these taxa as *Adamanasuchus eisenhardtae* and *Calyptosuchus wellesi* had been recovered outside of Desmatosuchinae in previous studies (e.g., Parker, 2007; Desojo et al., 2012). The presence of these five taxa within Desmatosuchinae is poorly supported with nodes having decay indices of only +1 and bootstrap values of less than 50% (Figure 6.16). Thus, this part of the tree may also prove to be highly labile in future analyses.

The subsequent nested clade within Desmatosuchinae; however, is highly supported by 13 unambiguous synapomorphies, a decay index of +5, and a bootstrap value of 94%. I name this clade Desmatosuchini and define it in the next section. In this study Desmatosuchini is well-resolved and includes NSCM 21723 (Heckert et al., in press), *Longosuchus meadei*, *Sierritasuchus macalpini*, *Lucasuchus hunti*, and *Desmatosuchus*. This clade has the same constituent taxa as Desmatosuchinae *sensu* Parker (2007).

Tree support

Character state transformations were evaluated under both the accelerated transformation (ACCTRAN) and delayed transformation (DELTRAN) options. Synapomorphies recovered under each option are listed for each node and character states placed at the same node under both ACCTRAN and DELTRAN criteria are considered to be unambiguous synapomorphies. Underlined numbers represent characters with a C.I. of 1.000 and can be considered to be robust synapomorphies.

Unnamed node (*Revueltosaurus callenderi* + Aetosauria)

Unambiguous synapomorphies -- 1) lateral surface of maxilla bears a sharp longitudinal ridge (7-1); 2) ventrolateral margin of the nasal forms part of the dorsal border of the antorbital fossa (10-1); 3) postfrontal-parietal contact is restricted by a posterolateral process of the frontal (14-1); 4) anterior process of the quadratojugal forms the ventral margin of lateral temporal fenestra (16-1); 5) transverse width of frontals greater than that

of the parietals at their anteroposterior mid-points (19-1); 6) basal tubera of the basicranial are clearly separated in ventral view (24-1); 7) The crown bases of the maxillary teeth are anteroposteriorly oval, but not strongly mediolaterally compressed in occlusal view (34-1); 8) articular face of the cervical centrum is round (38-1); 9) trunk vertebrae lack well-developed intervertebral articulations (hyposphene/hypantrum) (43-1); 10) anterior bar present and strongly raised om osteoderms (52-1); 11) lateral osteoderms only present in the sacral and anterior caudal regions (73-1); and 12) ventral osteoderms square and overlapping (83-2).

Other possible synapomorphies -- ACCTRAN: 1) shape of the maxillary tooth crown in labial/lingular view is bulbous with pointed or slightly recurved tips (35-2); 2) subglenoid 'pillar' absent on coracoid (46-1); and 3) acetabulum of ilium opens opens fully or mostly laterally (49-1). DELTRAN: none.

Aetosauria Marsh, 1884 *sensu* Parker, 2007. Modified by Nesbitt, 2011.

Definition -- The most inclusive clade containing *Aetosaurus ferratus* and *Desmatosuchus spurensis*, but not *Rutiodon carolinensis*, *Postosuchus kirkpatricki*, *Prestosuchus chiniquensis*, *Poposaurus gracilis*, *Crocodylus niloticus*, *Gracilisuchus stipanicicorum*, and *Revueltosaurus callenderi*.

Unambiguous synapomorphies -- 1) premaxillary teeth restricted to posterior portion of the element (3-1); 2) external nares longer than or equal to the antorbital fenestra (6-1); 3)

prefrontal-parietal contact is extensive (14-2); 4) supratemporal fenestra is dorsolaterally or laterally oriented and visible in lateral view (20-1); 4) posterodorsal process of dentary more elongate than the posteroventral process (26-1); 5) anterior portion of dentary edentulous (28-1); 6) radiate patterning on paramedian osteoderms (53-1); 7) dorsal eminence of paramedian osteoderm contacts the posterior margin of osteoderm in most osteoderm rows (54-1); 8) the dorsal eminence of the anterior caudal paramedian osteoderms are low and pyramidal or rounded and knob-like (71-1); and 9) lateral osteoderms present along the entire dorsal carapace (73-2).

Other possible synapomorphies -- ACCTRAN: 1) dorsally projecting tuber present on articular (33-1). DELTRAN: none.

Stagonolepididae Lydekker, 1887 *sensu* Heckert and Lucas, 2000.

Definition -- The last common ancestor of *Desmatosuchus spurensis* and *Aetosaurus ferratus* and all of their descendants.

1) maxilla contributes to the margin of the external naris (2-1); 2) premaxilla has prominent dorsal tubercle that extends dorsally into the external naris (5-1); 3) anterior ends of the dentary prolonged into an acute rostrum (slipper-shaped) (30-1); and 4) maxillary teeth are conical in cross section (34-2).

Other possible synapomorphies -- ACCTRAN: 1) A ventral 'chin' is present on the mandibular ramus formed by a ventral inflexion of the dentary, which covers the splenial (29-2) and 2) subglenoid pillar present on coracoid (46-1). DELTRAN: 1) dorsally projecting tuber present on articular (33-1); and 2) shape of the maxillary tooth crown in labial/lingular view is bulbous with pointed or slightly recurved tips (35-2).

Aetosaurinae Marsh 1884, *sensu* Heckert and Lucas, 2000.

Revised Definition – The least inclusive clade containing *Aetosaurus ferratus* but not *Desmatosuchus smalli*.

Unambiguous synapomorphies -- 1) transverse width of parietals greater than transverse width of the frontals (19-0); and 2), the anteroposterior diameter of the supratemporal fenestra is roughly half the size of the orbit (22-1).

Other possible synapomorphies -- ACCTRAN: 1) pubis symphysis short, less than one-half of element length (51-1). DELTRAN: none.

Typothoracinae Huene, 1915 *sensu* Parker, 2007. Emended clade name

Revised Definition – The least inclusive clade containing *Typothorax coccinarum* and *Paratypothorax andressorum,* but not *Aetosaurus ferratus*, *Stagonolepis robertsoni* or *Desmatosuchus smalli.*

Note: This clade was first named Typothoracisinae (Parker, 2007); however, the formation of this name is incorrect as the root for 'thorax' is 'thorac' not 'thoracis' so the proper formation of this clade name is Typothoracinae. The family name Typothoracidae was first proposed by Huene (1915), so he should also be credited for the name Typothoracinae.

Unambiguous synapomorphies -- 1) width/length ratio of widest paramedian osteoderms (rows 9-11) in dorsal trunk series is greater than 3.5 (64-2); and 2) carapace is broad and discoidal in dorsal view (82-2).

Other possible synapomorphies -- ACCTRAN: 1) anterior projection of quadratojugal underlies the posterior process of the jugal and excluded from the lateral temporal fenestra (16-2); 2) articular lacks strong dorsally projecting tuber (33-0); 3) cervical vertebrae with a transversely oval articular face of the centrum (38-0); 4) transverse processes of the trunk vertebrae are elongate, more than twice as wide as the centrum (40-1); 5) neural spine height of the mid-trunk vertebrae is equal to or less than the height of the centrum (41-1); 6) proximal head of the humerus is broadly expanded transversely, with significant lateral expansion (48-1); 7) acetabulum on ilium opens fully or mostly ventrally (49-0); 8) strongly developed ventral keel on the paramedian osteoderms (56-2); 9) dorsal eminence of cervical lateral osteoderms is a moderate length, dorsoventrally flattened, slightly recurved spine (74-1); 10) mid-trunk lateral osteoderms with a strongly acute angle of flexion between the dorsal and lateral flanges (79-2); and 11) lateral flange

of pelvic and anterior caudal lateral osteoderms is roughly triangular in lateral view with a semicircular ventrolateral border and a hook-like eminence (81-1). DELTRAN: none.

Unnamed node ((Paratypothoracini + (*Typothorax coccinarum* + *Redondasuchus rineharti*)).

Unambiguous synapomorphy -- lateral edge of the dorsal paramedian osteoderms in dorsal view are strongly sigmoidal with a strongly posteromedially oriented posterolateral corner (63-1).

Other possible synapomorphies – ACCTRAN: none. DELTRAN: 1) anterior projection of quadratojugal underlies the posterior process of the jugal and excluded from the lateral temporal fenestra (16-2); 2) transverse processes of the trunk vertebrae are elongate, more than twice as wide as the centrum (40-1); 3) neural spine height of the mid-trunk vertebrae is equal to or less than the height of the centrum (41-1); 4) dorsal eminence of cervical lateral osteoderms is a moderate length, dorsoventrally flattened, slightly recurved spine (74-1); 5) mid-dorsal lateral osteoderms with a strongly acute angle of flexion between the dorsal and lateral flanges (79-2); and 6) lateral flange of pelvic and anterior caudal lateral osteoderms is roughly triangular in lateral vie with a semicircular ventrolateral border and a hook-like eminence (81-1).

Unnamed node (*Typothorax coccinarum* + *Redondasuchus rineharti*)

Unambiguous synapomorphies -- 1) cervical vertebrae extremely shortened anteroposteriorly (37-1); and 2) surface pattern of dorsal paramedian osteoderms is reticulate (53-2).

Other possible synapomorphies -- ACCTRAN: 1) premaxilla lacks a prominent dorsal tubercle that extends dorsally into the external naris (5-0); 2) lateral surface of the maxilla is smooth, lacking longitudinal ridge (7-2); 3) lateral margin of the nasal does not form part of the dorsal border of the antorbital fossa (10-0); 4) supratemporal fenestra larger than or nearly same size as the orbit (22-0); 5) retroarticular process is longer than high (32-1); 6) ectepicondyle of the humerus proximodistally oriented foramen present on its lateral side (47-1); and 7) ratio of cervical vertebrae/paramedian osteoderms significantly less than 1:1 (58-1). DELTRAN: 1) ventral strut of paramedian osteoderms strongly developed (56-2).

Paratypothoracini Parker, 2007. Emended clade name.

Revised Definition -- The least inclusive clade containing *Tecovasuchus chatterjeei, Rioarribasuchus chamaensis,* and *Paratypothorax andressorum*.

Note: This clade was first named Paratypothoracisini (Parker, 2007); however, the formation of this name is incorrect as the root for 'thorax' is 'thorac' not 'thoracis' so the proper formation of this clade name is Paratypothoracini.

Unambiguous synapomorphies -- 1) caudal ribs of the caudal vertebrae attach near the base of the centrum (45-1); 2) anterior bar present, but weakly raised (52-2); 3) dorsal eminence of the paramedian osteoderms does not contact the posterior margin of the osteoderm in most rows (54-0); 5) dorsal eminence of the dorsal paramedian osteoderms is strongly offset medially (66-2); 5) dorsal flange of the dorsal lateral osteoderms is highly reduced and 'tongue-shaped' (76-2); and 6) dorsal eminence of the anterior and mid-dorsal lateral osteoderms is in the form of an elongate flattened horn (78-1).

Other possible synapomorphies -- ACCTRAN: 1) Transverse width of frontal wider than parietal (19-1); 2) strong posteroventral orientation of the posterior portion of the parietal forms a triangular supratemporal fenestra (21-1); 3) maxillary teeth are anteroposteriorly oval, but not strongly mediolaterally compressed in cross section (34-1); and 4) shape of the maxillary tooth crown in labial/lingular view is bulbous and partly recurved, anterior edge is concave, posterior edge straight (35-1). DELTRAN: none.

Unnamed node (SMNS 19003 + Paratypothoracini).

Unambiguous synapomorphy -- posterior margin of paramedian osteoderms bears a transverse, posteroventrally sloping flange (bevel) (57-1).

Other possible synapomorphies -- none.

Unnamed node (*Tecovasuchus chatterjeei* + *Paratypothorax*).

Unambiguous synapomorphy -- distinct sharp raised mediolateral ridge extends medially from dorsal eminence of paramedian osteoderm to medial osteoderm margin (65-1).

Other possible synapomorphy -- ACCTRAN: none. DELTRAN: ventral strut of paramedian osteoderms strongly developed (56-2).

Paratypothorax (*Paratypothorax andressorum* + *Paratypothorax* sp.).

Unambiguous synapomorphies -- 1) lateral faces of the posterior trunk vertebrae meet to form a sharp ventral edge or keel (44-1); and 2) dorsal eminence of the posterior trunk – anterior caudal paramedian osteoderms is a moderate, bulbous spike (71-2).

Other possible synapomorphies -- none.

Stagonolepidoidea Hoffstetter, 1955. New clade name.

Definition -- The most inclusive clade containing *Stagonolepis robertsoni* and *Desmatosuchus smalli*, but not *Aetosaurus ferratus* and *Paratypothorax andressorum*.

Unambiguous synapomorphies -- 1) anterior portion of the premaxilla laterally expanded in dorsal view (1-1); 2) anterior portion of nasal maintains an equal width in dorsal view (9-1); 3) triangular depression on the midline suture area of the nasals absent (11-1); 4) jugal contributes to the margin of the antorbital fenestra (13-1); 5) basal tubera are nearly or completely connected (24-0); and 6) surangular bears prominent dorsal tuber (31-1).

Other possible synapomorphies – ACCTRAN: none. DELTRAN: 1) A 'chin' is present on the mandibular ramus formed by a ventral inflexion of the dentary, which covers the splenial (29-2); and 2) acetabulum on ilium opens fully or mostly laterally (49-1).

Stagonolepidinae Huene 1936, sensu Heckert and Lucas, 2000.

Revised Definition – The most inclusive clade containing *Stagonolepis robertsoni*, but not *Desmatosuchus spurensis* or *Paratypothorax andressorum*.

Unambiguous synapomorphies – 1) proximal portion of pubis bears two foramina' (50-1).

Other possible synapomorphies -- ACCTRAN: 1) Postfrontal-parietal contact restricted by a posterolateral process of the frontal (14-1). DELTRAN: none.

Desmatosuchinae Huene 1936, *sensu* Heckert and Lucas, 2000.

Revised Definition – The most inclusive clade containing *Desmatosuchus smalli,* but not *Stagonolepis robertsoni*, *Aetosaurus ferratus*, or *Paratypothorax andressorum*.

Unambiguous synapomorphies -- 1) lateral surface of the maxilla is smooth, lacking longitudinal ridge (reversed in *Longosuchus meadei*) (7-2); 2) lateral margin of the nasal does not form part of the dorsal border of the antorbital fossa (10-0); 3) quadrate foramen

entirely within quadrate bone (18-1), and 4) fewer than nine tooth positions in the dentary (27-1).

Other possible synapomorphies -- ACCTRAN: 1) ventral margin of the jugal strongly anterodorsally inclined in lateral view (12-1); and 2) proximal head of the humerus broadly expanded transversely, with significant lateral expansion (48-1). DELTRAN: None.

Unnamed node (*Neoaetosauroides engaeus* + Desmatosuchinae).

Unambiguous synapomorphies -- 1) supratemporal fenestra is roughly half the size of the orbit (22-1); 3) dorsal and ventral posteroventral processes of the dentary are roughly equal in length (26-0); and 4) anterolateral projection of the anterior bar of the dorsal paramedian osteoderms is present and elongate (reversed in Desmatosuchini) (68-1).

Other possible synapomorphies -- ACCTRAN: 1) ventral portion of the antorbital fossa on the maxilla is very shallow or absent (8-1); 2) retroarticular process is longer than high (32-1); and 3) ectepicondyle of the humerus proximodistally oriented foramen present on its lateral side (47-1). DELTRAN: 1) ventral margin of the jugal strongly anterodorsally inclined in lateral view (12-1).

Unnamed node (((*Adamanasuchus eisenhardtae* + *Scutarx deltatylus*) + *Calyptosuchus wellesi*)) + Desmatosuchini))).

Unambiguous synapomorphies -- 1) basal tubera and basipterygoid processes widely separated anteroposteriorly (reversed in *Desmatosuchus smalli* and *Scutarx deltatylus*; convergent with *Tecovasuchus chatterjeei*) (25-1); and 2) cervical vertebrae with a transversely oval articular face of the centrum (38-0).

Other possible synapomorphies -- ACCTRAN: 1) edentulous premaxilla (3-2); 2) edentulous premaxilla (4-2); 3) postfrontal/parietal contact absent (14-0); and 4) ratio of cervical vertebrae/paramedian osteoderms significantly less than 1:1 (58-1). DELTRAN: none.

Desmatosuchini. Case, 1920. New clade name.

Definition – The most inclusive clade containing *Desmatosuchus smalli,* but not *Neoaetosauroides engaeus*, *Scutarx deltatylus, Stagonolepis robertsoni*, *Aetosaurus ferratus*, *Calyptosuchus wellesi*, and *Paratypothorax andressorum*.

Unambiguous synapomorphies -- 1) random surface patterning of paramedian osteoderms (reversed in *Lucasuchus hunti*) (53-0); 2) in the dorsal trunk paramedian osteoderms the anterior edge of the lateral osteoderm overlaps the anterior edge of the paramedian osteoderm (62-1); 3) lacks the sharp anteromedial projection of the anterior bar (reversed in *Lucasuchus hunti*) (67-1); 4) anterior bar of the dorsal trunk paramedian osteoderms lacks scalloping of the anterior margin on the medial side of the osteoderm (69-1); 5) dorsal eminence of the cervical lateral osteoderms is in the form of a moderately long,

faceted, slightly recurved spine (74-2); 6) rectangular dorsal flange of the dorsal lateral osteoderms (76-0); 7) approximately 90 degree angle between the dorsal and lateral flanges of the mid-trunk lateral osteoderms (79-1); 8) dorsal trunk lateral osteoderms strongly asymmetrical with the dorsal flange longest (80-1); and 9) overall shape in of the dorsal carapace in dorsal view is moderately spinose (82-1).

Other possible synapomorphies- ACCTRAN: 1) post-temporal fenestra is absent (23-1); 2) ventral 'chin' of the mandibular ramus present and formed by a ventral inflexion of the splenial (29-1); 3) in the paramedian osteoderms dorsal to the cervical and anterior trunk vertebrae, lateral edge articulation with lateral osteoderms is dorsoventrally thickened, angled contact, with deeply incised interdigitation (='tongue and groove') (60-1); 4) dorsal eminence shape in the cervical paramedian osteoderms are a low pyramidal or rounded boss, or elongate keel (61-1); 5) the anterior bar of the trunk distal paramedian osteoderms lacks an anterolateral pro69-jection (68-2); 6) dorsal eminence in the mid-trunk osteoderms is a conical spike (78-2); 7) lateral flange of the pelvic and anterior caudal lateral osteoderms are rectangular and ventral to a well-developed spine (81-2); and 8) ventral osteoderms absent (83-0). DELTRAN: ratio of cervical vertebrae/paramedian osteoderms significantly less than 1:1 (58-1).

Unnamed node (*Longosuchus meadei* + Desmatosuchini).

Unambiguous synapomorphies -- 1) cervical paramedian osteoderms are longer than wide (57-1); and 2) adjacent paramedian and lateral cervical osteoderms are often fused (59-1).

Other possible synapomorphies – ACCTRAN: none. DELTRAN: 1) ventral portion of the antorbital fossa on the maxilla is very shallow or absent (8-1); 2) post-temporal fenestra is absent (23-1); 3) ventral 'chin' of the mandibular ramus present and formed by a ventral inflexion of the splenial (29-1); 4) proximal head of humerus broadly expanded transversely with a significant lateral expansion (48-1); 5) in the paramedian osteoderms dorsal to the cervical and anterior trunk vertebrae, lateral edge articulation with lateral osteoderms is dorsoventrally thickened, angled contact, with deeply incised interdigitation (='tongue and groove') (60-1); 6) dorsal eminence shape in the cervical paramedian osteoderms are a low pyramidal or rounded boss, or elongate keel (61-1); 7) the anterior bar of the trunk dirsal paramedian osteoderms lacks an anterolateral projection (68-2); 8) dorsal eminence in the mid-dorsal osteoderms is a conical spike (78-2); 9) lateral flange of the pelvic and anterior caudal lateral osteoderms are rectangular and ventral to a well-developed spine (81-2); and 10) ventral osteoderms absent (83-0).

Unnamed node (*Sierritasuchus macalpini* + Desmatosuchini).

Unambiguous synapomorphies -- 1) neural spine height of the mid-dorsal vertebrae is low, equal to or less than the height of the centrum (41-1) and 2) dorsal eminence of dorsal paramedian osteoderms is centralized (66-0).

Other possible synapomorphies -- ACCTRAN: 1) quadrate foramen positioned between the quadrate and quadratojugal (18-0); 2) supratemporal fenestra larger than or nearly

same size as the orbit (22-0); 3) lower posteroventral process of the dentary is longer than the upper process (26-2); 4) dorsal tuber of surangular is absent (31-0); 5) articular lacks strong dorsally projecting tuber (33-0); and 6) hyposphene/hypantrum present in dorsal vertebrae (43-0). DELTRAN: none.

Unnamed node (*Lucasuchus hunti* + *Desmatosuchus*).

Unambiguous synapomorphies -- 1) dorsal eminence of the paramedian osteoderms almost never contacts the posterior osteoderm margin (54-0); and 2) posterior face of the dorsal trunk lateral osteoderms lack a ventral emargination (77-0).

Other possible synapomorphy -- ACCTRAN: 1) articular face of the cervical vertebral centrum is subrectangular (38-2). DELTRAN: none.

Desmatosuchus Case 1920 (= *Desmatosuchus smalli* + *Desmatosuchus spurensis*).

Unambiguous synapomorphies -- 1) osteoderms possess a depressed anterior lamina rather than a raised anterior bar (52-3); 2) dorsal eminence of the cervical lateral osteoderms is a greatly elongated horn (74-3); and 3) anteriormost dorsal trunk lateral osteoderms bear a mound-like dorsal eminence (75-1).

Other possible synapomorphies – ACCTRAN: none. DELTRAN: 1) postfrontal-parietal contact absent (14-0); 2) retroarticular process is longer than high (32-1); 3) articular lacks strong dorsally projecting tuber (33-0); 4) articular face of the cervical vertebral centrum is subrectangular (38-2); and 5) hyposphene/hypantrum present in trunk vertebrae (43-0).

Unnamed node (*Calyptosuchus wellesi* + (*Adamanasuchus eisenhardtae* + *Scutarx deltatylus*)).

Unambiguous synapomorphies -- 1) acetabulum on ilium opens fully or mostly ventrally (49-0); 2) ventral strut of the paramedian osteoderms weakly developed (56-1); and 3) width/length ratio of widest paramedian osteoderms is between 3.01 and 3.5 (64-1).

Other possible synapomorphies -- ACCTRAN: 1) dentary tooth count of nine or more (27-0); and 2) two pubic foramina (50-1). DELTRAN: none.

Unnamed node (*Adamanasuchus eisenhardtae* + *Scutarx deltatylus*).

Unambiguous synapomorphies -- 1) anterolateral projection of the anterior bar of the dorsal paramedian osteoderms is present and elongate (70-1).

Other possible synapomorphies -- ACCTRAN: none. DELTRAN: none.

DISCUSSION

Comparisons to previous analyses

Constituency and Status of Major Clades of Aetosauria

Four major clades have been defined within Aetosauria: Stagonolepididae, Aetosaurinae, Stagonolepininae (emended to Stagonolepidinae by Sereno, 2005), and Desmatosuchinae (Heckert and Lucas, 1999, 2000). A fifth, Typothoracinae, was added by Parker (2007).

Historically the terms Stagonolepididae and Aetosauria have been used interchangeably for family-group names under the Linnaean taxonomic system (see discussion in Walker, 1961), but were first defined cladistically by Heckert and Lucas (2000), the former as stem-based and the latter as node based, although in that analysis they contained the same taxa. Parker (2007) also recovered these clades at a shared node, but cautioned that the definition provided by Heckert and Lucas (2000) was based on *Aetosaurus* occupying the base of the tree and leaves open the possibility for non-stagonolepidid aetosaurs, which would alter the historic usage of the name. Rescoring of character states in *Aetosauroides* moved it to the base of Aetosauria as a non-stagonolepidid aetosaur (Desojo et al., 2012), a position recovered in all subsequent analyses including the present study (Heckert et al., in press; Roberto-da-Silva, et al, 2014).

In their original defining analysis (Heckert and Lucas, 1999a) Aetosaurinae included only *Aetosaurus*; however, Parker (2007) and Parker et al. (2008) recovered Aetosaurinae as a greatly expanded clade that included all non-Desmatosuchines; however, this clade was generally unsupported and its constituents not accepted by all workers (e.g., Schoch, 2007). Moreover, subsequent analyses (Desojo et al., 2012;

Heckert et al., in press) do not recover Aetosaurinae as a more inclusive clade with *Aetosaurus ferratus* the only constituent by original definition. In these analyses the remnant of the "Aetosaurines" (*sensu* Parker, 2007) are poorly resolved along the spine of Stagonolepididae.

The present study recovers a different result (Figure 6.16) with *Aetosaurus ferratus*, *Coahomasuchus kahleorum*, and *Stenomyti huangae*, which was originally referred to the genus *Aetosaurus* (Small and Martz, 2013), situated near the base of Aetosaurinae, which also includes the Typothoracinae. This still differs from Aetosaurinae as recovered by Parker (2007), which also included *Stagonolepis robertsoni*, *Aetosauroides scagliai*, *Neoaetosauroides engaeus*, and *Calyptosuchus wellesi*, all of which are now recovered as more closely related to *Desmatosuchus* (Figure 6.16). Constraining the analysis to recover all of these taxa in a monophyletic Aetosaurinae (*sensu* Parker, 2007) requires 11 additional steps.

As defined by Heckert and Lucas (2000) Stagonolepidinae consisted of *Stagonolepis robertsoni* and *Coahomasuchus kahleorum*. Parker (2007) recovered Stagonolepidinae at the same node as Aetosaurinae and chose to use the latter name for that clade. Subsequently the name Stagonolepidinae has fallen out of use in recent analyses although it would have pertained solely to *Stagonolepis robertsoni* in recovered topologies (Desojo et al., 2012) and Heckert et al., (in press). However, in the present study Stagonolepidinae is distinct from Aetosaurinae as originally conceived and consists of *Stagonolepis robertsoni* and *Polesinesuchus aurelioi* (Figure 6.16).

Desmatosuchinae was first recovered as a clade by Heckert and Lucas (1999a, 2000) where it was comprised of *Desmatosuchus*, *Typothorax*, *Paratypothorax*, and *Longosuchus*; however, the published tree was affected by typographical and scoring errors, as well as reductive coding methods according to Harris et al. (2003a), who

provided a revised version of the Heckert and Lucas (1999a) matrix. The cladogram in Harris et al. (2003a) based solely on the Heckert and Lucas (1999a) matrix recovered Desmatosuchinae as consisting of *Desmatosuchus*, *Longosuchus*, *Lucasuchus*, and *Acaenasuchus*, all of which have remained constituent taxa in all subsequent analyses (Parker, 2007; Parker et al., 2008; Desojo et al., 2012, Heckert et al., in press; this study), although this present study did not include *Acaenasuchus* as an Operational Taxonomic Unit (see explanation above).

The present study differs from all others in recovering several taxa within Desmatosuchinae for the first time, including *Stagonolepis olenkae*, *Neoaetosauroides engaeus*, *Adamanasuchus eisenhardtae*, *Scutarx deltatylus*, and *Calyptosuchus wellesi* (Figure 6.16). Nevertheless, support for these included taxa is weak, and it is probable that in future analyses they may continue to migrate between the bases of Aetosaurinae and Stagonolepidoidea. A new robust clade, Desmatosuchini, is erected for the taxa originally within Desmatosuchinae (*sensu stricto*) as originally recovered by Harris et al. (2003) and Parker (2007).

Typothoracinae was first recovered and defined by Parker (2007) and is comprised of taxa more closely related to *Typothorax* and *Paratypothorax* than to *Aetosaurus*, *Stagonolepis*, or *Desmatosuchus*. This clade was well-supported by Parker (2007) and has been recovered in all subsequent analyses including the present analysis (Figure 6.16).

Desmatosuchinae and Aetosaurinae were recovered as sister taxa, with Typothoracinae nested within Aetosaurinae (Parker, 2007). Desojo et al. (2012) and Heckert et al. (in press) did not recover a similar topology after rescoring and adding taxa to the Parker (2007) matrix. Instead they presented trees with Desmatosuchinae and

Typothoracinae as sister taxa. The present analysis recovers Typothoracinae within Aetosaurinae and a distinct Desmatosuchinae (Figure 6.16).

In sum, the results of five most recent phylogenetic analyses demonstrate that Typothoracinae and Desmatosuchinae are robust clades within Aetosauria, well-supported and stable when taxa are added and scorings are changed. Recovery of an inclusive Aetosaurinae is not consistent across studies, with weak support values for non-desmatosuchine and typothoracine taxa causing the constituent taxa to be shuffled around the base of the tree in most studies. The significance of and possible reason for this is addressed below.

The Monophyly of Stagonolepis

It has been recognized that aetosaurian material, especially osteoderms, recovered from southwestern North America (Chinle Formation, Dockum Group) is very similar in overall anatomy to that of *Stagonolepis robertsoni*. In fact the first person to directly compare these materials was convinced of their congeneric status (Charles Lewis Camp, unpublished notes, 1935). The North American material was eventually named *Calyptosuchus wellesi* by Long and Ballew (1985); however, soon afterwards that species was reassigned to the genus *Stagonolepis* (Murry and Long, 1989; Long and Murry, 1995).

This potential relationship was first discussed in a numerical phylogenetic framework by Heckert and Lucas (1999a:62) who noted that *Calyptosuchus wellesi* and *Stagonolepis robertsoni* "score almost identically throughout the matrix", and therefore they removed *Calyptosuchus wellesi* prior to their final run. For the same reasons they removed *Aetosauroides scagliai*, considering it also to represent *Stagonolepis robertsoni*

and several anatomical descriptions were published detailing these proposed synonymies (Lucas and Heckert, 2001; Heckert and Lucas, 2002a). However, investigation of the original matrix by Harris et al., (2003a) determined that because these three taxa were not scored identically, *Calyptosuchus wellesi* and *Aetosauroides scagliai* could not be removed without affecting the final analysis. A reanalysis did not recover a "*Stagonolepis*" clade with *Calyptosuchus wellesi* and *Stagonolepis robertsoni*, but did find a clade with *Stagonolepis robertsoni* and *Aetosauroides scagliai* (Harris et al., 2003a: fig. 9).

The strict consensus tree published by Parker (2007: fig. 13) offered no resolution to this problem, recovering all three taxa in an unresolved polytomy with *Aetosaurus ferratus*. However, Desojo (2005) argued against the synonymy of *Aetosauroides* and *Stagonolepis* and in a recent redescription of *Aetosauroides scagliai* demonstrated key differences in the skull and postcranial skeleton that preclude an assignment of that material to *Stagonolepis robertsoni* (Desojo and Ezcurra, 2011). More recent phylogenetic analyses featuring a rescoring of *Aetosauroides scagliai* do not recover the three '*Stagonolepis*-like' species as a discrete clade (Desojo et al., 2012; Heckert et al., in press). The present study provides a redescription of *Calyptosuchus wellesi* and lists differences between it and *Stagonolepis robertsoni*. Likewise the associated phylogenetic analysis does not recover them as a discrete clade. Constraining the present analysis to recover them in an exclusive clade requires 10 additional steps. Thus, anatomical comparisons and several phylogenetic analyses strongly support the separation of these three taxa and *Calyptosuchus* and *Aetosauroides* should no longer be considered junior synonyms of *Stagonolepis* (Parker, 2008a; Desojo and Ezcurra, 2011).

Numerous well-preserved cranial bones from Poland were described as a new species of *Stagonolepis*, *Stagonolepis olenkae* (Sulej, 2010). Postcranial bones and

osteoderms were also recovered from the same quarry (Dzik, 2001; Dzik and Sulez, 2007) and were assigned to *Stagonolepis robertsoni* by Lucas et al., (2007d). In a traditional (i.e., non-cladistic) analysis *Stagonolepis olenkae* was considered to be an early member of an anagenetic '*Stagonolepis-Aetosaurus*' lineage (Sulej, 2010). Differences between *Stagonolepis olenkae* and *Stagonolepis robertsoni* appear to all be in the skull and include contrasting dimensions of various cranial bones, the presence of a massive ridge on the anterior end of the palatine in *S. olenkae*, the presence of a lateral ridge on the maxilla of *Stagonolepis robertsoni*, and most notably a reduced number of dentary teeth and the presence of large tubercles on the parietals of *Stagonolepis olenkae* (Sulej, 2010). In the phylogenetic analysis presented here they are scored differently for five characters, four are cranial and the fifth is that the humeral head is more expanded in *Stagonolepis olenkae*. In the recovered tree *Stagonolepis robertsoni* + *Polesinesuchus aurelioi* is the sister taxon to *Stagonolepis olenkae* + Desmatosuchinae. A topological constraint to force the two purported species of *Stagonolepis* to form an exclusive clade requires only an additional two steps. Therefore, even though they were not recovered as monophyletic, I do not suggest erecting a new generic name to receive *Stagonolepis olenkae*. Differences between the taxa are too few and potentially explained by the much larger size of *Stagonolepis olenkae*, although Sulej (2010) explicitly argued against this possibility. A full description of the postcranial material and osteoderms will hopefully provide further evidence for or against the potential generic synonymy of these two taxa.

The Phylogenetic Position of Aetosaurus ferratus

The earliest exhaustive treatment of the Aetosauria (Walker, 1961) considered *Aetosaurus ferratus* as the 'basal' aetosaurian, a position supported by the first

phylogenetic analyses of the Aetosauria (Parrish, 1994; Heckert et al., 1996; Heckert and Lucas, 1999a). Indeed, an early study constrained *Aetosaurus ferratus* to this position by utilizing it as the sole outgroup for the entire analysis (Heckert et al., 1996). Nonetheless that study considered other aetosaurs to be more 'advanced' than *Aetosaurus* based on characters of the teeth, especially the presence of bulbous rather than recurved teeth and an edentulous anterior portion of the dentary. Those characters and scorings for *Aetosaurus* were taken directly from Parrish (1994), and used again by Heckert and Lucas (1999a) to diagnose *Aetosaurus*. Parker (2007) followed Walker (1961:164) in considering the teeth of *Aetosaurus* bulbous and the anterior portion of the dentary edentulous. In his accompanying analysis *Aetosaurus ferratus* was recovered more deeply nested within Stagonolepididae, the first time it had not been recovered at the base of Aetosauria in a phylogenetic analysis (Parker, 2007). This alternate placement prompted detailed discussion by Schoch (2007) who acknowledged that the teeth were as Walker (1961) had described, but argued that the more nested placement of *Aetosaurus* was somewhat ambiguous as other character states found in *Aetosaurus ferratus* supported a position closer to the base of Aetosauria.

In subsequent analyses (Desojo et al., 2012; Heckert et al., in press) *Aetosaurus* has been recovered closer to the base of Aetosauria in part mainly because of a change in character polarities based on the scoring of *Aetosauroides scagliai* as having a maxilla that is excluded from the margin of the external naris (Desojo and Ezcurra, 2011); a change that pulled both *Aetosauroides* and *Aetosaurus* towards the root of the tree. In the present analysis *Aetosaurus* is recovered in a polytomy with *Coahomasuchus* and Typothoracisinae, and two taxa are still fairly close to the base of Aetosauria (Figure 6.16), but constraining the clade of *Aetosaurus* plus *Coahomasuchus* to the base of Aetosauria requires an additional six steps.

Low Support Values in Data Partitions

Overall, the tree of Heckert et al. (in press) is the most similar of all past studies to the one presented here, suggesting that incorrect scorings that affected the earliest analyses (Parrish, 1994; Heckert et al., 1996; Heckert and Lucas, 1999a) still played a major role in the recovered topology of Parker (2007). Some of these errors were directly inherited from the previous studies (Parrish, 1994; Heckert et al., 1996), but others resulted from a general lack of good specimens and a necessary reliance on outdated literature to score characters as redescriptions of key taxa such as *Aetosaurus ferratus*, *Aetosauroides scagliai*, *Neoaetosauroides engaeus*, and *Desmatosuchus spurensis* had not yet been published (Desojo and Báez, 2005, 2007; Schoch, 2007; Parker, 2008b; Desojo and Ezcurra, 2011). Still, this early work should be recognized for pioneering phylogenetic studies of aetosaurians, especially the study of Heckert et al., (1996), which introduced many key characters still used in current analyses. However, this also demonstrates the importance of discovering and utilizing new specimens of existing taxa (e.g., MNA V9300, YPM 58121; NMMNH P-56299; TMM 31100-437), as well as crucial reinvestigations of original type materials (e.g, Desojo and Báez, 2005, 2007; Schoch, 2007), in phylogenetic work.

I find the results of the new study presented here generally disappointing because of the lack of support for the base of the tree, essentially all nodes outside of Typothoracinae and Desmatosuchini. This problem also plagued the previous study by Parker (2007) and was apparent in the way topologies shifted significantly in new studies when characters were rescored and new taxa added (Desojo et al., 2012; Heckert et al., in press). The present work sought to increase character support by creating as many new

characters as possible, particularly those from skeletal elements outside of the dorsal carapace. Inclusion of endoskeletal (non-armor) characters was suggested as a way to provide tree stability (Desojo et al., 2012; Heckert et al., in press).

Parker (2007) scored 35 parsimony informative characters with 23 (66%) of these characters from the osteoderms. This new study has expanded the dataset to 80 parsimony informative characters, an increase of over 100%, with only 31 of these characters scoring osteoderm characters (39%). Thus, it was expected to see an increase in stability in the overall tree metrics utilizing a dataset with better skeletal region sampling, but unfortunately this was not realized in the final results.

One of the possible reasons for these low support values is that the non-osteoderm characters of aetosaurians appear to generally have higher levels of homoplasy. For example, the 35 parsimony informative cranial characters have an average Consistency Index value of 0.596. This value was computed by simply adding up the C.I. scores for each character and dividing the resulting number by the number of characters, thus this is a calculation of a 'raw' C.I. average and does not equate the final reported C.I. number for the MPTs as determined by PAUP*. Vertebral characters score much higher with an average C.I. value of 0.767. However, the paramedian osteoderm characters have an average value of 0.697, whereas the lateral osteoderms have an average value of 0.833 demonstrating the value of the osteoderm characters. Overall the non-osteoderm characters have an average C.I. value of 0.606, compared to an average value of 0.746 for the osteoderm characters. What this signifies is that the non-osteoderm characters included in the study are more apt to change across the tree than the osteoderm characters, which signifies a higher degree of homoplasy in non-osteoderm characters or that non-comparable maturity at time of death among specimens plays a greater role than expected.

Overall, sampling of non-osteoderm characters remains poor, with the majority of characters taken from the cranial region. Only four characters sample the appendicular skeleton, and the limbs and girdles represent a potential area for character expansion. Unfortunately, many aetosaur taxa do not have limb and girdle material referred to them, and, in some cases, these materials are present but covered by an articulated carapace and not accessible for study without non-invasive (e.g., CT) scanning. Where limb and girdle elements are known (e.g., femora, scapulae, ilia) many of the characters appear to be conserved across taxa. Still, with increasing sample sizes and better comparisons, more informative characters can probably be derived from this dataset in future analyses.

Dataset Partitioning

An interesting question brought up during the construction of this dataset is what if aetosaurians did not possess an extensive armor carapace? What if all of the characters and character states used in phylogenetic analyses of the Aetosauria were derived from the skull, axial, and appendicular portions of the skeleton as is the case for the majority of vertebrates? In sum, what would the phylogeny of aetosaurians look like without utilizing characters of the osteoderms?

Fundamental limitations of phylogenetic analyses lie in the various properties of the data set being utilized. These properties define the data set and thus are intrinsic to the final results as factors such as the number of taxa and characters included, amount of missing data, and degree of character weighting dictate the most parsimonious tree(s), but also the number of plausible topologies available to be chosen from. The literature is replete with studies addressing these various aspects of phylogenetic analysis, not simply because they are of some statistical interest, but because they are fundamental to the

process itself. One particular aspect of data set analysis is the discussion of data partitioning, which entails the separation of a data set of phylogenetic characters into discrete parts based on types of characters (e.g., molecular sequences vs. morphological), or positional (e.g., skull vs. postcranium). In most published cases, the debate on data partitioning in phylogenetic analyses revolves around the advantages or disadvantages of combining of molecular sequence and morphological data into a single data set (e.g., Bull et al., 1993). Considerable discussion is available regarding partitioning of strictly morphological data into discrete character sets based mainly on anatomical subregions (Rowe 1988; Gauthier et al. 1988; Donoghue et al. 1989; Rae, 1999; Clarke and Middleton, 2008), but none pertains to the special case of osteoderms versus endoskeletal features.

The purpose of this section is to differentiate morphological (anatomical) characters from the study presented earlier in the chapter into discrete partitions. As discussed throughout this study, aetosaurs have an elaborate bony armor carapace covering the main skeleton and characteristics such as the surface ornamentation, size, osteoderm geometry, and articulation patterns of this armor are the main factor utilized for aetosaurian taxonomy, whereas characters from the rest of the skeleton have generally been under-developed (Desojo, 2005). Thus, aetosaurs provide an excellent example of a group where historically the taxonomy is based almost entirely on characters of a single anatomical subregion. A major assumption of students of aetosaurs is that not only is osteoderm anatomy taxonomically informative, but that it is also phylogenetically informative, providing an accurate signal of evolutionary relationships (Parker, 2007). Dataset partitioning provides a test of which characters, in this case integumentary versus non-integumentary, are providing the main phylogenetic signal for this group and allows

for in-depth examination of possible underlying factors regarding the poorly resolved phylogenetic relationships recovered in past studies (Harris et al., 2003a).

Why partition?

Osteoderms represent a mineralized component of the dermis in tetrapods (Hill, 2005). As such they are hypothetically an autonomous (i.e., they are not found in all vertebrates) unit (module) of the skeleton and circulatory system. This independence is further supported by the finding that onset of osteoderm development is delayed, by as much as a year, in comparison with the rest of the skeleton in *Alligator* with the result that they are absent in very young animals (Vickaryous and Hall, 2008). This independence also suggests that the osteoderms, with specific proposed functions (e.g., defense, heat transfer, species recognition; Seidel, 1979; Parker, 2007), may be under different evolutionary selection pressures than other parts of the body such as the head, which is mainly focused on resource acquisition, or the limbs, which are mainly focused on locomotion and/or environmental manipulation. Although the presence of osteoderms can hypothetically influence some factors of the rest of the skeleton, such as the development of transversely expanded apices on the neural spines, a robust olecranon process of the ulna for bearing additional weight, and modified parietal bones of the skull for reception of the anterior portion of the armor characters, they can be considered a distinct module of the skeleton. This begs the question of how does the non-integumentary portion of the aetosaur skeleton compare to other taxonomic groups, but more importantly how does it compare within Aetosauria proper?

Methods

Morphobank (O'Leary and Kaufmann, 2012) was used to divide the main dataset into smaller partitions based on cranial characters, osteoderm characters, and the full set of non-osteoderm characters. The cranial dataset consists of characters 1-35, the osteoderm dataset consists of characters 52-83, and the full endoskeletal set consists of characters 1-51. All analyses for this study were run using PAUP* version 4.0.b10 (Swofford, 2003). All characters were weighted equally and the most parsimonious trees (MPTs) were subject to an exact solution search using the branch and bound implementation under the program default settings. Bootstrap support values for each dataset were calculated from 1000 replicates with only scores above 50% being recorded as informative, although only values above 70% probably represent well-supported clades (Hillis and Bull, 1993). Distribution of character states was analyzed in Mesquite 2.75 (Maddison and Maddison, 2011).

The consensus tree provided earlier in the chapter utilized the full data set for this entire project (26 in-group taxa and 83 characters) and establishes the baseline relationships for this study. For this portion of the study runs used the subsets outlined above. Because some taxa are only known from osteoderms (e.g., *Apachesuchus heckerti*) it was necessary to remove taxa where no characters could be scored for one of the partitions, as inclusion of taxa with no scored characters causes the algorithm to generate all possible trees, which increases exponentially given the total number of taxa with the end result of a completely unresolved consensus tree. Therefore all taxa lacking skull material were also removed from the matrices so that the final trees could be directly compared. Taxa were also removed if taxonomic equivalence could be demonstrated, utilizing the Safe Taxonomic Reduction method of Wilkinson (1995a) to reduce the number of MPTs and increase resolution. For the cranial set this included

Tecovasuchus chatterjeei, which can be scored only for two characters, and for *Desmatosuchus spurensis*, which for this partition is identically coded to *Desmatosuchus smalli*. *Desmatosuchus smalli* was retained for the analysis as its overall scoring contains fewer missing data (98% complete). For the osteoderm dataset this included *Stagonolepis olenkae*, which is scored identical to *Stagonolepis robertsoni*, *Desmatosuchus spurensis* which is scored the same as *Desmatosuchus smalli*, and *Redondasuchus rineharti*, which is scored the same as *Typothorax coccinarum*. The final partition datasets initially contain 13 taxa. *Postosuchus kirkpatricki* and *Revueltosaurus callenderi* are utilized as the outgroup, and the in-group taxa consist of *Aetosaurus ferratus*, *Stagonolepis robertsoni*, *Scutarx deltatylus*, *Aetosauroides scagliai*, *Coahomasuchus kahleorum*, *Desmatosuchus smalli*, *Longosuchus meadei*, *Neoaetosauroides engaeus*, *Typothorax coccinarum*, SMNS 19003, and *Stenomyti huangae*.

A 'Simultaneous Analysis' dataset (all 83 characters; *sensu* Baker and DeSalle, 1997), although with the reduced number of taxa (13), was run to see the effects of reduced taxon sampling, which has been hypothesized to reduce phylogenetic accuracy (Hillis, 1998), and to establish a baseline topology for comparison with the partitioned datasets. Nonetheless, it should be recognized that portioning datasets is an analytical tool and should not be expected to represent the final phylogenetic hypothesis. This simultaneous analysis matrix was subsequently portioned into three datasets, one including only cranial characters, another including only osteoderm characters, and a third including all non-osteoderm characters including the cranial set. All uninformative and constant characters were excluded, further reducing the matrix sizes (13 taxa, 35 characters from the cranial set; 13 taxa, 24 characters for the osteoderm only set, and 13 taxa, 46 characters for the non-osteoderm only set). Because the datasets were reduced, Permutation Tail Probability (PTP) tests were run in PAUP* to test the null hypothesis

that the datasets are no better than random and thus phylogenetically uninformative (Faith and Cranston, 1991). The cranial and the armor only datasets had PTP scores of 0.01 and the endoskeletal dataset had a score of 0.02 which are less than the required PTP of 0.05 that is considered to be significant, thus falsifying the null hypothesis. These datasets were run under the branch and bound settings in PAUP* and the results of the partition sets were compared with each other, as well as to the full and reduced taxon datasets containing all 83 characters.

Results

Reduction of the number of taxa in the full working matrix from 28 to 13 taxa produced 14 parsimony-uninformative characters (including four constant characters) out of the original set of 83. The uninformative characters were excluded *a priori* from the final matrix of 69 characters and 12 in-group taxa. Ten characters were unordered. The initial run (branch and bound) resulted in three most parsimonious trees of 178 steps. (C.I. = 0.6067, H.I. = 0.3933, R.I. = 0.5270, R.C. = 0.3198), which is provided in Figure 6.17a. This tree is somewhat similar to the strict consensus tree recovered in the complete analysis presented earlier except that the base of Aetosauria is unresolved, consisting of *Stenomyti*, *Stagonolepis*, Aetosaurinae and Desmatosuchinae. Nonetheless, taxa recovered in Aetosaurinae and Desmatosuchinae in the full analysis are recovered in those same clades in this reduced analysis. Thus the reduction of taxa as well as the loss of the 14 constant/uninformative does not significantly change relationships within the tree.

Overall clade support in the base of the reduced matrix tree is not good with some clades collapsing with one additional step. However, Typothoracinae (*Typothorax* +

SMSN 19003) collapses after six steps, and Desmatosuchini (*Desmatosuchus* + *Longosuchus*) is particularly well-supported, not collapsing until nine additional steps. Thus, there appears to be no negative effects to clade support as a result of reduced taxon sampling as the nodes are even better supported than in the tree recovered for the complete analysis. Thus, this reduced matrix tree provides a suitable baseline topology to compare to the other partition sets.

A branch and bound search of the reduced matrix utilizing the osteoderm only dataset (12 in-group taxa, 24 informative characters, eight ordered; outgroup constrained) results in three MPTs (Figure 6.17b) of 58 steps each (C.I. = 0.8276, R.I. = 0.7727, R.C. = 0.6395). These metrics are high, suggesting that there is reduced homoplasy in this data partition (H.I. = 0.1724). Nonetheless, the recovered tree topology is mostly unresolved and poorly supported. Four clades are recovered; 1) *Desmatosuchus smalli* + *Longosuchus meadei*, which is the sister taxon to all of the other aetosaurians; 2) all of the non-desmatosuchine taxa; 3) *Stenomyti huangae* + *Neoaetosauroides engaeus*, and 4) *Typothorax coccinarum* + SMNS 19003 (Figure 6.17b). In this partitioned analysis *Stenomyti* + *Neoaetosauroides* is supported by two unambiguous synapomorphies, dorsal eminence of the dorsal paramedian osteoderms is strongly offset medially (66-2), and anterolateral projection of the anterior bar of the dorsal paramedian osteoderms is present and elongate (68-1). *Typothorax coccinarum* + SMNS 19003 are supported by six unambiguous synapomorphies: 1) lateral edge of the dorsal paramedian osteoderms in dorsal view are strongly sigmoidal with a strongly posteromedially oriented posterolateral corner (63-1); 2) width/length ratio of widest paramedian osteoderms (rows 9-11) in dorsal trunk series is greater than 3.5 (64-2); 3) dorsal eminence of cervical lateral osteoderms is a moderate length, dorsoventrally flattened, slightly recurved spine (74-1); 4) mid-dorsal lateral osteoderms with a strongly acute angle of flexion between the dorsal

and lateral flanges (79-2); 5) lateral flange of pelvic and anterior caudal lateral osteoderms is roughly triangular in lateral vie with a semicircular ventrolateral border and a hook-like eminence (81-1); and 6) carapace is broad and discoidal in dorsal view (82-2).

Desmatosuchus plus *Longosuchus* (Desmatosuchini) is the best supported clade with 14 unambiguous synapomorphies: 1) cervical paramedian osteoderms are longer than wide (57-1); 2) ratio of cervical vertebrae/paramedian osteoderms significantly less than 1:1 (58-1); 3) adjacent paramedian and lateral cervical osteoderms are often fused (59-1); 4) in the paramedian osteoderms dorsal to the cervical and anterior trunk vertebrae, lateral edge articulation with lateral osteoderms is dorsoventrally thickened, angled contact, with deeply incised interdigitation (='tongue and groove') (60-1); 5) dorsal eminence shape in the cervical paramedian osteoderms are a low pyramidal or rounded boss, or elongate keel (61-1); 6) in the dorsal trunk paramedian osteoderms the anterior edge of the lateral osteoderm overlaps the anterior edge of the paramedian osteoderm (62-1); 7) lacks the sharp anteromedial projection of the anterior bar (reversed in *Lucasuchus hunti*) (67-1); 8) the anterior bar of the trunk distal paramedian osteoderms lacks an anterolateral projection (68-2); 9) anterior bar of the dorsal trunk paramedian osteoderms lacks scalloping of the anterior margin on the medial side of the osteoderm (69-1); 10) dorsal eminence in the mid-trunk osteoderms is a conical spike (78-2); 11) approximately 90 degree angle between the dorsal and lateral flanges of the mid-trunk lateral osteoderms (79-1); 12) dorsal trunk lateral osteoderms strongly asymmetrical with the dorsal flange longest (80-1); 13) lateral flange of the pelvic and anterior caudal lateral osteoderms are rectangular and ventral to a well-developed spine (81-2); and 14) overall shape in of the dorsal carapace in dorsal view is moderately spinose (82-1).

Overall support is mixed with the clade *Neoaetosauroides* + *Stenomyti Typothorax* + SMNS 19003 having Decay Indices of +1 and +2 respectively, but *Desmatosuchus* plus *Longosuchus* is very strongly supported with a Decay Index of +9. *Typothorax* + SMNS 19003 has a bootstrap value of 86% for 1000 replicates, and *Desmatosuchus* plus *Longosuchus* occurs in 100% of the replicates (Figure 6.17b).

A branch and bound run of the endoskeletal (non-osteoderm) dataset (12 in-group taxa, 46 informative characters, four ordered) results in two MPTs of 115 steps (C.I. = 0.5217, H.I. = 0.4783, R.I. = 0.4762, R.C. = 0.2484), the strict consensus of which is shown as figure 6.17c. The tree is nearly completely resolved and the topology more closely resembles the total evidence tree rather than the cranial only tree. *Aetosauroides* is recovered at the base of the tree, and the clade (*Neoaetosauroides* + (*Scutarx* + (*Desmatosuchus* + *Longosuchus*))) is recovered. A significant difference, however, is that SMNS 19003 forms a novel clade with *Aetosaurus* in this partion tree rather than with *Typothorax*. Therefore the clade Typothoracinae is not supported by this character set. Support for this topology is weak with only clade (Aetosauria) with a bootstrap value higher than 50%. *Aetosaurus* + SMNS 19003 has a Decay Index of +1, a bootstrap value of 48%, and is supported by three unambiguous synapomorphies: 1) ventrolateral margin of the nasal forms part of the dorsal border of the antorbital fossa (10-1); 2) postorbital contacts quadratojugal (15-1); and 3)) supratemporal fenestra is greatly reduced in size compared to the orbit (22-2).

A subset of the non-osteoderm dataset, consisting of only cranial characters, was also run using the branch and bound search criteria. This run (12 in-group taxa, 35 informative characters, four ordered) resulted in thirteen MPTs of 82 steps (C.I. = 0.5488, H.I. = 0.4512, R.I. = 0.5542, R. C. = 0.3041) shown as figure 6.17d. This tree is most similar to the non-osteoderm dataset tree, but less resolved. The base of the tree is a large

polytomy with *Aetosaurus*, *Aetosaurioides, Typothorax*, *Coahomasuchus*, SMSN 19003, and *Stenomyti*. *Longosuchus* and Desamtosuchus form a clade (Desmatosuchini) with *Scutarx*, *Neoaetosauroides*, and *Stagonolepis robertsoni* as successive sister taxa. Support is no better than in the endoskeletal (non-osteoderm) tree, with all clades a Decay Indices of +1 and a bootstrap values less than 50% (Figure 6.17d). As with the endocranial set Typothoracinae is not recovered. However, neither is the clade *Aetosaurus* + SMNS 19003, which was recovered in the endocranial set.

Dataset Incongruence

A partition homogeneity test was conducted in PAUP* for the 'simultaneous analysis' matrix (excluding uninformative characters following the recommendations of Lee, 2001) divided into three partitions (osteoderm, postcranial, and cranial) using the CHARSET command in PAUP*. The test resulted in a p-value score of 0.03 suggesting that some character conflict exists between the partitioned datasets. Incongruence Length Difference (ILD) tests (Farris et al., 1995) were run for each partition set, comparing each to the other two sets. The test without the cranial set had a p-value score of 0.70, that without the endoskeletal (non-osteoderm) set had a score of 0.08, and the test excluding the osteoderm set had a p-value of 0.35. These results all show significant incongruence over the 0.05 threshhold. These numbers also suggest that although the cranial and osteoderm sets are the most compatible, with low conflict, the osteoderm and postcranial sets and the cranial and postcranial sets have very high levels of conflict. Size differences between the partitions (e.g., number of characters) do not influence the ILD test, thus datasets with higher amounts of characters do not 'overwhelm' partitions with lower

numbers of characters (Farris et al., 1995; Baker et al., 1998). Therefore these numbers are the result of dataset incongruence.

Bull et al., (1993) argued that dataset partitions with high levels of character conflict should not be combined for analyses (the prior agreement approach), whereas others (e.g., Kluge, 1989; Barrett et al., 1991) argue that data should be combined in all cases (the total evidence approach). Still others argued that these debates have been mostly theoretical and it is important to examine the actual data to understand the consequences of these approaches (Baker and DeSalle, 1997). The Partition Homogeneity Test (and ILD) measures levels of disagreement between partitions, but does not identify specific nodes where this conflict occurs (Lambkin et al., 2002). Baker and DeSalle (1997) developed a new measure, Partitioned Bremer Support (PBS) to determine the amount of support individual data partitions contribute to the branch support of the full matrix. Partition datasets that conflict with other datasets at the same node will contribute negatively to the overall branch support. Therefore isolating Bremer Support values for nodes by partition allows for the determination of localized areas of disagreement. The higher the negative PBS number, the greater the support that partition provides for an alternative node that is not present in the combined data tree (Lambkin, 2004; Brower, 2006). Moreover, strong variance in PBS scores for nodes, demonstrates conflict between partitions for node resolution (Lambkin, 2004). Neutral (0) scores indicate that there is within-dataset incongruence and that the particular partition is ambivalent about the node, reducing overall support (Lambkin et al., 2002).

I employed the program TreeRot.v3 (Sorenson and Franzosa, 2007) to calculate PBS values for the partitioned dataset. This method works back and forth between the TreeRot.v3 program and PAUP*. First the 'simultaneous analysis' matrix is run in PAUP* using the same parameters as the earlier run (12 in-group taxa, 69 informative

characters, ten characters ordered, branch and bound search) with the three partitions set-up using the CHARSET command. I also used PAUP* to calculate Bremer Support (BS) values for the entire dataset. The resulting tree file is then entered into TreeRot to generate a PAUP* command file, which includes the Partitioned Bremer Support (PBS) values. Minimum, maximum and averaged values are given for each partition at each node. Baker and DeSalle (1997) recommended utilizing the averaged value, but Lambkin et al., (2002) argued that averaging masks some of the conflict found at each node. For this study I did use the averaged values, however, because it is the averaged values for each partition that sum to match the Bremer Support value listed for each node. The values for this analysis are provided for branches in Figure 6.17a. There are three numbers listed, the first is from the cranial character set, the second from the postcranial (vertebrae, girdles, limbs) character set, and the third from the osteoderm character set. Note that the three PBS values equal the total BS value for that branch and as mentioned earlier negative numbers denote negative support (homoplasy) and neutral numbers indicate node ambivalence for that dataset. Also note that these character set (CHARSET) divisions are for the purpose of determining the PBS and do not pertain directly to the partition dataset trees presented in Figures 6.17b-d.

The cranial character set supports eight nodes, showing no conflict with the other character sets, although support is low for four of these nodes (below +0.5). The postcranial character set supports only a single node (*Coahomasuchus* + Typothoracinae), but is mostly neutral except for two nodes where it shows moderate conflict with the other datasets, especially in one node, *Desmatosuchus* + *Longosuchus* (=Desmatosuchini), which has a PBS of -1.50. The osteoderm character set shows positive, but low, for seven out of eight nodes, including good support (+5.53) for Desmatosuchinae. The osteoderm character set shows conflict for Desmatosuchini (-

1.17). In sum, character dataset conflict occurs in two nodes, Aetosauria and Desmatosuchini, with all conflict occurring with the postcranial and osteoderm datasets (Figure 6.17a).

Discussion

Dataset partitioning and partition homogeneity tests (PHT) strongly suggest that the main character suites (i.e. cranial, postcranial, osteoderm) possess some conflicting phylogenetic signals. The PHT suggests that the postcranial dataset conflicts the most with the other datasets, and Partitioned Bremer Support analyses identify the nodes where this conflict exists.

It had been suggested by previous studies that adding more non-osteoderm character data would stabilize weakly supported and labile relationships outside of the Typothoracinae and Desmatosuchini (Desojo, 2005; Desojo et al., 2012; Heckert et al., in press; Roberto-da-Silva et al., 2014), but doubling the size of the matrix and increasing the number of endoskeletal characters to be dominant did not create more support, these inner tree relationships still remain weakly supported, and there is little confidence in the recovered clades. It is presently unclear how stable these nodes will be. Lack of support and accuracy could be caused by the need for more taxon sampling or by large amounts of missing data (Wiens, 1998b; Heath et al., 2008), but it is also possible that it is caused by incongruence between and within character suites (Lambkin et al., 2002). Moreover, missing or inapplicable data has been argued to cause ambiguous character optimizations at nodes (Ezcurra et al., 2014).

Using the total evidence approach of Kluge (1989) and adding more solid character data could overcome dataset noise (Barrett et al., 1991), and this should be

tested in future analyses. Furthermore, the present matrix contains little data from the appendicular skeleton, where the characters appear to be well-conserved, or what differences are apparent cannot be viewed outside of the realm of ontogenetic or sexual variation, but this should be a source of future characters where possible. Increased taxonomic sampling from future discoveries, including the potential discovery of other suchian taxa with lateral armor to serve as improved outgroup taxa, will undoubtedly help improve dataset resolution.

Bull et al., (1993) argued that combining heterogeneous datasets can result in an erroneous parsimony estimates and that it is better to keep these data separate to avoid getting a single wrong answer. Data that fail statistical tests for heterogeneity should not be combined and used in analyses that assume the data to be homogeneous, because character datasets that appear to be independent may in fact be the result of two distinct histories of character change (Bull et al., 1993). However, according to those authors Hillis (1987) argued that because some character sets may be useful in resolving certain areas of the tree that all data should be combined. If incongruent datasets are combined, any underlying positive signal will be amplified and can cancel out dataset noise (Lee, 2009).

In the tree recovered in the main part of this study (Figure 6.16) it is encouraging that the topology 'makes sense', that is that there is nothing in the topology that will be a major surprise to an aetosaur worker suggesting that an underlying positive signal is present. For example, *Scutarx deltatylus* and *Calyptosuchus wellesi*, are recovered in the same clade, which is expected as the material of *Scutarx* was once assigned to *Calyptosuchus* (Parker and Martz, 2011). *Stenomyti huangae* and *Aetosaurus ferratus* are recovered close together just outside of Typothoracinae (Figure 6.16) and therefore presents a proposed relationship with little statistical support, yet when originally

discovered the material of *Stenomyti* was originally assigned to *Aetosaurus* (Small, 1998) and utilizing only anatomical comparisons it would be expected for the two to be recovered close together, again suggesting an underlying positive signal. In contrast, the tree presented by Parker (2007) introduced two strong clades (Typothoracinae, Desmatosuchinae), but generally the overall recovered topology did not 'make sense' in regards that, 1) no terminal taxa stemmed from the base of the tree (i.e. there is no 'basal' species-group taxon), and 2) outside of the two strong clades, all of the other taxa were an unresolved 'hodge-podge' unsupported by synapomorphies other than a few armor characters.

Nonetheless, caution is warranted when equating 'sense' with accuracy. For example, at one time it was thought that taxa with a radial ornamentation on the paramedian osteoderms, and similar lateral osteoderm anatomy formed a widely inclusive clade (Aetosaurinae, Parker, 2007), or a genus-group taxon (*Stagonolepis sensu* Heckert and Lucas, 2000) and the tree presented by Parker (2007) supported those hypotheses to some extent. However, these hypotheses quickly fell apart when new cranial data were added showing that these osteoderm characters are potentially homoplastic (Parker, 2008b; Desojo et al., 2012). Indeed, the partition analyses presented here show that those clades are not recovered in the endoskeletal analyses (Figure 6.17c, d) are therefore are based almost entirely on osteoderm characters. Moreover, the full analysis shows that the main character combining these taxa, radial ornamentation of the paramedian osteoderms, is simply a plesiomorphic character of non-desmatosuchins. Thus, these data strongly suggest that even in a tree with much 'noise' (conflicting character data, weak clade support) that a well-supported phylogenetic signal is coming through that is only amplified over the 'noise' when all of the data are combined (Baker and DeSalle, 1997).

Prospectus

Many of the discussions of dataset partitioning and character congruence and the strategies devised to deal with problems are from studies where morphological and molecular data are being combined (e.g., Bull et al., 1993; Huelsenbeck et al., 1996; Cunningham, 1997; DeSalle and Brower, 1997; Wiens, 1998a). However, there is no reason not to suspect that the same phenomena may occur in studies using purely morphological data. Different anatomical modules may possess different histories and thus present conflicting character data that can mask true phylogenetic relationships or support false ones. I would encourage workers conducting phylogenetic analyses of morphological datasets to explore the possibilities of incongruent subsets in their data.

Furthermore, ontogenetic change in aetosaurians is still poorly understood and it is important that specimens scored are at the same relative ontogenetic stage to rule out the possibility of differences caused by developmental history. Determination of maturity indicators can identify synonymous taxa (originally scored separately) and provide a baseline for morphological equivalence of taxa (or specimens) used in phylogenetic studies (Brochu, 1996). Presently the most often used indicator for pseudosuchians, including aetosaurians) is the progression of neurocentral suture close in the vertebral column (Brochu, 1996). In aetosaurians this progression begins in the caudal series and ends with the axis/atlas (Irmis, 2007). Unfortunately, many aetosaurian specimens lack relatively complete series (e.g, *Tecovasuchus chatterjeei*, TTU P-545) or completely lack preserved vertebrae (e.g., *Paratypothorax andressorum*, SMNS unnumbered). In others, the vertebral column is covered by the articulated carapace (*Coahomasuchus kahleorum*, NMMNH P-18496). Fortunately, other methods such as CT scanning and histological sectioning are available, but to date only a handful of specimens have been sampled and only two of these are holotypes (e.g., Parker et al., 2008; Cerda and Desojo, 2011). I

encourage all aetosaur workers to carefully determine and document maturity indicators for as many specimens as possible with a future goal of incorporating this information into phylogenetic analyses.

As with any scientific study, this is a work in progress. Unfortunately, it is presently unclear whether phylogenetic relationships resulting from a matrix with an abundance of osteoderm characters (e.g., Parker, 2007) are any more correct (accurate) than those formed by a matrix with an abundance of endoskeletal (non-osteoderm) characters (this study), although I have given my reasons above for preferring the latter. I've attempted to carefully reexamine all characters used in past analyses and to construct unambiguous characters and states. I've tried to score characters as carefully as possible, but certainly errors exist. The Partitioned Bremer Support analysis shows where character support for individual nodes is weak or conflicting for suites of characters and therefore can be used to examine node stability when new data are added (Gatesy et al., 2003; Wahlberg and Nylin, 2003; Lambkin, 2004). Thus, future analyses should look to increase the number of informative characters, fill in blanks caused by missing data and correct erroneous scorings to improve accuracy and clade support. However, they should avoid adding large numbers of poorly supported characters (i.e. heavy on missing data) just for the sake of increasing characters numbers and instead focus on creating characters that can be fully or nearly fully coded to avoid decreasing overall accuracy (Wiens, 1998b).

Taxon	Number of characters scored	Percent complete
Desmatosuchus smalli	80	98%
Stagonolepis robertsoni	78	95%
Aetosaurus ferratus	77	94%
Typothorax coccinarum	74	90%
Aetosauroides scagliai	72	88%
Longosuchus meadei	72	88%
Coahomasuchus kahleorum	68	83%
Stagonolepis olenkae	68	83%
Neoaetosauroides engaeus	67	82%
Desmatosuchus spurensis	65	79%
Stenomyti huangae	59	72%
SMSN 19003	54	66%
Scutarx deltatylus	52	63%
Calyptosuchus wellesi	44	54%
Sierritasuchus macalpini	38	46%
Paratypothorax sp.	36	44%
Paratypothorax andressorum	33	40%
Tecovasuchus chatterjeei	32	39%
Polesinesuchus aurelioi	31	38%
Rioarribasuchus chamaensis	30	37%
Redondasuchus rineharti	30	37%
Lucasuchus hunti	29	35%
NCSM 21723	26	32%
Adamanasuchus eisenhardtae	24	29%
Aetobarbakinoides brasiliensis	22	27%
Apachesuchus heckerti	18	22%
AVERAGE		60%

Table 1. Completeness of taxa scored for this phylogenetic analysis. Number of characters scored is out of 83 potential scored characters.

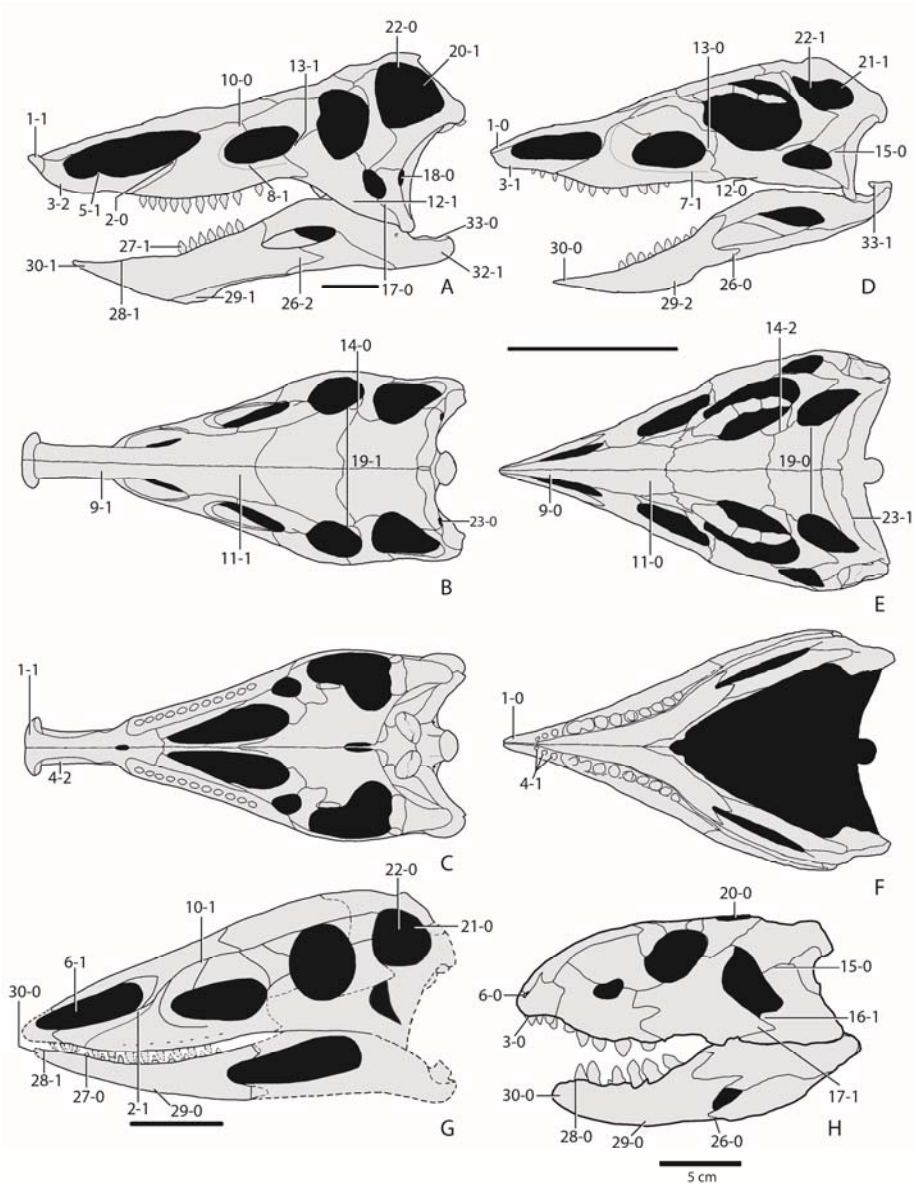

Figure 6.1. Skull reconstructions of suchian archosaurs showing defined character states. A, B, C, *Desmatosuchus smalli* in lateral, dorsal and ventral views (redrawn from Small, 2002); D, E, F, *Stenomyti huangae* in lateral, dorsal, and ventral views (redrawn from Small and Martz, 2013); G, *Aetosauroides scagliai* in lateral view (redrawn from Desojo and Ezcurra, 2011); H, *Revueltosaurus callenderi* (based on PEFO 34561) in lateral view. Scale bars equal 5 cm.

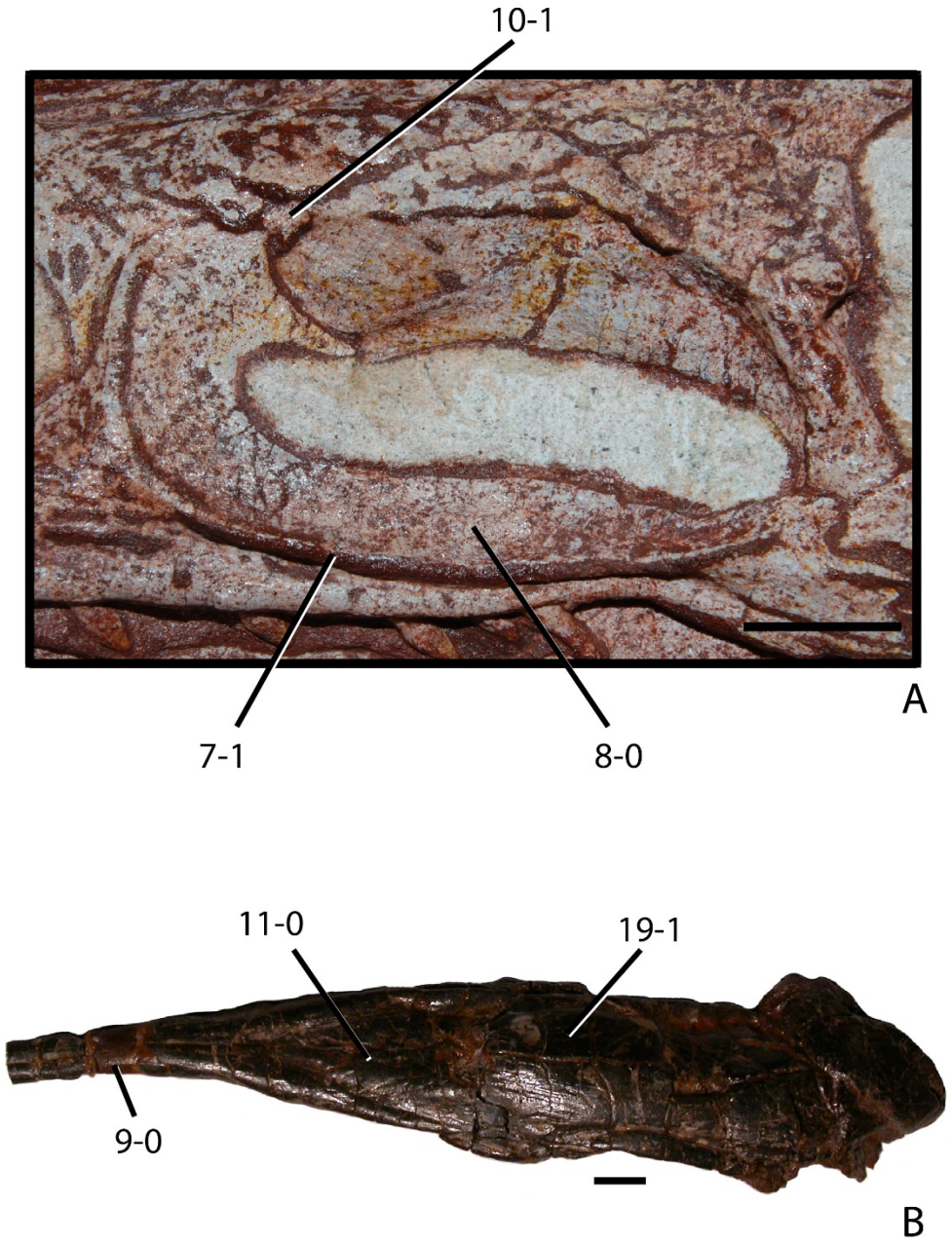

Figure 6.2. Photos of aetosaurian crania showing defined character states. A, close-up view of the antorbital fenestra in SMNS 19003, showing the extent of the antorbital fossa and the upper contact with the frontal; B, skull of *Aetosauroides scagliai* (PVL 2073) in dorsal view. Scale bars equal 1 cm.

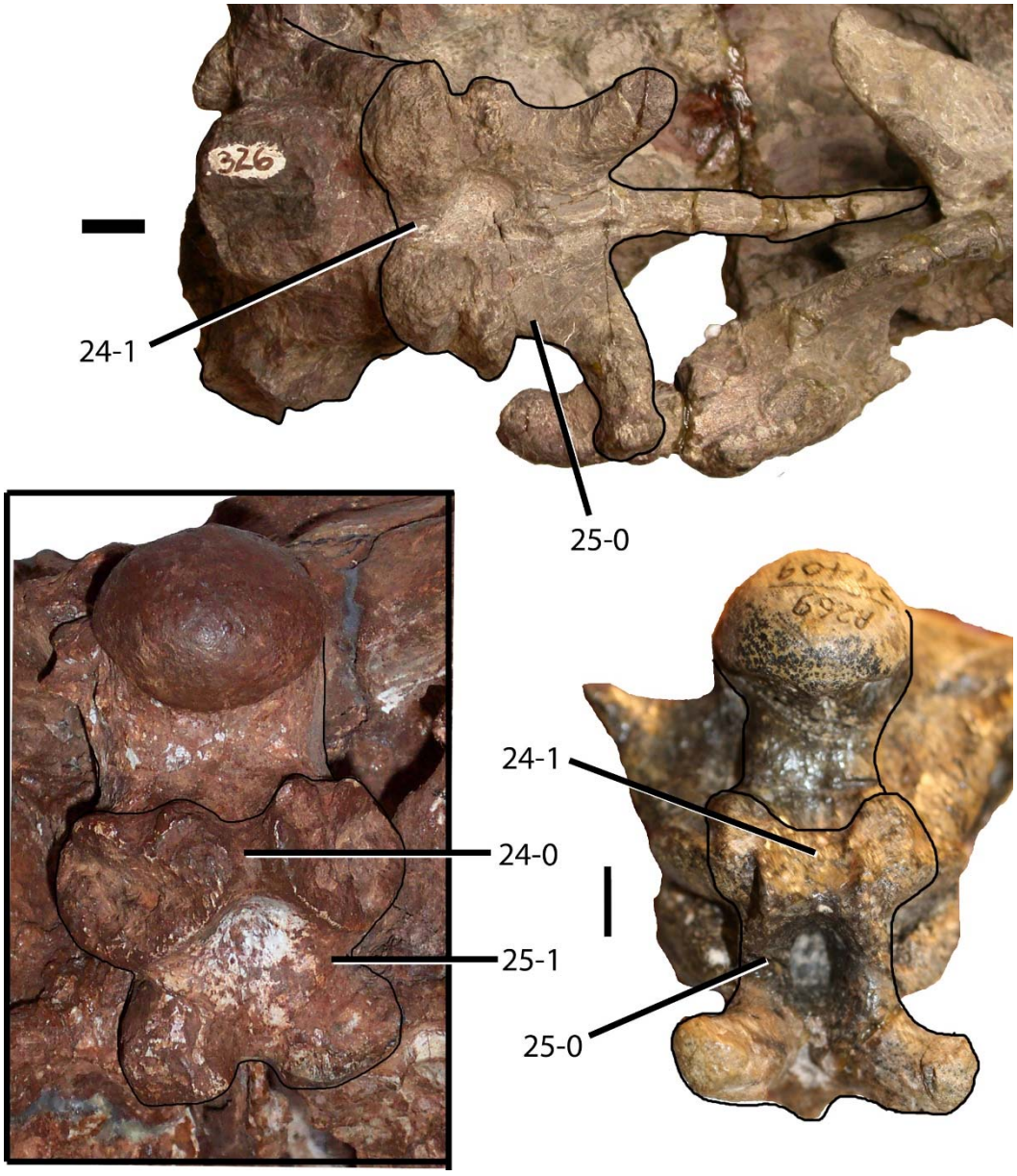

Figure 6.3. Photos of aetosaurian basicrania showing defined character states. A, PVSJ 326, parabasisphenoid of *Aetosauroides scagliai* in ventral view; B, TTU P-9024, parabasisphenoid of *Desmatosuchus smalli* in ventral view; C, UCMP 27409, parabasisphenoid of an aetosaurian, possibly *Calyptosuchus wellesi*, in ventral view; Scale bars equal 1 cm.

Figure 6.4. Posterior portion of the left mandible of *Stagonolepis olenkae* (ABIII 578/34) in lateral view showing defined character states. Scale bar equal 1 cm.

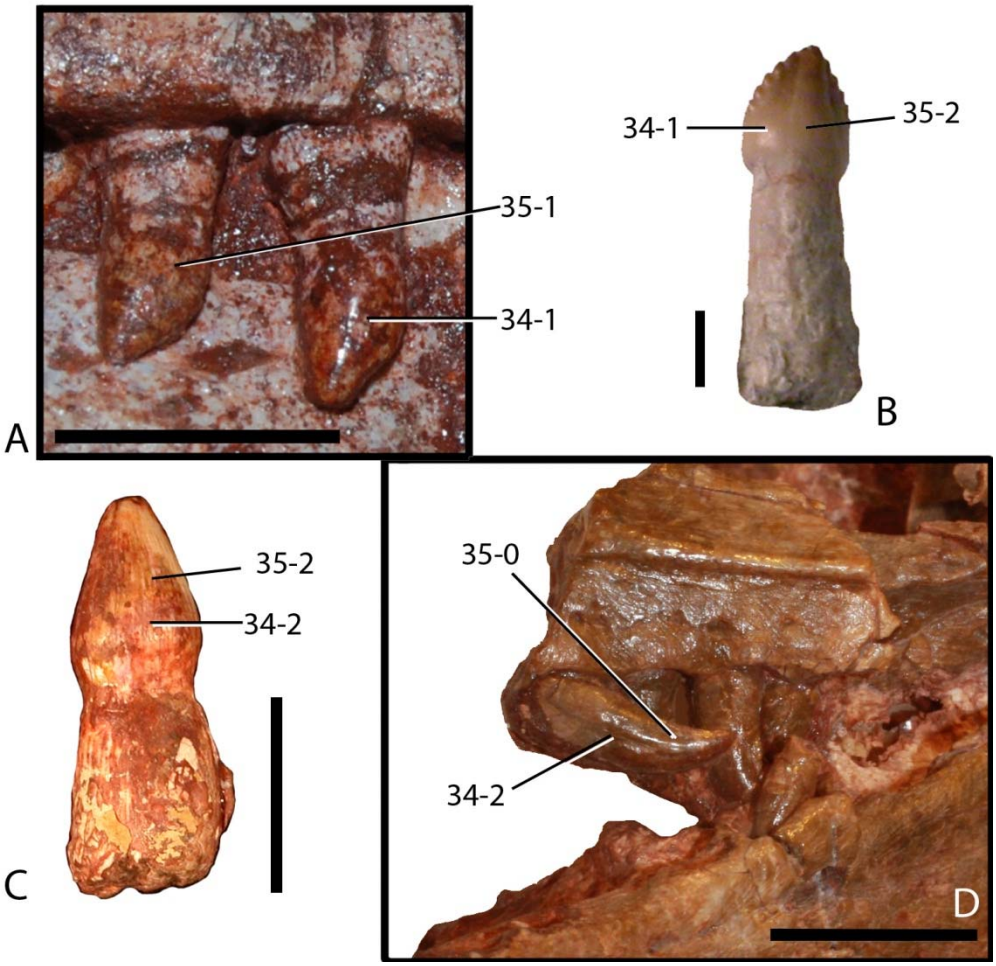

Figure 6.5. Maxillary teeth of various aetosaurians and *Revueltosaurus callenderi* showing defined character states. A, SMNS 19003; B, *Revueltosaurus callenderi* (PEFO 34561); C, *Desmatosuchus smalli* (TTU P-9024); D, *Coahomasuchus kahleorum* (TMM 31100-437). Scale bars equal 1 cm.

Figure 6.6. Cervical series centra of aetosaurians showing defined character states. A, *Desmatosuchus spurensis* (UMMP 7504) in anterior view; B, *Redondasuchus rineharti* (MDM 20080809BDM006RRF 34561) in lateral view; C, *Sierritasuchus macalpini* (UMMP V60817) in ventral view; D, *Calyptosuchus wellesi* (UMCP 139837) in posterior view; E, *Calyptosuchus wellesi* (UCMP 139794) in lateral view; F, *Calyptosuchus wellesi* (UCMP 78714) in ventral view . Scale bars equal 1 cm.

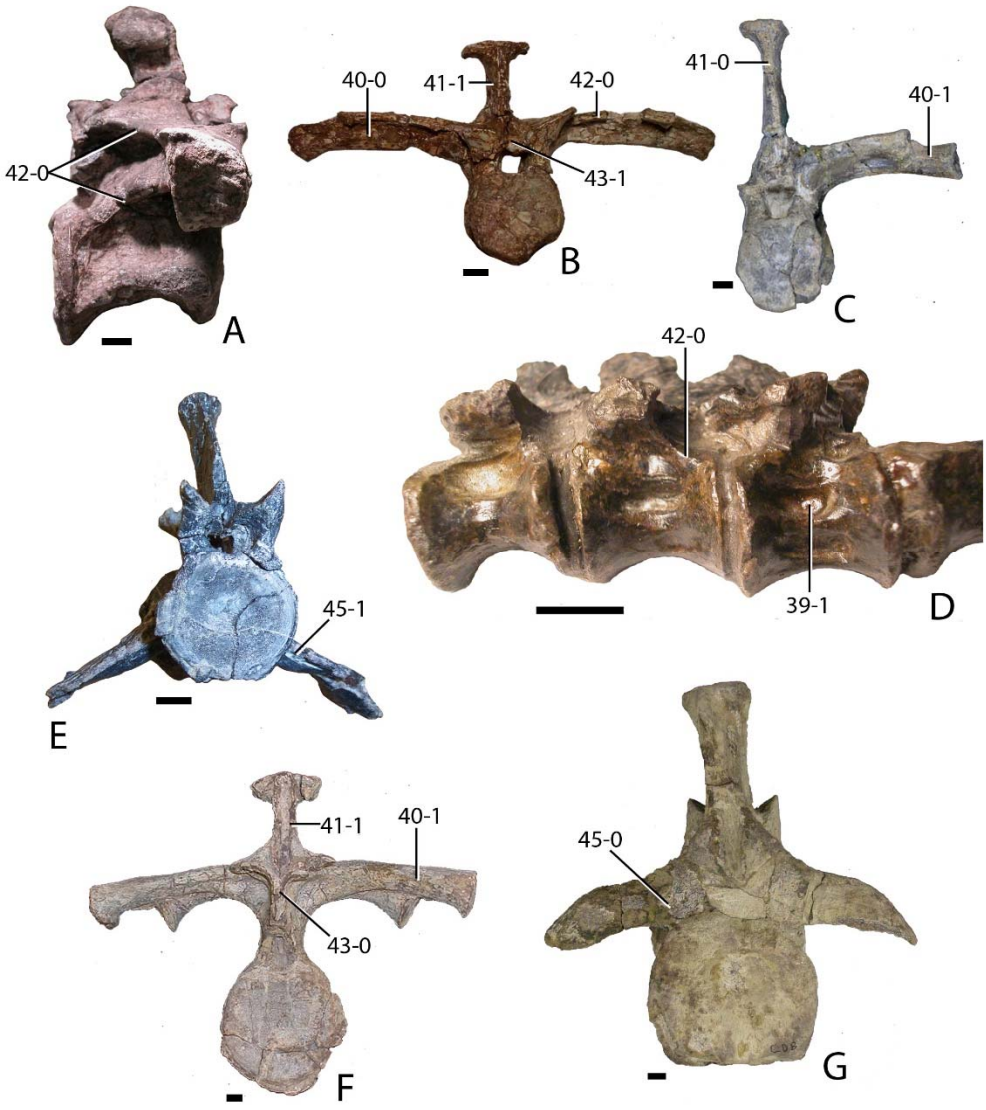

Figure 6.7. Dorsal and caudal series vertebrae of aetosaurians showing defined character states. A, *Desmatosuchus spurensis* (MNA V9300) anterior dorsal vertebra in lateral view; B, *Typothorax coccinarum* (TTU P-09214) posterior dorsal vertebra in anterior view; C, *Calyptosuchus wellesi* (UMCP 139702) mid-dorsal vertebra in anterior view; D, *Aetosauroides scagliai* (PVL 2073) dorsal vertebrae in lateral view; E, *Paratypothorax* sp. (PEFO 3004) anterior caudal vertebra in anterior view; F, *Desmatosuchus spurensis* (MNA V9300) mid-dorsal vertebra in posterior view; G, *Desmatosuchus spurensis* (MNA V9300) anterior mid-caudal vertebra in posterior view. Scale bars equal 1 cm.

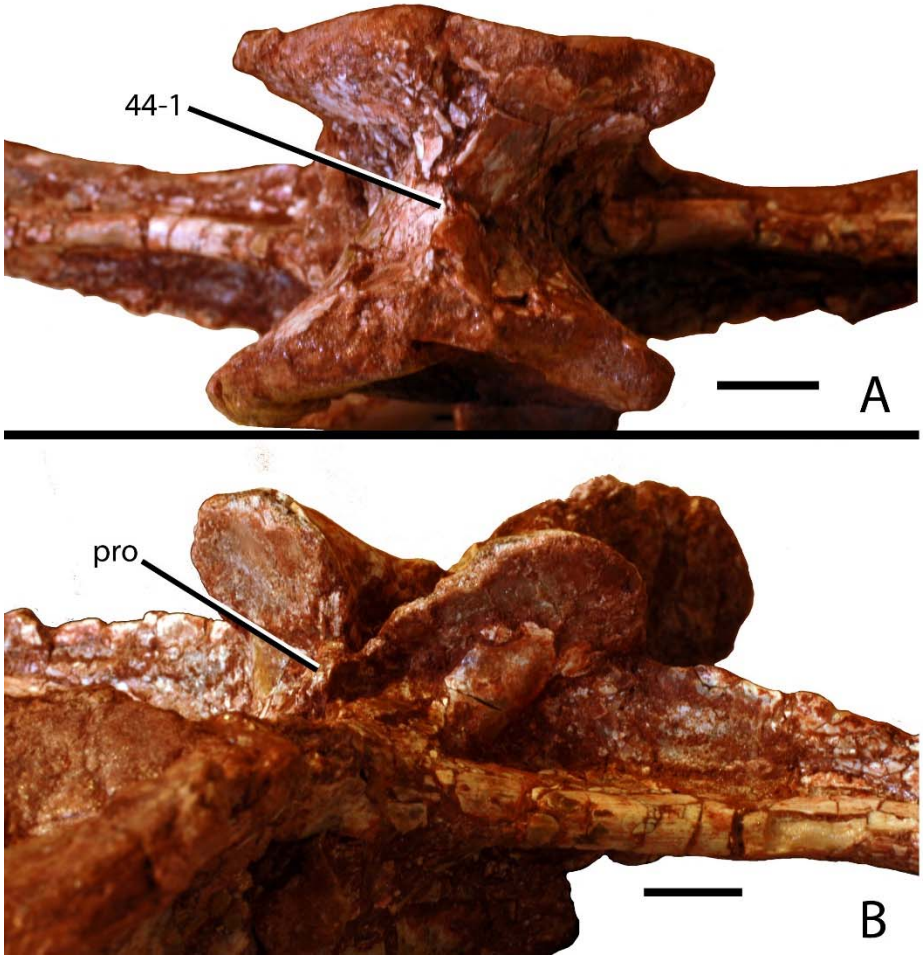

Figure 6.8. TTU P-9416, posterior dorsal vertebra of *Paratypothorax* sp. showing defined character states. A, centrum in ventral view; B, neural arch in posterolateral view showing posterior projection (pro). Scale bars equal 1 cm.

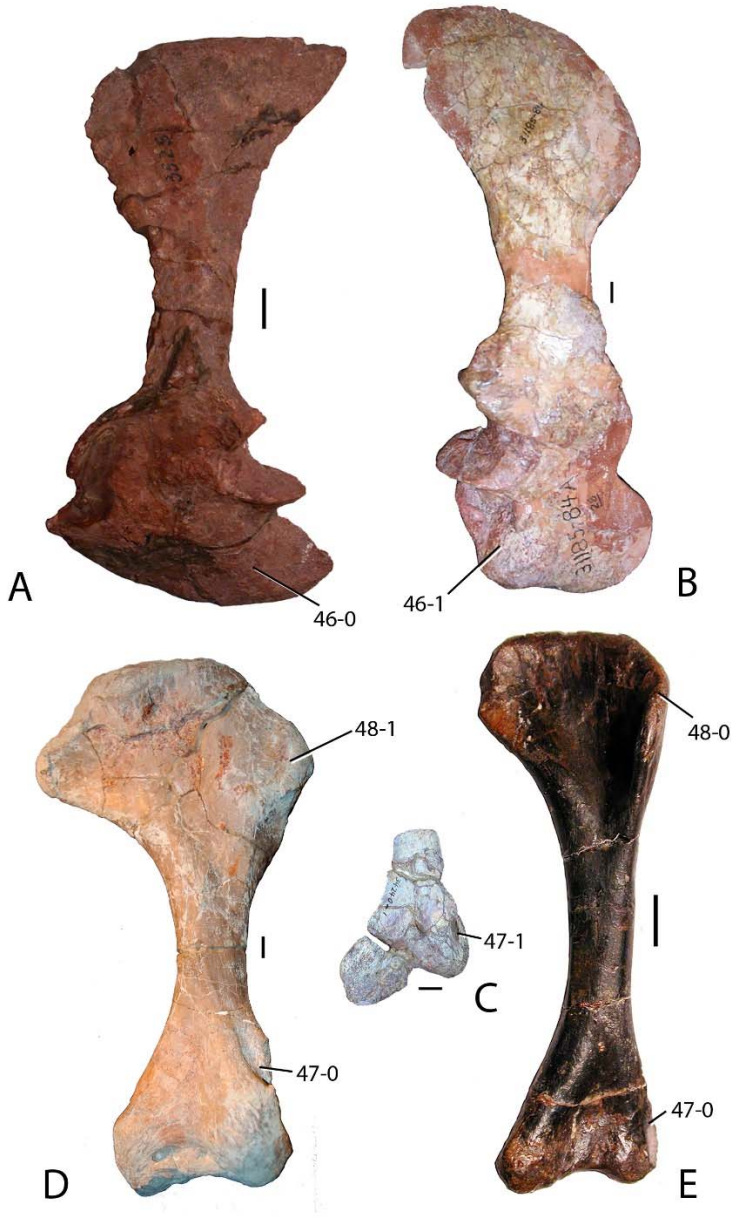

Figure 6.9. Scapulocoracoids and humeri of aetosaurians showing defined character states. A, *Neoaetosauroides engaeus* (PVL 3525) left scapulocoracoid in lateral view; B, *Longosuchus meadei* (TMM 31185-84a) right scapulocoracoid in lateral view; C, *Typothorax coccinarum* (UCMP 34240) distal end of left humerus in anterior view; D, *Stagonolepis olenkae* (ABIII 1175) right humerus in posterior view; E, *Aetosauroides scagliai* (PVL 2073) left humerus in anterior view. Scale bars equal 1 cm.

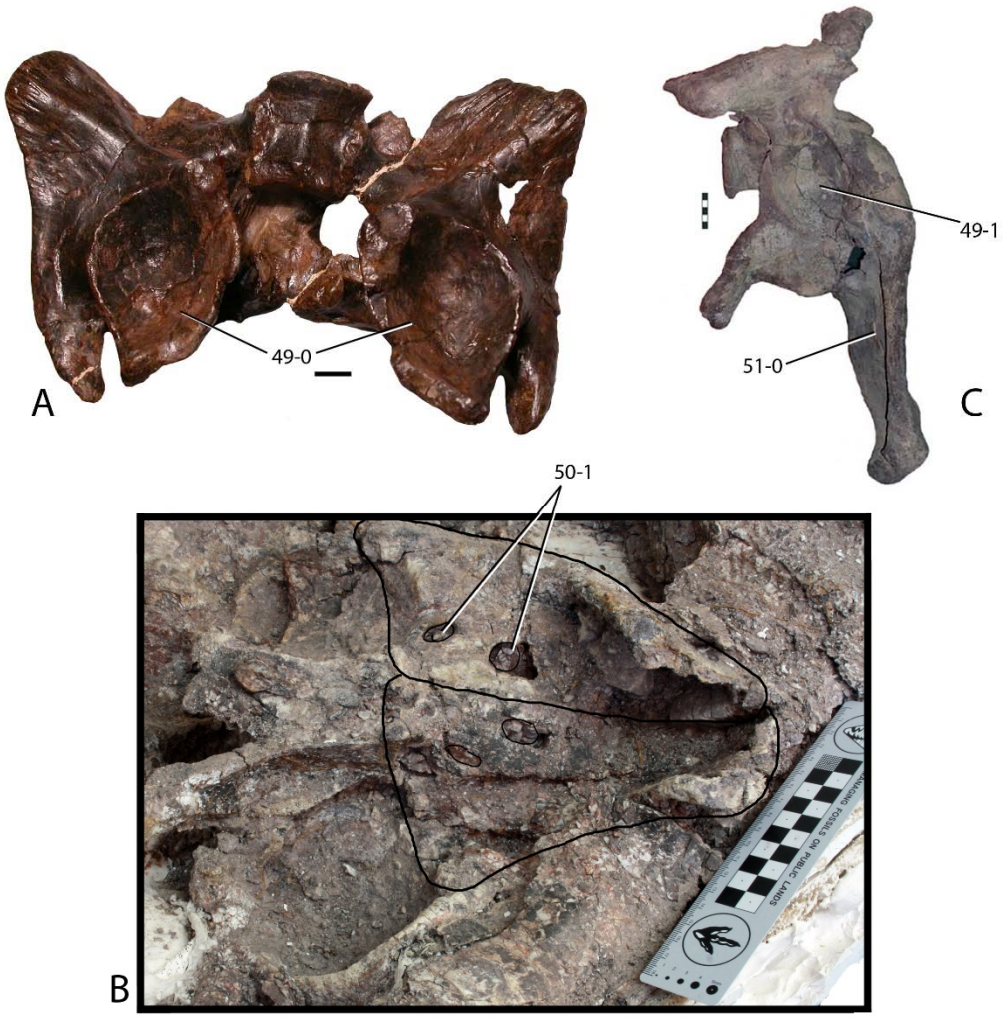

Figure 6.10. Sacra of aetosaurians showing defined character states. A, *Aetosauroides scagliai* (PVL 2073) ventral view; B, *Desmatosuchus spurensis* (MNA V9300) right lateral view; C, *Scutarx deltatylus* (PEFO 31217) ventral view. Scale bar for A equals 1 cm, for B equals 5 cm.

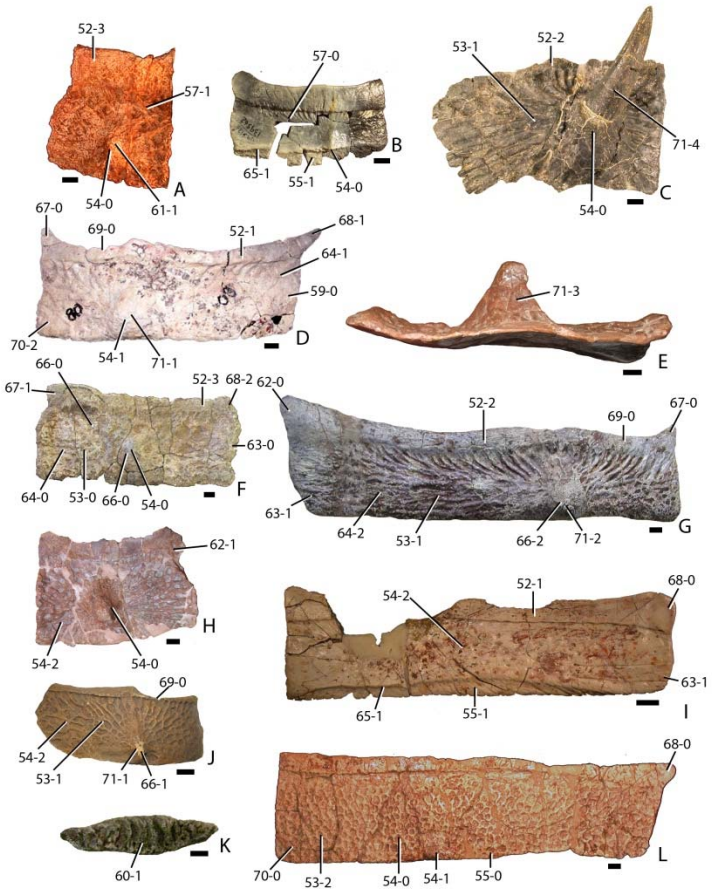

Figure 6.11. Paramedian osteoderms of aetosaurians showing defined character states. A, *Desmatosuchus smalli* (TTU P-9024) left posterior cervical osteoderm in dorsal view; B, Paratypothoracini (UCMP 139562) left cervical osteoderm in dorsal view; C, *Rioarribasuchus chamaensis* (NMMNH P-35459) left anterior caudal paramedian in dorsal view; D, *Scutarx deltatylus* (PEFO 34045) right dorsal trunk paramedian in dorsal view; E, *Lucasuchus hunti* (TMM 31100-361) right dorsal trunk osteoderm in posterior view; F, *Desmatosuchus spurensis* (MNA V9300) right dorsal trunk osteoderm in dorsal view; G, *Paratypothorax andressorum* (SMNS numbered L16) left dorsal trunk osteoderm in dorsal view; H, *Lucasuchus hunti* (TMM 31100-361) right dorsal trunk osteoderm in dorsal view; I, *Tecovasuchus chatterjeei* (TTU P-00545) right dorsal trunk osteoderm in dorsal view; J, *Stagonolepis robertsoni* (NHMUK 4789a) cast of left dorsal trunk osteoderm in dorsal view; K, *Desmatosuchus spurensis* (PEFO 26668) left dorsal trunk osteoderm in lateral view; L, *Paratypothorax* sp. (UCMP 34227) right dorsal trunk osteoderm in dorsal view. Scale bars equal 1 cm.

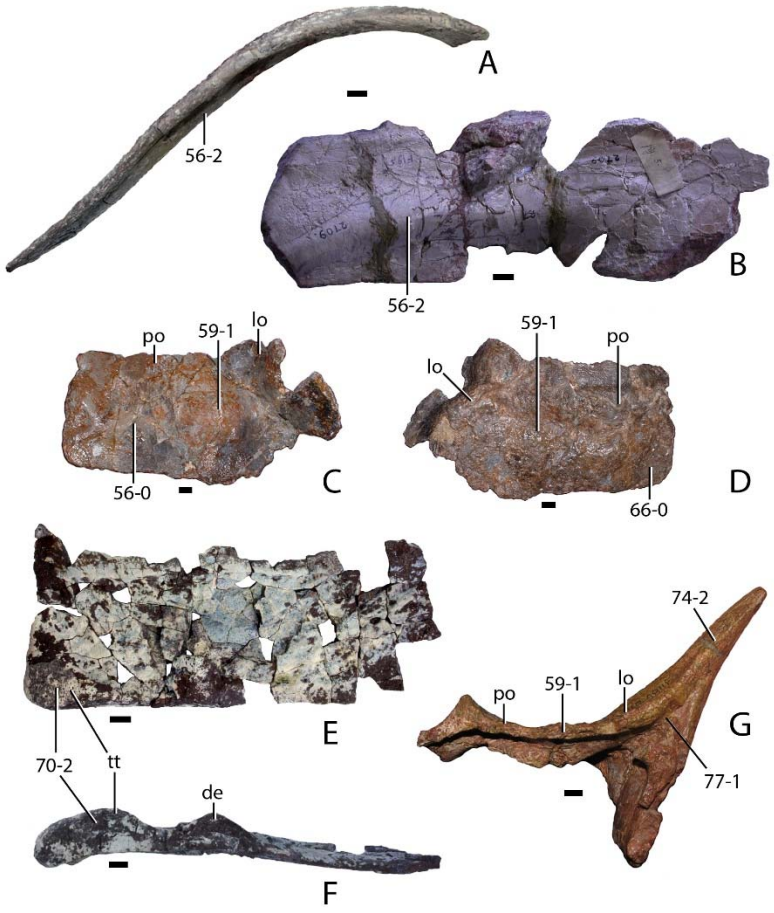

Figure 6.12. Paramedian and lateral osteoderms of aetosaurians showing defined character states. A, *Typothorax coccinarum* (PEFO 34848) left dorsal trunk paramedian osteoderm in posterior view; B, *Typothorax coccinarum* (AMNH FR 2709) left paramedian osteoderm in ventral view; C-D, *Desmatosuchus spurensis* (MNA V687) fused left anterior dorsal trunk paramedian and lateral trunk osteoderms in ventral (C) and dorsal (D) views; E-F, *Scutarx delatatylus* (PEFO 34045) right dorsal trunk paramedian osteoderm in dorsal (E) and posterior (F) views; G, *Longosuchus meadei* (TMM 31185-84B) fused right anterior dorsal trunk and lateral trunk osteoderms in posterior view. Scale bars equal 1 cm. Abbreviations: de, dorsal eminence, lo, lateral osteoderm, po, paramedian osteoderm, tt, triangular tuber.

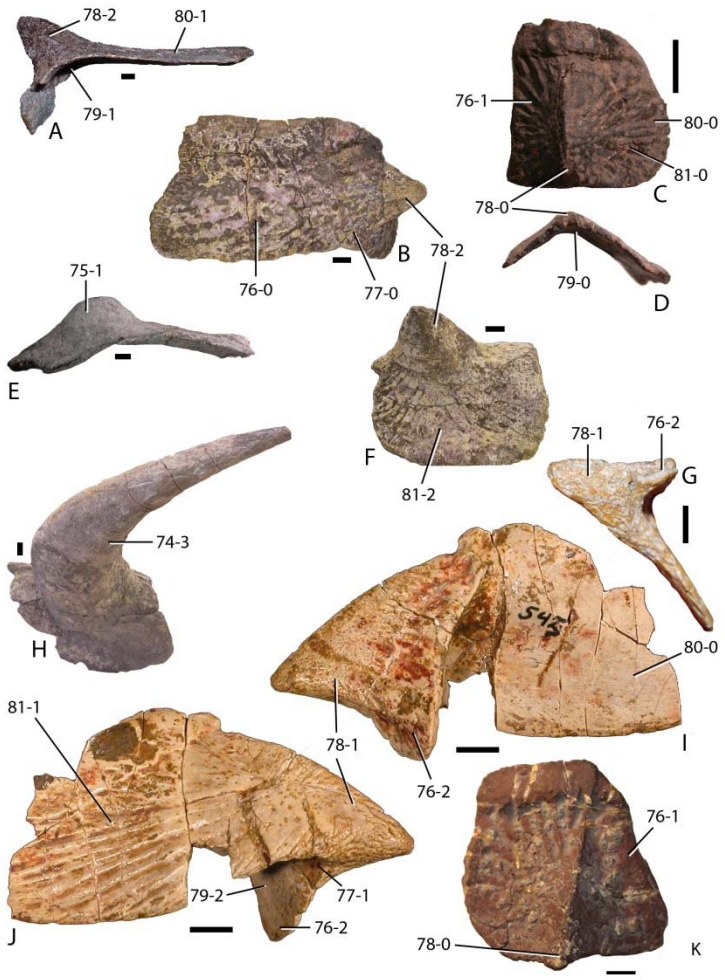

Figure 6.13. Lateral osteoderms of aetosaurians showing defined character states. A, *Desmatosuchus spurensis* (MNA V9300) right dorsal trunk osteoderm in anterior view; B, *Desmatosuchus spurensis* (MNA V9300) right dorsal trunk osteoderm in dorsal view; C-D, *Aetosauroides scagliai* (PVL 2073) right dorsal trunk osteoderm in dorsolateral (C) and posterior (D) views; E, *Desmatosuchus spurensis* (MNA V9300) left anterior dorsal trunk osteoderm in posterior view; F, *Desmatosuchus spurensis* (MNA V9300) right dorsal trunk osteoderm in lateral view; G, *Redondasuchus rineharti* (MDM 20110607RRBW006#2) left dorsal trunk osteoderm in posterior view; H, *Desmatosuchus spurensis* (MNA V9300) left cervical osteoderm in lateral view; I-J, *Tecovasuchus chatterjeei* (TTU P-00545) left dorsal trunk osteoderm in dorsomedial (I) and lateral views; K, *Calyptosuchus wellesi* (UCMP 27225) left dorsal trunk osteoderm in dorsolateral view. Scale bars equal 1 cm.

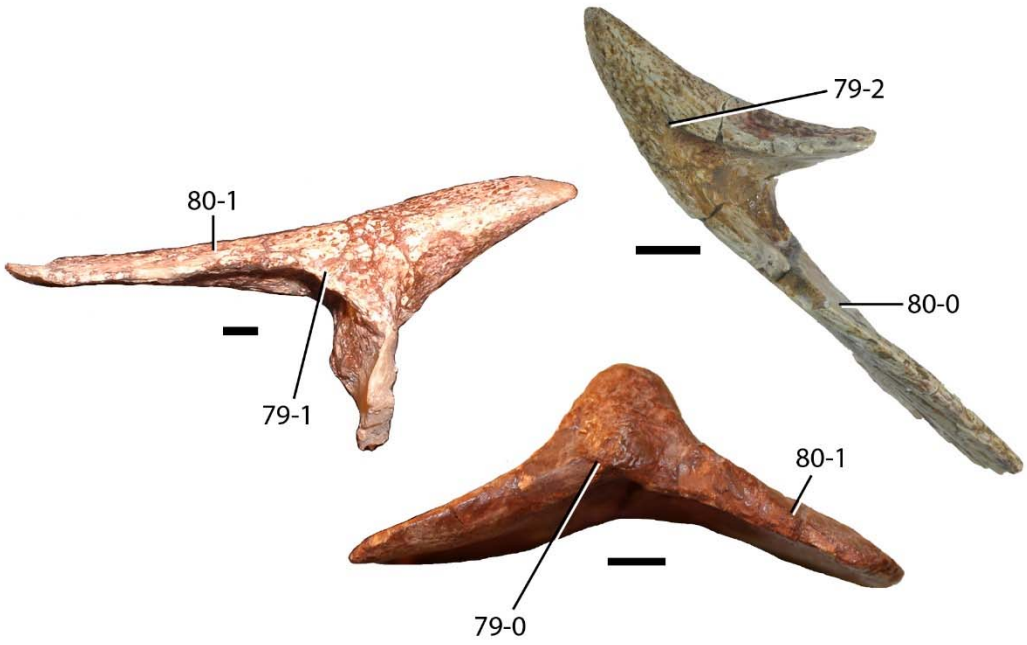

Figure 6.14. Lateral osteoderms of aetosaurians showing defined character states. A, *Desmatosuchus smalli* (TTU P-9024) right posterior dorsal trunk osteoderm in posterior view; B, *Tecovasuchus chatterjeei* (TTU P-00545) left dorsal trunk osteoderm in posterior view; C, *Scutarx deltatylus* (UCMP 35738) right dorsal trunk osteoderm in posterior view. Scale bars equal 1 cm.

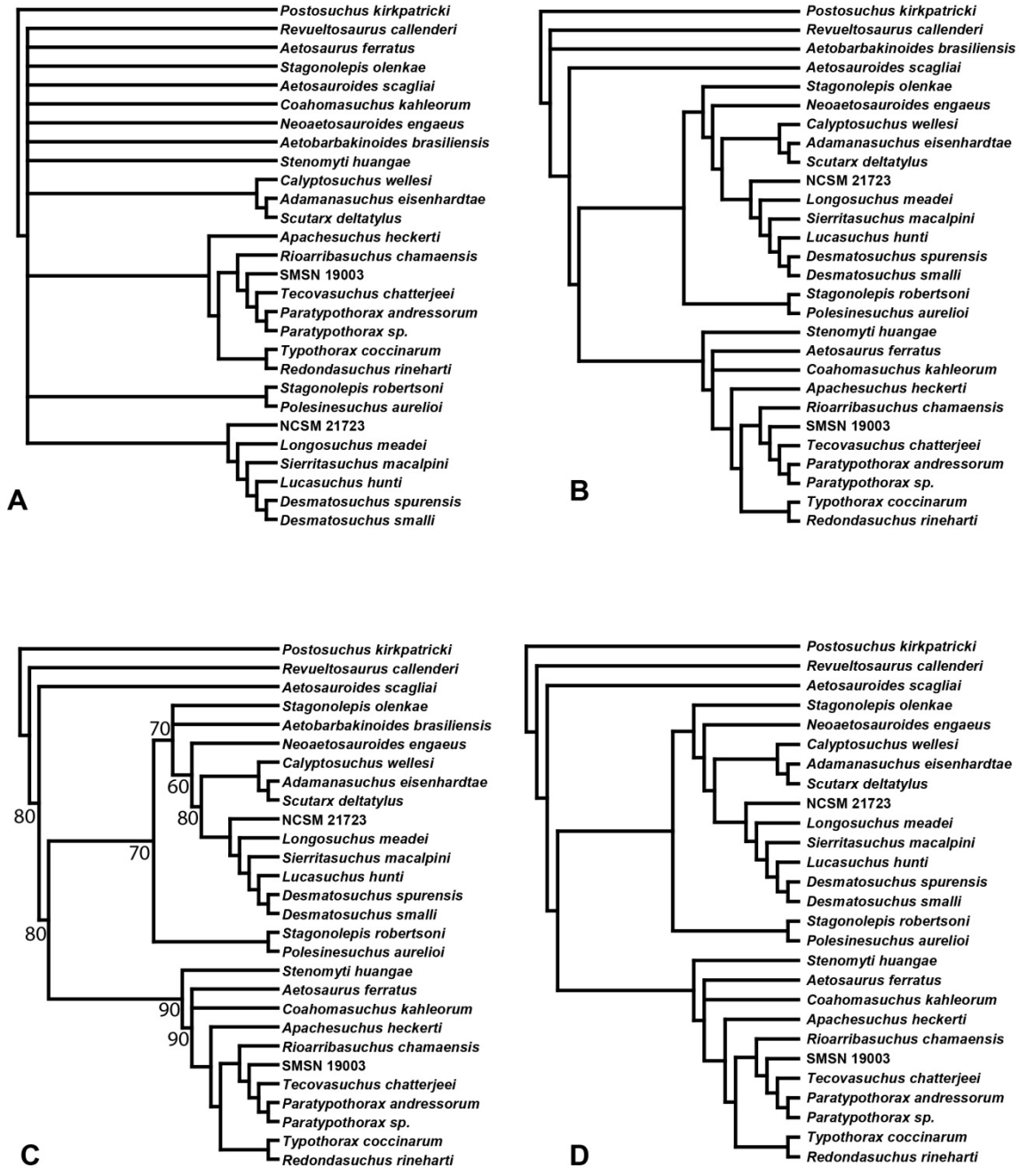

Figure 6.15. Phylogenetic trees recovered from the initial run of the main dataset. A, Strict component consensus of 30 MPTs; B, Adams consensus of 30 MPTs; 50% Majority Rule consensus of 30 MPTs. Only values under 100% are shown; D, Maximum agreement subtree after *a priori* pruning of *Aetobarbakinoides brasiliensis*.

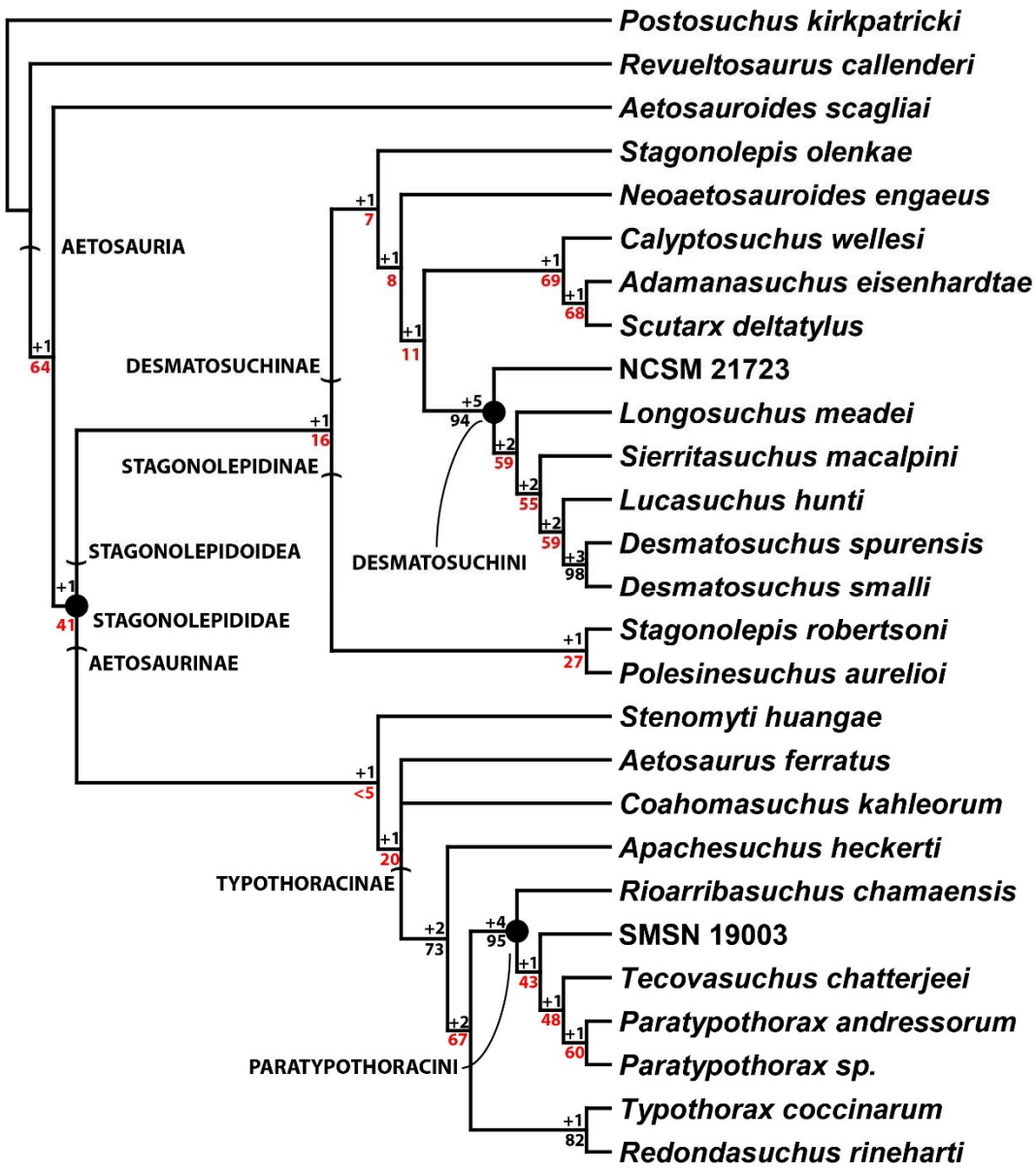

Figure 6.16. The reduced strict consensus of 3 MPTs used for this study with *Aetobarbakinoides brasiliensis* removed, with all named clades. Decay indices and bootstrap values are shown for all nodes, with bootstrap values under 70% (the confidence threshold of Hillis and Bull, 1993) shown in red.

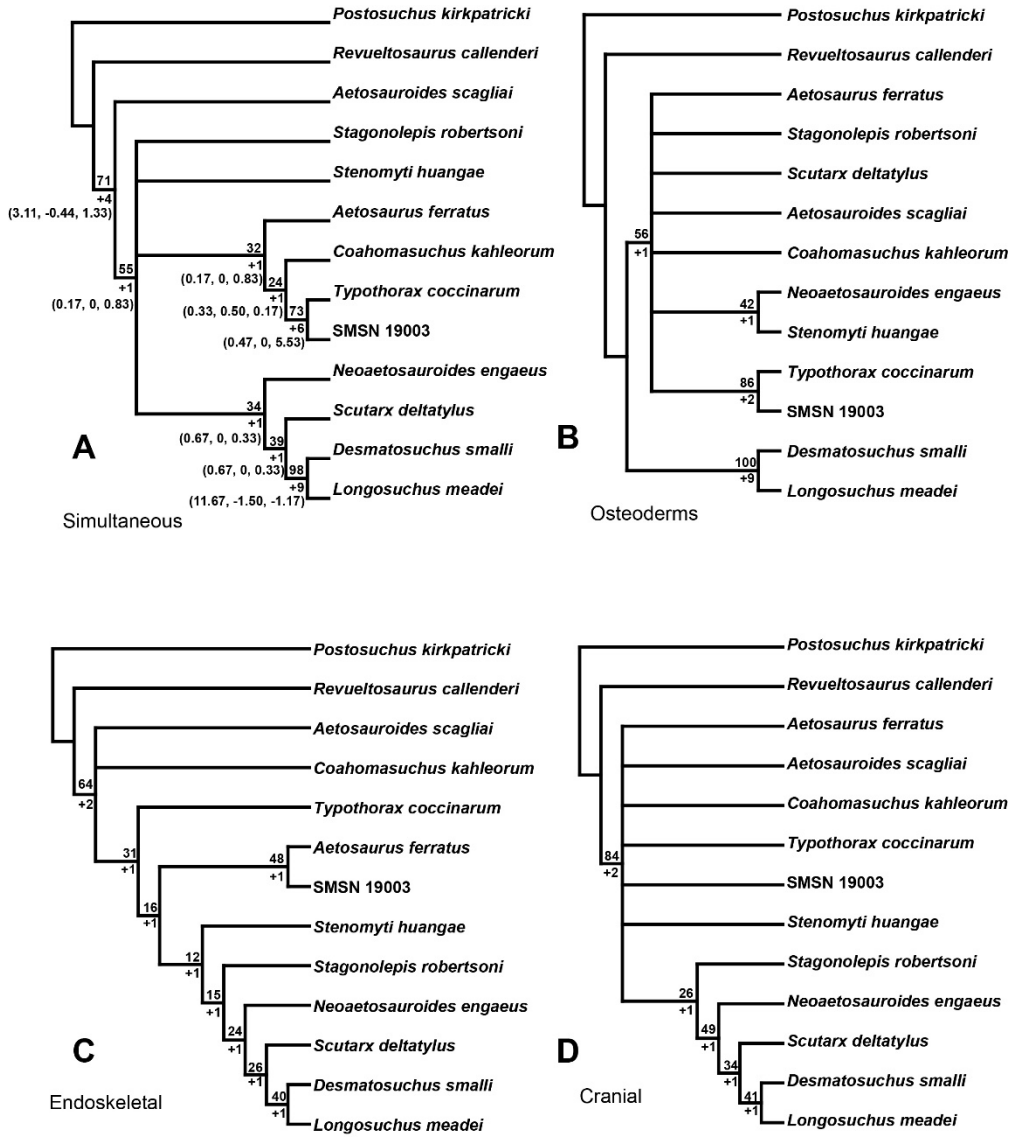

Figure 6.17. Phylogenetic trees recovered from partitioning the main dataset. Decay indices and bootstrap values (1000 replicates) listed for all nodes. A, Topology of a three MPTs from the simultaneous (13 taxa, 83 characters) dataset. Partitioned Bremer Support values for nodes are given in parentheses. The first value pertains to the cranial only characters, the second from the postcranial characters, and the third from the osteoderm characters; B, Topology of a three MPTs recovered for the osteoderm dataset; C, Strict consensus tree from two MPTs from the complete non-osteoderm (endoskeletal) dataset (cranial, axial, appendicular); D) Strict consensus of 13 MPTs from analysis of the cranial dataset.

CHAPTER 7: GLOBAL BIOSTRATIGRAPHIC RELATIONSHIPS OF THE AETOSAURIA

INTRODUCTION

More than two decades ago the need to establish a non-marine tetrapod biostratigraphy for the Late Triassic was articulated and rudimentary divisions established based on early work done in the 1930s through the 1950s (Huene, 1927; Camp, 1930; Colbert and Gregory, 1957; Long and Ballew, 1985; Lucas, 1990; Lucas and Hunt, 1993). The four Land Vertebrate Faunachrons (LVFs) established by (Lucas and Hunt, 1993) for the southwestern United States and their original age equivalents are the Otischalkian (early to middle Carnian), Adamanian (late Carnian), Revueltian (early to middle Norian) and the Apachean (latest Norian). These faunachrons were originally regional in scope based on non-marine tetrapods with the bases fixed by the first appearance of phytosaurian taxa, *Paleorhinus* (Otischalkian), *Smilosuchus* (="*Rutiodon*") (Adamanian), *Machaeroprosopus* (="*Pseudopalatus*") (Revueltian), and *Redondasuchus* (Apachean) (Lucas and Hunt, 1993). These concepts were later expanded to hypothetically be globally applicable (Lucas, 1998a; Lucas and Heckert, 2000), and refinements have been continually proposed as new discoveries are made (e.g., Hunt, 2001; Hunt et al., 2005; Heckert et al., 2007a, b; Lucas, 2010). Recently it has been argued that these faunachrons are better defined as biozones (Parker and Martz, 2011), although it has subsequently been argued that the term 'biozone' is not a superpositional

or biostratigraphic term and still lacks precise meaning for defining these intervals (Stocker, 2013b).

The global applicability of these biozones has been debated (e.g., Schultz, 2005; Langer, 2005; Rayfield et al., 2005, 2009; Lucas et al., 2007c, d; Lucas, 2010; Irmis et al., 2011; Desojo and Ezcurra, 2011; Stocker, 2013b; Butler, 2013; Butler et al., 2013) and it has been suggested that these biozones are best only used for regional correlations (Irmis et al., 2011; Parker and Martz, 2011). New radioisotopic dates from the Chinle Formation of Arizona demonstrate that the entire unit was deposited between 227 and ~205 Ma (Ramezani et al., 2011; Irmis et al., 2011; Atchley et al., 2013) ages that are now believed to range from the earliest Norian to the earliest Rhaetian based on recent revisions of the Triassic timescale (Ogg, 2012). These new data allow for the assignment of high precision radioisotopic ages to these biozones, enhancing their utility, although because the ages do not agree with the original stage correlations provided by Lucas (1998a) based on invertebrate and pollen biostratigraphy these new stage correlations (e.g., the 'long Norian') have been critized (Lucas et al., 2012).

The largest obstacle in the establishment of a global system of Late Triassic biozones is disagreements about the taxonomy of potentially biostratigraphically significant specimens (e.g., Lucas et al., 2007b; Desojo and Ezcurra, 2011; Irmis et al., 2011; Butler et al., 2013). Recent focus on apomorphy-based identifications of specimens has resulted in the recognition of greater taxonomic diversity and increased endemism in Late Triassic tetrapod faunas than previously assumed (e.g., Nesbitt et al., 2007; Irmis et al., 2007b; Nesbitt and Stocker, 2008; Stocker, 2010, 2012, 2013b; Butler et al., 2014).

Current apomorphy-based work has recognized at least one Late Triassic taxon, the phytosaurian *Paleorhinus,* that may have global biostratigraphic applicability; *Paleorhinus bransoni*, is known from the Popo Agie Formation of Wyoming, the lower part of the Dockum Group of Texas, and *Paleorhinus augustifrons* from the Blasensandstein of Germany, which is believed to be latest Carnian (Tuvalian) in age (Butler et al., 2014).

Two other proposed index taxa are more ambiguous. *Paratypothorax andressorum* occurs in the lower part of the Löwenstein Formation of Germany, which is Norian in age (Schoch and Wild, 1999) and paratypothoracin aetosaurs are found in established Adamanian and Revueltian strata (Norian) in the Chinle Formation and Dockum Group of the American Southwest, including what could be a new species of *Paratypothorax* (Long and Murry, 1995).

Aetosaurus ferratus co-occurs with *Paratypothorax* in the Löwenstein Formation and *Aetosaurus*-like specimens have been found in Norian strata in North America and Greenland (e.g., Jenkins et al., 1994; Small, 1998; Lucas et al., 1998; Heckert and Lucas, 1998). Recent re-examination of these materials, however, demonstrates that at least some of the western North American material belongs to a distinct taxon (*Stenomyti huangae*, Small and Martz, 2013) whereas the rest currently represents undiagnostic aetosaurines, including the eastern taxon *Stegomus arcuatus* (W. Parker, unpublished data). Detailed apomorphy-based revision of these specimens is needed to affirm their taxonomic affinities.

Rhynchosaurian archosauromorphs have been proposed as global biostratigraphic index taxa for the Late Triassic in particular *Hyperodapedon* (e.g., Lucas et al., 2003b; Langer, 2005). Whereas this taxon is widespread across Gondwana, it is rare in Laurasia making exact correlations difficult (Langer, 2005). Nonetheless I have used it here to suggest that the Lossiemouth Sandstone Formation of Scotland, which contains *Hyperodapedon gordoni* and *Stagonolepis robertsoni*, is roughly equivalent to the lower parts of the Santa Maria and Ischigualasto Formations of South America, which are date to about 230 Ma, and feature the Ischigualastian faunal assemblage that contains *Aetosauroides scagliai* (Lucas, 2010; Furin et al, 2006; Martinez et al., 2011).

CALIBRATING AETOSAURIAN PHYLOGENY

Figure 7.1 shows the phylogenetic relationships determined in Chapter 6 against the Triassic timescale, which includes the recent stage revisions as well as current biozonations from North and South America. The age of the Otischalkian-Adamanian boundary is presently unresolved, but the boundaries between the other Late Triassic biozones are generally established within the Chinle Formation of Arizona (Martz and Parker, 2010; Parker and Martz, 2011). Figures 7.2-7.5 depict the global distribution of aetosaurians in Pangea during these biozones.

Otischalkian (~232 - ~225 Ma)

The Otischalkian dates to at least 231.4 Ma based on the revised age of the Herr Toba bentonite from the lower part of the Ischigualasto Formation of Argentina, which contains the aetosaurian *Aetosauroides scagliai* (Rogers et al., 1993; Furin et al., 2006; Martinez et al., 2011). The Otischalkian, named for a vertebrate fossil assemblage I the Dockum Group near Otis Chalk Texas, is presently not recognized in the Chinle Formation, the base of which is now dated to 227.604±0.082 (Atchley et al., 2013; W. Parker unpublished data). The base of the Adamanian (i.e. lowest stratigraphic datum of *Smilosuchus*) is at 223.036± 0.059 (Ramezani et al., 2011). Thus the Otischalkian-Adamanian boundary is somewhere within this interval (Figure 7.1), which unfortunately is non-fossiliferous in the area where the isotopic ages were determined (i.e., Petrified Forest National Park (PEFO), Arizona). Moreover, there are no published ages from the Dockum Group to directly date the Otischalkian type assemblage.

The non-stagonolepidid *Aetosauroides scagliai* is Otischalkian as are both species of *Stagonolepis*, the problematic taxa *Coahomasuchus, Aetobarbakinoides*, and *Polesinesuchus*, as well as the desmatosuchines *Longosuchus*, *Lucasuchus*, and NCSM 21723. The sister taxon relationship of *Coahomasuchus* with *Aetosaurus*, and the close relationship of *Stenomyti* creates a long proposed ghost lineage for the latter two taxa, which are known from strata in Germany that are the same age as Revueltian strata in the western United States. Desmatosuchini has clear Otischalkian origins, but no typothoracines (*sensu* Parker, 2007) or paratypothoracines are presently known from Otischalkian strata (Figure 7.2).

Adamanian (~225 – 215 Ma)

The type faunal assemblage of the Adamanian biozone is from the upper part of the Blue Mesa Member in Petrified Forest National Park (Lucas and Hunt, 1993) and its base is marked by the lowest stratigraphic datum of the phytosaur *Smilosuchus* (=*Rutiodon*). The Adamanian is the acme for aetosaurian diversity in North America with no fewer than eight taxa currently recognized from the western United States. These include the initial appearance of the typothoracine aetosaurs with *Tecovasuchus chatterjeei* from the Tecovas Formation of Texas and *Tecovasuchus*-like form from the Blue Mesa Member of the Chinle Formation of Arizona (Figure 7.3; Parker, 2005a; Small and Martz, 2006). Lateral osteoderms from Morocco are referred to *Longosuchus* (Lucas, 1998a, b), but are more consistent with typothoracine lateral osteoderms (Parker and Martz, 2010). A typothoracine is also known from the upper Maleri Formation of India, which is possibly Adamanian based on the presence of a *Smilosuchus*-like phytosaurian (Lucas, 2010). The narrow-bodied form *Neoaetosauroides engaeus* is from the Los Colorados Formation of Argentina. This unit was assigned an Apachean age because of the presence of sauropodomorph dinosaurs and crocodyliformes (Lucas, 1998a, 2010). However, recent magnetostratigraphic work instead places it at the same time interval as the late Adamanian through early Revueltian. Presently no aetosaurian material is known from this time period in Europe or Brazil. *Chilenosuchus fortae* is a probable typothoracine (Desojo, 2003) from the Estratos El Bordo of northern Chile, which are of Late Triassic age, possibly equivalent in age to the Adamanian or Revueltian of western North America where typothoracines are common.

Revueltian (215 - ~208 Ma)

Parker and Martz (2011) identified the precise stratigraphic level of the Adamanian – Revueltian boundary in the Chinle Formation at PEFO, represented by the lowest stratigraphic datum of the phytosaur *Machaeroprosopus* (=*Pseudopalatus*). This level occurs near the base of the Jim Camp Wash beds of the Sonsela Member a few meters above the persistent red silcrete (Martz and Parker, 2010). The age of this level is presently constrained by two dates, 218.017± 0.088 Ma for the underlying Jasper Forest bed, and 213.124±0.069 Ma for the overlying Martha's Butte beds (Ramezani et al., 2011) with the actual boundary closer to 215 Ma (Figure 7.1; Dunlavey et al., 2009).

The Revueltian sees a sharp reduction in the number of North American aetosaurian taxa, including the complete disappearance of the desmatosuchines (Figure 7.4). Only a single osteoderm of *Desmatosuchus smalli* from the Chinle Formation of Arizona is possibly from Revueltian strata (Parker, 2005c; Parker and Martz, 2011). Paratypothoracins become much more taxonomically diverse with *Paratypothorax andressorum* in Germany, and *Rioarribasuchus chamaensis* and *Paratypothorax* sp. from the western United States (Long and Ballew, 1985; Long and Murry, 1995; Zeigler et al., 2003). Once considered rare in the Chinle Formation (Long and Ballew, 1985) paratypothoracins are now some of the most commonly recovered fossils from the Sonsela Member (Parker and Martz, 2011). SMNS 19003 is an exquisitely preserved paratypothoracin from the Revueltian of Germany (Desojo et al., 2013).

The Revueltian also represents the acme for *Aetosaurus*-like taxa, with *Aetosaurus ferratus* in Germany and *Stenomyti huangae* in Colorado and *Stegomus arcuatus* in eastern North America (Baird, 1986; Schoch, 2007; Small and Martz, 2013). However, the most commonly aetosaur recovered in North America from Revueltian age strata is *Typothorax coccinarum*. In the Petrified Forest Member of the Chinle Formation and the Bull Canyon Formation of New Mexico is *Typothorax*, of which fossils are extremely numerous (Long and Murry, 1995; Hunt, 2001; Martz, 2002; Heckert et al., 2010; Parker and Martz, 2011).

Apachean (~208 – 201 Ma)

The Revueltian-Apachean boundary is not as well-constrained in PEFO because of the lack of the index fossil *Redondasaurus*; however, the lowest stratigraphic datum of *Redondasaurus* occurs in the Owl Rock Member at Ward Terrace, Arizona (Kirby, 1991). Here *Redondasaurus* (e.g., MNA V3495) overlaps with *Machaeroprosopus* (e.g., MNA V1595) about 30 meters below the contact with the Rock Point Member in the 'limy' portion of the Owl Rock that is characterized by thick layers of carbonate (Kirby, 1991). At PEFO the base of these beds begin in the middle of the Owl Rock Member at Chinde Mesa (Atchley et al., 2013). An estimated age of 207.8 Ma was obtained just below these beds (Ramezani et al., 2011). This provides a maximum age for the Revueltian-Apachean boundary (Figure 7.1) and is now considered to be early Rhaetian (Hüsing et al., 2010).

The Apachean biozone sees the most marked decline in aetosaurian diversity, with taxa being extremely rare except in North America (Figure 7.5). In North America the majority of known taxa are from the Redonda Formation of New Mexico and the Owl Rock Member of the Chinle Formation of Arizona. Aetosaurians are commonly recovered in these strata, but all recognized taxa from the Redonda Formation, *Apachesaurus heckerti*, *Redondasuchus reseri*, and *Redondasuchus rineharti* (Spielmann and Lucas, 2012) are all typothoracines similar to *Typothorax coccinarum*. At Ward Terrace in Arizona *Typothorax coccinarum* (e.g., MNA V5583, MNA V6802) has been reported from the Owl Rock Member at MNA localities 360 and the Tohachi Wash localities (Kirby, 1991; Spielmann et al., 2007). These localities occur at the same level, and up to thirty meters above the lowest occurrence of the phytosaur *Redondasaurus* (MNA V3495), extending these records of *Typothorax* into the Apachean (Figure 7.1).

An undescribed aetosaur (GR 249) with some similarities to *Aetosaurus ferratus* is known from the siltstone member of the Chinle Formation near Ghost Ranch, New Mexico (J. Martz, W. Parker, and B. Small, unpublished data). The stratigraphic relationship between the siltstone member and other upper Chinle Formation strata is controversial, with some workers assigning it to the Rock Point Member (e.g., Lucas and Hunt, 1992; Heckert et al., 2008) and others considering it to be a possible Owl Rock equivalent (e.g., Dubiel, 1989a, b). The presence of *Redondasuchus* in the siltstone member and not in the Owl Rock was some of the strongest evidence for assigning these strata to the Rock Point Member (Lucas and Hunt, 1992), but the recognition of *Redondasuchus* in the Owl Rock Member now makes this ambiguous. Moreover, the

siltstone member records a different paleomagnetic polarity signal than the type Rock Point Member suggesting that the two are not equivalents (Zeigler and Geissman, 2011).

Three osteoderms with a radial surface ornamentation pattern and strongly raised anterior bar are from the Trossingen Formation of Germany (Matzke and Maisch, 2011), but these two cervical or dorsal paramedians and one mid-caudal paramedian are poorly preserved and offer no more information except that an aetosaurian was present in the Trossingen Quarry of Germany.

The general lack of aetosaurians outside of North America may be attributed to a provincialization of faunas in the latest Triassic or a sampling bias (Lucas, 2010). Aetosaurians are not known from earliest Jurassic strata.

DISCUSSION

The earliest known aetosaurians are from the late Carnian of South America and Europe, and possibly North America, demonstrating that the Aetosaurinae and Stagonolepidoidea had already diverged by that time. Unfortunately early Carnian continental rocks are presently unrecognized, so the earliest records of aetosaurians are unrecognized.

Aetosaurians sharply diversify through the Norian and then appear to decline significantly in diversity during the Rhaetian, becoming extinct at some point before the beginning of the Jurassic. However, as with origins of the group in the Carnian, the lack of Apachean aetosaurians could also be the result of a sampling bias because of the reduced amount of accessible fossiliferous outcrop from that time period compared to the other Late Triassic biozones (Lucas, 2010).

Typothorax does not appear until the Adamanian and desmatosuchines disappear shortly afterwards, but it is unclear if these events are linked (Figures 7.3, 7.4). The disappearance of the Desmatosuchinae in the latest Adamanian/early Revueltian and the radiation of *Typothorax* in the North American Southwest may be related to an increase in arid conditions in the middle Norian of western Pangaea (e.g., Colbert, 1958; Tanner, 2003; Martz and Parker, 2010; Dubiel and Hasiotis, 2011; Atchley et al., 2013). By the Apachean typothoracines, including *Typothorax* and *Redondasuchus* are the most common aetosaurian group found in North America (Figure 2.5).

Aetosaurians appear to have a regional biostratigraphic utility during the Carnian and Norian. *Lucasuchus* and *Coahomasuchus* occur in the Colorado City Member of the Dockum Group in Texas and also in the Pekin Formation of North Carolina providing a strong biostratigraphic link between those strata (Heckert et al., in press). *Aetosauroides scagliai* occurs in both the Ischigualasto Formation of Argentina and the Sequence 2 of the Santa Maria Supersequence in Brazil and appears to be a robust index taxon for South American basins. *Stagonolepis* occurs in the Lossiemouth Formation of Scotland and at Krasiejów in Poland, providing a potential tie between those strata. The Polish strata are considered to be the equivalent of the Lehrberg beds (now the Steigerwald Formation) of the Germanic Basin in Bavaria, which are late Carnian in age (Deutsche Stratigraphische Kommission, 2005). The Polish and Scottish materials are currently assigned to different species and that taxonomy is upheld here. Gondwanan aetosaurian material is rare and generally non-diagnostic during the Adamanian with the exception of *Neoaetosauroides engaeus* from Argentina (Figure 7.3). The Maleri Formation of India produces isolated

osteoderms that may be desmatosuchine and paratypothoracin, but these are rarely figured and have never been formally described (Desojo et al., 2013). The aetosaurians of western North American can presently be correlated no farther than within the Chinle and Dockum basins (Parker and Martz, 2011).

Vertebrate biostratigraphy, including aetosaurians, can also be used to correlate the new Chinle radioisotopic dates to Dockum Group strata to constrain the ages of significant fossils such as the turtle *Chinlechelys* (Joyce et al., 2009) and the mammaliamorph *Adelobasileus* (Lucas and Luo, 1993). The former is from the Bull Canyon Formation (Dockum Group) of New Mexico where it was found with *Revueltosaurus callenderi* (NMMNH P-16932) and *Typothorax coccinarum* (Hunt, 2001; Joyce et al., 2009). In the Chinle Formation *Revueltosaurus callenderi* is constrained to the middle portion of the Petrified Forest Member, below the Black Forest bed (Parker and Martz, 2011). These strata are constrained by two dates: 209.926±0.072 Ma for the Black Forest bed and 213.124±0.069 Ma for the Marthas Butte beds of the Sonsela Member (Ramezani et al., 2011). Thus *Chinlechelys* holotype is probably from between 210-213 Ma and early Revueltian in age (Parker and Martz, 2011).

Adelobasileus is from the lower part of the Tecovas Formation (Dockum Group) of Texas and co-occurs with *Trilophosaurus buettneri* (NMMNH P-34373) and *Trilophosaurus jacobsi* (NMMNH P-34073; Heckert, 2004). The holotype of *Trilophosaurus jacobsi* (MNA V3192) occurs at the *Placerias* Quarry of Arizona where it co-occurs with the aetosaurians *Desmatosuchus spurensis* and *Calytosuchus wellesi* in the upper part of the Blue Mesa Member (Murry, 1987; Long and Murry, 1995; Parker

and Martz, 2011). The holotypes of *Desmatosuchus spurensis* and *Calyptosuchus wellesi* are both from the Tecovas Formation of Texas (Long and Murry, 1995). At PEFO the upper part of the Blue Mesa Member has been dated to 223.036±0.059 Ma (Ramezani et al., 2011) and is no younger than 220.124±0.068 Ma, which is a date for the top of the Blue Mesa Member (Atchley et al., 2013). These dates are Adamanian in age (Parker and Martz, 2011).

In the Revueltian, the two species of *Paratypothorax* may provide a correlation between the lower part of the Löwenstein Formation and the middle and upper portion of the Sonsela Member of the Chinle Formation. *Aetosaurus* has been proposed as an index taxon of the Revueltian (e.g., Lucas, 2010); however, the genus is presently restricted to the Löwenstein Formation of Germany and the Calcare de Zorzino Formation of Italy (Wild, 1999; Schoch, 2007). A potential species of *Aetosaurus, Aetosaurus arcuatus*, is represented mostly by natural molds in sandstone from the Newark Supergroup of the eastern United States. This taxon is presently not diagnostic above the level of aetosaurinae and the material is undergoing revision (W. Parker, unpublished data).

Currently no long-range correlations are available for Apachean strata using aetosaurians because the only good material of this age is typothoracines from Arizona and New Mexico. The Redonda Formation has been considered an equivalent to the Rock Point Member of the Chinle Formation and younger than the Owl Rock Member (e.g., Lucas, 2010). However, skulls of the phytosaur *Redondasaurus* have been recovered from the Owl Rock near Ward Terrace, Arizona and from the upper part of the Cooper Canyon Formation of Texas (Chavez, 2010; Parker et al., 2011; Spielmann and Lucas,

2012), making those correlations problematic as the upper portion of the Owl Rock is actually Apachean. This includes the majority of the MNA and MCZ localities along Ward Terrace (Kirby, 1989, 1991). The fauna from these sites includes the hybodont shark *Reticulodus synergus* (MNA V6059), the metoposaurid *Apachesuchus* (MNA V5575), the phytosaurs *Redondasuchus gregorii* (MNA V3495) and *Machaeroprosopus buceros* (MNA V1595), the aetosaur *Typothorax coccinarum* (e.g., MNA V6802), and a paracrocodylomorph (e.g., MNA V249a), which with the exception of *Redondasaurus* is very similar to the composition of Revueltian faunas from the American southwest. Thus differentiating Apachean and Revueltian faunas at fossil localities with poor stratigraphic control can be problematic for these areas limiting the effectiveness of these biozones.

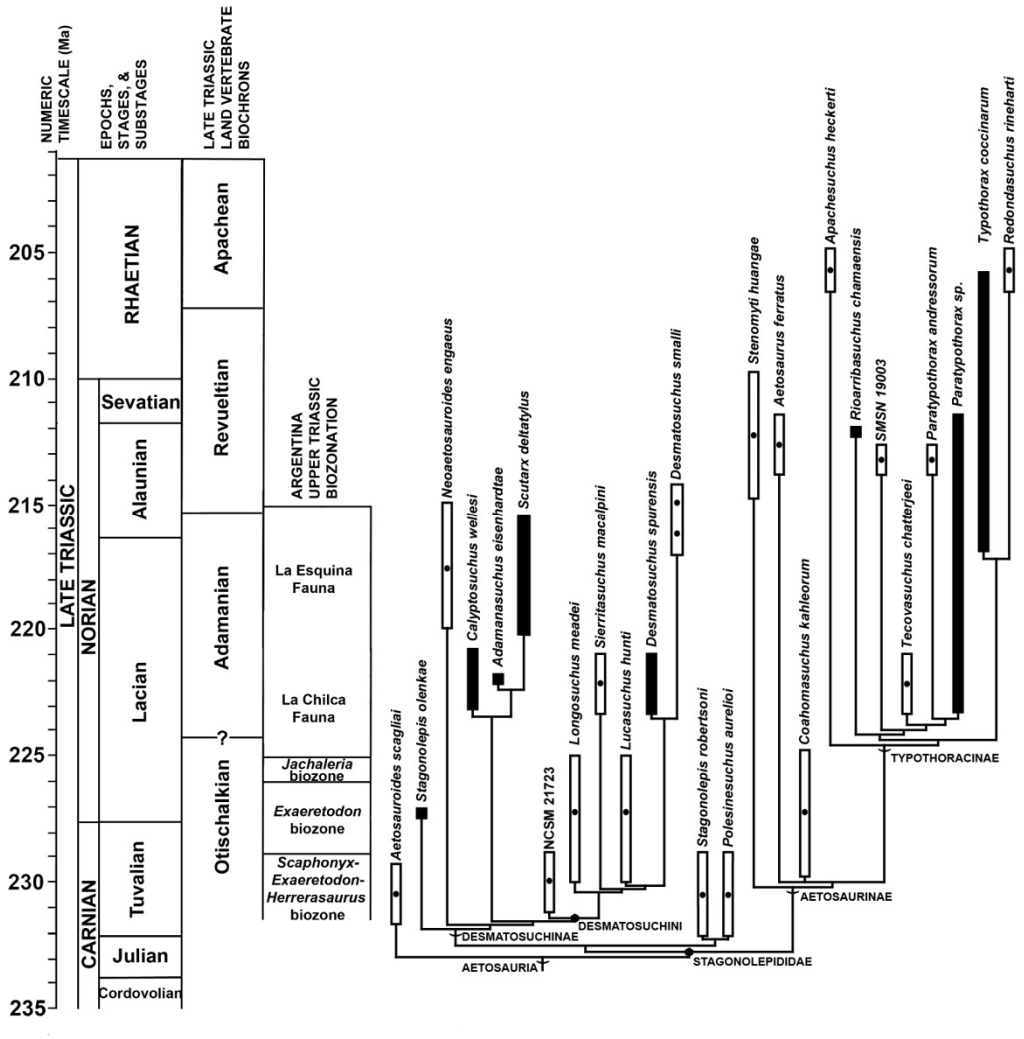

Figure 7.1. The current phylogeny of the Aetosauria set to the Triassic timescale. White bars represent estimated ranges for taxa known from only single or a few specimens (dots). Black bars represent ranges known from numerous specimens Question marks indicate uncertainty in placement. Dates and biozonation data are from Deutsche Stratigraphische Kommission, 2005; Hüsing et al., 2010; Ramezani et al., 2011; Irmis et al., 2011; Parker and Martz, 2011; Martinez et al., 2011, and Desojo et al., 2013. Modified from Desojo et al., 2013.

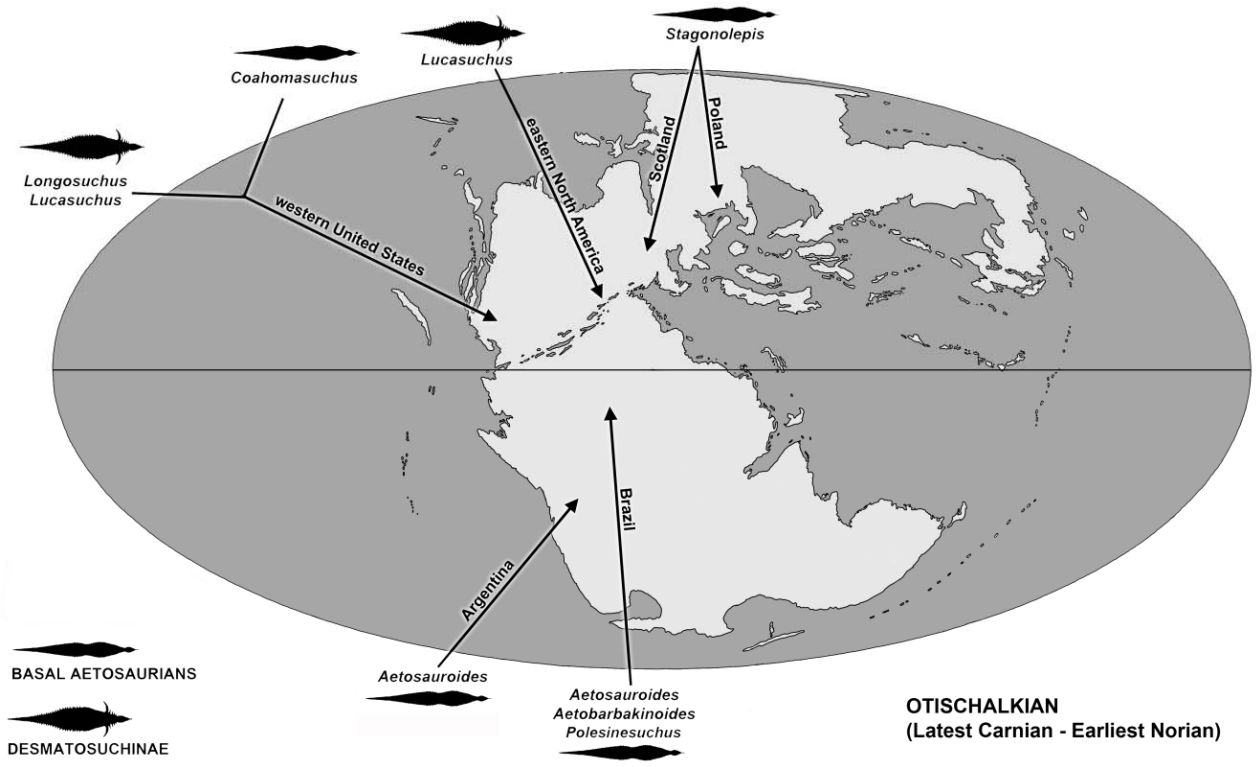

Figure 7.2. Paleogeographic map of Pangaea during the Late Triassic showing the global distribution of Otischalkian aetosaurian assemblages. Modified from Desojo et al., 2013.

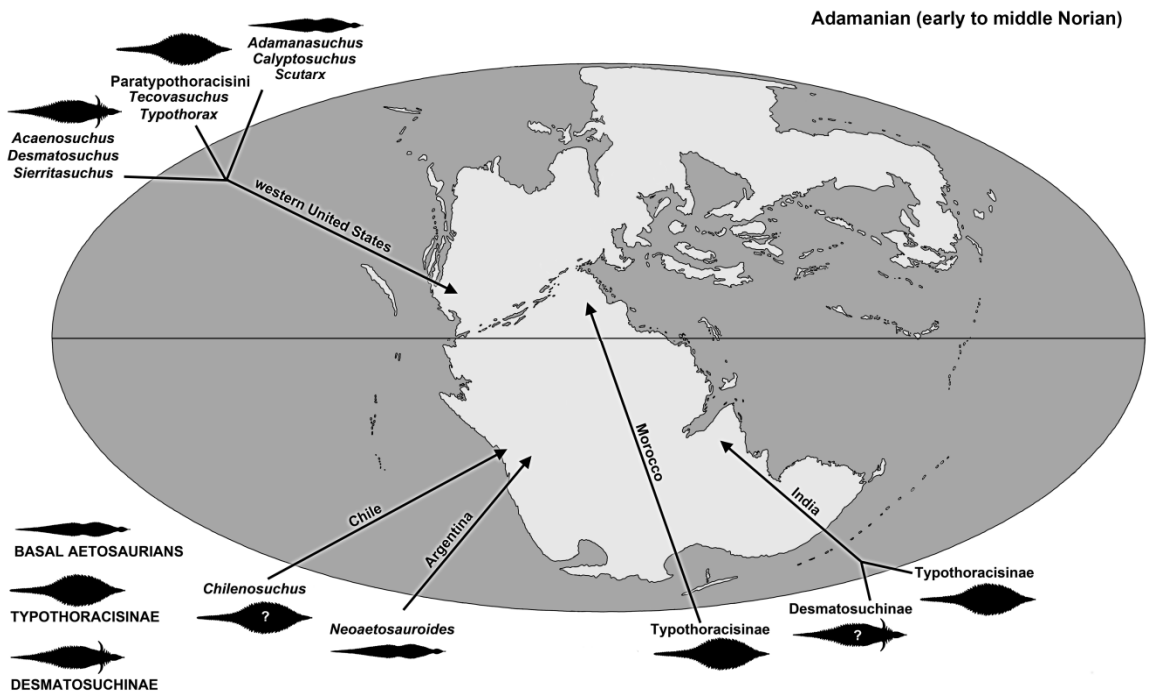

Figure 7.3. Paleogeographic map of Pangaea during the Late Triassic showing the global distribution of Adamanian aetosaurian assemblages. Modified from Desojo et al., 2013.

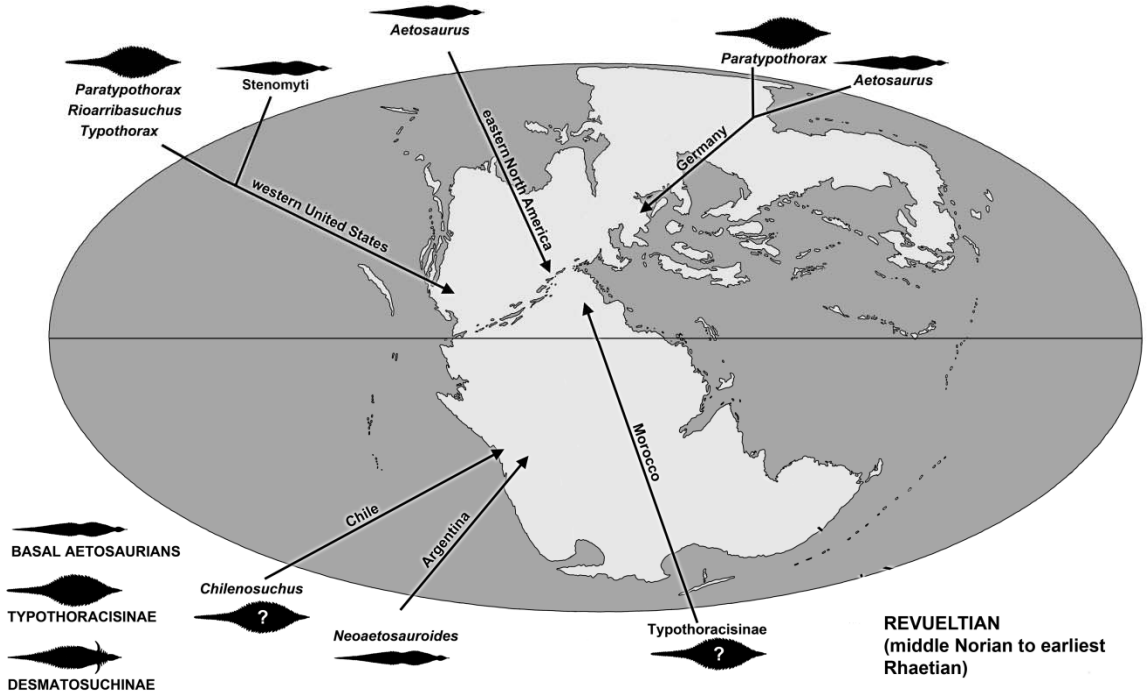

Figure 7.4. Paleogeographic map of Pangaea during the Late Triassic showing the global distribution of Revueltian aetosaurian assemblages. Modified from Desojo et al., 2013.

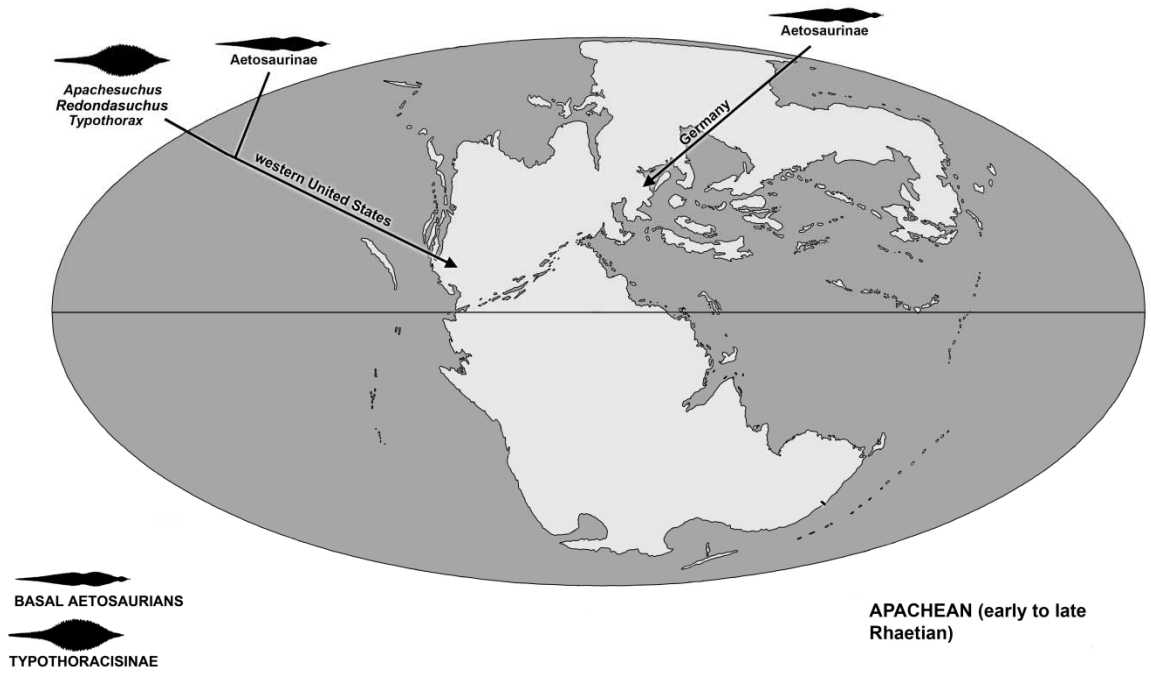

Figure 7.5. Paleogeographic map of Pangaea during the Late Triassic showing the global distribution of Apachean aetosaurian assemblages. Modified from Desojo et al., 2013.

APPENDIX

PHYLOGENETIC MATRIX:

```
      MATRIX
      'Postosuchus kirkpatricki'
0000000000000000000000000000000000000000000000000000-------------
------00---------0
      'Revueltosaurus callenderi'
00000010011001011010000110000000012001000110010110110000000000000
-0000011---------2
      'Adamanasuchus eisenhardtae'
???????????????????????????????????????????????????11101?????0110
10101?120?1-00000?
      'Aetosaurus ferratus'
0110111001000211110102?101111100122?01000??000001?111100000000010
10000112001-000002
      'Apachesuchus heckerti'
???????????????????????????????????????????????????1310?0?00?0020
100?0???????????2?
      'Stagonolepis robertsoni'
111011101110110??0?100?00101211012200100001000001101110000000000
10000112001-000002
      'Stagonolepis olenkae'
11101120101??20??111000001111110122???00001??0011??11100??0000000
10000112001-00000?
      'Calyptosuchus wellesi'
??????????????????????????0????????0000000100???0?0111010?0000010
10100112001-000002
      'Scutarx deltatylus'
?????1????1???????101001???2???????0000000100???010111010?0000010
10102112001-000002
      'Aetosauroides scagliai'
?0100110010??2????1100?1010100???10001100010010000011100000000000
10000112001-000002
      'Coahomasuchus kahleorum'
?????10???00??111?1??01000?0?0?120001000010?11????111000000000010
10000112001-000002
      'Desmatosuchus spurensis'
?1???121101110??0?1100101??????10??1020010000???1003000011111000
012101123100211210
      'Desmatosuchus smalli'
11221121101110010011??1012111101022002001000000111003000011111000
012101123100211210
```

```
      'Rioarribasuchus chamaensis'
????????????????????????????????????????????1??????10000?0000120
20004121021120l2?
      'Longosuchus meadei'
?1???121?0010????1?10111101111101221000000100101100101001111110000
1121011220012112l0
      'Lucasuchus hunti'
????????????????????????????????????????????????11000111121000
002103122000211?1?
      'NCSM 21723'
????????????????????????????????????????????????20100010?210?0
11?10?122000?11?1?
      'Neoaetosauroides engaeus'
1110?12?0?1112???1?10100001121?1?22011000????01010?1100?000000000
20100112001-000002
      'Typothorax coccinarum'
011?012000?0???2?10100?10?0101010221100110100011001121020100001l0
10000112101-020122
      'Redondasuchus rineharti'
????????????????????????????????120???????????121020?0000120
100?01121?1-02012?
      'Paratypothorax andressorum'
????????????????????????????????????1011???????210120?0000121
20000212102112012?
      'Paratypothorax sp.'
????????????????????????????????????110111?0????210020?0000121
20000212102112012?
      'Tecovasuchus chatterjeei'
????????????????????????10???????????0?0????0???????110120???00121
20000112102112012?
      'Sierritasuchus macalpini'
????????????????????????????????????000001?0???????10100111111000
0121011220012112?1?
      'SMSN 19003'
011011100100021212111????1??01?0?11????????????????2101?000000120
200?01121021120l2?
      'Aetobarbakinoides brasiliensis'
????????????????????????????????????10?000000??01???11?0?0??000?00
1????1???????????
      'Stenomyti huangae'
011111100000020100011l???10121?1122????????????????1110?0000?0000
20100112001-000001
      'Polesinesuchus aurelioi'
????????????????????????0???????????00100??100000111111000?0010000
10?0011??????????2
      ;
ENDBLOCK;
```

REFERENCES

Adams, E. N. 1972. Consensus techniques and the comparison of taxonomic trees. Systematic Zoology 21:390-397.

Agassiz, L. 1844. Monographie des poisons fossiles du vieux grés rouge ou Système Dévonian (Old Red Sandstone) des Isles Britanniques ed de Russie. Jent et Gassman, Neuchâtel, 171 pp.

Atchley, S. C., Nordt, L. C., Dworkin, S. I., Ramezani, J., Parker, W. G., Ash, S. R., and S. A. Bowring. 2013. A linkage among Pangean tectonism, cyclic alluviation, climate change, and biologic turnover in the Late Triassic: the record from the Chinle Formation, southwestern United States. Journal of Sedimentary Research 83:1147-1161.

Baker, R. H., and R. DeSalle. 1997. Multiple sources of character information and the phylogeny of Hawaiian dropsophilids. Systematic Biology 46:654-673.

Baird, D. 1986. Some Upper Triassic reptiles, footprints, and an amphibian from New Jersey. The Mosasaur 3:125-153.

Barbarena, M. C., Araújo, D. C., and E. L. Lavina. 1985. Late Permian and Triassic tetrapods of southern Brazil. National Geographic Research 1:5-20.

Barrett, M, Donoghue, M. J., and E. Sober. 1991. Against consensus. Systematic Zoology 40:486-493.

Bell, C. J., Head, J. J., and J. I. Mead. 2004. Synopsis of the herpetofauna from Porcupine Cave; pp. 117-126 *in* Barnosky, A. D. (ed.), Biodiversity Response to Climate Change in the

Middle Pleistocene: the Porcupine Cave Fauna from Colorado. University of California Press, Berkeley.

Bell, C. J., Gauthier, J. A., and G. S. Bever. 2010. Covert biases, circularity, and apomorphies: a critical look at the North American Quaternary herpetofaunal stability hypothesis. Quaternary International 217:30-36.

Bever, G. S. 2005. Variation in the ilium of North American *Bufo* (Lissamphibia: Anura) and its implications for species-level identification of fragmentary anuran fossils. Journal of Vertebrate Paleontology 25:548-560.

Bonaparte, J. F. 1969. Dos nuevas "faunas" de reptiles Triásicos de Argentina; pp. 283-306 *in* Amos, A. J. (ed.), Gondwana Stratigraphy, IUGS Symposium, Buenos Aires, 1-15 October 1967. United Nations Educational Scientific and Cultural Organization, Paris.

Bonaparte, J. F. 1972 [imprint 1971]. Los tetrápodos del sector superior de la Formación Los Colorados, La Rioja, Argentina (Triásico Superior). I Parte. Opera Lilloana 22:1-183.

Bonaparte, J. F. 1982. Classification of the Thecodontia; pp. 99-122 *in* Buffetaut, E., Janvier, P., Rage, J. –C., and P. Tassy (eds.), Phylogénie et Paléobiogéographie: Livre Jubilaire en L'honneur de R. Hoffstetter. Géobios Mémoire Spécial 6. Université Claude Bernard, Département de Géologie, Centre National de la Recherche Scientifique, Lyon.

Brady, L. F. 1958. New occurrence of *Desmatosuchus* in Northern Arizona. Plateau 30:61-63.

Brochu, C. A. 1992. Ontogeny of the postcranium in crocodylomorph archosaurs. Unpublished M.S. thesis, The University of Texas, Austin, TX, 340 pp.

Brochu, C. A., 1996. Closure of neurocentral sutures during crocodilian ontogeny: implications for maturity assessment in fossil archosaurs. Journal of Vertebrate Paleontology 16:49-62.

Brower, A. V. Z. 2006. The how and why of branch support and partioned branch support, with a new index to assess partition incongruence. Cladistics 22:378-386.

Brusatte, S. L., Benton, M. J., Desojo, J. B., and M. C. Langer. 2010. The higher-level phylogeny of Archosauria (Tetrapoda: Diapsida). Journal of Systematic Palaeontology 8:3-47.

Butler R. J. 2013. '*Francosuchus*' *trauthi* is not *Paleorhinus*: implications for Late Triassic vertebrate biostratigraphy. Journal of Vertebrate Paleontology 33:856–864.

Butler, R. J., Barrett, P. M., and D. J. Gower. 2012. Reassessment of the evidence for postcranial skeletal pneumaticity in archosaurs, and the early evolution of the avian respiratory system. PLoS ONE 7(3):e34094.

Butler, R. J., Rauhut, O. W. M., Stocker, M. R., and R. Bronowicz. 2014. Redescription of the phytosaurs *Paleorhinus* ('*Francosuchus*') *angustifrons* and *Ebrachosuchus neukami* from Germany, with implications for Late Triassic biochronology. Zoological Journal of the Linnaean Society 170:155-208.

Cadena, E. A., Bloch, J. I., and C. A. Jaramillo. 2010. New podocnemidid turtle (Testudines: Pleurodira) from the Middle-Upper Paleocene of South America. Journal of Vertebrate Paleontology 30:367-382.

Camp, C. L. 1930. A study of the phytosaurs with description of new material from Western North America. Memoirs of the University of California 10:1-174.

Camp, C. L., and S. P. Welles. 1956. Triassic dicynodont reptiles: part I, the North American genus *Placerias*. Memoirs of the University of California 13:255-304.

Casamiquela, R. M. 1960. Noticia preliminar sobre dos nuevos estagonolepoideos Argentinos. Ameghiniana 2:3-9.

Casamiquela, R. M. 1961. Dos nuevos estagonolepoideos Argentinos (de Ischigualasto, San Juan). Revista de la Asociación Geológica de Argentina 16:143-203.

Casamiquela, R. M. 1967. Materiales adicionales y reinterpretación de *Aetosauroides scagliai* (de Ischigualasto, San Juan). Revista del Museo de La Plata (nueva serie), Tomo 5, Sección Paleontología 33:173-196.

Casamiquela, R. M. 1980. Nota sobre restos de un reptile aetosauroideo (Thecodontia, Aetosauria) de Quimal, Cordillera de Domeyko, Antofagasta. Prueba de la existencia del Neotriásico continental en los Andes del Norte de Chile; pp. 135-142 *in* Anonymous (ed.), Actas del Segundo Congreso Argentino de Paleontología y Bioestratigrafía y Primer Congreso Latinoamericano de Paleontología, Buenos Aires, Argentina, 2-6 de Abril, 1978, Volume 1. Asociación Paleontológica Argentina, Buenos Aires.

Case, E. C. 1920. Preliminary description of a new suborder of phytosaurian reptiles with a description of a new species of *Phytosaurus*. Journal of Geology 28:524–535.

Case, E. C. 1922. New reptiles and stegocephalians from the Upper Triassic of western Texas. Carnegie Institution of Washington Publication 321:1-84.

Case, E. C. 1929. Description of the skull of a new form of phytosaur with notes on the characters of described North American phytosaurs. Memoirs of the University of Michigan Museums, Museum of Paleontology 2:1-56.

Case, E. C. 1932. A perfectly preserved segment of the armor of a phytosaur, with associated vertebrae. Contributions from the Museum of Paleontology, University of Michigan 4:57-80.

Cerda, I. A., and J. B. Desojo. 2011. Dermal armour histology of aetosaurs (Archosauria: Pseudosuchia), from the Upper Triassic of Argentina and Brazil. Lethaia 44:417-428.

Chatterjee, S. 1985. *Postosuchus,* a new thecodontian reptile from the Triassic of Texas and the origin of tyrannosaurs. Philosophical Transactions of the Royal Society of London, Series B 309:395-460.

Chavez, C., 2010. A new phytosaur (Archosauria: Pseudosuchia) from the Late Triassic Dockum Group of Texas. Unpublished M.S. thesis, Texas Tech University, Lubbock, TX, 77 pp.

Clarke, J. A. 2004. Morphology, phylogenetic taxonomy, and systematic of *Ichthyornis* and *Apatornis* (Avialae: Ornithurae). Bulletin of the American Museum of Natural History 286:1-179.

Clarke, J. A., and K. M. Middleton. 1998. Mosaicism, modules, and the evolution of birds: results from a Bayesian approach to the study of morphological evolution using discrete character data. Systematic Biology 57:185-201.

Coddington, J., and N. Scharff. 1994. Problems with zero-length branches. Cladistics 10:415-423.

Colbert, E. H. 1958. Triassic tetrapod extinction at the end of the Triassic Period. Proceedings of the National Academy of Sciences of the U.S.A. 44:973-977.

Colbert, E. H. 1971. Tetrapods and continents. The Quarterly Review of Biology 46:250-269.

Colbert, E. H., and J. T. Gregory. 1957. Correlation of continental Triassic sediments by vertebrate fossils; pp. 1458-1467 *in* Reeside, J. B. Jr., Applin, P. L., Colbert, E. H., Gregory, J. T., Hadley, H. D., Kummel, B., Lewis, P. J., Love J. D., Maldonado-Koerdell, M., McKee, E. D., McLaughlin, D. B., Muller, S. W., Reinemund, J. A., Rodgers, J., Sanders, J., Silberling, N. J., and K. Waagé (eds.), Correlation of the Triassic formations of North America exclusive of Canada. Bulletin of the Geological Society of America 68:1451-1514.

Cope, E. D. 1869. Synopsis of the extinct Batrachia, Reptilia, and Aves of North America. Transactions of the American Philosophical Society 14:1-252.

Cope, E. D. 1875. Report on the geology of that part of northwestern New Mexico examined during the field season of 1874; pp. 981-1017 (61-97 of separate report LL) *in* Wheeler, G. M. (ed.) Annual report upon the geographical explorations west of the one hundredth meridian in California, Nevada, Nebraska, Utah, Arizona, Colorado, New Mexico, Wyoming and Montana. United States Government Printing Office, Washington, DC.

Cope, E. D. 1877. The extinct vertebrata obtained in New Mexico by parties of the expedition of 1874; pp.1-36B *in* Wheeler, G. M. (ed.), Report upon United States geographical surveys west of the one hundredth meridian, volume 4, paleontology. United States Government Printing Office, Washington, D. C.

Cope, E. D. 1887. A contribution to the history of the Vertebrata of the Trias of North America. Proceedings of the American Philosophical Society 24:209-228.

Cope, E. D. 1892. A contribution to the vertebrate paleontology of Texas. Proceedings of the American Philosophical Society 30:123-131.

Cunningham, C. W. 1997. Can three incongruence tests predict when data should be combined? Molecular Biology and Evolution 14:733-740.

Dalton, R. 2008. Fossil reptiles mired in controversy. Nature 451:510.

Dayrat, B., Cantino, P. D., Clarke, J. A., and K. de Queiroz. 2008. Species names in the PhyloCode: the approach adopted by the International Society for Phylogenetic Nomenclature. Systematic Biology 57:507-514.

de Queiroz, K. 2007. Species concepts and species delimitation. Systematic Biology 56:879-886.

de Queiroz, K., and J. A. Gauthier. 1992. Phylogenetic taxonomy. Annual Review of Ecology and Systematics 23:449-480.

de Ricqlés, A. J., Padian, K., and J. R. Horner. 2003. On the bone histology of some Triassic pseudosuchian archosaurs and related taxa. Annales de Paléontologie 89:67-101.

DeSalle, R., and A. V. Z. Brower. 1997. Process partitions, congruence, and the independence of characters: inferring relationships among closely related Hawaiian *Drosophilla* from multiple gene regions. Systematic Biology 46:751-764.

Desojo, J. B. 2003. Redescripción del aetosaurio *Chilenosuchus forttae* Casamiquela (Diapsida: Arcosauria): presencia de Triásico continental en el norte de Chile. Revista Geológica de Chile 30:53-63.

Desojo, J. B. 2005. Los aetosaurios (Amniota, Diapsida) de América Del Sur: sus relaciones y aportes a la biogeografía y bioestratigrafía del Triásico continental. Unpublished Ph.D dissertation, Universidad de Buenos Aires, Buenos Aires, 176 pp.

Desojo, J. B., and A. M. Báez. 2005. El esqueleto postcraneano de *Neoaetosauroides* (Archosauria: Aetosauria) del Triásico Superior del centro-oeste de Argentina. Ameghiniana 42:115-126.

Desojo, J. B., and A. M. Báez. 2007. Cranial morphology of the Late Triassic South American archosaur *Neoaetosauroides engaeus*: evidence for aetosaurian diversity. Palaeontology 50:267-276.

Desojo, J. B., and M. D. Ezcurra. 2011. A reappraisal of the taxonomic status of *Aetosauroides* (Archosauria, Aetosauria) specimens from the Late Triassic of South America and their proposed synonymy with *Stagonolepis*. Journal of Vertebrate Paleontology 31:596-609.

Desojo, J. B., and A. B. Heckert. 2004. New information on the braincase and mandible of *Coahomasuchus* (Archosauria: Aetosauria) from the Otischalkian (Carnian) of Texas. Neues Jahrbuch für Geologie und Paläontologie, Monatshefte 2004:605-616.

Desojo, J. B., and S. F. Vizcaíno. 2009. Jaw biomechanics in the South American aetosaur *Neoaetosauroides engaeus*. Paläontologische Zeitschrift 83:499–510.

Desojo, J. B., Ezcurra, M. D., and E. E. Kischlat. 2012. A new aetosaur genus (Archosauria: Pseudosuchia) from the early Late Triassic of southern Brazil. Zootaxa 3166:1-33.

Desojo, J. B., Heckert, A. B., Martz, J. W., Parker, W. G., Schoch, R. R., Small, B. J., and T. Sulej. 2013. Aetosauria: a clade of armoured pseudosuchians from the Upper Triassic continental beds; pp. 203-239 *in* Nesbitt, S.J., Desojo, J. B., and R. B. Irmis (eds.), Anatomy, Phylogeny, and Palaeobiology of Early Archosaurs and their Kin. Geological Society, London, Special Publications 379. The Geological Society Publishing House, Bath.

Deutsche Stratigraphische Kommission. 2005. Stratigraphie von Deutschland IV: Keuper. Courier Forschungs-Institut Senckenberg 253:1-296.

Donoghue, M. J., Doyle, Gauthier, J. A., Kluge, A. G., and T. Rowe. 1989. The importance of fossils in phylogeny reconstruction. Annual Review of Ecology and Systematics 20:431-460.

Dubiel, R. F. 1989a. Depositional and paleoclimatic setting of the Upper Triassic Chinle Formation, Colorado Plateau; pp. 171-187 *in* Lucas, S. G. and A. P. Hunt (eds.), Dawn of the Age of Dinosaurs in the American Southwest. New Mexico Museum of Natural History, Albuquerque.

Dubiel, R. F. 1989b. Paleoclimate cycles and tectonic controls on fluvial, lacustrine, and eolian strata of the Upper Triassic Chinle Formation, San Juan Basin. American Association of Petroleum Geologists Bulletin 73:1153-1154.

Dubiel, R. F., and S. T. Hasiotis. 2011. Deposystems, paleosols, and climatic variability in a continental-scale system: the Upper Triassic Chinle Formation, Colorado Plateau, USA; pp. 393-421 *in* Davidson, S., and C. North (eds.), From River to Rock Record: The Preservation of Fluvial Sediments and Their Subsequent Interpretation. SEPM Special Publication 97. Society for Sedimentary Geology, Tulsa.

Dunlavey, M. G., Whiteside, J. H., and R. B. Irmis. 2009. Ecosystem instability during the rise of the dinosaurs: evidence from the Late Triassic in New Mexico and Arizona. Geological Society of America Abstracts with Programs 41:477.

Dzik, J. 2001. A new *Paleorhinus* fauna in the early Late Triassic of Poland. Journal of Vertebrate Paleontology 21:625-627.

Dzik, J., and T. Sulej. 2007. A review of the early Late Triassic Krasiejów biota from Silesia, Poland. Palaeontologia Polonica 64:3–27.

Efron, B., Halloran, E., and S. Holmes. 1996. Bootstrap confidence levels for phylogenetic trees. Proceedings of the National Academy of Sciences of the U. S. A. 93:7085-7090.

Ezcurra, M. D., Scheyer, T. M., and R. J. Butler. 2014. The origin and early evolution of Sauria: reassessing the Permian saurian fossil record and the timing of crocodile-lizard divergence. PLoS ONE 9(2):e89165.

Faith, D. P. 1991. Cladistic permutation tests for monophyly and nonmonophyly. Systematic Biology 40:366-375.

Faith, D. P., and P. S. Cranston. 1991. Could a cladogram this short have arisen by chance alone? On permutation tests for cladistic structure. Cladistics 7:1-28.

Farris, J. S., Källersjö, M., Kluge, A. G., and C. Bult. 1995. Testing significance of incongruence. Cladistics 10:315-319.

Fraser, N. 2006. Dawn of the Dinosaurs: Life in the Triassic. Indiana University Press, Bloomington, 328 pp.

Fraser, N. C., Heckert, A. B., Lucas, S. G., and V. P. Schneider. 2006. The first record of *Coahomasuchus* (Archosauria: Stagonolepididae) from the Carnian of eastern North America. Journal of Vertebrate Paleontology 26 (supplement to number 3):63A.

Furin, S., Preto, N., Rigo, M., Roghi, G., Gianolla, P., Crowley, J. L., and S. A. Bowring. 2006. High-precision U-Pb zircon age from the Triassic of Italy: implications for the Triassic time scale and the Carnian origin of calcareous nannoplankton and dinosaurs. Geology 34:1009-1012.

Gatesy, J., Amato, G., Norell, M., DeSalle, R., and C. Hayashi. 2003. Combined support for wholesale taxic atavism in gavialine crocodylians. Systematic Biology 52:403-433.

Gauthier, J. A. 1986. Saurischian monophyly and the origin of birds; pp. 1-55 *in* Padian, K. (ed.). The origin of birds and the evolution of flight. Memoirs of the California Academy of Sciences 8. California Academy of Sciences, San Francisco.

Gauthier, J. A., and K. Padian. 1985. Phylogenetic, functional, and aerodynamic analyses of the origin of birds and their flight; pp. 185-197 *in* Hecht, M. K., Ostrom, J. H., Viohl, G., and P. Wellnhofer (eds.), the Beginning of Birds: Proceedings of the International *Archaeopteryx* Conference, Eichstätt, 1984. Freunde des Jura-Museums Eichstätt, Eichstätt.

Gauthier, J. A., Kluge, A. G., and T. Rowe. 1988. Amniote phylogeny and the importance of fossils. Cladistics 4:105-209.

Gill, F. B., Slikas, B., and F. H. Sheldon. 2005. Phylogeny of titmice (Paridae) II: species relationships based on sequences of the mitochondrial cytochrome-B gene. The Auk 122:121-143.

Gower, D. J., and A. D. Walker. 2002. New data on the braincase of the aetosaurian archosaur (Reptilia: Diapsida) *Stagonolepis robertsoni* Agassiz; pp. 7-23 in Norman D. B. and D. J. Gower (eds.), Archosaurian Anatomy and Paleontology. Essays in Memory of Alick D. Walker. Zoological Journal of the Linnaean Society 136. The Linnaean Society of London, London.

Gregory, J. T. 1953a. *Typothorax* and *Desmatosuchus.* Postilla 16**:**1-27.

Gregory, J. T. 1953b. *Typothorax* scutes from Germany. Postilla 15:1-6.

Gregory, J. T. 1962. The genera of phyosaurs. American Journal of Science 260:652-690.

Gregory, J. T., and F. Westphal. 1969. Remarks on the phytosaur genera of the European Trias. Journal of Paleontology 43:1296-1298.

Harris, S. R., Gower, D. J., and M. Wilkinson. 2003a. Intraorganismal homology, character construction, and the phylogeny of aetosaurian archosaurs (Reptilia, Diapsida). Systematic Biology 52:239-252.

Harris, S. R., Gower, D. J., and M. Wilkinson. 2003b. Phylogenetic methods and aetosaur interrelationships: a rejoinder. Systematic Biology 52:851-852.

Heath, T. A., Hedtke, S. M., and D. M. Hillis. 2008. Taxon sampling and the accuracy of phylogenetic analysis. Journal of Systematics and Evolution 46:239-257.

Heckert, A. B. 1997. The tetrapod fauna of the Upper Triassic lower Chinle Group (Adamanian: Latest Carnian) of the Zuni Mountains, west-central New Mexico; pp. 29-39 *in* Lucas, S. G., Estep, J. W., Williamson, T. E., and G. S. Morgan (eds.), New Mexico's Fossil Record 1. New Mexico Museum of Natural History and Science Bulletin 11, New Mexico Museum of Natural History and Science Bulletin, Albuquerque.

Heckert, A. B. 2003 [imprint 2002]. A revision of the Upper Triassic ornithischian dinosaur *Revueltosaurus*, with a description of a new species; pp. 253-268 *in* Heckert, A. B., and S. G. Lucas (eds.), Upper Triassic Stratigraphy and Paleontology. New Mexico Museum of Natural History and Science Bulletin 21. New Mexico Museum of Natural History and Science, Albuquerque.

Heckert, A. B. 2004. Late Triassic microvertebrates from the lower Chinle Group (Otischalkian – Adamanian: Carnian), southwestern U. S. A. New Mexico Museum of Natural History and Science Bulletin 27:1-170.

Heckert, A. B., and S. G. Lucas. 1997. Lower Chinle Group (Adamanian: Latest Carnian) tetrapod biostratigraphy and biochronology, eastern Arizona and west-central New Mexico; pp. 11-23 *in* Anderson, B., Boaz, D., and R. D. McCord (eds.), Southwest Paleontological Symposium 1997, Proceedings 5. Mesa Southwest Museum and Southwest Paleontological Society, Mesa (erroneously labeled Volume 1 on cover).

Heckert, A. B., and S. G. Lucas. 1998. First occurrence of *Aetosaurus* (Reptilia: Archosauria) in the Upper Triassic Chinle Group (USA) and its biochronological significance. Neues Jahrbuch für Geologie und Paläontologie, Monatshefte 1998:604-612.

Heckert, A. B., and S. G. Lucas. 1999a. A new aetosaur (Reptilia: Archosauria) from the Upper Triassic of Texas and the phylogeny of aetosaurs. Journal of Vertebrate Paleontology 19:50-68.

Heckert, A. B., and S. G. Lucas. 1999b. Global correlation and chronology of Triassic theropods (Archosauria: Dinosauria). Albertiana 23:22-35.

Heckert, A. B., and S. G. Lucas. 2000. Taxonomy, phylogeny, biostratigraphy, biochronology, paleobiogeography, and evolution of the Late Triassic Aetosauria (Archosauria: Crurotarsi). Zentralblatt für Geologie und Paläontologie Teil I 1998 Heft 11–12:1539-1587.

Heckert, A. B., and S. G. Lucas. 2002a. South American occurrences of the Adamanian (Late Triassic: latest Carnian) index taxon *Stagonolepis* (Archosauria: Aetosauria) and their biochronological significance. Journal of Paleontology 76:852-863.

Heckert, A. B., and S. G. Lucas. 2002b [imprint 2001]. Stratigraphy, biostratigraphy and biochronology of lower Chinle Group (Adamanian: Latest Carnian) vertebrate fossil assemblages in the vicinity of St. Johns, Arizona; pp. 9-15 *in* McCord, R. D., and D. Boaz (eds.), Western Association of Vertebrate Paleontologists with Mesa Southwest Museum and Southwest Paleontological Society Mesa, Arizona, First Meeting of the New Millennium. Mesa Southwest Museum Bulletin 8. Southwest Paleontological Society, Mesa Southwest Museum, and the City of Mesa, Mesa.

Heckert, A. B., and S. G. Lucas. 2003. Clarifying aetosaur phylogeny requires more fossils, not more trees: reply to intraorganismal homology, character construction, and the phylogeny of aetosaurian archosaurs (Reptilia, Diapsida). Systematic Biology 52:253-255.

Heckert, A. B., and K. E. Zeigler. 2003. The Late Triassic Snyder Quarry: A brief history of discovery and excavation; pp. 5-13 *in* Zeigler, K. E., Heckert, A. B., and S. G. Lucas (eds.), Paleontology and Geology of the Upper Triassic (Revueltian) Snyder Quarry, New Mexico. New Mexico Museum of Natural History and Science Bulletin 24. New Mexico Museum of Natural History and Science, Albuquerque.

Heckert, A. B., Lucas, S. G., Hunt, A. P., and J. D. Harris. 2001. A giant phytosaur (Reptilia: Archosauria) skull from the Redonda Formation (Upper Triassic: Apachean) of east-central New Mexico; pp. 169-176 *in* Lucas, S. G., and D. S. Ulmer-Scholle (eds.),

Geology of the Llano Estacado, 52nd Field Conference. New Mexico Geological Society Guidebook. New Mexico Geological Society, Socorro.

Heckert, A. B., Zeigler, K. E., and S. G. Lucas. 2003. Aetosaurs (Archosauria: Stagonolepididae) from the Upper Triassic (Revueltian) Snyder Quarry, New Mexico; pp. 115-126 *in* Zeigler, K. E., Heckert, A. B., and S. G. Lucas (eds.), Paleontology and Geology of the Upper Triassic (Revueltian) Snyder Quarry, New Mexico. New Mexico Museum of Natural History and Science Bulletin 24. New Mexico Museum of Natural History and Science, Albuquerque.

Heckert, A. B., Lucas, S. G., and A. P. Hunt. 2005a. Triassic vertebrate fossils in Arizona; pp. 16-44 *in* Heckert, A. B., and S. G. Lucas (eds.), Vertebrate Paleontology in Arizona. New Mexico Museum of Natural History and Science Bulletin 29. New Mexico Museum of Natural History and Science, Albuquerque.

Heckert, A. B., Lucas, S. G., Sullivan, R. M., Hunt, A. P., and J. A. Spielmann. 2005b. The vertebrate fauna of the Upper Triassic (Revueltian: early-mid Norian) Painted Desert Member (Petrified Forest Formation: Chinle Group) in the Chama Basin, northern New Mexico; pp. 302-318 *in* Lucas, S. G., Zeigler, K. E., Lueth, V. W., and D. E. Owen (eds.), Geology of the Chama Basin, 56th Field Conference. New Mexico Geological Society Guidebook. New Mexico Geological Society, Socorro.

Heckert, A. B., Lucas, S. G., Hunt, A. P., and J. A. Spielmann. 2007a. Late Triassic aetosaur biochronology revisited; pp. 49-50 *in* Lucas, S. G., and J. A. Spielmann (eds.), The Global Triassic. New Mexico Museum of Natural History and Science Bulletin 41. New Mexico Museum of Natural History and Science, Albuquerque.

Heckert, A. B., Spielmann, J. A., Lucas, S. G., and A. P. Hunt. 2007b. Biostratigraphic utility of the Upper Triassic aetosaur *Tecovasuchus* (Archosauria: Stagonolepididae), an index taxon of St. Johnsian (Adamanian: Late Carnian) time; pp. 51-57 *in* Lucas, S. G., and J. A. Spielmann (eds.), The Global Triassic. New Mexico Museum of Natural History and Science Bulletin 41. New Mexico Museum of Natural History and Science, Albuquerque.

Heckert, A. B., Lucas, S. G., Rinehart, L. F., and A. P. Hunt. 2008. A new genus and species of sphenodontian from the Ghost Ranch *Coelophysis* Quarry (Upper Triassic: Apachean), Rock Point Formation, New Mexico, USA. Palaeontology 51:827-845.

Heckert, A. B., Lucas, S. G., Rinehart, L. F., Celeskey, M. D., Spielmann, J. A., and A. P. Hunt. 2010. Articulated skeletons of the aetosaur *Typothorax coccinarum* Cope (Archosauria: Stagonolepididae) from the Upper Triassic Bull Canyon Formation (Revueltian: early-mid Norian), eastern New Mexico, USA. Journal of Vertebrate Paleontology 30:619-642.

Heckert, A. B., Lucas, S. G., and J. A. Spielmann. 2012. A new species of the enigmatic archosauromorph *Doswellia* from the Upper Triassic Bluewater Creek Formation, New Mexico, USA. Palaeontology 55:1333-1348.

Heckert, A. B., Schneider, V. P., Fraser, N. C., and R. A. Webb. In Press. A new aetosaur (Archosauria: Suchia) from the Upper Triassic Pekin Formation, Deep River Basin, North Carolina, U. S. A., and its implications for early aetosaur evolution. Journal of Vertebrate Paleontology.

Hill, R. V. 2005. Integration of morphological data sets for phylogenetic analysis of Amniota: the importance of integumentary characters and increased taxonomic sampling. Systematic Biology 54:530-547.

Hillis, D. M., 1987. Molecular vs. morphological approaches to systematics. Annual Review of Ecology and Systematics 18:23-42.

Hillis, D. M. 1998. Taxonomic sampling, phylogenetic accuracy, and investigator bias. Systematic Biology 47:3-8.

Hillis, D. M., and J. P. Huelsenbeck. 1992. Signal, noise, and reliability in molecular phylogenetic analyses. Journal of Heredity 83:189-195.

Hillis, D. M., and J. J. Bull. 1993. An empirical test of bootstrapping as a method for accessing confidence in phylogenetic analysis. Systematic Biology 42:182-192.

Hillis, D. M., Huelsenbeck, J. P., and C. W. Cunningham. 1994. Application and accuracy of molecular phylogenies. Science 264:671-677.

Hoffstetter, R. 1955. Thecodontia; pp. 665-694 *in* Piviteau, J. (ed.), Traité de Paléontologie 5. Masson et Cie Éditeurs, Paris.

Hopson, J. A. 1979. Paleoneurology; pp. 39-146 *in* Gans, C., Northcutt, R. G., and P. Ulinsky (eds.), Biology of the Reptilia 9, Neurology A. Academic Press, London.

Howell, E. R., and R. C. Blakey. 2013. Sedimentological constraints on the evolution of the Cordilleran arc: New insights from the Sonsela Member, Upper Triassic Chinle Formation, Petrified Forest National Park (Arizona, USA). Geological Society of America Bulletin 125:1349-1368.

Huber, P., Lucas, S. G., and A. P. Hunt. 1993. Vertebrate biochronology of the Newark Supergroup Triassic, eastern North America; pp. 179-186 *in* Lucas, S. G., and M. Morales (eds.), The Nonmarine Triassic, Transactions of the International Symposium and Field Trip on the Nonmarine Triassic 17-24 October 1993 Albuquerque, New

Mexico. New Mexico Museum of Natural History and Science Bulletin 3. New Mexico Museum of Natural History and Science, Albuquerque.

Huelsenbeck, J. P, Bull, J. J., and C. W. Cunningham., 1996. Combining data in phylogenetic analysis. Tree 11:152-157.

Huene, F. v. 1915. On reptiles of the New Mexican Trias in the Cope collection. American Museum of Natural History Bulletin 34:485-507.

Huene, F. v. 1927 [imprint 1926]. Notes on the age of the continental Triassic strata in North America. Proceedings of the United States National Museum 69, Number 2644, Article 18:1-10.

Huene, F. v. 1936. The constitution of the Thecodontia. American Journal of Science 32:207-217.

Hunt, A. P. 1998. Preliminary results of the dawn of the dinosaurs project at Petrified Forest National Park, Arizona; pp. 135-137 *in* Santucci, V. L., and L. McClelland (eds.), National Park Service Paleontological Research. Geological Resources Division Technical Report NPS/NRGRD/GRDTR-98/01, October, 1998. Geological Resources Division, Lakewood.

Hunt, A. P. 1989. A new ?ornithischian dinosaur from the Bull Canyon Formation (Upper Triassic) of east-central New Mexico; pp. 355-358 *in* Lucas, S. G. and A. P. Hunt (eds.), Dawn of the Age of Dinosaurs in the American Southwest. New Mexico Museum of Natural History, Albuquerque.

Hunt, A. P. 2001. The vertebrate fauna, biostratigraphy and biochronology of the type Revueltian land-vertebrate faunachron, Bull Canyon Formation (Upper Triassic), east-central New

Mexico; pp. 123-151 *in* Lucas, S. G., and D. S. Ulmer-Scholle (eds.), Geology of the Llano Estacado, 52nd Field Conference. New Mexico Geological Society Guidebook. New Mexico Geological Society, Socorro.

Hunt, A. P., and S. G. Lucas. 1990. Re-evaluation of '*Typothorax*' *meadei*, a Late Triassic aetosaur from the United States. Paläontologische Zeitschrift 64:317-328.

Hunt, A. P., and S. G. Lucas. 1991. A new aetosaur from the Redonda Formation (Late Triassic: middle Norian) of east-central New Mexico, U.S.A. Neues Jahrbuch für Geologie und Paläontologie, Monatshefte 1991:728-736.

Hunt, A. P., and S. G. Lucas. 1992. The first occurrence of the aetosaur *Paratypothorax andressi* (Reptilia: Archosauria) in the western United States and its biochronological significance. Paläontologische Zeitschrift 66:147-157.

Hunt, A. P., Lucas, S. G., and A. B. Heckert. 2005. Definition and correlation of the Lamyan: A new biochronological unit for the non-marine late Carnian (Late Triassic); pp. 357-366 *in* Lucas, S. G., Zeigler, K. E., Lueth, V. W., and D. E. Owen (eds.), Geology of the Chama Basin, 56th Field Conference. New Mexico Geological Society Guidebook. New Mexico Geological Society, Socorro.

Hüsing, S. K., Deenen, M. H. L., Koopmans, J. G., and W. Krijgsman. 2011. Magnetostratigraphic dating of the proposed Rhaetian GSSP at Steinbergkogel (Upper Triassic, Austria): implications for the Late Triassic time scale. Earth and Planetary Science Letters 302:203-16.

Huxley, T. H. 1859. On the *Stagonolepis robertsoni* (Agassiz) of the Elgin Sandstone; and on the recently discovered footmarks in the Sandstones of Cummingstone. Proceedings of the Geological Society 15:440-460.

Huxley, T. H. 1875. On *Stagonolepis robertsoni*, and on the evolution of the crocodylia. Quarterly Journal of the Geological Society 31:423-438.

Huxley, T. H. 1877. The crocodilian remains found in the Elgin sandstones, with remarks on the ichnites of Cummingstone. Memoirs of the Geological Survey of the United Kingdom 3:1-58.

Irmis, R. B. 2005. The vertebrate fauna of the Upper Triassic Chinle Formation in northern Arizona; pp. 63-88 *in* Nesbitt, S. J., Parker, W. G., and R. B. Irmis (eds.), Guidebook to the Triassic Formations of the Colorado Plateau in Northern Arizona: Geology, Paleontology, and History. Fieldtrip for the 65th Annual Meeting for the Society of Vertebrate Paleontology. Mesa Southwest Museum Bulletin 9. Southwest Paleontological Society and Mesa Southwest Museum, Mesa.

Irmis, R. B. 2007. Axial skeleton ontogeny in the Parasuchia (Archosauria: Pseudosuchia) and its implications for ontogenetic determination in archosaurs. Journal of Vertebrate Paleontology 27:350-361.

Irmis, R. B. 2008. Perspectives on the origin and early diversification of dinosaurs. Unpublished Ph.D. dissertation, University of California, Berkeley, 421 pp.

Irmis, R. B., Nesbitt, S. J., Padian, K., Smith, N. D., Turner, A. H., Woody, D., and A. Downs. 2007a. A Late Triassic dinosauromorph assemblage from New Mexico and the rise of dinosaurs. Science 317:358-361.

Irmis, R. B., Parker, W. G., Nesbitt, S. J., and J. Liu. 2007b. Early ornithischian dinosaurs: the Triassic record. Historical Biology 19:3-22.

Irmis, R. B., Martz, J. W., Parker, W. G., and S. J. Nesbitt. 2010. Re-evaluating the correlation between Late Triassic terrestrial vertebrate biostratigraphy and the GSSP-defined marine stages. Albertiana 38:40-52.

Irmis, R. B., Mundil, R., Martz, J. W., and W. G. Parker. 2011. High-resolution U-Pb ages from the Upper Triassic Chinle Formation (New Mexico, USA) support a diachronous rise of dinosaurs. Earth and Planetary Science Letters 309:258-267.

Jacobs, L. L., and P. A. Murry. 1980. The vertebrate community of the Triassic Chinle Formation near St. Johns, Arizona; pp. 55-71 *in* Jacobs, L. L. (ed.), Aspects of Vertebrate History: Essays in Honor of Edwin Harris Colbert. Museum of Northern Arizona Press, Flagstaff.

Jenkins, F. A. Jr., Shubin, N. H., Amaral, W. W., Gatesy, S. M., Schaff, C. R., Clemmensen, L. B., Downs, W. R., Davidson, A. R., Bonde, N., and F. Osbæck. 1994. Late Triassic continental vertebrates and depositional environments of the Fleming Fjord Formation, Jameson Land, East Greenland. Meddelelser om Grønland Geoscience 32:1-25.

Jepsen, G. L. 1948. A Triassic armored reptile from New Jersey; pp. 5-20 in Johnson, M. E. (ed.), A Triassic Armored Reptile from New Jersey. State of New Jersey Department of Conservation Miscellaneous Geologic Paper. New Jersey Geologic Survey, Trenton.

Joyce, W. G., Lucas, S. G., Scheyer, T. M., Heckert, A. B., and A. P. Hunt. 2009. A thin-shelled reptile from the Late Triassic of North America and the origin of the turtle shell. Proceedings of the Royal Society B 276:507-513.

Kirby, R. E. 1989. Late Triassic vertebrate localities of the Owl Rock Member (Chinle Formation) in the Ward Terrace area of northern Arizona; pp. 12-28 *in* Lucas, S.G. and A. P. Hunt (eds.), Dawn of the age of dinosaurs in the American Southwest. New Mexico Museum of Natural History, Albuquerque.

Kirby, R. E. 1991. A vertebrate fauna from the Upper Triassic Owl Rock Member of the Chinle Formation in northern Arizona. Unpublished M.S. thesis. Northern Arizona University, Flagstaff, 476 pp.

Kitching, I. J., Forey, P. L., Humphries, C. J., and D. M. Williams. 1998. Cladistics: the Theory and Practice of Parsimony Analysis, 2nd edition. The Systematics Association Publication 11. Oxford University Press, Oxford.

Kluge, A. G. 1989. A concern for evidence and a phylogenetic hypothesis of relationships among *Epicrates* (Boidae, Serpentes). Systematic Zoology 38:7-25.

Kuhn, O., 1936. Weitere parasuchier und labyrinthodonten aus dem Blasensandstein des Mittleren Keuper von Ebrach. Palaeontographica Abteilung A 83:61-98.

Lambkin, C. L. 2004. Partitioned Bremer support localizes significant conflict in bee flies (Diptera: Bombyliidae: Anthracinae). Invertebrate Systematics 18:351-360.

Lambkin, C. L., Lee, M. S. Y., Winterton, S. L., and D. K. Yeates. 2002. Partitioned Bremer support and multiple trees. Cladistics 18:436-444.

Landry, S. O. 1958. The function of the entepicondylar foramen in mammals. American Midland Naturalist 60:100-112.

Langer, M. C. 2005. Studies on continental Late Triassic tetrapod biochronology II. The Ischigualastian and a Carnian global correlation. Journal of South American Earth Sciences 19:205–218.

Langer, M. C., Ribeiro, A. M., Schultz, C. L., and J. Ferigolo. 2007. The continental tetrapod-bearing Triassic of South Brazil; pp. 201-218 *in* Lucas, S. G., and J. A. Spielmann (eds.), The Global Triassic. New Mexico Museum of Natural History and Science Bulletin 41. New Mexico Museum of Natural History and Science, Albuquerque.

Lee, M. S. Y. 2001. Uninformative characters and apparent conflict between molecules and morphology. Molecular Biology and Evolution 18:676-680.

Lee, M. S. Y. 2003. Species concepts and species reality: Salvaging a Linnaean rank. *Journal of Evolutionary Biology* 16:179-188.

Lee, M. S. Y. 2009. Hidden support from unpromising data sets strongly unites snakes with anguimorph 'lizards.' Journal of Evolutionary Biology 22:1308-1316,

Lehman, T., and S. Chatterjee. 2005. Depositional setting and vertebrate biostratigraphy of the Triassic Dockum Group of Texas. Journal of Earth System Science 114:325–351.

Loeuille, B., Sinischalchi, C. M., and J. R. Pirani. 2014. New names in Vernonieae (Asteraceae) of northeastern Brazil. Phytoneuron 2014-8:1-11.

Long, R. A., and K. L. Ballew. 1985. Aetosaur dermal armor from the late Triassic of southwestern North America, with special reference to material from the Chinle Formation of Petrified Forest National Park; pp. 45-68 *in* Colbert, E. H., and R. R. Johnson (eds.), The Petrified Forest Through the Ages, 75th Anniversary Symposium

November 7, 1981. Museum of Northern Arizona Bulletin 54. Museum of Northern Arizona Press, Flagstaff.

Long, R. A., and R. Houk. 1988. Dawn of the Dinosaurs: The Triassic in Petrified Forest. Petrified Forest Museum Association, Holbrook, Arizona, 96 pp.

Long, R. A., and P. A. Murry. 1995. Late Triassic (Carnian and Norian) tetrapods from the southwestern United States. New Mexico Museum of Natural History and Science Bulletin 4:1–254.

Lucas, S. G. 1990. Toward a vertebrate biochronology of the Triassic. Albertiana 8:36–41.

Lucas, S. G., 1998a. Global Triassic tetrapod biostratigraphy and biochronology. Palaeogeography, Palaeoclimatology, Palaeoecology 143:347-384.

Lucas, S. G. 1998b. The aetosaur *Longosuchus* from the Triassic of Morocco and its biochronological significance. Compte Rendus de l'Académie des Science Paris. Sciences de la Terre et des Planètes 326:589–594.

Lucas, S. G. 2000. Pathological aetosaur armor from the Upper Triassic of Germany: Stuttgarter Beiträge zur Naturkunde Serie B (Geologie und Paläontologie) 281:1-6.

Lucas, S. G. 2010. The Triassic timescale based on nonmarine tetrapod biostratigraphy and biochronology, pp. 447-500 *in* Lucas, S. G. (ed.) The Triassic Timescale. Geological Society, London, Special Publications 334. The Geological Society Publishing House, Bath.

Lucas, S. G., and A. P. Hunt. 1992. Triassic stratigraphy and paleontology, Chama Basin and adjacent areas, north-central New Mexico; pp. 151-167 *in* Lucas, S. G., Kues, B. S.,

Williamson, T. E., and A. P. Hunt (eds.), San Juan Basin IV, 43rd Field Conference. New Mexico Geological Society, Albuquerque.

Lucas, S. G., and A. P. Hunt. 1993. Tetrapod biochronology of the Chinle Group (Upper Triassic), western United States; pp. 327-329 *in* Lucas, S. G., and M. Morales (eds.), The Nonmarine Triassic, Transactions of the International Symposium and Field Trip on the Nonmarine Triassic 17-24 October 1993 Albuquerque, New Mexico. New Mexico Museum of Natural History and Science Bulletin 3. New Mexico Museum of Natural History and Science, Albuquerque.

Lucas, S. G., and Z. Luo. 1993. *Adelobasileus* from the Upper Triassic of west Texas: the oldest mammal. Journal of Vertebrate Paleontology 13:309-334.

Lucas, S. G., and A. B. Heckert. 1996a. Late Triassic aetosaur biochronology. Albertiana 17:57-64.

Lucas, S. G., and A. B. Heckert. 1996b. Vertebrate biochronology of the Late Triassic of Arizona; pp. 63-81 *in* Boaz, D., Dierking, P., Dornan, M., McGeorge, R., and B. J. Tegowski (eds.), Proceedings of the Fossils of Arizona Symposium Volume 4. Mesa Southwest Museum Bulletin and the City of Mesa, Mesa.

Lucas, S. G., and A. B. Heckert. 2000. Biochronological significance of Triassic nonmarine tetrapod records from marine strata. Albertiana 24:30–36.

Lucas, S. G., and A. B. Heckert. 2001. The aetosaur *Stagonolepis* from the Upper Triassic of Brazil and its biochronological significance. Neues Jahrbuch für Geologie und Paläontologie, Monatshefte 2001:719–732.

Lucas, S. G., and P. E. Kondrashov. 2004. Early Eocene (Bumbanian) perissodactyls from Mongolia and their biochronological significance; pp. 215-220 *in* Lucas, S. G., Zeigler, K. E., and P. E. Kondrashov (eds.), Paleogene Mammals. New Mexico Museum of Natural History and Science Bulletin 26. New Mexico Museum of Natural History and Science, Albuquerque.

Lucas, S. G., and S. Connealy. 2008. Triassic New Mexico: Dawn of the Dinosaurs. New Mexico Museum of Natural History and Science, Albuquerque, 48 pp.

Lucas, S. G., Hunt, A. P., and R. Kahle. 1993. Late Triassic vertebrates from the Dockum Formation near Otis Chalk, Howard County, Texas; pp. 237–244 *in* Love, D. W., Hawley, J. W., Kues, B. S., Adams, J. W., Austin, G. S., and J. M. Barker (eds.), Carlsbad Region, New Mexico and West Texas, 44th Field Conference. New Mexico Geological Society, Albuquerque.

Lucas, S. G., Heckert, A. B., and A. P. Hunt. 1995. Unusual aetosaur armor from the Upper Triassic of west Texas. Paläontologische Zeitschrift 69:467-473.

Lucas, S. G., Heckert, A. B., and A. P. Hunt. 1997. Stratigraphy and biochronological significance of the Late Triassic *Placerias* Quarry, eastern Arizona (U.S.A.). Neues Jahrbuch für Geologie und Paläontologie, Abhandlungen 203:23-46.

Lucas, S. G., Heckert, A. B., and A. P. Hunt. 2003a [imprint 2002]. A new species of the aetosaur *Typothorax* (Archosauria: Stagonolepididae) from the Upper Triassic of east-central New Mexico; pp. 221-233 *in* Heckert, A. B., and S. G. Lucas (eds.), Upper Triassic Stratigraphy and Paleontology. New Mexico Museum of Natural History and Science Bulletin 21. New Mexico Museum of Natural History and Science, Albuquerque.

Lucas, S. G., Heckert, A. B., and N. Hotton III. 2003b [imprint 2002]. The rhynchosaur *Hyperodapedon* from the Upper Triassic of Wyoming and its global biochronological significance; pp. 149-156 *in* Heckert, A. B., and S. G. Lucas (eds.), Upper Triassic Stratigraphy and Paleontology. New Mexico Museum of Natural History and Science Bulletin 21. New Mexico Museum of Natural History and Science, Albuquerque.

Lucas, S. G., Zeigler, K. E., Heckert, A. B., and A. P. Hunt. 2005. Review of Upper Triassic stratigraphy and biostratigraphy in the Chama Basin, northern New Mexico; pp. 170-181 *in* Lucas, S. G., Zeigler, K. E., Lueth, V. W., and D. E. Owen (eds.), Geology of the Chama Basin, 56th Field Conference. New Mexico Geological Society Guidebook. New Mexico Geological Society, Socorro.

Lucas, S. G., Hunt, A. P., and J. A. Spielmann. 2006a. *Rioarribasuchus*, a new name for an aetosaur from the Upper Triassic of north-central New Mexico; pp. 581-582 *in* Harris, J. D., Lucas, S. G., Spielmann, J. A., Lockley, M. G., Milner, A. R. C., and J. I. Kirkland (eds.), The Triassic-Jurassic Terrestrial Transition. New Mexico Museum of Natural History and Science Bulletin 37. New Mexico Museum of Natural History and Science, Albuquerque.

Lucas, S. G., Heckert, A. B., and L. F. Rinehart. 2006b. The Late Triassic aetosaur *Paratypothorax*; pp. 575-580 *in* Harris, J. D., Lucas, S. G., Spielmann, J. A., Lockley, M. G., Milner, A. R. C., and J. I. Kirkland (eds.), The Triassic-Jurassic Terrestrial Transition. New Mexico Museum of Natural History and Science Bulletin 37. New Mexico Museum of Natural History and Science, Albuquerque.

Lucas, S. G., Hunt, A. P., and J. A. Spielmann. 2007a. A new aetosaur from the Upper Triassic (Adamanian: Carnian) of Arizona; pp. 241-247 *in* Lucas, S. G. and J. A. Spielmann (eds.), Triassic of the American West. New Mexico Museum of Natural History and Science Bulletin 40. New Mexico Museum of Natural History and Science, Albuquerque.

Lucas, S. G., Hunt, A. P., Heckert, A. B., and J. A. Spielmann. 2007b. Global Triassic tetrapod biostratigraphy and biochronology: 2007 status; pp. 229-240 *in* Lucas, S. G. and J. A. Spielmann (eds.), The Global Triassic. New Mexico Museum of Natural History and Science Bulletin 41. New Mexico Museum of Natural History and Science, Albuquerque.

Lucas, S. G., Heckert, A. B., and L. Rinehart. 2007c. A giant skull, ontogenetic variation and taxonomic validity of the Late Triassic phytosaur *Parasuchus*; pp. 222-228 *in* Lucas, S. G. and J. A. Spielmann (eds.), The Global Triassic. New Mexico Museum of Natural History and Science Bulletin 41. New Mexico Museum of Natural History and Science, Albuquerque.

Lucas, S. G., Spielmann, J. A., and A. P. Hunt. 2007d. Biochronological significance of Late Triassic tetrapods from Krasiejów, Poland; pp. 248-258 *in* Lucas, S. G. and J. A. Spielmann (eds.), The Global Triassic. New Mexico Museum of Natural History and Science Bulletin 41. New Mexico Museum of Natural History and Science, Albuquerque.

Lucas, S. G., Tanner, L. H., Kozur, H. W., Weems, R. E., and A. B. Heckert. 2012. The Late Triassic timescale: age and correlation of the Carnian-Norian boundary. Earth-Science Reviews 114:1-18.

Lydekker, R. 1887. The fossil Vertebrata of India. Records of the Geological Survey of India 20:51–80.

Lyson, T. R., and W. G. Joyce. 2010. A new baenid turtle from the Upper Cretaceous (Maastrichtian) Hell Creek Formation of North Dakota and a preliminary taxonomic review of Cretaceous Baenidae. Journal of Vertebrate Paleontology 30:394-402.

Maddison, W. P. and D. R. Maddison. 2011. Mesquite: a modular system for evolutionary analysis. Version 2.75. http://mesquiteproject.org.

Matzke, A. T., and M. W. Maisch. 2011. The first aetosaurid archosaur from the Trossingen *Plateosaurus* Quarry (Upper Triassic, Germany). Neues Jahrbuch für Geologie und Paläontologie, Abhandlungen 262:355-358.

Marsh, O. C. 1884. The classification and affinities of dinosaurian reptiles. Nature 31:68–69.

Martinez, R. N., Sereno, P. C., Alcober, O. A., Colombi, C. E., Renne, P. R., Montañez, I. P., and B. S. Currie. 2011. A basal dinosaur from the dawn of the dinosaur era in southwestern Pangaea. Science 331:206–210.

Martinez, R. N., Apaldetti, C., Alcober, O. A., Columbi, C. E., Sereno, P. E., Fernandez, E., Santi Malnis, P., Correa, G. A., and D. Abelin. 2013 [imprint 2012]. Vertebrate succession in the Ischigualasto Formation; pp. 10-30 *in* Sereno, P. C. (ed.), Basal Sauropodomorphs and the Vertebrate Fossil Record of the Ischigualasto Formation (Late Triassic: Carnian-Norian) of Argentina. Society of Vertebrate Paleontology Memoir 12. Journal of Vertebrate Paleontology 32 (supplement to number 6), November 2012.

Martz, J. W. 2002. The morphology and ontogeny of *Typothorax coccinarum* (Archosauria, Stagonolepididae) from the Upper Triassic of the American Southwest. Unpublished M.S. thesis, Texas Tech University, Lubbock, TX, 279 pp.

Martz, J. W. 2008. Lithostratigraphy, chemostratigraphy, and vertebrate biostratigraphy of the Dockum Group (Upper Triassic), of southern Garza County, West Texas. Unpublished Ph.D. dissertation, Texas Tech University, Lubbock, Texas, 504 pp.

Martz, J. W., and B. J. Small. 2006. *Tecovasuchus chatterjeei*, a new aetosaur (Archosauria: Aetosauria) from the Tecovas Formation (Upper Triassic, Carnian) of Texas. Journal of Vertebrate Paleontology 26:308–320.

Martz, J. W., and W. G. Parker. 2010. Revised lithostratigraphy of the Sonsela Member (Chinle Formation, Upper Triassic) in the southern part of Petrified Forest National Park, Arizona. PLoS ONE 5(2): e9329.

Martz, J. W., Mueller, B., Nesbitt, S. J., Stocker, M. R., Parker, W. G., Atanassov, M., Fraser, N., Weinbaum J., and J. R. Lehane. 2013. A taxonomic and biostratigraphic re-evaluation of the Post Quarry vertebrate assemblage from the Cooper Canyon Formation (Dockum Group, Upper Triassic) of southern Garza County, western Texas; pp. 339-364 *in* Parker, W., Bell, C., Brochu, C., Irmis, R., Jass, C, Stocker, M., and M. Benton (eds.), The Full Profession: A Celebration of the Life and Career of Wann Langston Jr., Quintessential Vertebrate Paleontologist. Earth and Environmental Science Transactions of the Royal Society of Edinburgh 103.

Maxwell, E. E. 2010. Generic reassignment of an ichthyosaur from the Queen Elizabeth Islands, Northwest Territories, Canada. Journal of Vertebrate Paleontology 30:403-415.

Mayden, R. L. 1997. A hierarchy of species concepts: the denouement in the saga of the species problem; pp. 381-424 *in* Claridge, M. F., Dawah, H. A., and M. R. Wilson (eds.), Species: the Units of Biodiversity. Chapman and Hall, London.

Murry, P. A. 1986. Vertebrate paleontology of the Dockum Group, western Texas and eastern New Mexico; pp. 109-136 *in* Padian, K. (ed.) The Beginning of the Age of Dinosaurs. Cambridge University Press, Cambridge.

Murry, P. A. 1987. New reptiles from the Upper Triassic Chinle Formation of Arizona. Journal of Paleontology 61:773-786.

Murry, P. A., and R. A. Long. 1989. Geology and paleontology of the Chinle Formation, Petrified Forest National Park and vicinity, Arizona and a discussion of vertebrate fossils of the southwestern Upper Triassic; pp. 29–64 *in* S. G. Lucas and A. P. Hunt (eds.), Dawn of the Age of Dinosaurs in the American Southwest. New Mexico Museum of Natural History, Albuquerque.

Murry, P. A., and R. A. Long. 1996. A diminutive carnivorous aetosaur from the Upper Triassic of Howard County, Texas. Journal of Vertebrate Paleontology 16 (supplement to number 3):55A.

Nesbitt, S. J. 2011. The early evolution of archosaurs: relationships and the origin of major clades. Bulletin of the American Museum of Natural History 352:1–292.

Nesbitt, S. J., and M. R. Stocker. 2008. The vertebrate assemblage of the Late Triassic Canjilon Quarry (northern New Mexico, U.S.A.), and the importance of apomorphy-based assemblage comparisons. Journal of Vertebrate Paleontology 28:1063–72.

Nesbitt, S. J., Irmis, R. B., and W. G. Parker. 2007. A critical re-evaluation of the Late Triassic dinosaur taxa of North America. Journal of Systematic Palaeontology 5:209–243.

Nesbitt, S. J., Smith, N. D., Irmis, R. B., Turner, A. H., Downs, A., and M. Norell. 2009a. A complete skeleton of a Late Triassic saurischian and the early evolution of dinosaurs. Science 326:1530-1533.

Nesbitt, S. J., Irmis, R. B., Parker, W. G., Smith, N. D., Turner, A. H., and T. Rowe. 2009. Hindlimb osteology and distribution of basal dinosauromorphs from the Late Triassic of North America. Journal of Vertebrate Paleontology 29:498-516.

Nesbitt, S. J., Sidor, C. A., Irmis, R. B., Angielczyk, K. D., Smith, R. M. H., and L. A. Tsuji. 2010. Ecologically distinct dinosaurian sister group shows early diversification of Ornithodira. Nature 464:95-98.

Nixon, K. C., and Q. D. Wheeler. 1992. Extinction and the origin of species; pp. 119–143 *in* Novacek M. J. and Q. D. Wheeler (eds.), Extinction and Phylogeny. Columbia University Press, New York.

O'Leary, M. A., and S. G. Kaufman. 2012. MorphoBank 3.0: Web application for morphological phylogenetics and taxonomy. http://www.morphobank.org.

Ogg, J. G. 2012. Triassic; pp. 681-730 *in* Gradstein, F. M., Ogg, J. G. Schmitz, M. and G. Ogg (eds.), The Geologic Time Scale 2012. Elsevier, B.V., Netherlands.

Page, R. D. M. 2001. Nexus Data Editor for Windows (NDE), version 0.5.0. Program and documentation. Available online at: http://taxonomy.zoology.gla.ac.uk/rod/NDE/nde.html. Published by the author, Glasgow, U.K.

Parker, W. G. 2002 [imprint 2001]. An enigmatic aetosaur specimen from the Upper Triassic Dockum Formation of Texas (Abstract); p. 17 *in* McCord, R. D., and D. Boaz (eds.),

Western Association of Vertebrate Paleontologists with Mesa Southwest Museum and Southwest Paleontological Society Mesa, Arizona, First Meeting of the New Millennium. Mesa Southwest Museum Bulletin 8. Southwest Paleontological Society, Mesa Southwest Museum, and the City of Mesa, Mesa.

Parker, W. G. 2003. Description of a new specimen of *Desmatosuchus haplocerus* from the Late Triassic of northern Arizona. Unpublished M. S. Thesis, Northern Arizona University, Flagstaff, 315 pp.

Parker, W. G. 2005a. Faunal review of the Upper Triassic Chinle Formation of Arizona; pp. 34-54 *in* McCord, R. D. (ed.), Vertebrate Paleontology of Arizona. Mesa Southwest Museum Bulletin 11. Southwest Paleontological Society, Mesa Southwest Museum and the City of Mesa, Mesa.

Parker, W. G. 2005b. Petrified Forest National Park: A roadlog; pp. 33-51 *in* Nesbitt, S. J., Parker, W. G., and R. B. Irmis (eds.), Guidebook to the Triassic Formations of the Colorado Plateau in Northern Arizona: Geology, Paleontology, and History. Fieldtrip for the 65th Annual Meeting for the Society of Vertebrate Paleontology. Mesa Southwest Museum Bulletin 9. Southwest Paleontological Society and Mesa Southwest Museum, Mesa.

Parker, W. G. 2005c. A new species of the Late Triassic aetosaur *Desmatosuchus* (Archosauria: Pseudosuchia). Compte Rendus Paleovol 4:327-340.

Parker, W. G. 2006. The stratigraphic distribution of major fossil localities in Petrified Forest National Park, Arizona; pp. 46-62 *in* Parker, W. G., Ash, S. R., and R. B. Irmis (eds.), A Century of Research at Petrified Forest National Park 1906-2006: Geology and

Paleontology. Museum of Northern Arizona Bulletin 62. Petrified Forest Museum Association, Holbrook.

Parker, W. G. 2007. Reassessment of the aetosaur "*Desmatosuchus*" *chamaensis* with a reanalysis of the phylogeny of the Aetosauria (Archosauria: Pseudosuchia). Journal of Systematic Palaeontology 5:1–28.

Parker, W. G. 2008a. How many valid aetosaur species are there? Reviewing the alpha-taxonomy of the Aetosauria (Archosauria: Pseudosuchia) and its implications for Late Triassic global biostratigraphy. Journal of Vertebrate Paleontology 28 (supplement to number 3):125A.

Parker, W. G. 2008b. Description of new material of the aetosaur *Desmatosuchus spurensis* (Archosauria: Suchia) from the Chinle Formation of Arizona and a revision of the genus *Desmatosuchus*. PaleoBios new series 28:1–40.

Parker, W. G. 2013. Redescription and taxonomic status of specimens of *Episcoposaurus* and *Typothorax*, the earliest known aetosaurs (Archosauria: Suchia) from the Upper Triassic of western North America, and the problem of proxy 'holotypes;' pp. 313-338 *in* Parker, W., Bell, C., Brochu, C., Irmis, R., Jass, C, Stocker, M., and M. Benton (eds.), The Full Profession: A Celebration of the Life and Career of Wann Langston Jr., Quintessential Vertebrate Paleontologist. Earth and Environmental Science Transactions of the Royal Society of Edinburgh 103.

Parker, W. G., and R. B. Irmis. 2005. Advances in Late Triassic vertebrate paleontology based on material from Petrified Forest National Park, Arizona; pp. 45-58 *in* Heckert, A. B. and S. G. Lucas (eds.), Vertebrate Paleontology in Arizona. New Mexico Museum of Natural

History and Science Bulletin 29. New Mexico Museum of Natural History and Science, Albuquerque.

Parker, W. G., and J. W. Martz. 2010. Using positional homology in aetosaur (Archosauria: Pseudosuchia) osteoderms to evaluate the taxonomic status of *Lucasuchus hunti*. Journal of Vertebrate Paleontology 30:1100–1104.

Parker, W. G., and J. W. Martz. 2011. The Late Triassic (Norian) Adamanian–Revueltian tetrapod faunal transition in the Chinle Formation of Petrified Forest National Park, Arizona; pp. 231-260 *in* Butler, R. J., Irmis, R. B., Langer, M. C., and A. B. Smith (eds.), Late Triassic Terrestrial Biotas and the Rise of Dinosaurs. Earth and Environmental Science Transactions of the Royal Society of Edinburgh 101 (for 2010).

Parker, W. G., Stocker, M. R., and R. B. Irmis. 2008. A new desmatosuchine aetosaur (Archosauria: Suchia) from the Upper Triassic Tecovas Formation (Dockum Group) of Texas. Journal of Vertebrate Paleontology 28:692–701.

Parker, W. G., Irmis, R. B., Nesbitt, S. J., Martz, J. W., and L. S. Browne. 2005. The Late Triassic pseudosuchian *Revueltosaurus callenderi* and its implications for the diversity of early ornithischians dinosaurs. Proceedings of the Royal Society, Series B 272:963–969.

Parker, W. G., Brown, M. B., Nesbitt, S. J., Stocker, M. R., and R. B. Irmis. 2007. Revised osteology of *Revueltosaurus callenderi* (Archosauria: Pseudosuchia) based on new material from Petrified Forest National Park, Arizona. Journal of Vertebrate Paleontology 27 (supplement to number 3):127A.

Parker, W. G., Martz, J. W., and R. Dubiel. 2011. A newly recognized specimen of the phytosaur *Redondasaurus* from the Upper Triassic Owl Rock Member (Chinle Formation) and its

biostratigraphic implications. Society of Vertebrate Paleontology Abstracts of Papers Seventy-First Annual Meeting of the Society of Vertebrate Paleontology, Paris Las Vegas Hotel Las Vegas, Nevada, USA November 2-5, 2011, p. 171.

Parrish, J. M. 1994. Cranial osteology of *Longosuchus meadei* and the phylogeny and distribution of the Aetosauria. Journal of Vertebrate Paleontology 14:196-209.

Parrish, J. M., and K. Carpenter. 1986. A new vertebrate fauna from the Dockum Formation (Late Triassic) of eastern New Mexico; pp. 151-160 *in* Padian, K. (ed.), The Beginning of the Age of Dinosaurs. Cambridge University Press, Cambridge.

Platnick, N. I. 1976. Are monotypic genera possible? Systematic Zoology 25:198-199.

Platnick, N. I. 1977a. Paraphyletic and polyphyletic groups. Systematic Zoology 26:195-200.

Platnick. N. I. 1977b. Monotypy and the origin of higher taxa: a reply to E. O. Wiley. Systematic Zoology 26:355-357.

Rae, T. C. 1999. Mosaic evolution in the origin of the Hominoidea. Folia Primatologia 70:125-135.

Ramezani, J., Hoke, G. D., Fastovsky, D. E., Bowring, S. A., Therrien, F., Dworkin, S. I., Atchley, S. C., and L. C. Nordt. 2011. High-precision U–Pb zircon geochronology of the Late Triassic Chinle Formation, Petrified Forest National Park (Arizona, USA): temporal constraints on the early evolution of dinosaurs. Geological Society of America Bulletin 123:2142-2159.

Rauhut, O. W. M., 2004. Braincase structure of the Middle Jurassic theropod dinosaur *Piatnitzkysaurus.* Canadian Journal of Earth Sciences 41:1109-1122.

Rayfield, E. J, Barrett, P. M., McDonnell, R. A., and K. J. Willis. 2005. A geographical information system (GIS) study of Triassic vertebrate biochronology. Geological Magazine 142:327-354.

Rayfield, E. J., Barrett, P. M., and A. R. Milner. 2009. Utility and validity of Middle and Late Triassic 'land vertebrate faunachrons.' Journal of Vertebrate Paleontology 29:80-87.

Reese, A. M. 1915. The Alligator and Its Allies. Knickerbocker Press, New York, 358 pp.

Rieppel, O. 1985. The recessus scalae tympani and its bearing on the classification of lizards. Journal of Herpetology 19:373-384.

Roberto-Da-Silva, L., Desojo, J. B., Cabriera, S. F., Aires, A. S. S., Müller, S. T., Pacheco, C. P., and S. Dias-Da-Silva. 2014. A new aetosaur from the Upper Triassic of the Santa Maria Formation, southern Brazil. Zootaxa 3764:240-278.

Romer, A. S. 1966. Vertebrate Paleontology. University of Chicago Press, Chicago, 468 pp.

Rogers, R. R., Swisher III, C. C., Sereno, P. C., Monetta, A. M., Forster, C. A., and R. N. Martinez. 1993. The Ischigualasto Tetrapod Assemblage (Late Triassic, Argentina) and $^{40}Ar/^{39}Ar$ dating of dinosaur origins. Science 260:794-797.

Rowe, T. 1988. Definition, diagnosis, and the origin of Mammalia. Journal of Vertebrate Paleontology 8:241-264.

Santi Malnis, P., Kent, D. V., Colombi, C. E., and S. E. Geuna. 2011. Quebrada de la Sal magnetostratigraphic section, Los Colorados Formation, Upper Triassic Ischigualasto Villa Unión basin, Argentina; pp. B15, 1-7 *in* Sinito, A. M., Caballero Miranda, C. I., Soler Arrechadle, A. M., Sánchez Bettucci, L, and M. Aldana (eds), Proceedings of the Second Biennial Meeting of the Latin American Association of Paleomagnetism and

Geomagnetism, Tandil, Argentina, November 2011. Latinmag Letters Proceedings 1, Special Issue LL11-02SP. Instituto de Geofisica, Universidad Nacional Autónoma de México, Mexico City.

Sawin, H. J. 1947. The pseudosuchian reptile *Typothorax meadei*. Journal of Paleontology 21:201–238.

Schachner, E. R., Manning, P. L., and P. Dodson. 2011. Pelvic and hindlimb myology of the basal archosaur *Poposaurus gracilis* (Archosauria:Poposauroidea). Journal of Morphology 272:1464-1491.

Schneider, V. P., Heckert, A. B., and N. C. Fraser. 2011. Diversity of aetosaurs (Archosauria: Stagonolepididae) in the Upper Triassic Pekin Formation (Deep River Basin), North Carolina. Society of Vertebrate Paleontology Abstracts of Papers Seventy-First Annual Meeting of the Society of Vertebrate Paleontology, Paris Las Vegas Hotel Las Vegas, Nevada, USA November 2-5, 2011, p. 188.

Schoch, R. R. 2007. Osteology of the small archosaur *Aetosaurus* from the Upper Triassic of Germany. Neues Jahrbuch für Geologie und Paläontologie, Abhandlungen 246:1–35.

Schoch, R. R. and R. Wild. 1999. Die Tetrapoden-Fauna im Keuper Süddeutschlands; pp. 395–408 *in* Hauschke, N. and V. Wilde (eds.), Die Trias – Eine Ganz Andere Welt: Mitteleuropa im frühen Erdmittelalter. Verlag Dr. Freidrich Pfeil, Munich.

Schrire, B. D. and G. P. Lewis. 1996. Monophyly: a criterion for generic delimitation, with special reference to Leguminosae; pp. 353-370 *in* van der Maesen, L. J. G., van der Burgt, X. M., and J. M. van Medenbach de Rooy (eds.), The Biodiversity of African Plants. Kluwer Academic Publishers, Dordrecht.

Schultz, C. L. 2005. Biostratigraphy of the non-marine Triassic: is a global correlation based on tetrapod faunas possible? Pp. 123-145 *in* Koutsoukos, E. A. M. (ed.), Applied Stratigraphy. Springer, Dordrecht.

Seidel, M. R. 1979. The osteoderms of the American Alligator and their functional significance. Herpetologica 35:375-380.

Sereno, P. C. 1985. The logical basis of phylogenetic taxonomy. Systematic Biology 54:595-619.

Slowinski, J. 1993. ‘‘Unordered’’ versus ‘‘ordered’’ characters. Systematic Biology 42:155-165.

Small, B. J. 1985. The Triassic thecodontian reptile *Desmatosuchus*: osteology and relationships. Unpublished M.S. thesis, Texas Tech University, Lubbock, Texas, 83 pp.

Small, B. J. 1989. Aetosaurs from the Upper Triassic Dockum Formation, Post Quarry, West Texas; pp. 301-308 *in* Lucas, S. G., and A. P. Hunt (eds.), Dawn of the Age of Dinosaurs in the American Southwest, New Mexico Museum of Natural History, Albuquerque.

Small, B. J. 1998. The occurrence of *Aetosaurus* in the Chinle Formation (Late Triassic, USA) and its biostratigraphic significance. Neues Jahrbuch für Geologie und Paläontologie, Monatshefte 1998:285-296.

Small, B. J. 2002. Cranial anatomy of *Desmatosuchus haplocerus* (Reptilia: Archosauria: Stagonolepididae). Zoological Journal of the Linnean Society 136:97-111.

Small, B. J., and J. W. Martz. 2013. A new basal aetosaur from the Upper Triassic Chinle Formation of the Eagle Basin, Colorado, USA; pp. 393-412 *in* Nesbitt, S. J., Desojo, J. B., and R. B. Irmis (eds.), Anatomy, Phylogeny and Palaeobiology of Early Archosaurs and their Kin. Geological Society, London, Special Publications 379. The Geological Society Publishing House, Bath.

Sorenson, M. D. and E. A. Franzosa. 2007. TreeRot, version 3. Boston University, Boston, MA.

Spielmann, J. A., and S. G. Lucas. 2012. Tetrapod fauna of the Upper Triassic Redonda Formation, east-central New Mexico: the characteristic assemblage of the Apachean land-vertebrate faunachron. New Mexico Museum of Natural History and Science Bulletin 55:1-119.

Spielmann, J. A., Hunt, A. P., Lucas, S. G., and A. B. Heckert. 2006. Revision of *Redondasuchus* (Archosauria: Aetosauria) from the Upper Triassic Redonda Formation, New Mexico, with a description of a new species; pp. 583-587 *in* Harris, J. D., Lucas, S. G., Spielmann, J. A., Lockley, M. G., Milner, A. R. C., and J. I. Kirkland (eds.), The Triassic-Jurassic Terrestrial Transition. New Mexico Museum of Natural History and Science Bulletin 37. New Mexico Museum of Natural History and Science, Albuquerque.

Stocker, M. R. 2010. A new taxon of phytosaur (Archosauria: Pseudosuchia) from the Late Triassic (Norian) Sonsela Member (Chinle Formation) in Arizona, and a critical reevaluation of *Leptosuchus* Case, 1922. Palaeontology 53:997-1022.

Stocker, M. R. 2012. A new phytosaur (Archosauriformes, Phytosauria) from the Lot's Wife beds (Sonsela Member) within the Chinle Formation (Upper Triassic) of Petrified Forest National Park, Arizona. Journal of Vertebrate Paleontology 32:573-586.

Stocker, M. R. 2013a. A new taxonomic arrangement for *Paleorhinus scurriensis*; pp. 251-263 *in* Parker, W., Bell, C., Brochu, C., Irmis, R., Jass, C, Stocker, M., and M. Benton (eds.), The Full Profession: A Celebration of the Life and Career of Wann Langston Jr., Quintessential Vertebrate Paleontologist. Earth and Environmental Science Transactions of the Royal Society of Edinburgh 103.

Stocker, M. R. 2013b. Contextualizing vertebrate faunal dynamics: new perspectives from the Triassic and Eocene of western North America. Unpublished Ph.D. dissertation, The University of Texas at Austin, Austin, 297 pp.

Stuessy, T. F. 2009. Plant Taxonomy: the Systematic Evaluation of Comparative Data. Columbia University Press, New York, 568 pp.

Sulej, T. 2010. The skull of an early Late Triassic aetosaur and the evolution of the stagonolepidid archosaurian reptiles. Zoological Journal of the Linnean Society 158:860-881.

Swofford, D.L. 2003. PAUP*. Phylogenetic Analysis Using Parsimony (*and Other Methods). Version 4. Sinauer Associates: Sunderland, Massachusetts.

Swofford, D. L., and D. P. Begle. 1993. User manual for PAUP*, Phylogenetic Analysis Using Parsimony, version 3.1. Illinois Natural History Survey, Champaign.

Tanner, L. H. 2003. Pedogenic features of the Chinle Group, Four Corners regions: evidence of Late Triassic aridification; pp. 269-280 *in* Lucas, S. G., Semken, S. C., Berglof, W., and D. Ulmer-Scholle (eds.), Geology of the Zuni Plateau, 54th Guidebook. New Mexico Geological Society, Socorro.

Vences, M., Guayasamin, J. M., Miralles, A., and I. de la Riva. 2010. To name or not to name: Criteria to promote economy of change in Linnaean classification schemes. Zootaxa 3636:201-244.

Vickaryous, M. K., and B. K. Hall. 2008. Development of the dermal skeleton in *Alligator mississippiensis* (Archosauria, Crocodylia) with comments on the homology of osteoderms. Journal of Morphology 269:398-422,

Wahlberg, N., and S. Nylin. 2003. Morphology versus molecules: resolution of the positions of *Nymphalis*, *Polygonia*, and related genera (Lepidoptera: Nymphalidae). Cladistics 19:213-223.

Wake, M. H. 1992. Hyman's comparative vertebrate anatomy, revised third edition. University of Chicago Press, Chicago, 795 pp.

Walker, A. D. 1961. Triassic Reptiles from the Elgin Area: *Stagonolepis*, *Dasygnathus*, and their allies. Philosophical Transactions of the Royal Society of London 244:103–204.

Walker, A. D. 1990. A revision of *Sphenosuchus acutus* Haughton, a crocodylomorph reptile from the Elliott Formation (Late Triassic or Early Jurassic) of South Africa. Philosophical Transactions of the Royal Society of London B 330:1-120.

Weinbaum, J. C. 2011. The skull of *Postosuchus kirkpatricki* (Archosauria: Paracrocodyliformes) from the Upper Triassic of the United States. PaleoBios new series 30:18-44.

Weinbaum, J. C. 2013. Postcranial skeleton of *Postosuchus kirkpatricki* (Archosauria: Paracrocodylomorpha) from the Upper Triassic of the United States; pp. 525-553 *in* Nesbitt, S. J., Desojo, J. B. and R. B. Irmis, (eds.), Anatomy, Phylogeny and Palaeobiology of Early Archosaurs and their Kin. Geological Society, London, Special Publications 379. The Geological Society Publishing House, Bath.

Wiens, J. J. 1998a. Combining datasets with different phylogenetic histories. Systematic Biology 47:568-581.

Wiens, J. J. 1998b. Does adding characters with missing data increase or decrease phylogenetic accuracy? Systematic Biology 47:625-640.

Wiens, J. J. 2004. What is speciation and why should we study it? The American Naturalist 163:914-923.

Wild, R. 1989. *Aetosaurus* (Reptilia: Thecodontia) from the Upper Triassic (Norian) of Cene near Bergamo, Italy, with a revision of the genus. Rivista del Museo Civico di Scienze Naturali 14:1–24.

Wiley, E. O. 1977. Are Monotypic Genera Paraphyletic? A Response to Norman Platnick. Systematic Zoology 26:352-355.

Wilkinson, M. 1995a. Coping with abundant missing entries in phylogenetic inference using parsimony. Systematic Biology 44:501-514.

Wilkinson, M. 1995b. A comparison of two methods of character construction. Cladistics 11:297-308.

Wilson, J. A. 1999. Vertebral laminae in sauropods and other saurischian dinosaurs. Journal of Vertebrate Paleontology 19:639-653.

Wilson, J. A., D'Emic, M. D., Ikejiri, T., Moacdieh, E. M., and J. A. Whitlock. 2011. A nomenclature for vertebral fossae in sauropods and other saurischian dinosaurs. PLoS ONE 6(2):e17114.

Witmer, L. M. 1997. Craniofacial air sinus systems; pp. 151-159 *in* Currie, P. J. and K. Padian (eds.), The Encyclopedia of Dinosaurs. Academic Press, San Diego.

Woody, D. T. 2006. Revised stratigraphy of the lower Chinle Formation (Upper Triassic) of Petrified Forest National Park, Arizona; pp. 17-45 in Parker, W. G., Ash, S. R., and R. B. Irmis (eds.), A Century of Research at Petrified Forest National Park 1906-2006:

Geology and Paleontology. Museum of Northern Arizona Bulletin 62. Petrified Forest Museum Association, Holbrook.

Zacarias, J. D. 1982. Una nova especie de tecodonte aetosaurio (*Aetosauroides subsulcatus*, sp. nov.) de Formaçáo Santa Maria, Triassico de Rio Grande du Sul, Basil. Unpublished M.S. thesis, Federal University of the State of Rio Grande, Porto Alegre, Brazil, 69 pp.

Zeigler, K. E., and J. W. Geissman. 2011. Magnetostratigraphy of the Upper Triassic Chinle Group of New Mexico: implications for regional and global correlations among Upper Triassic sequences. Geosphere 7:802-829.

Zeigler, K. E., Heckert, A. B., and S. G. Lucas. 2003 [imprint 2002]. A new species of *Desmatosuchus* (Archosauria: Aetosauria) from the Upper Triassic of the Chama Basin, north-central New Mexico; pp. 215-219 *in* Heckert, A. B. and S. G. Lucas (eds.), Upper Triassic Stratigraphy and Paleontology. New Mexico Museum of Natural History and Science Bulletin 21. New Mexico Museum of Natural History and Science, Albuquerque.

Zittel, K. A. v. 1887–1890. Handbuch der Palaeontologie. 1. Abteilung: Paläozoologie, Band 3, Vertebrata (Pisces, Amphibia, Reptilia, Aves). Druck und Verlag von R. Oldenbourg, Münich und Leipzig, 900 pp.